Taxonomy, phylogeny and genomics of the Wallemiomycetes and a newly discovered class of extremophilic fungi

Hai Nguyen

A thesis submitted to the Faculty of Graduate and Postdoctoral Studies in partial fulfillment of the requirements for the degree of Doctor of Philosophy in Biology

Department of Biology
Faculty of Science
University of Ottawa

“We are what we think.
All that we are arises with our thoughts.
With our thoughts we make the world.”
-- Buddha (As translated by T. Byrom (1993), Shambhala Publications)

Table of Contents

Abstract

New species of fungi that belong to the class Wallemiomycetes and related lineages were discovered and characterized. The Wallemiomycetes includes species of brown moulds from the genus *Wallemia.* Further study was warranted for *Wallemia sebi* because of its ubiquity in the human indoor environments and its potential roles in food spoilage, human allergy and disease. A survey of *Wallemia* in house dust was conducted. Sequencing of DNA and application of the genealogical concordance phylogenetic species recognition (GCPSR) led to recognition of four species within the *W. sebi* species complex (WSSC) and served as the foundation for phenotypic assessment and the formal description of three new species called *W. mellicola*, *W. canadensis* and *W. tropicalis*. A survey of heat resistant fungi in soils coincidentally resulted in the discovery of a new lineage of fungi related to *Wallemia*. This new lineage included a previously described monotypic genus *Basidioascus* and a new sister genus given the name *Geminibasidium*. A part of the morphological life cycle of these fungi was documented where two new basidial types were discovered, followed by the description of three new species called *B. magus*, *G. donsium* and *G. hirsutum*. Further studies on the sexuality and origins of the species *B. undulatus* were carried out with genome sequencing, genome analysis, confocal microscopy and electron microscopy. These results led to the creation of a new class of fungi called the Geminibasidiomycetes, which are distantly related to the Wallemiomycetes. Solving the WSSC, circumscribing a new class of fungi called Geminibasidiomycetes and characterizing the species of Geminibasidiomycetes on a taxonomic and genomic level are my original contributions to scientific knowledge.

Resumé

De nouvelles espèces de moisissures appartenant à la classe des Wallemiomycètes ainsi que d'autres lignées apparentées ont été découvertes et caractérisées. Les Wallemiomycètes comprennent certaines espèces de moisissures brunes appartenant au genre *Wallemia*. De plus amples études sont nécessaires afin de mieux comprendre les rôle potentiels de *Wallemia sebi*, une espèce ubiquitaire dans la poussière domestique, sur la détérioration des aliments, le développement d'allergies et les maladies cutanées. Alors, une enquête sur la présence de *Wallemia* dans la poussière domestique a donc été réalisée. Les séquences d'ADN et l'application de la reconnaissance et la concordance généalogiques d'espèces phylogénétiques (RCGEP) ont conduit à l'identification de quatre espèces phylogénétiques dans le complexe d'espèces *W. sebi* (CEWS). Ces données ont guidé l'évaluation phénotypique et la description formelle de trois nouvelles espèces appelées: *W. mellicola*, *W. canadensis* et *W. tropicalis*. De plus, une enquête sur les moisissures résistantes à la chaleur dans les sols a abouti à la découverte fortuite d'une nouvelle lignée de moisissures. Cette nouvelle lignée comprenait un genre monotypique précédemment décrit, i.e. *Basidioascus,* et un nouveau genre apparenté auquel le nom *Geminibasidium* fut donné. Seulement une partie du cycle de vie morphologique de ces espèces de moisissures, durant lequel deux nouveaux types de basides ont été découverts, a pu être observée pour la première fois. Ses caractéristiques ont permis, par la suite, de décrire trois nouvelles espèces appelées: *B. magus*, *G. donsium* et *G. hirsutum*. De plus amples études sur la sexualité et les origines de l'espèce *B. undulatus* ont été réalisées par séquençage et analyse génomique, ainsi que par microscopie confocale et microscopie électronique. Ce travail a mené à la création d'une nouvelle classe de moisissures appelées Geminibasidiomycètes, qui sont apparentées à la classe Wallemiomycètes, mais plus éloignées. Trouver la solution pour reconnaitre les espèces dans l'CEWS, découvrir une nouvelle classe de moisissures Geminibasidiomycètes et caractériser ces espèces de Geminibasidiomycètes avec la taxonomie et la génomique sont mes contributions originales à la connaissance scientifique.

Acknowledgements

The research described in this thesis was performed within the Biodiversity (Mycology) Group at the Canadian federal department Agriculture and Agri-Food Canada (AAFC) at the Eastern Cereal and Oilseed Research Centre (ECORC). This research was funded by the Alfred P. Sloan Foundation Program on the Microbiology of the Built Environment, the Ontario Graduate Scholarship (OGS), Queen Elizabeth II graduate scholarship in Science and Technology (QEII-GSST) and the University of Ottawa excellence scholarship.

This thesis was four years in the making. I owe a great deal of gratitude to my colleagues, family, and friends who have supported me through these times.

First, I want to thank my mentor/supervisor/advisor Keith A. Seifert (KAS) for showing me the gateway to the hidden world and guiding me after I have stepped through it. Keith, I learned an incredible amount from you. I am lucky that you fostered an environment where I am able to intuitively feel my way through the unknown and not be afraid of it. I am so grateful for your support and advice. I am also grateful for all the opportunities you have given me to travel and to network with the prominent people in the field. I'll never forget what we accomplished together in these short years. We have a rare great working relationship and I hope this is just the beginning to a life long collaboration.

Next, I want to thank some members of the KAS lab whom I have spent the majority of my time with during my doctoral studies. Gerrry Louis-Seize, thank you for your help around the lab. Joey Tanney, thank you for being a great office mate and a collaborator. Allison Walker, thank you for being like a big sister, for your letters of support for scholarships, manuscript edits, and your great sense of humour. Yuuri Hirooka, thank you for being a great collaborator and a wonderful close friend outside of work.

I have extensively collaborated with Denise Chabot from the Microscopy Centre at ECORC. Thank you Denise for making time for me. I always felt like we were embarking on a spaceship going somewhere exciting every time we started the electron or confocal microscope. I also want to thank Nancy Nickerson for isolating all the cool fungi that I got to work with.

I want to thank other people from AAFC: the research scientists André Levesque, Scott Redhead, Yolande Dalpé, Sarah Hambleton, Wen Chen, and John Bissett for their general help/advice on research. Thanks Wen for our various discussions, Scott for reading over my manuscripts, and Yolande for help with preliminary nuclear staining experiments. I want to thank the technicians Tara Rintoul (technical advice), Julie Chapados (technical advice and ordering materials), Quinn Eggertson (phylogenetics advice), Parivash Shoukouhi (yeast cultures), Katia Ponomareva (DNA/RNA extractions), Wayne McCormick and Rafik Assabgui (Sanger sequencing). Many thanks go to the bioinformaticians Satpal Bilkhu (databases, bash, Perl), Jeff Cullis (genomics), Chris Lewis (general informatics), Christine Lowe (phylobayes), Glen Newton (software installation), Zaky Adam (genome assembly) and Iyad Kandalaft (Galaxy). Thanks Kelly Babcock and Jennifer Wilkinson at DAOM/CCFC for help with depositing fungi. I want to thank my first boss at AAFC Tharcisse Barasubiye for teaching me the basics and introducing me to everyone when I first arrived as an undergrad. Finally, I want to thank the various postdocs I had the chance of meeting at AAFC: Miao Liu, Prasad Kesanakurti Samba Siva, Kanak Bala.

I am also part of the University of Ottawa. Thanks to the people at the biology department for all your support: Doreen Smith et al. for stipends and travel reimbursements, Lise Bergeron for your support in the mini-course. Thanks John Basso for inspiring me to stay and continue in the life sciences. Thanks Guy Drouin for being part of my thesis committee. Thanks Stephane Aris-Brosou for teaching me bioinformatics. As for the qualifying exam, thanks Nicolas Corradi for chairing and Doug Johnson for being an examiner. Thanks Myron Smith at Carleton University for letters of references, teaching me fungal genetics, and being part of my thesis committee. I want to thank the other admin staff at uOttawa: the ladies at the science grad office (Elvira Evangelista, Lorraine Houle, Diane Perras, Manon Gauvreau) for all your help, the awards officers at FGPS (Daniel Melanson and Paulette Arsenault) for your time/patience.

I am so fortunate to have the chance to travel for conferences and collaborate with many around the world. Thank you Cobus Visagie and Neriman Yilmaz for your hospitality in the Netherlands. You are now in Canada and I hope we will become great friends and colleagues. Thanks Timon Wyatt for various discussions and trying out some experiments with me (even though they didn't work). I want to give thanks to other collaborators in Europe: Martin Meijer, Rob Samson, Saso Jančič, Polona Zalar and Nina Gunde-Cimerman. Thank you Dominik Begerow for inviting me to Bochum and your hospitality. Thank you M. Cathie Aime for inviting me to visit you in West Lafayette, for your hospitality, and for driving me to East Lansing. Thank you Shaghayegh Nasr, Robby Roberson, Yen Le, Erick Cardenas Poire, Yutaka Kikoku, Peter Johnston, for research collaboration.

My family means a lot to me. I want to thank my father Dinh-Van Nguyen and my mother Hong Le for their support and love. I did not turn out exactly as you expected but at least I did something you are proud of. I want to thank my sister Susan Nguyen and my cousins for a great time during the Christmas holidays.

My friends have done a good job at keeping me grounded. A special thank you to Kevin Ripley for your friendship, patience, understanding and companionship. We have been through so many good times together these past four years. Thank you D. Brisson, J. Laframboise, S. Yardy, D. Geissler, K. J-G & T. Geraghty, E. Chiang, D. Lambert, D. Boucher, J. Em, S. Butler, A. Belov & G. Chudov, J. Weiss & K. Go, T. Grewal & M. Langlet, A. Flint, B. Marquez, for your friendship during my studies.

List of abbreviations

AFTOL – Assembling the Fungal Tree of Life
A_w – water activity
bp – base pairs
CBS – CBS-KNAW Fungal Biodiversity Centre culture collection in Utrecht, the Netherlands
DAOM – Canadian National Mycological Herbarium, Agriculture and Agri-Food Canada, Ottawa, Canada
DAOMC or CCFC – Canadian Collection of Fungal Cultures, Agriculture and Agri-Food Canada, Ottawa, Canada
DAPI – 4',6-diamidino-2-phenylindole. It is a fluorescent stain that binds to DNA.
DG18 – Dichloran Glycerol Agar
EXF – Ex Culture Collection of the Department of Biology, Biotechnical Faculty, University of Ljubljana in Ljubljana, Slovenia
ET – epitype
Gb – Gigabases (=1,000,000,000 bp)
GCPSR – Genealogical concordance phylogenetic species recognition
GTR – Generalized time-reversible
HAL2 – 3´-phosphoadenosine-5´-phosphatase
HMG – high mobility group
HPLC – High performance liquid chromatography
HT – holotype
ITS – internal transcribed spacers of the nuclear ribosomal DNA, including the 5.8S gene. The official fungal barcode.
JGI – Joint Genome Institute in Walnut Creek, California, USA
Kb – kilobases (1,000 bp)
LSU – large (28S) subunit of the ribosome
M40Y – 40% sucrose with malt and yeast extract agar
MAPK – mitogen-activated protein kinases
Mb – Megabases (=1,000,000 bp)
MCM7 – DNA replication licensing factor
MEA – Malt extract agar
MUCL – Mycotheque of the Catholic University of Louvain, Louvain la Neuve, Belgium
MYA – Malt yeast extract agar
Mya – Million years ago
MZKI – Microbiological Culture Collection of the National Institute of Chemistry, Ljubljana, Slovenia
NT – neotype
PCR – Polymerase chain reaction
RPB1 – RNA polymerase II largest subunit
RPB2 – RNA polymerase II second largest subunit
SSU – small (18S) subunit of the ribosome
SYTO-9 – A green-fluorescent nucleic acid stains (DNA and RNA)
TEM – transmission electron microscopy
TSR1 – pre-rRNA processing protein
UAMH – University of Alberta Microfungus Collection and Herbarium, Edmonton, Canada
WSSC – *Wallemia sebi* species complex

List of Tables

Supplementary Table 4.2. Nuclear single copy genes selected for phylogenomic analysis and molecular dating.

Supplementary Table 4.3. Molecular clock calibrations in molecular dating analysis.

Supplementary Table 4.4. List of known and putative meiosis genes in the genome of *Saccharomyces cerevisiae*, *Cryptococcus neoformans* and *Basidioascus undulatus*.

Supplementary Table 4.5. List of mating genes.

List of Figures

List of Supplementary Files

Supplementary File 2.1. All trees resulting from single gene phylogenetic analyses.

Supplementary File 2.2. BPP3 analyses.

Supplementary File 4.1. *Basidioascus undulatus* scaffolds in fasta format.

Supplementary File 4.2. *Basidioascus undulatus* transcripts by LocusID in fasta format.

Supplementary File 4.3. *Basidioascus undulatus* proteins by LocusID in fasta format.

Supplementary File 4.4. *Basidioascus undulatus* annotations listing coordinates of all genes by LocusID in the genome in gff3 format

Supplementary File 4.5. Annotations of the *B. undulatus* genome by Locus ID.

Chapter 1: General introduction

Hai D.T. Nguyen[1,2]

[1] Department of Biology, Faculty of Science, University of Ottawa, Ottawa, Ontario, Canada

[2] Biodiversity (Mycology), Eastern Cereal and Oilseed Research Centre, Agriculture and Agri-Food Canada, Ottawa, Ontario, Canada

Overview

Environmental sequencing of fungi revealed large unprecedented gaps in knowledge of the biodiversity of fungi on Earth (e.g. O'Brien et al. 2005; Jumpponen and Jones 2009; Buee et al. 2009). This thesis is about the discovery and characterization of new species of fungi that belong to the class Wallemiomycetes (Basidiomycota) and related lineages.

The Wallemiomycetes includes three species of brown moulds in the genus *Wallemia*. These species are called *W. sebi*, *W. muriae* and *W. ichthyophaga*. They thrive in environments of high cellular osmotic stress and are often referred to as osmotolerant/osmophilic or xerotolerant/xerophilic. *Wallemia ichthyophaga* is an obligate halophile previously isolated from the water of salterns (Zalar et al. 2005). The other two species, *W. sebi* and *W. muriae*, are often isolated from sweet (fruits, jams, cakes) or salty (fish, bacon, salted beans) foods, soil, and also water of salterns (Zalar et al. 2005). Also, *W. sebi* and *W. muriae* are the two species of *Wallemia* most commonly isolated from the indoor environment (Takahashi 1997; Pieckova and Jesenská 1999; Ren et al. 1999; Engelhart and Exner 2002; Zalar et al. 2005; Nakayama and Morimoto 2009; Lappalainen et al. 2012).

Chronic exposure to indoor mould is known to be associated with allergy and asthma (reviewed in Li and Yang 2004) and *W. sebi* produces the metabolites walleminol, walleminone (Frank et al. 1999), and an azasteroid called UCA1064-B (Takahashi et al. 1993). Walleminol has an LD50 of 40 µg/ml for brine shrimp and a minimum inhibitory dose of 50 µg/ml for rat liver cells (Wood et al. 1990). The UCA1064-B compound has weak activity against *Saccharomyces cerevisae*, Gram-

positive bacteria and cytotoxic to HeLa cells (Takahashi et al. 1993). *Wallemia sebi* produces some antimicrobial activity towards *Enterobacter aerogenes* (Peng et al. 2011). Botic et al. (2012) showed that salt induces biosynthesis of active compounds in *W. sebi* that are hemolytic towards mammalian erythrocytes. Despite the ubiquity of *Wallemia* in house dust and awareness of its potential to cause an inflammatory response, no allergens were reported until Desroches et al. (2014) demonstrated that human antibodies react to compounds produced by *W. sebi* spores. The ubiquitous presence of *W. sebi and W. muriae* in human dwellings and the potential *of W. sebi* to make toxic metabolites and cause allergies make further investigation on these fungi worthwhile.

Furthermore*, Wallemia* is interesting because it occupies an isolated evolutionary position in kingdom Fungi according to phylogenetic analyses (Zalar et al. 2005; Matheny et al. 2006; Padamsee et al. 2012). Environmental sequences on public databases hint at the existence of entire uncharacterized lineages. Therefore, new species of fungi, including those in or related to the Wallemiomycetes, remain to be studied and characterized taxonomically.

The thesis contains five main sections, presented as chapters 1 through 5. The main chapters are manuscripts that were either submitted to, or published in, peer-reviewed journals. Minor reformatting was done for uniformity but the contents essentially mirror the published papers. Supplementary Tables are found in the Appendix. However, very lengthy supplementary tables, figures and additional data are provided as downloadable Supplementary Files instead.

This thesis is deeply rooted in fungal taxonomy but infused with contemporary techniques from other areas of biology. **Chapter 1** touches on basic concepts in

fungal taxonomy, phylogenetic analysis, fungal species concepts, fungal sexuality, and genomics. Traditionally, fungal taxonomy involved describing and classifying new species using morphology. In the past decade, phylogenetic analyses with DNA sequences helped with the description and classification of new species, and an introduction to phylogenetic analysis is presented. To circumscribe species, one must apply a testable species concept and these concepts are summarized. Fungal genome data are now being generated at unprecedented rates. Illumina sequencing, genome assembly and genome annotation are briefly discussed.

In **chapter 2**, an in-depth survey of *Wallemia* in the indoor environment was conducted. Strains of *Wallemia* were isolated and cultured from indoor house dust and surfaces. Multi-locus DNA sequencing and application of the genealogical concordance phylogenetic species recognition (GCPSR) resulted in the recognition of four phylogenetic species within the *W. sebi* species complex (WSSC). The phylogenetic species hypotheses from chapter 2 were used to guide phenotypic assessment of *W. sebi* strains from a wide range of environments in a companion study (Jančič et al. 2015) not included in this thesis. The results from the companion study led to the formal description of the new species *W. mellicola*, *W. canadensis*, and *W. tropicalis.*

Next, we went outdoors to look for members of the Wallemiomycetes. In **chapter 3**, a survey of heat resistant fungi in soils resulted in the discovery of a new lineage of fungi distantly related to *Wallemia*. These fungi included species of a previously known genus, *Basidioascus,* and a newly discovered genus *Geminibasidium*. Morphological, ontogenetic, physiological and phylogenetic

studies were performed, which led to the proposal of a new order Geminibasidiales tentatively classified in the class Wallemiomycetes.

Our newly discovered species of fungi in the Geminibasidiales are interesting because they are unique morphologically and phylogenetically isolated from other fungi. *Basidioascus undulatus* was selected as a representative model organism. In **chapter 4**, *de novo* genome sequencing, assembly, annotation and analysis were combined with confocal microscopy and electron microscopy to further study sexuality and evolutionary origins of *B. undulatus*. Taken together, the results led to the confirmation of the sexual structures in *B. undulatus* and the movement of the Geminibasidiales (and its subordinal ranks) out of the Wallemiomycetes, and into the new class Geminibasidiomycetes.

Chapter 5 summarizes all results and provides future directions for research on the fungi in the Wallemiomycetes and the Geminibasidiomycetes.

Kingdom Fungi

Fungi are a diverse collection of heterotrophic eukaryotes. They comprise of mushrooms, rusts, smuts, puffballs, truffles, morels, moulds, lichens, and yeasts, and many unfamiliar microscopic organisms (Figure 1.1). Fungi are generally aerobic, have cell walls with β-glucan and chitin, have mitochondria and peroxisomes, but they lack plastids (Kendrick 2001). Fungi are unicellular, and/or filamentous. The term **hypha** (*pl.* **hyphae**) is used to refer to the filamentous cells of some fungi. The growth and branching of hyphae form a network of filaments called

a **mycelium**. Fungi can reproduce both sexually and asexually by spores and other kinds of propagules.

Historically, fungi were studied as a branch of botany and were lumped in the now obsolete phylum Thallophyta of the plant kingdom (Kendrick 2001). In the 1990's, progress was made toward a phylogenetic classification of fungi based on analyses of DNA (Bruns et al. 1991; Bruns et al. 1992) while prior to this time, morphological characters, physiological characters (e.g. growth at different temperatures and water activity (Pitt 1973), biochemical characters (e.g. isozyme profiles (Joslyn and Boucias 1981), cell wall composition (Bartnicki-Garcia 1968), substrate utilization profiles (Van der Walk and Yarrow 1984) were used to classify fungi. Furthermore, septal pore ultrastructure traditionally played a large role in fungal systematics (Khan and Kimbrough 1982) and is still relevant today for delineating fungal classes (van Driel et al. 2009).

The contemporary concept of kingdom Fungi is different than the traditional concept of fungi. Analyses with DNA sequences from fungal organisms, as understood in the traditional sense, were placed in the eukaryotic tree of life by several studies (Baldauf and Palmer 1993; Baldauf and Doolittle 1997; Baldauf et al. 2000). Researchers realized that the traditional treatment of the fungi is a polyphyletic assemblage of organisms (Figure 1.2A). The contemporary concept of fungi excludes the slime moulds (Dictyostelia, Myxogastria, Acrasida) and water moulds (Oomycota). Members of kingdom Fungi, considered as the 'true' fungi, are more closely related to animals than to plants (Baldauf et al. 2000).

Figure 1.1. Fungal growth forms. A. The mushroom *Amanita muscaria* (*JJ Harrison*). B. Close up of stem rust, *Puccinia graminis*, on a wheat plant (*Yue Jin*). C. The galls of the smut *Ustilago maydis* on corn (*Boom10ful*). D. The puffball *Lycoperdon pyriforme* on a decaying pine log (*Sasata*). E. The truffle *Tuber melanosporum* (*moi-même*). F. The morel *Morchella elata* (photo credit unknown). G. The mould *Penicillium expansum* on a rotting pear (*H.J. Larsen*). H. The lichen *Xanthoria elegans* on exposed sandstone (photo credit unknown). I. The red yeast *Rhodotorula mucilaginosa* on agar (*A doubt*). J. An obscure fungus called *Rozella allomycis* parasitizing the chytrid *Allomyces* (*Timothy James*). All photos were taken from the Wikimedia Commons and are licensed under Creative Commons Attribution-Share Alike 3.0 Unported license.


A
B
C
D
1 cm
E
F
G
H
I
J

Figure 1.2. Phylogenetic tree of fungi and fungal-like organims. A. This eukaryotic tree of life is based on the one shown in Baldauf et al. (2000) and is derived from phylogenetic analyses of sequences of rDNA and up to four protein-coding genes. Circled in black are the organisms traditionally studied by mycologists. B. This fungal tree of life is based on the one shown in Schoch et al. (2012) and it depicts the 17 main lineages recognized in kingdom fungi today. Many basal relationships, indicated by dashed lines, have high levels of uncertainty.

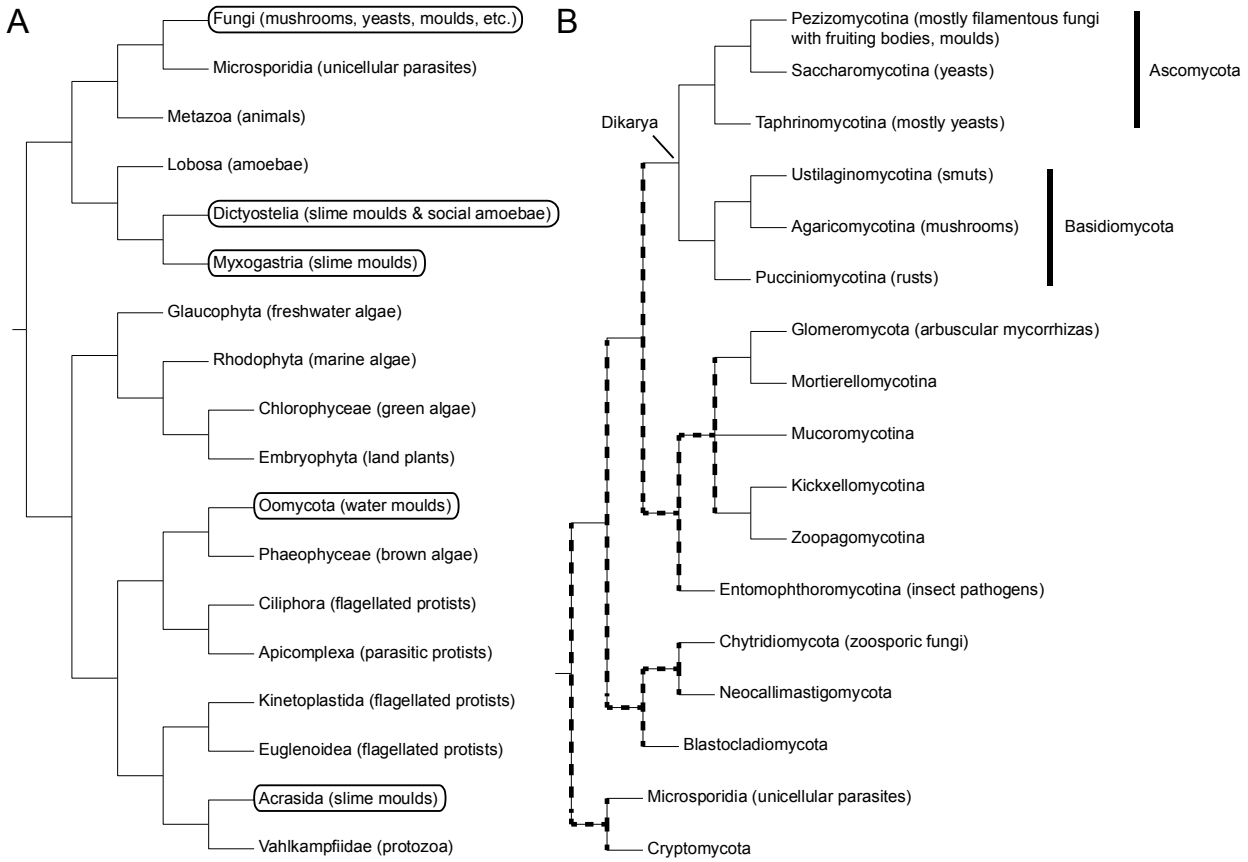
A
Fungi (mushrooms, yeasts, moulds, etc.)
Microsporidia (unicellular parasites)
Metazoa (animals)
Lobosa (amoebae)
Dictyostelia (slime moulds & social amoebae)
Myxogastria (slime moulds)
Glaucophyta (freshwater algae)
Rhodophyta (marine algae)
Chlorophyceae (green algae)
Embryophyta (land plants)
Oomycota (water moulds)
Phaeophyceae (brown algae)
Ciliphora (flagellated protists)
Apicomplexa (parasitic protists)
Kinetoplastida (flagellated protists)
Euglenoidea (flagellated protists)
Acrasida (slime moulds)
Vahlkampfiidae (protozoa)
B
Pezizomycotina (mostly filamentous fungi with fruiting bodies, moulds)
Saccharomycotina (yeasts)
Taphrinomycotina (mostly yeasts)
Ascomycota
Dikarya
Ustilaginomycotina (smuts)
Agaricomycotina (mushrooms)
Pucciniomycotina (rusts)
Basidiomycota
Glomeromycota (arbuscular mycorrhizas)
Mortierellomycotina
Mucoromycotina
Kickxellomycotina
Zoopagomycotina
Entomophthoromycotina (insect pathogens)
Chytridiomycota (zoosporic fungi)
Neocallimastigomycota
Blastocladiomycota
Microsporidia (unicellular parasites)
Cryptomycota

Seventeen major lineages are currently recognized in Kingdom Fungi (Figure 1.2B). The phyla Ascomycota and Basidiomycota together make up the subkingdom Dikarya. Fungi that belong to Ascomycota and Basidiomycota are also referred to casually as **ascomycetes** and **basidiomycetes,** respectively. Most of the described species belong to Dikarya (64163 ascomycetes and 31515 basidiomycetes, totaling 95678) according to the 10th edition of the Dictionary of the Fungi (Kirk et al. 2008).

Many well-studied and important fungi belong to the phylum Ascomycota. As a group, ascomycetes have many specialized ecological roles. They are parasites, pathogens, and mutualists of plants, algae, and animals, and saprobes. Economically important ascomycetes include *Saccharomyces cerevisiae* (brewer's yeast) and *Penicillium chrysogenum* (producer of the antibiotic penicillin). Ascomycetes produce meiospores (ascospores) within sac-shaped cells (asci). Asci are found in fruiting bodies called ascomata. There are many types of ascomata. For example, a cleistothecium is an enclosed spherical structure such as that found in the mould *Penicillium*, a perithecium is an opened bottle-like structure found, for example, in *Neurospora*, and an apothecium is a completely open structure found in cup fungi such as *Peziza*. Ascomycetes also produce a large diversity of asexual structures and spores.

Basidiomycota is the sister phylum to Ascomycota. Basidiomycetes used to be divided into two taxonomic groups called the phragmobasidiomycetes and holobasidiomycetes (Tulasne and Tulasne 1847) based on morphology of the basidium. The alternative classification system is the division of basidiomycetes into two groups called the heterobasidiomycetes and homobasidiomycetes (Crous et al.

2009) based on mating behaviour. Both of these two group systems are slowly being phased out because phylogenetic analyses with DNA sequences are now the standard for classifying fungi into major groups. Pioneering studies by Swann and Taylor (1995) using rDNA sequences in phylogenetic analyses divided the Basidiomycota into three major groups (subphyla), which are now called the Pucciniomycotina, Ustilaginomycotina and Agaricomycotina (Bauer et al. 2006; Hibbett 2006).

Basidiomycetes have diverse ecological roles (Aime et al. 2006; Begerow et al. 2006; Hibbett 2006). Species in the Pucciniomycotina and Ustilaginomycotina are predominantly plant pathogens but are also asymptomatic species of the leaf surface, fungal pathogens and saprobes (Aime et al. 2014; Begerow et al. 2014). The Agaricomycotina includes the jelly fungi and yeasts that are classified in the Tremellomycetes and Dacrymycetes, the mushrooms that are classified in the Agaricomycetes (Weiss et al. 2014; Oberwinkler 2014; Hibbett et al. 2014), and more recently the mould *Wallemia* that is classified in the Wallemiomycetes (Padamsee et al. 2012; Zajc et al. 2013). Species of Tremellomycetes can be found living on leaf surfaces, seawater, freshwater, soil, animals, or other fungi (Weiss et al. 2014). Fungi in the Agaricomycetes function as saprotrophs, pathogens, and mutualists. The Agaricomycetes contains the majority of root-associated fungi called ectomycorrhizal fungi (ECM), as well as white-rot and brown-rot decayers of massive woody substrates like tree logs (Hibbett et al. 2014). The ecological role of *Wallemia* is unknown or uncertain at best.

Fungi in the Basidiomycota are economically important. The most commonly cited example of Pucciniomycotina is the stem rust species *Puccinia graminis*, which

causes economically important disease of wheat and barley (Singh et al. 2011). Well-known genera in Ustilaginomycotina are *Ustilago* and *Tilletia*, which are important species causing bunt of wheat, loose smut of barley, and corn smut (Begerow et al. 2014). Edible mushrooms are familiar examples of fungi in the Agaricomycotina and they include *Pleurotus ostreatus* (oyster mushroom) and *Lentinula edodes* (shiitake), which grow on logs (Hibbett et al. 2014). Yeast species are found in all three major groups (Kurtzman et al. 2011). Examples of important basidiomycetous yeasts are *Pseudozyma flocculosa* that causes disease in cucumber and *Cryptococcus neoformans* is a pathogen of concern for immunocompromised patients (Kurtzman et al. 2011).

Despite some differences, basidiomycetes have many underlying common features. Typically in fungi of the Agaricomycotina, a club-shaped cell called the **basidium** (*pl.* **basidia**) gives rise to four meiospores (basidiospores) attached by a horn shaped structure called the **sterigma** (*pl.* **sterigmata**). In fungi of the Pucciniomycotina, a resting spore called a teliospore gives rise to a basidium bearing four basidiospores. Basidium morphology is diverse across the phylum (Figure 1.3) and can be divided into two major types. Phragmobasidia are basidia that have longitudinal or transverse cross-walls, whereas the holobasidia lack cross-walls. The basidia are organized as a fruiting body called the **basidiome** (*pl.* **basidiomata**). An example of a basidiome is the mushroom.

Figure 1.3. Some examples of basidial types. A. *Puccinia* basidium germinating from a teliospore. B. *Ustilago* basidium germinating from a teliospore. C. Typical basidium of fungi in the Auriculariales. D. *Tremella* basidium. E. *Dacrymyces* forked basidium. F. Typical basidium of fungi in the Agaricales. A–D. Phragmobasidia. E–F. Holobasidia. Figures after Begerow et al. (2014) and Crous et al. (2009).

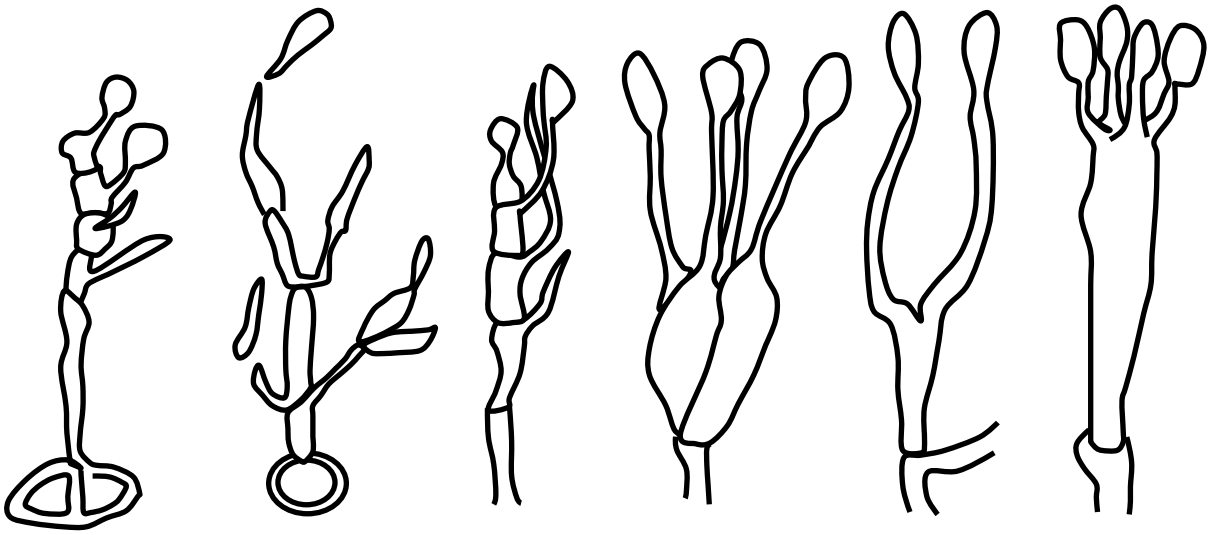
A
B
C
D
E
F

Basidiomycetes have diverse life cycles. The life cycles of Pucciniomycotina species range from simple yeasts such as *Rhodosporidium toruloides* where basidia germinate from a teliospore and produce budding spores as yeast cells. These yeast cells can mate to give hyphae where teliospores are produced once again (Aime et al. 2014). Some Pucciniomycotina species such as the rusts *Puccinia graminis* and *Melampsora larici-epitea* have complex life cycles involving alternate plant hosts and additional sexual structures such as spermagonia, aecia, and urediniospores (Aime et al. 2014). In general, species of Ustilaginomycotina have a dimorphic life cycle consisting of a saprobic haploid phase beginning with the formation of basidiospores that germinate into yeast cells and ending with the conjugation of compatible haploid yeast cells to produce dikaryotic hyphae capable of infecting plant tissues (Begerow et al. 2014). In species of Agaricomycetes, the basidiospores germinate and produce haploid hyphae. These hyphae can become fragmented to give rise to asexual spores called **arthroconidia**. If the hyphae from one individual encounter the hyphae of another individual and both individuals are compatible for mating, their hyphae will fuse. After fusion, the resulting hyphae become bi-nucleated (dikaryotic) and **clamp connections** are formed. A clamp connection is an outgrowth developing at a septum that grows backward and fuses with the preceding cell so that a daughter nucleus can return to the mother cell during hyphal growth. The dikaryotic hyphae eventually make basidia where the two nuclei will fuse, undergo meiosis, and produce basidiospores once again (Kues 2000).

The life cycle of *Wallemia* species is different than most other fungi in Agaricomycotina. *Wallemia* species grow as brown moulds that only produce chains

of asexual spores called **conidia** (Figure 1.4). The morphology of *Wallemia* is reminiscent of the ascomycetous mould *Torulomyces*. The chains of conidia develop in tetrads. At one point, it was hypothesized that tetrad conidia might actually be meiotic products (e.g. basidiospores) and the conidiogenous cells may be some kind of previously uncharacterized basidium (Moore 1986). However, the latest investigation does not support the interpretation of tetrad conidia as basidiospores (Padamsee et al. 2012). Basidiospores and basidia of *Wallemia* have never been observed before. Therefore the life cycle of *Wallemia* is not fully known yet.

Figure 1.4. *Wallemia* conidium ontogeny. The conidiogenous cell (a) develops basauxically where it increases its length near the base while unbranched chains of conidia (b) are produced basipetally where the youngest conidium is at the base. Each dashed line connects the same point on the fungus. This figure was adapted from Hill (1974).

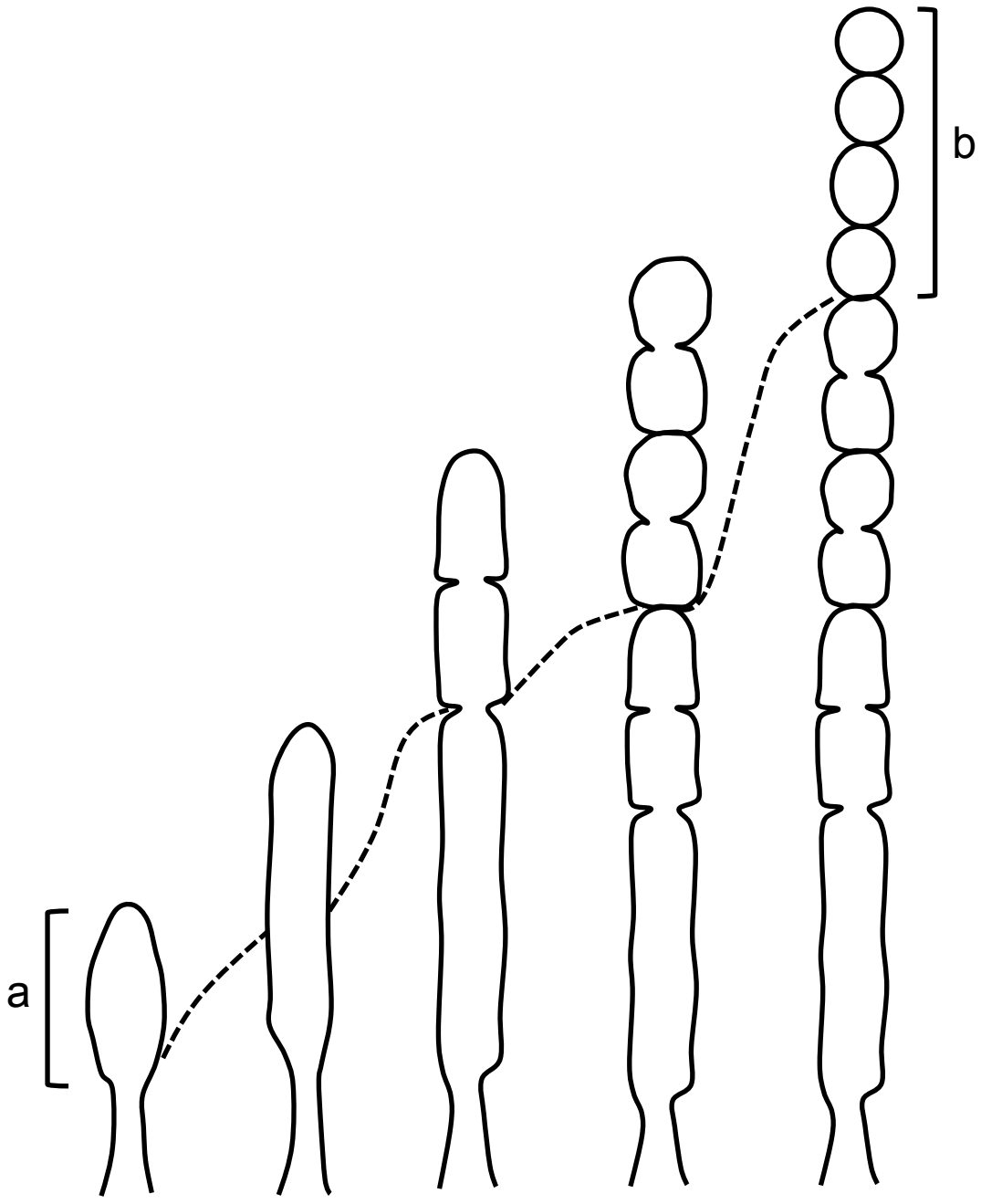
a
b

Fungal biodiversity and taxonomy

Described fungal species make up only a small percentage (5–10%) of all the fungi that exist on Earth. Published estimates of the actual number of fungal species on Earth vary from 1.62 million (Hawksworth 1991) to 2.27 million species (Hawksworth 2001). These estimates assume a certain ratio of fungi to vascular plant species because fungi are well known to associate with plants as pathogens or mutualists. O'Brien et al. (2005) estimates 3.5 to 5.1 million species based on environmental sequencing of soil. However, the estimated figure of 1.5 million fungal species is widely accepted by mycologists (Bass and Richards 2011).

Fungal taxonomy is concerned with naming, identifying and classifying fungal species. The International Code of Nomenclature for algae, fungi, and plants (also known as the Melbourne Code) is a complex document (http://www.iapt-taxon.org/nomen/main.php) outlining all the rules for naming fungi. A DNA barcode is a standardized 500-800 bp sequence used to identify species (Hebert et al. 2003) and the internal transcribed spacer (ITS) region is the official fungal DNA barcode (Schoch et al. 2012). A taxonomic hierarchy of ranks characterized by a set of endings is used to classify fungi (Table 1.1).

Table 1.1. The fungal taxonomic hierarchy with endings and two examples.

Ranks	Endings	Example 1	Example 2
Phylum	-mycota	Ascomycota	Basidiomycota
Subphylum	-mycotina	Saccharomycotina	Agaricomycotina
Class	-mycetes	Saccharomycetes	Wallemiomycetes
Order	-ales	Saccharomycetales	Wallemiales
Family	-aceae	Saccharomycetaceae	Wallemiaceae
Genus	N/A	*Saccharomyces*	*Wallemia*
Species	N/A	*cerevisiae*	*sebi*

Type specimens play an important role in fungal taxonomy. A type specimen is a permanent reference for a taxon (e.g. species or genus) that defines features of that taxon. Every fungal species must have a single preserved type specimen called a **holotype** usually deposited in a herbarium. The holotype is designated when a new species is described. There have been many cases where the holotype is in poor condition or simply lost. When the holotype is in poor shape but still exists, additional material to supplement the holotype can be designated instead and this material is called an **epitype**. However, when the holotype is completely lost, the designated representative material is called a **neotype**.

Phylogenetic analysis

Phylogenetic analysis is useful for revealing relationships among taxa. These relationships can be monophyletic, paraphyletic or polyphyletic. Monophyletic relationships are observed when all members of a group are derived from a common ancestor. Paraphyletic relationships describe a hypothesized group of related organisms that excludes one or more of the common descendants. A polyphyletic group includes descendants of two or more different evolutionary

ancestral organisms. Divergence of character states (e.g. nucleotide or amino acid sequences) between organisms is calculated as the first step in phylogenetic analysis. This is followed by the application of phylogenetic reconstruction methods to infer a phylogenetic tree. The phylogenetic tree depicts the best hypothesis about the relationships among organisms.

Before DNA sequencing technologies were common, morphological characters were widely used in phylogenetic analyses. However, today most phylogenetic analyses are carried out using DNA or amino acid sequences. In the first step of phylogenetic analysis, computer algorithms (e.g. (Edgar 2004; Katoh and Standley 2013)) align nucleotide or amino acid sequences producing a multiple sequence **alignment**. In this alignment, divergence is calculated between all pairs of nucleotide or amino acid sequences by counting the number of sites where they differ and calculating the proportion of this difference. Divergence is essentially a product of nucleotide or amino acid substitution. This substitution process can be modeled mathematically. One can develop time reversible models, which are models that assume for any two nucleotides, the rate of change from one to another, and vice versa, is the same. One of the simplest models is the JC69 nucleotide substitution model (Jukes and Cantor 1969) where the equilibrium frequencies of the four nucleotides of DNA (A, T, G, and C) are 25% each and that during evolution, any nucleotide has the same probability to be replaced by any other. Each model is defined by a set of **parameters**.

There are two additional ways nucleotide substitution can be modeled. The rate of nucleotide substitution can vary for different positions in a sequence. For example, in a protein coding sequence, the third codon position tends to mutate

faster than the first position because a change in the third codon position does not usually lead to a change in amino acid. In this case, nucleotide substitution can be modeled further with what is called **rate heterogeneity among sites**, which accounts for different rates at each site (Yang 1993). In some cases, a certain mutation at a given site is strongly deleterious and an **invariable-sites model** can be used to account for such phenomenon (Fitch 1986).

Once the divergence is measured, the next step is to infer phylogenetic relationships. Many phylogeny reconstruction methods are available to make this inference. Some methods are distance-based such as neighbor joining while others are character-based such as Bayesian inference, maximum likelihood and maximum parsimony.

Neighbor joining (Saitou and Nei 1987) is a distance-based method where divergence is computed for every sequence pair in the alignment and stored in a matrix of pairwise distances. The divergence values can be left as observed distance or adjusted by applying a nucleotide substitution model. The algorithm starts with an unresolved star tree with a central node, finds a pair of sequences with the lowest distance value, and joins them together to a newly created node connected to the central node. Then, the distance values in the matrix are updated by calculating the distance from this newly created node to other sequences followed by the joining of the next two closest neighbours. This is repeated until the relationships between all sequences are resolved, producing a phylogenetic tree.

Bayesian inference is becoming more popular in phylogenetics. Its use in phylogenetics began in the 1990's (Yang and Rannala 1997). **Bayesian inference** begins with the statement of a **prior** belief about the tree (the relationships between

organisms). Aligned sequence data and a model of substitution are used to update this **prior** to a **posterior probability** distribution. If the data are informative, most of the posterior probability will be focused or said to **converge** on one tree topology.

In **maximum likelihood** (Felsenstein 1981), each site in the alignment is evaluated by summing the probabilities of every possible reconstruction of ancestral states given a model of nucleotide substitution. This is done to find the values of the parameters in the model and tree that maximizes the likelihood.

Maximum parsimony is method of phylogenetic inference where the tree with the minimum number of evolutionary changes is considered as the best hypothesis of relationship among organisms (Fitch 1971). Maximum parsimony used to be a common approach but it has now been replaced by Bayesian inference and maximum likelihood in the fungal taxonomy literature.

Often a **bootstrap analysis** is used to evaluate the reliability of specific clades in a phylogenetic tree (Felsenstein 1985). Bootstrap analysis is a sampling technique for estimating statistical error when the underlying sampling distribution is unknown. In bootstrap analysis, a new alignment is generated by randomly choosing columns from the original alignment, where each column can be selected more than once or not at all, until a new set of sequences, called a **bootstrap replicate**, with the same length as the original one is assembled. Then, for each bootstrap replicate, a tree is computed and the proportion of each clade that appear from all bootstrap replicates is taken as the statistical confidence to support the topology of the phylogenetic tree produced from the original alignment.

Fungal species recognition and delimitation

The species is the basic unit of biological taxonomy. Most biologists will agree that a species is made up of one or many populations of individuals. A species evolves independently and is genetically isolated from other species.

There are many **species concepts** that can be applied to recognize fungal species. Here, the species concept is defined as a standard for recognizing whether individuals should be considered members of the same species. Each fungal species is unique so the genetic events and relevant characters indicating speciation are unique too. Fungal species can be delineated with the biological species concept (BSC) emphasizing reproductive isolation, the morphological species concept (MSC) focusing on morphological differences, the ecological species concept (ESC) highlighting adaptation to an ecological niche, and the phylogenetic species concept (PSC) asserting nucleotide divergence. Some of these concepts will describe consequence of speciation (e.g. phylogeny in PSC) and others the mechanism that initiates speciation (e.g. introduction of a species to a new environment in ESC). One or more of these concepts may be applicable to a particular taxonomic group but the same concept(s) will not necessarily be applicable to all species in that group.

Species can be recognized by various concepts but how can they be delimited in a practical sense? This is an important issue for fungal taxonomists who want to describe and classify new species. The Genealogical Concordance Phylogenetic Species Recognition (GCPSR) (Taylor et al. 2000), an extension of the PSC, is currently a popular method for delimiting species. In this approach,

sequences of multiple unlinked genes are analyzed in phylogenetic analyses with software packages such as PAUP v4.0 (Swofford 2002), RAxML v8 (Stamatakis 2014), MrBayes v3 (Ronquist and Huelsenbeck 2003), or BEAST v2 (Bouckaert et al. 2014). The discordant groupings, showing evidence of lack of genetic exchange, represent the species limit (Figure 1.5). This approach is often used to solve a **species complex** or to delimit **cryptic species** of fungi. A species complex is a group of two or more species that are morphologically similar but the species boundaries are unclear until circumscribed with a species concept. Similar to the definition of the species complex, but expressed differently, cryptic species are genetically distinct, phylogenetic fungal species that cannot be distinguished by morphological characters.

Yang and Rannala (2010) introduced a Bayesian modeling approach using multi-locus sequence data to generate posterior probabilities of species assignment. This approach accounts for uncertainties because of poorly resolved or conflicted genealogies and the ancestral coalescent process. Coalescence is the tracking of each individual's lineage in a population back in time until the first ancestor (Kingman 1982). In other words, coalescence is the merging of the genealogy of multiple gene copies into their common ancestor where "merging" only makes sense when viewed backwards in time. This approach is implemented in a program called BPP3 (Yang and Rannala 2010). Sequence alignments of multiple loci and a mapping file assigning the species for each sequence are provided. The analysis is run multiple times and the output provides the posterior probability for the number of species that exist.

Another way to delimit species is by testing the BSC. The BSC is an intuitively satisfying species concept because of its applicability to other familiar organisms like animals. A way of testing the BSC for fungi is with a mating test, which involves growing two individuals in culture on the same Petri dish. If the two individuals are of the same biological species and they are 'compatible' (discussed below), they will produce fertile progeny and the BSC is fulfilled. However, mating in culture may not indicate mating in nature. On the other hand, getting fungi to mate in culture does not always work either because often many factors like optimal physiological conditions or genetic compatibility are unknown. Fortunately, the occurrence of mating can sometimes be inferred without observing it (discussed below).

Figure 1.5. Genealogical Concordance Phylogenetic Species Recognition (GCSPR). Hypothetical phylogenetic analysis of three genes (genes 1-3) shows transition from concordance among branches to incongruity and it can be used to diagnose the species limit of 8 strains (A to H). Based on a figure in Taylor et al. (2000).

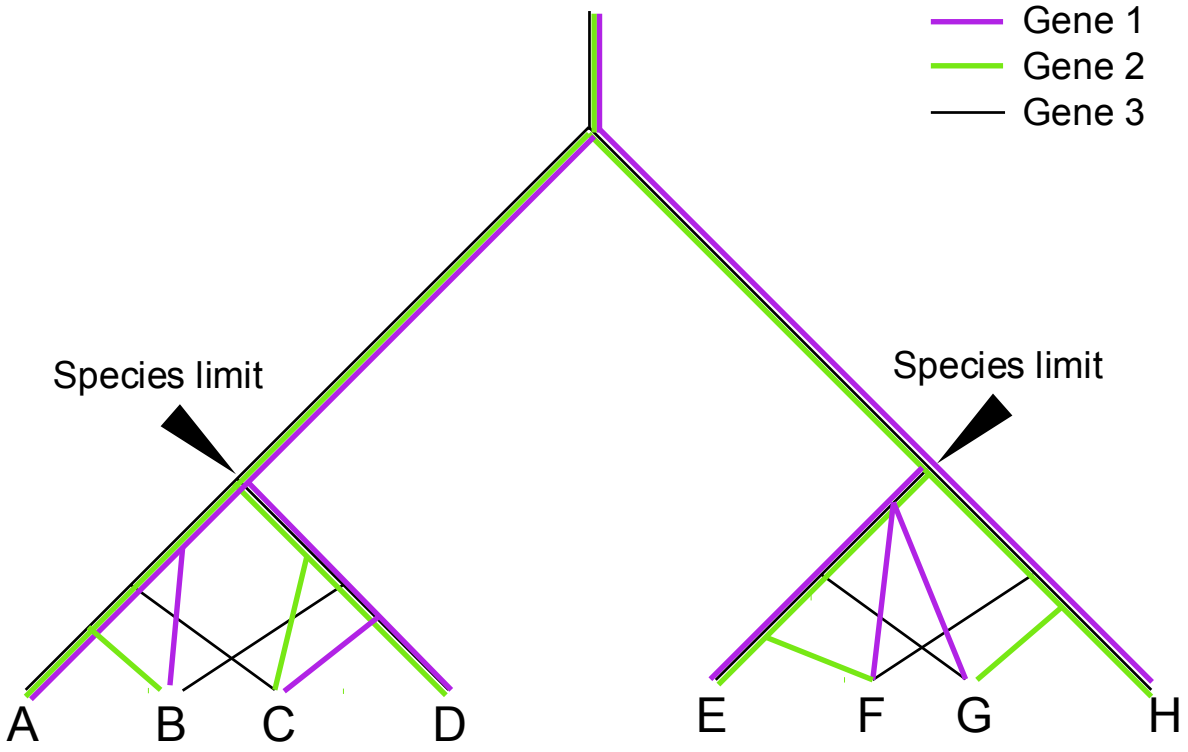
Gene 1
Gene 2
Gene 3
Species limit
Species limit
A
B
C
D
E
F
G
H

Fungal sexuality

Fungal sexuality is a complicated topic but is well summarized in Lee et al. (2010) and Ni et al. (2011). Fungi can reproduce sexually, asexually, and/or parasexually. The sexual stage or morph of a fungus is called the **teleomorph** while the asexual stage or morph is called the **anamorph**.

The function of sexual reproduction is to purge deleterious mutations and to mix genes creating progeny better adapted for colonization of a new environment. When two compatible mating partners recognize each other by chemicals called pheromones, they undergo cell fusion (plasmogamy) followed by nuclear fusion (karyogamy) and meiosis and produces usually four haploid cells (Lee et al. 2010).

Sexual reproduction in fungi is governed by the MAT locus, which is a special genomic region that gives mating identity, sexual identity or gender (e.g. analogous to male or female in animals). This sexual identity is called a **mating type**. The MAT locus encodes for genes that play a role in mate attraction and recognition. Most species of fungi have a single MAT locus, that segregates as a single unit during meiosis, with two possible mating types (e.g. **a** or **α**; + or -). When this is the case, those species of fungi are said to have a **bipolar** mating system. For example, *Wallemia* has a bipolar mating system (Padamsee et al. 2012). However, in some species of basidiomycetes (James et al. 2013), sexual identity is governed by two unlinked MAT loci segregating independently during meiosis. More than two possible alleles can occur at each MAT locus. These basidiomycetes are said to have a **tetrapolar** mating system.

Mating partners recognize each other by the binding of pheromones to pheromone receptors on their cell surfaces (Jones and Bennett 2011). For example, in *S. cerevisiae*, an **α** cell would release α pheromones but would have pheromone receptors for binding **a** pheromones. The binding of pheromones initiates a complex signal transduction cascade that includes a mitogen-activated protein kinase (MAPK) pathway turning on other mating genes.

Fungi that have either the bipolar or tetrapolar mating systems are called **heterothallic**, which means they need another individual of a different mating type to initiate mating and the sexual cycle. On the other hand, **homothallic** fungi are self-compatible and have no need for a genetically distinct mate to undergo a sexual cycle. Outcrossing is difficult to prove for species of homothallic fungi when they are spontaneously producing sexual structures all the time. To delineate species of homothallic fungi with the BSC, one would have to cross two strains, each with unique markers, and show evidence of meiotic recombination in the offspring.

Fungi can also reproduce asexually and some will *only* reproduce asexually. One form of asexual reproduction is the clonal dispersion of spores, where mitospores (conidia) are produced from conidiogenous cells on structures called conidiophores. Fungi that are strictly asexual do not ever produce sexual structures and do not undergo mating. As a consequence, they may be considered clones. If asexual fungal species are clones, they will probably go extinct because deleterious mutations will accumulate over time (Muller 1964). However, the apparent success of asexual species argues against the idea that they are clonal and suggests that another mechanism for maintaining a common gene pool is utilized or that sex must be occurring but not observed. The mechanism for genetic exchange in the absence

of meiosis is called **parasexuality**. For example, *Candida albicans* undergoes a parasexual cycle where two diploid cells fuse in a process called **anastomosis** and the ploidy level increases (2N to 4N). Then, the tetraploid undergoes mitosis and random chromosome loss to return to the diploid state with no recognized meiosis (Noble and Johnson 2007). We do not know how parasexuality functions in most fungi. **Cryptic sexuality** is when the meiosis genes and a mating type locus are present but the sexual cycle of the fungus is not observed. *Wallemia sebi* is said to be sexually cryptic (Padamsee et al. 2012). The implied occurrence of cryptic sexuality and parasexuality leads to challenging fundamental questions about fungal sexuality that can be a focus of genomic studies.

Fungal taxonomy in the age of genomics

Next generation sequencing technologies (e.g. Illumina sequencing, Pyrosequencing, Ion Torrent, etc.) and developments in computing and bioinformatics, now allow low cost sequencing of entire genomes of fungi. Illumina is a next-generation sequencing platform commonly used for genome sequencing. A high quality sample of total DNA is first prepared from the tissue of the fungus. In Illumina sequencing (reviewed in Morey et al. 2013), a library is prepared by fragmenting the genomic DNA to a target size of usually 300–400 bp long. This is followed by the ligase of universal DNA **adaptor** oligonucleotides at both ends of each DNA fragment. These DNA fragments are denatured and in the first step, single stranded DNA fragments are bound to the surface of the flow cell by complementarity of its adaptor to other adaptors on the flow cell surface. In the

second step, the single strand's unattached end hybridizes to adjacent complimentary adaptors forming a bridge. This closed amplicon is extended by polymerases to a double-stranded bridge in a process called **bridge-PCR**. Additional cycles produce more copies of each initial fragment as spatially separated clusters on the flow cell. After bridge-PCR, **sequencing-by-synthesis** is performed where reversable-terminator fluorescently labeled nucleotides are added simultaneously to the sequencing reaction. Each nucleotide has a different fluorescence and they compete for incorporation with amplified fragments in the clusters. An imaging step is performed after nucleotide incorporation to record fluorescence and hence the identity of the nucleotide that was incorporated. Sequencing-by-synthesis is performed until the fluorescence in each position of the entire fragment in each cluster is recorded. When both ends of the fragment are sequenced this is called **paired-end** sequencing. In paired-end sequencing, two files are created where one represents the forward read and the other the reverse read.

Genome assembly is the process where reads are aligned together and overlapping reads that form longer fragments of DNA represent portions of chromosomes. Only few studies so far were able to assemble these fragments into complete chromosomes. Genome assembly can be **reference-based,** where a previously assembled genome of the same or related species is used to guide assembly. Alternatively, genome assembly can be performed ***de novo***, which means starting from the beginning, without the use of a reference genome to guide assembly. Before genome assembly, low-quality data is trimmed and error correction is performed on the reads using specialized bioinformatics programs. A plethora of *de novo* genome assembly programs now exist. Some use an assembly

approach known as overlap-layout-consensus (OLC) and many use De Bruijn graphs. In genome assemblies based on De Bruijn graphs, reads are partitioned into substrings of length *k* called **k-mers. K-mers** then form the nodes of a network called a graph. When nodes share an overlap of *k-1*, a link called an edge is created between them. A De Bruijn graph is a graph whose nodes are sequences of symbols from some alphabet (e.g. DNA letters) and whose edges indicate the sequences which might overlap. This approach was first formalized by Pevzner et al. (2001). The path travelled through the graph forms the basis for a longer stretch of a sequence called a **contig**. Contigs can be oriented and joined together into even longer sequences called **scaffolds**. Assembly quality is assessed by measuring **N50.** N50 is a number representing the length for which the collection of all contigs of that length or longer contains at least 50% of the sum of the lengths of all contigs. Assemblies are also assessed by the presence and completeness of orthologous core eukaryotic genes (CEG's).

Genome annotation is primarily the process of identifying the location and function of genes and other genomic features like coding regions or untranslated regions. Genome annotation comes after genome assembly. It begins with masking repetitive and low complexity sequences in the genome by replacing them with the letter N. Algorithms are used to detect gene models. Protein alignments and RNA-seq data can be provided to support the predicted gene models. The sum of evidence from gene predictions, protein and RNA alignments are put together to create gene annotations. BLAST searches and protein domain scans are performed to assign function to annotated genes. Despite advancements in these tools, many gene products are still characterized as "hypothetical protein".

Once the genome is annotated, it becomes useful for developing testable hypotheses in fungal taxonomy. For example, hypotheses about a particular classification for a species could be tested using phylogenomic analyses that employ multiple genes extracted from genomic information.

Conclusion

Fungi are a group of eukaryotic organisms that are diverse morphologically and ecologically. Fungal taxonomy helps in the process of uncovering unknown fungal biodiversity with collection, identification and classification of fungal species. Fungal species can be delimited with various species concepts and validated using phylogenetic analyses. The entity of a fungal species is maintained through sexual, cryptic, asexual and/or parasexual life cycles. Recent developments in sequencing technologies and bioinformatics now open the door for affordable genomic studies in fungal evolution and sexuality.

Acknowledgements

Thanks J. Chapados for reviewing the section on Illumina sequencing and K.A. Seifert for reading and commenting on the draft.

Chapter 2: Application of the phylogenetic species concept to *Wallemia sebi* from house dust and indoor air revealed by multi-locus genealogical concordance

Hai D.T. Nguyen[1,2], Sašo Jančič[3], Martin Meijer[4], Joey B. Tanney[2], Polona Zalar[3], Nina Gunde-Cimerman[3], Keith A. Seifert[1,2]

[1] Department of Biology, Faculty of Science, University of Ottawa, Ottawa, Ontario, Canada

[2] Biodiversity (Mycology), Eastern Cereal and Oilseed Research Centre, Agriculture and Agri-Food Canada, Ottawa, Ontario, Canada

[3] Department of Biology, Biotechnical Faculty, University of Ljubljana, Ljubljana, Slovenia

[4] CBS-KNAW Fungal Biodiversity Centre, Utrecht, The Netherlands

Abstract

A worldwide survey of *Wallemia* occurring in house dust and indoor air was conducted. The isolated strains were identified as *W. sebi* and *W. muriae*. Previous studies suggested that the *W. sebi* phylogenetic clade contained cryptic species but conclusive evidence was lacking because only the internal transcribed spacer (ITS) marker was analyzed. The ITS and four protein-coding genes (*MCM7*, *RPB*1, *RPB*2, and *TSR*1) were sequenced for 85 isolates. Based on an initial neighbor joining analysis of the concatenated genes, *W. muriae* remained monophyletic but four clades were found in *W. sebi,* which we designated as *W. sebi* clades 1, 2, 3, and 4. We hypothesized that these clades represent distinct phylogenetic species within the *Wallemia sebi* species complex (WSSC). We then conducted multiple phylogenetic analyses and demonstrated genealogical concordance, which supports the existence of four phylogenetic species within the WSSC. Geographically, *W. muriae* was only found in Europe, *W. sebi* clade 3 was only found in Canada, *W. sebi* clade 4 was found in subtropical regions, while *W. sebi* clade 1 and 2 were found worldwide. Haplotype analysis showed that *W. sebi* clades 1 and 2 had multiple haplotypes while *W. sebi* clades 3 and 4 had one haplotype and may have been under sampled. We describe *W. sebi* clades 2, 3, and 4 as new species in a companion study.

Keywords

Internal transcribed spacer (ITS); DNA replication licensing factor (*MCM7*); pre-rRNA processing protein (*TSR*1); RNA polymerase II largest subunit (*RPB*1); RNA

polymerase II second largest subunit (*RPB*2); Wallemia sebi species complex (WSSC); Genealogical concordance phylogenetic species recognition (GCPSR); indoor fungi; Basidiomycota

Introduction

The genus *Wallemia* was introduced over a century ago by Johan-Olsen (1887) for *W. ichthyophaga,* discovered on dried salted fish. However, *Wallemia* remained obscure and what are now recognized as *Wallemia* species were reported under several generic names. Von Arx (1970) proposed the combination *W. sebi* for the species originally described as *Sporendonema sebi* Fr. and today it is the most frequently reported *Wallemia* species. In a recent study, some species names used in the old literature for *Wallemia* were synonymized and other doubtful names were listed as synonyms of *W. sebi* (Zalar et al. 2005). That study connected the old literature with modern concepts of *Wallemia* with molecular data (Zalar et al. 2005). As a consequence, three asexual species, namely *W. sebi*, *W. muriae*, and *W. ichthyophaga*, were now recognized and grouped in the newly erected class Wallemiomycetes and order Wallemiales (Zalar et al. 2005). A more detailed review of the taxonomic history of *Wallemia* and its species is provided in the accompanying paper (Jančič et al. 2015).

Wallemia was considered an enigma in the fungal kingdom and its taxonomic position remained uncertain for over a hundred years. Terracina (1974) showed dolipore-like septal structures in *W. sebi*, similar to those formed by many fungi in the Basidiomycota and some yeasts in the Ascomycota. A few decades later, Moore

(1996) interpreted this as a special kind of parenthesome and described a new family, the Wallemiaceae, to accommodate *Wallemia*. The Wallemiaceae was first classified in the Filobasidiales (Basidiomycota). Subsequent studies could not confirm the exact evolutionary position of *Wallemia* within Basidiomycota by phylogenetic analysis with ribosomal DNA sequences and a few protein-coding gene sequences (Matheny et al. 2006). Recently, the genome of *W. sebi* was sequenced and a phylogenomic analysis with 71 protein-coding genes showed clearly that *Wallemia* belonged to a lineage basal to the Agaricomycotina (Basidiomycota) (Padamsee et al. 2012).

Morphologically, *Wallemia* species grow as powdery, brown colonies on low water activity media and are considered xerophilic or at least xerotolerant. The spore ontogenesis of this fungus is unusual and was the focus of many studies (Hill 1974; Madelin and Dorabjee 1974; Moore 1986; Padamsee et al. 2012) because mycologists were undecided on whether *Wallemia* produces asexual or sexual spores. *Wallemia sebi* produces chains of blastic conidia that mature in basipetal succession by differentiation of a basauxically developing fertile hypha (Cole and Samson 1979). The elongating fertile hypha undergoes septation and subdivides into four cylindrical cells that swell and then disarticulate, a process that is reminiscent of thallic ontogeny. Recently, nuclear behavior during spore development was observed using differential interference contrast and epifluorescence microscopy (Padamsee et al. 2012). Researchers reported no evidence of meiosis, concluding that the known morphology of this fungus represents an asexual morph (Padamsee et al. 2012). Although the sexual stage of *Wallemia* has never been observed, a mating type locus and meiotic genes were

detected in the genome of *W. sebi* CBS 633.66 (Padamsee et al. 2012). Distantly related to *W. sebi* CBS 633.66, *Wallemia ichthyophaga* EXF-994 lacks a complete set of core meiosis genes and it might be incapable of sexual reproduction (Zajc et al. 2013). Thus, some *Wallemia* species may be capable of sexual reproduction but their sexual morphs remain undiscovered.

Many fungi exhibit cryptic speciation. A single morphological or biological species with a cosmopolitan distribution is often composed of multiple cryptic, phylogenetic species that are often geographically separated (Dettman et al. 2003). Sequence variation in the rDNA internal transcribed spacers region (ITS, i.e. ITS1-5.8S-ITS2) hints at the existence of cryptic species within *W. sebi* and this was noted previously (Zalar et al. 2005). Although ITS is the formally recognized fungal barcode (Schoch et al. 2012), it sometimes does not distinguish among closely related phylogenetic species. The genealogical concordance phylogenetic species recognition concept (GCPSR) was proposed as an empirical method for recognizing cryptic speciation (Taylor et al. 2000). GCPSR involves sequencing multiple genes that are then combined in phylogenetic analyses. Incongruent nodes are identified as the point of genetic isolation and therefore the species limit (see Leavitt et al. (2011) for *Xanthoparmelia*; Henk et al. (2011) for *Penicillium*; Dettman et al. (2003) for *Neurospora*; O'Donnell et al. (2008) for *Fusarium*). The GCPSR is especially practical for delimiting species in morphologically reduced fungi or fungi that only exhibit their asexual morph like *Wallemia*.

Ecologically, *Wallemia* is a ubiquitous genus that is usually isolated from xeric environments, including sweet (fruits, jams, cakes) and salty (fish, bacon, salted beans) foods, soil, hypersaline water of salterns (Zalar et al. 2005; Samson et al.

2010), and plants (Jančič et al. unpublished). In rare cases, *W. sebi* causes subcutaneous phaeohyphomycosis (Auvrey 1909; Beurmann et al. 1909; Guarro et al. 2008). Chronic exposure to mould is often associated with allergy and asthma (reviewed in Li and Yang (2004)). Sensitization to *W. sebi* was first reported in Japan (Sakamoto et al. 1989) and another study showed that 0.2% of 1790 children aged 3–14 in Germany had IgE sensitization to *W. sebi* (Kolossa-Gehring et al. 2007). Occupational allergy to *W. sebi* was also reported in European farmers (Lappalainen et al. 1998; Reboux et al. 2001; Roussel et al. 2004; Sennekamp et al. 2012) as a condition called farmer's lung disease, which is characterized by the inflammation of the lungs caused by inhalation of dust from mouldy hay or grain. It was reported recently that human antibodies react to compounds produced by *W. sebi* spores (Desroches et al. 2014).

Wallemia sebi and *W. muriae* are the two species of *Wallemia* most commonly isolated from the indoor environment, an arid niche where xerophiles are common (Takahashi 1997; Pieckova and Jesenska 1999; Ren et al. 1999; Engelhart and Exner 2002; Zalar et al. 2005; Nakayama and Morimoto 2009; Lappalainen et al. 2012). *Wallemia sebi* was frequently isolated from house dust (Sakamoto et al. 1989; Takahashi 1997) and detected by 454 pyrosequencing of house dust in Canada, USA, and Western Europe (Amend et al. 2010; Nonnenmann et al. 2012). At the same time as our metagenomic study (Amend et al. 2010), a parallel project was initiated to investigate the fungal biodiversity of the same samples using high throughput dilution-to-extinction culturing methods. The current study is part of that project. Here, we combined indoor *Wallemia* strains from two other studies that used air and swab sampling as isolation methods, to increase our sample size and

geographic coverage. For reference, we included ex-neotype strains of *W. sebi* and *W. muriae*, and the genome sequenced strain of *W. sebi* (CBS 633.66). Our first objective was to identify what *Wallemia* species occurred in the indoor environment. Our second objective was to develop additional DNA markers to apply the GCPSR to delimit putative cryptic species in the *W. sebi* species complex (WSSC). We chose two protein-coding genes, RNA polymerase II largest subunit (*RPB*1) and RNA polymerase II second largest subunit (*RPB*2) that were previously used to separate species in the Basidiomycota (Matheny et al. 2002; Matheny 2005; Matheny et al. 2007). Additionally, we selected two other genes, DNA replication licensing factor (*MCM*7) and pre-rRNA processing protein (*TSR*1), both recently identified as reliable markers for fungal molecular phylogenetics (Aguileta et al. 2008; Schmitt et al. 2009). After sequencing all five genes for all our isolates, we performed single gene and combined gene phylogenetic analyses. As a third objective, we analyzed two *W. sebi* strains reported to cause skin lesions and a strain of indoor *W. sebi* reported to produce compounds that react to human antibodies (Desroches et al. 2014) with our indoor strains to determine whether potentially medically relevant phylogenetic species exist in the WSSC.

This study establishes four DNA markers not previously used for *Wallemia* to detect cryptic speciation in the WSSC. The observed clades in the WSSC are taxonomically described as new species in a companion study (Jančič et al. 2015), where physiological and secondary metabolite profiling are applied as phenotypic tests of the phylogenetic species hypotheses derived here.

Materials and Methods

Sample collection, isolation and culture

House dust samples were collected as previously described (Amend et al. 2010). Briefly, sterilized dust stream collectors (Indoor Biotechnologies) were attached to domestic vacuum cleaners. Samples were collected through a 2-mm sieve and refrigerated at 4 °C until further processing. For house dust, cultures were isolated either by a modified dilution-to-extinction plating technique of house dust (Visagie et al. 2014). Air samples of 100 L were collected approximately 1 m above the ground with a viable impaction sampler (Sas Super ISO, PBI International). Indoor surfaces (ie. walls, ceilings) were sampled with the swab (Heinz Herenz, Hamburg, Germany). For air and swab sampling, cultures were isolated using standard microbiological techniques. Media for xerophilic fungi were used for isolation, such as malt extract agar with 20% sucrose (M20S: 20 g Bacto malt extract (Difco Laboratories, Sparks, USA); 200 g sucrose (EMD Chemicals Inc., Gibbstown, USA); 15 g agar (EMD Chemicals Inc., Gibbstown, USA); 1000 mL distilled water), malt and yeast extract with 40% sucrose (M40Y: 20 g Bacto malt extract (Difco Laboratories, Sparks, USA); 5 g Bacto yeast extract (Difco Laboratories, Sparks, USA); 400 g of sucrose (EMD Chemicals Inc., Gibbstown, USA); 15 g agar (EMD Chemicals Inc., Gibbstown, USA); 1000 mL distilled water), or dichloran 18% glycerol (DG18: Oxoid Ltd, Hampshire, UK) agar and incubated at room temperature and inspected regularly. Putative *Wallemia* colonies were morphologically identified using a light microscope, transferred to M20S, and then transferred to M40Y prior to long-term preservation. Cultures were deposited and

maintained at the Canadian Collection of Fungal Cultures, Agriculture and Agri-Food Canada (CCFC/DAOM), in Ottawa, Canada; CBS-KNAW Fungal Biodiversity Centre, Utrecht, the Netherlands (CBS); and the Ex Culture Collection of the Department of Biology, Biotechnical Faculty, University of Ljubljana, Infrastructural Centre Mycosmo, MRIC UL, Ljubljana, Slovenia (EXF). Supplementary Table 2.1 includes information on all strains used in this study.

Genetic marker development and evaluation

Wallemia sebi specific primers were designed using PrimaClade (Gadberry et al. 2005) for *RPB*1 and *RPB*2 genes from MAFFT v7.122b (Katoh and Standley 2013) alignment of existing *Wallemia* sequences (Matheny et al. 2006). *Wallemia sebi* specific primers for *MCM*7 and *TSR*1 genes were designed from the genome annotations of *W. sebi* CBS 633.66 (Padamsee et al. 2012) using Primer3 (Koressaar and Remm 2007; Untergasser et al. 2012). Markers were checked by BLAST against the *W. sebi* CBS 633.66 genome. This was done to verify that they were single copy and could be assumed to be unlinked because they are located on different scaffolds. All primer sequences used are shown in Supplementary Table 2.2.

DNA extraction, PCR and sequencing

DNA extraction, PCR and sequencing were performed using a previously described methods (Nguyen et al. 2013) (see Chapter 3). The following PCR profile was used to amplify ITS, *MCM*7, *RPB*1, and *TSR*1: 95 °C for 3 min (initial denaturation), then 40 cycles at 95 °C for 30 sec (denaturation), 55 °C for 30 sec (annealing), 72 °C for 1 min (extension), followed by 72 °C for 5 min (final extension). A touchdown PCR profile was used to amplify *RPB*2. This profile was

the same as the profile described above except that the annealing temperature started at 65 °C (1 cycle), then changed to 63 °C (1 cycle), then to 61 °C (1 cycle), then to 59 °C (1 cycle) then finally to 57 °C (35 cycles).

Clade assignment and phylogenetic analysis

Sequences of each gene were aligned using MAFFT v7.122b (Katoh and Standley 2013) with option L-INS-i for ITS and G-INS-i for *MCM7*, *TSR*1, *RPB*1, and *RPB*2. Alignments were trimmed with BioEdit v7.2.2 (Hall 1999) and analyzed as described below.

To initially assess whether strains formed distinct phylogenetic clusters, a preliminary neighbor joining (NJ) analysis was performed on a concatenated dataset of all aligned genes using SeaView v4.4.2 (Gouy et al. 2010) with the following options: NJ; observed distance; do not ignore all gap sites.

Next, individual genes were analyzed using four methods: neighbor joining, maximum parsimony, maximum likelihood and Bayesian inference. NJ was performed in SeaView v4.4.2 (Gouy et al. 2010) as described above with 1000 bootstrap replicates. Maximum parsimony heuristic searches were performed using PAUP4.10b (Swofford 2002) with these parameters: uninformative characters excluded, midpoint rooting, simple sequence addition, TBR swapping algorithm, collapse and multitrees in effect, 100 maximum trees saved. This was followed by the computation of a parsimony strict consensus tree. RAxML 8.0.20 (Stamatakis 2014) was used to compute a maximum likelihood tree using the GTRGAMMA model. This model was chosen because it includes the parameter G for rate heterogeneity among sites. In RAxML, by default, G has 25 rate categories making the estimation of proportion of invariable sites (I) unnecessary because G

mathematically accounts for I (Stamatakis 2006). Support values were assessed using the 'rapid bootstrapping' option with 1000 replicates. Prior to Bayesian inference, jmodeltest v2.1.4 (Darriba et al. 2012; Guindon and Gascuel 2003) was used to calculate the best evolutionary model for each gene; for each gene alignment, likelihood scores were computed with the following options: 3 substitution schemes, base frequencies on (+F); rate variation on with 8 rate categories (+G, nCat=8); ML optimized base tree; NNI search algorithm. The proportion of invariable sites (+I) was not considered in our model testing because it had minimal impact on estimates of rates and coalescence times for closely related species (Jia et al. 2014). The HKY + G model was selected for ITS, *RPB*2 and *TSR*1 loci, and K80 + G was chosen for *MCM7* and *RPB*1, according to the Bayesian Information Criterion (BIC) (Schwarz 1978). Bayesian inference analyses were performed with BEAST v2.1.3 (Bouckaert et al. 2014). BEAUTi v2.1.3 was used to generate the input XML file. Gene alignments were loaded in BEAUTi and each gene partition was assigned a separate site model, clock model and tree model. The site model was chosen according to the results from jmodeltest described above and the gamma category count was set to 8. All substitution rates, the gamma shape, and the kappa parameter were estimated and left on default settings. All of our *Wallemia* strains were closely related, so we chose the estimated strict clock and the Yule model of speciation, which does not take into account species extinction, conditional on the root for all gene partitions. The birth rate, clock rate and mutation rate priors were set to exponential, except the mutation rate for *RPB2* was set to uniform. Kappa parameters for the HKY models were left on lognormal. Then, the MCMC chain length was set to 1.0×10^8 and storing one tree every 20000 generations. Three

independent BEAST experiments were run with a different random seed. Convergence and effective sample size was monitored with Tracer v1.6. All gene trees from each independent run were combined with LogCombiner v2.1.3 with a burn-in of 10%. The consensus tree was generated with TreeAnnotator v2.1.3 with the target tree type set to maximum clade credibility tree and node heights set to mean heights.

All trees generated from these analyses (Supplementary File 2.1) were imported into FigTree v1.3.1 (http://tree.bio.ed.ac.uk/software/figtree/). Isolates were assigned to a clade number if they were recovered as a distinct group in the strict parsimony analyses and with >80% support values in the NJ, maximum likelihood and Bayesian analyses. We started the assessment on the right hand side of the tree (most recent in molecular time) and worked to the left, using groupings in the initial NJ tree based on the concatenated alignment.

After the isolates were assigned to clades, we used the species phylogeny approach implemented in *BEAST (Heled and Drummond 2010). *BEAST infers a species tree by considering divergence times, population sizes, and gene trees from multiple genes sampled from multiple individuals using a mixture of coalescent and Yule processes. Alignments were imported into the *BEAST template inside BEAUTi. We used the same setup parameters as for the Bayesian analysis described above for the site models, clock models and priors. Additionally, the Yule model conditional on the root was chosen for the species tree branching prior, the species birthrate and the population mean prior distributions were set to normal. Each strain was designated as a separate species using a mapping tab delimited file. Isolates that lacked sequence information for certain genes were included but

the missing sequences were filled in with "?" treated by BEAST as missing information. As above, the MCMC chain length was set to 1.0×10^8 and storing one tree every 20000 generations. A total of 3 independent *BEAST experiments were run with a different random seed. Convergence and effective sample size was monitored with Tracer v1.6. The species trees from all independent runs were combined with LogCombiner v2.1.3 with a burn-in of 25%. The consensus species tree was generated with TreeAnnotator v2.1.3 with the target tree type set to maximum clade credibility tree and node heights set to mean heights.

To provide stronger support for the species hypothesis, a species delimitation analysis was conducted using the program BPP3 (Rannala and Yang 2003; Yang and Rannala 2010), which uses a Bayesian approach to evaluate species delimitation. We used the preliminary NJ tree from the concatenated data set of all aligned genes described above as a guide tree. This method accommodates the species phylogeny as well as incomplete lineage sorting caused by ancestral polymorphism. A gamma prior *G*(2, 1000), with mean 2/2000 = 0.001, is used on the population size parameters (θs). The age of the root in the species tree (τ0) is assigned the gamma prior *G*(2, 1000), while the other divergence time parameters are assigned the Dirichlet prior (Yang and Rannala 2010). Each analysis was run three times to confirm consistency between runs.

To compare the resolution of these markers as potential secondary barcodes, MEGA 5 (Tamura et al. 2011) was used to calculate uncorrected pairwise distances (p-distance) between each sequence for each gene. This information was used to calculate the between clades and within clades p-distances using Microsoft Excel.

All sequences were deposited in GenBank (Supplementary Table 2.1). Alignments and trees were deposited in TreeBASE under study accession no. S15232.

Haplotype analysis and geography

The program COLLAPSE v1.2 (Posada 2004) was used to determine the haplotypes (i.e. unique sequences) in each gene alignment. We obtained a sequence of all strains for *MCM*7, *RPB*1 and *TSR*1. Missing data may have a negligible effect on species tree reconstruction (Hovmoller et al. 2013), but haplotyping using DNA sequences would be sensitive to missing data; therefore our incomplete *RPB*2 *and ITS* data sets were excluded. Alignments were further trimmed with BioEdit v7.2.2 to eliminate all columns with missing data, then concatenated in SeaView v4.4.2 (Gouy et al. 2010). Following this, COLLAPSE v1.2 was run with default settings (gaps treated as 5^{th} state; sequences with 0 difference collapsed) to calculate the number of haplotypes.

Results

Isolates

A total of 85 isolates of *Wallemia* were isolated from our survey of house dust or indoor air in 12 countries: 22 strains from Slovenia; 15 from the Netherlands; 10 from the Federation of Micronesia; 7 from Germany; 6 from Denmark; 6 from Uruguay; 5 from Indonesia; 4 from Canada; 4 from United Kingdom; 3 from Thailand; 2 from Mexico; and 1 from South Africa. The source and method of isolation for each strain are summarized in Supplementary Table 2.1.

Genetic marker assessment

For *Wallemia*, the ITS region amplifies easily but has a high sequencing failure rate, despite repeated attempts. ITS sequence chromatograms often had multiple overlapping peaks. We attempted to design *Wallemia* specific primers for the ITS region, but after pilot testing, they were no more reliable for sequencing than standard primers (White et al. 1990). Finally, with much difficulty, we were able to obtain ITS sequences for 70 of 90 (78%) strains. Even with 78% completion of the data from our indoor *Wallemia* strains, we were able to confirm the observation of potentially cryptic species within the WSSC (Zalar et al. 2005).

To demonstrate cryptic speciation within the WSSC using GCPSR, we designed primers to amplify other markers. We designed primers for the genes *MCM7*, *RPB*1, *RPB*2, and *TSR*1 yielding amplicons of 603, 610, 738, and 607 bp respectively (Table 2.1). Our primers for *MCM7*, *RPB*1, and *TSR*1 yielded 100% sequencing success, while those for *RPB*2 were successful for 85 of 90 (94%) of the strains.

Table 2.1. Genetic variability of sampled loci.

Locus	# sequences	# unique sequences	Aligned bp	# alignment patterns[a]	# parsimony informative sites[b]	model[c]
ITS	70	50	513	123	39	HKY+G
MCM7	90	57	603	127	74	K80+G
*RPB*1	90	37	610	131	74	K80+G
*RPB*2	85	45	738	89	60	HKY+G
*TSR*1	90	49	607	128	69	HKY+G
Combined	90	NA	3071	598	316	NA

NA = not applicable
[a]RAxML v8.0.20 (Stamatakis 2014) detected the number of alignment patterns
[b]Number of parsimony informative sites were determined by PAUP v4.10b (Swofford 2002)
[c]The best model of sequence evolution was found by running jmodeltest v2.1.4 (Darriba et al. 2012; Guindon and Gascuel 2003)

To compare the resolution of these markers as potential secondary barcodes, we calculated the pairwise distance (p-distance) between all sequences. We then organized these values into two groups: the p-distances obtained from between clade comparisons and those obtained from within clade comparisons according to our species hypothesis. Ranges were graphed for each marker (Figure 2.1). *MCM7*, *TSR*1, and *RPB*1 had high percentages of informative characters per sequenced base (11–12%), while ITS and *RPB*2 were lower at 8%. Additionally, *MCM7*, *TSR*1, and *RPB*1 showed a high mean between clade p-distance (0.053–0.064) while retaining low mean within clade p-distance (0.002–0.003). *RPB*2 had a lower mean between clade p-distance of 0.038 and a comparable mean within clade p-distance of 0.002. Meanwhile, ITS showed the lowest mean between clades p-distance (0.024) while having the highest mean within clades p-distance (0.005). We observed that the within clade and between clades p-distances overlapped for ITS, while these did not overlap for *MCM7*, *RPB*1, *RPB*2, and *TSR*1.

Figure 2.1. Comparison of pair-wise distance (p-distance), alignment length, and parsimony informative characters of each gene. The grey bars show the distribution range of the p-distance within clades while the blue bars show the range of p-distances between clades. The mean p-distances and the number of observations (N) used to calculate each mean are shown. AL = alignment length in base pairs. PIC = number and percentage of parsimony informative characters in the alignment.

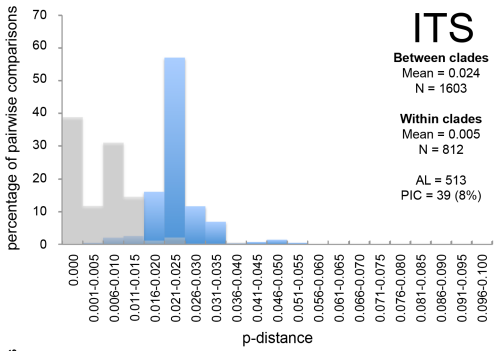
ITS
Between clades
Mean = 0.024
N = 1603
Within clades
Mean = 0.005
N = 812
AL = 513
PIC = 39 (8%)
percentage of pairwise comparisons
p-distance

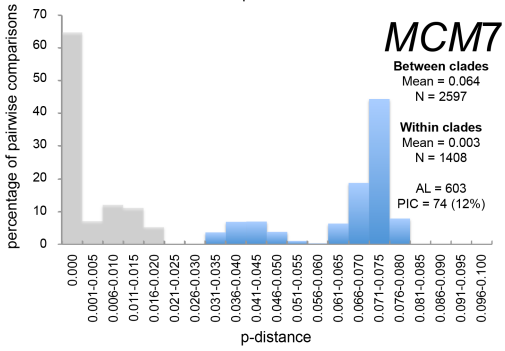
MCM7
Between clades
Mean = 0.064
N = 2597
Within clades
Mean = 0.003
N = 1408
AL = 603
PIC = 74 (12%)
percentage of pairwise comparisons
p-distance

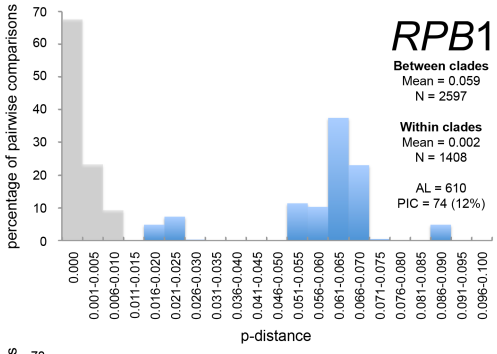
RPB1
Between clades
Mean = 0.059
N = 2597
Within clades
Mean = 0.002
N = 1408
AL = 610
PIC = 74 (12%)
percentage of pairwise comparisons
p-distance

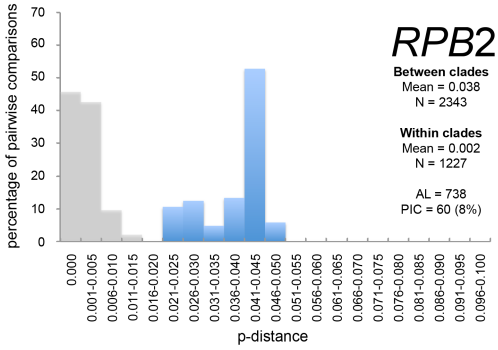
RPB2
Between clades
Mean = 0.038
N = 2343
Within clades
Mean = 0.002
N = 1227
AL = 738
PIC = 60 (8%)
percentage of pairwise comparisons
p-distance

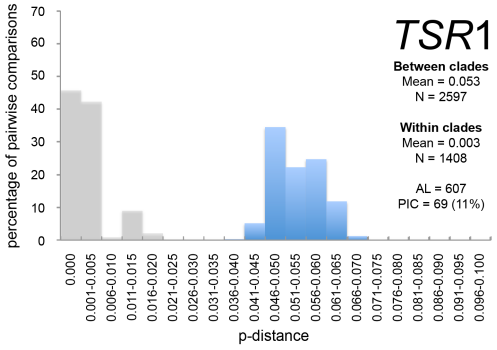
TSR1
Between clades
Mean = 0.053
N = 2597
Within clades
Mean = 0.003
N = 1408
AL = 607
PIC = 69 (11%)
percentage of pairwise comparisons
p-distance

Phylogenetic analysis

The initial neighbor joining (NJ) analysis with concatenated gene sequences revealed four distinct clades near the *W. sebi* neotype, comprising what we call the *W. sebi* complex (WSSC). We provisionally named them *W. sebi* clades 1, 2, 3, and 4. The isolates that made up clade 1 clustered around the neotype strain of *W. sebi* (CBS 818.96). Those comprising clade 2 grouped with the genome sequenced strain of *W. sebi* (CBS 633.66). Clade 3 and 4 were not detected previously (Zalar et al. 2005) and did not group with any strains previously analyzed. The *W. muriae* strains grouped in the clade including the ex-neotype strain of *W. muriae* (CBS 116628).

We formulated species hypotheses based on this initial NJ analysis and designated nodes delineating monophyletic groups, numbered as above, with *W. muriae*, as the species limit. To support these hypotheses, genealogical concordance and monophyly must be demonstrated consistently across multiple loci. We performed single gene phylogenetic analyses with four different methods of phylogenetic reconstruction: NJ, parsimony, maximum likelihood and Bayesian inference. The support values for nodes in each single gene phylogeny are summarized in Supplementary Table 2.4 and Figure 2.2. Concordance for our designated clades was found for all single gene analyses with all four methods of reconstruction, with a few exceptions. The most obvious exception was found in the phylogeny of the ITS locus, where *W. sebi* clade 2 was polytomous instead of monophyletic, as found in the phylogeny of the other four loci. The second exception was that *W. sebi* clade 1 had a low bootstrap support value (51%), but only in the maximum likelihood analysis of the *RPB*2 locus.

Figure 2.2. Single gene phylogenies of ITS, *MCM*7, *RPB*1, *RPB*2 and *TSR*1. The star trees topologies from the Bayesian analyses are illustrated. The black dot shows recovered distinct groups in the strict parsimony analyses and with >80% support values the NJ, maximum likelihood and Bayesian analyses. The grey dot in the *RPB*2 phylogeny marks the node supported by all analyses but with low bootstrap support in maximum likelihood. In each gene, certain nodes internal to our species hypothesis were well supported and these clades are depicted beside each gene tree.

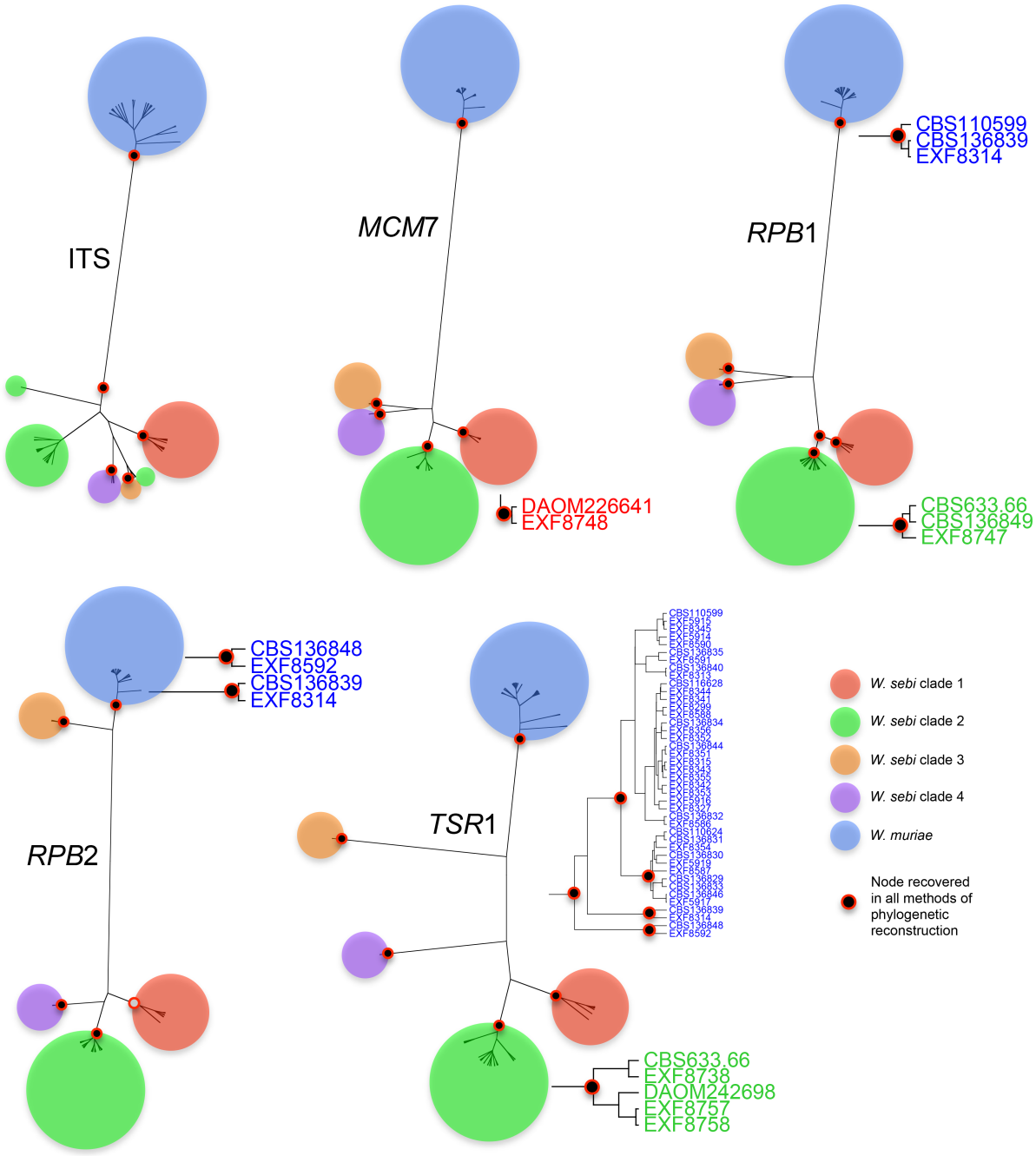
ITS
MCM7
RPB1
RPB2
TSR1
CBS110599
CBS136839
EXF8314
DAOM226641
EXF8748
CBS633.66
CBS136849
EXF8747
CBS136848
EXF8592
CBS633.66
EXF8738
DAOM242698
EXF8757
EXF8758
W. sebi clade 1
W. sebi clade 2
W. sebi clade 3
W. sebi clade 4
W. muriae
Node recovered in all methods of phylogenetic reconstruction

MCM7, *RPB*1, *RPB*2, and *TSR*1 had a higher sequencing success rate than ITS and could easily distinguish *W. sebi* clades 1, 2, 3, and 4. However, as shown in the phylogenies (Supplementary File 2.1), ITS sequences can still recognize *W. muriae* and *W. sebi* clades 1, 3, and 4 but cannot distinguish *W. sebi* clade 2 as a monophyletic group.

We then performed a *BEAST analysis, which combines the information from multiple loci to yield a species tree. The nodes with strong support indicate the location of genealogical concordance, in essence the species limit. We considered nodes strongly supported if they received posterior probabilities (PP) ≥0.95. The *BEAST analysis strongly supported *W. sebi* clades 1, 2, 3, 4 and *W. muriae* as distinct clades. However, the branch length between *W. muriae* and all four *W. sebi* clades was long. Our species hypothesis was supported by the *BEAST analysis, but low posterior probability values were found in the backbone, which represent the confidence that can be applied to the relationships among the four *W. sebi* clades. This was consistent with results from the single gene phylogenies because backbone topologies varied from one gene to the next. The initial NJ tree marked with concordant nodes found across all single gene phylogenies and the *BEAST tree are summarized in Figure 2.3. Supporting these results, the species delimitation analyses in BPP3 consistently reported a posterior probability of 0.99 to 1.00 for the five species (Supplementary File 2.2).

The clinically derived strains (CBS 196.56, EXF-8754, DAOM 226642) were in different clades, and there was no discernable support for a pathogenic clade in the WSSC.

Figure 2.3. Multi-gene phylogenies. A. Neighbour joining tree based on the concatenated alignment. Nodes marked with black dots indicate the concordant groups detected consistently in all 5 genealogies. The grey dots indicate somewhat concordant groups detected 2 out of 5 genealogies. B. The inferred species tree from *BEAST. Posterior probabilities on important backbone nodes and strongly supported nodes (>0.80) are shown on the tree. Long branches were represented by a double break in the line. T = neotype strain, **O** = genome sequenced strain, ✚ = strains reported to cause subcutaneous lesions, ◆ = strain reported to produce metabolites that react to human antibodies.

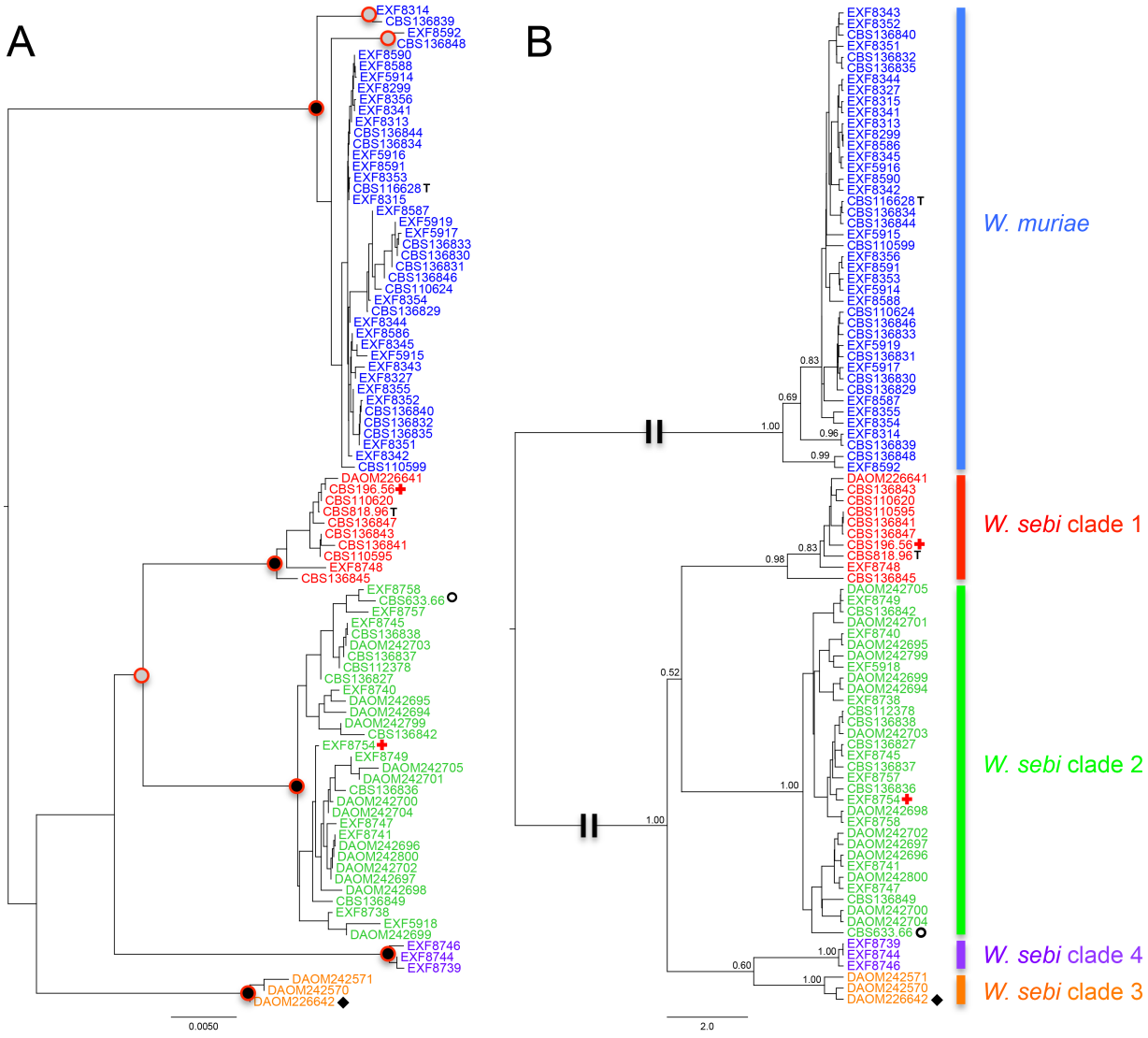
A
EXF8314
CBS136839
EXF8592
CBS136848
EXF8590
EXF8588
EXF5914
EXF8299
EXF8356
EXF8341
EXF8313
CBS136844
CBS136834
EXF5916
EXF8591
EXF8353
CBS116628T
EXF8315
EXF8587
EXF5919
EXF5917
CBS136833
CBS136830
CBS136831
CBS136846
CBS110624
EXF8354
CBS136829
EXF8344
EXF8586
EXF8345
EXF5915
EXF8343
EXF8327
EXF8355
EXF8352
CBS136840
CBS136832
CBS136835
EXF8351
EXF8342
CBS110599
DAOM226641
CBS196.56
CBS110620
CBS818.96T
CBS136847
CBS136843
CBS136841
CBS110595
EXF8748
CBS136845
EXF8758
CBS633.66
EXF8757
EXF8745
CBS136838
DAOM242703
CBS136837
CBS112378
CBS136827
EXF8740
DAOM242695
DAOM242694
DAOM242799
CBS136842
EXF8754
EXF8749
DAOM242705
DAOM242701
CBS136836
DAOM242700
DAOM242704
EXF8747
EXF8741
DAOM242696
DAOM242800
DAOM242702
DAOM242697
DAOM242698
CBS136849
EXF8738
EXF5918
DAOM242699
EXF8746
EXF8744
EXF8739
DAOM242571
DAOM242570
DAOM226642
0.0050
B
EXF8343
EXF8352
CBS136840
EXF8351
CBS136832
CBS136835
EXF8344
EXF8327
EXF8315
EXF8341
EXF8313
EXF8299
EXF8586
EXF8345
EXF5916
EXF8590
EXF8342
CBS116628T
CBS136834
CBS136844
EXF5915
CBS110599
EXF8356
EXF8591
EXF8353
EXF5914
EXF8588
CBS110624
CBS136846
CBS136833
EXF5919
CBS136831
EXF5917
CBS136830
CBS136829
EXF8587
EXF8355
EXF8354
EXF8314
CBS136839
CBS136848
EXF8592
DAOM226641
CBS136843
CBS110620
CBS110595
CBS136841
CBS136847
CBS196.56
CBS818.96T
EXF8748
CBS136845
DAOM242705
EXF8749
CBS136842
DAOM242701
EXF8740
DAOM242695
DAOM242799
EXF5918
DAOM242699
DAOM242694
EXF8738
CBS112378
CBS136838
DAOM242703
CBS136827
EXF8745
CBS136837
EXF8757
CBS136836
EXF8754
DAOM242698
EXF8758
DAOM242702
DAOM242697
DAOM242696
EXF8741
DAOM242800
EXF8747
CBS136849
DAOM242700
DAOM242704
CBS633.66
EXF8739
EXF8744
EXF8746
DAOM242571
DAOM242570
DAOM226642
0.83
0.69
1.00
0.96
0.99
0.83
0.98
0.52
1.00
1.00
1.00
0.60
1.00
2.0
W. muriae
W. sebi clade 1
W. sebi clade 2
W. sebi clade 4
W. sebi clade 3

Geography and haplotype analysis

Often, a single fungal species with an assumed cosmopolitan distribution is shown to be composed of multiple cryptic species that are geographically separated (Dettman et al. 2003). We mapped the approximate geographical origin of our strains, but there was no obvious geographical correlation with clade number (Figure 2.4) among our samples.

To analyze the diversity of sampling, we used a haplotyping approach where each unique sequence (rather than each strain) was grouped. These results are summarized in Supplementary Table 2.3. The concatenated alignment used for haplotyping had 1255 sites, of which 176 were variable. Thirty-one distinct haplotypes were detected. Out of these, 19 were singletons. Overall, the strains that grouped together as a clade in our phylogenetic analyses also grouped together in our haplotype analysis, but the different clades we postulated in our species hypothesis were further dissected. This is expected because a species should have different haplotypes. For example, *W. sebi* clade 1 included five haplotypes, *W. sebi* clade 2 was separated into 18 haplotypes and *W. muriae* had six distinct haplotypes. However, *W. sebi* clade 3 and clade 4 contained single haplotypes, which is an indication that these clades were not well sampled or that they are clonal.

Figure 2.4. Approximate geographic location of our *Wallemia* isolates on the global map. Since most of our sampling came from Europe, the map of Europe is enlarged on the upper right hand corner.

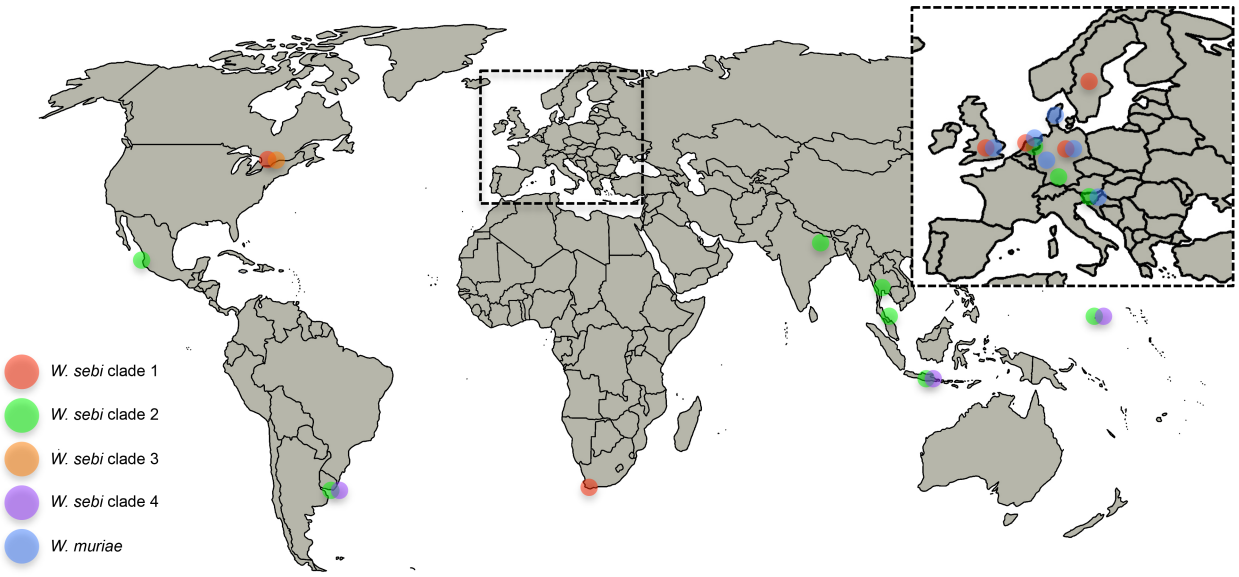
W. sebi clade 1
W. sebi clade 2
W. sebi clade 3
W. sebi clade 4
W. muriae

When we took into consideration the geography of the non-singleton haplotypes, we observed some patterns. Haplotype 1 and 4 are strictly European, haplotype 12 was found only in Micronesia while haplotype 17 and 18 contained a mixture of strains from Indonesia and Thailand, suggestive of a south Asian population. Haplotype 24, also known as *W. sebi* clade 3, included only Canadian strains. However, after adding singleton haplotypes and comparing all haplotypes, geographical ranges overlapped. Haplotype 13 contained a mixture of European and Micronesian strains. Haplotype 16 was also a mixture of strains from India, Indonesia and one strain from the Netherlands. Haplotype 25 corresponded to *W. sebi* clade 4 and it contained several strains from Uruguay, Micronesia and Indonesia. All of our strains identified as *W. muriae* came from Europe, although the species exhibited three different haplotypes.

Discussion

Previous studies suggest that *Wallemia* is a common genus in the indoor environment, with *W. sebi* and *W. muriae* as the dominant species (Amend et al. 2010; Nonnenmann et al. 2012; Sakamoto et al. 1989; Takahashi 1997; Zalar et al. 2005). As shown by our investigation, *W. sebi* and *W. muriae* are the two most common species of *Wallemia* found indoors, confirming previous findings. We did not detect any novel species distantly related to *W. sebi* and *W. muriae sensu* Zalar et al. (2005).

There is unexplained ITS diversity in *W. sebi* that hints at the existence of cryptic species, as suggested previously (Zalar et al. 2005). We were able to

amplify the ITS locus in all species but it often failed to sequence. Fungi can have multiple copies of the ITS in tandem or even located on different chromosomes (Maleszka and Clark-Walker 1993). Because this region is not translated, multiple copies of ITS can evolve differently. However, concerted evolution may reduce infragenomic variation among copies, although some variation still exists (Ganley and Kobayashi 2007; Simon and Weiss 2008). Lindner and Banik (2011) showed that cloned ITS sequences of the same *Laetiporus* species (Polyporales, Basidiomycota) contained variation that could be interpreted as different species in a phylogenetic analysis. We speculate that *W. sebi* and *W. muriae* have multiple copies of the ITS region with high infragenomic variation. This could explain our inability to sequence the ITS marker with a high success rate.

We designed primers to amplify four other DNA markers (*MCM7*, *RPB*1, *RPB*2, and *TSR*1) and then conducted GCPSR-based multilocus phylogenetic analyses to detect cryptic species. We first conducted a neighbor joining phylogenetic analysis from a concatenated alignment to formulate our species hypothesis. Then, we tested genealogical concordance by reconstructing single gene phylogenies using four different methodologies and finally a multi-gene phylogenetic analysis using *BEAST. *Wallemia muriae* cohered as a monophyletic group in all analyses and was found only in Europe. However, this species may be in the early stages of speciation. Two basal clades to the main *W. muriae* group were detected in 2 of 5 genealogies (Figure 2.3A). One of the clades consisted of strains EXF 8314 and CBS 136839 while the other included EXF 8592 and CBS 136848. Based on our data and given that only two strains comprised each clade, we could not see any supporting characters to suggest recognizing these clades as

species at this time. However, four clades of *W. sebi* emerged from the phylogenetic analyses and fulfilled the requirements for phylogenetic species recognition. These clades are genealogically concordant and we found no disagreement. However, the ITS phylogeny did not support *W. sebi* clade 2 as a monophyletic group in any of the phylogenetic reconstructions. The high infragenomic variation allows for a high number of substitutions in a given site in short molecular time, possibly masking the phylogenetic signal, and could explain why *W. sebi* clade 2 was not monophyletic in the ITS phylogeny.

The phylogenetic signal produced from the other four markers (*MCM*7, *RPB*1, *RPB*2, and *TSR*1) is probably more accurate at representing genealogical concordance. Because all four DNA markers showed monophyly of the four clades of *W. sebi,* we suggest they should be recognized as different phylogenetic species. This was supported by our species delimitation analyses with BPP3. Although we used multiple loci to derive our phylogenetic species concept, only one of the four other protein coding markers is necessary to identify a *W. sebi* isolate to clade. Sequencing one other marker in addition to the official fungal barcode ITS would be more practical and economical. The sequence variation between species should exceed the variation within species. In DNA barcoding terms, this is referred to as the barcode gap. Of the four protein coding markers we tested, we recommend *TSR*1 as a secondary marker because of its clear barcode gap (Figure 2.1).

We performed a haplotype analysis to estimate the haplotype diversity within the phylogenetic species. Generally, we did not find a strong link between geography and haplotype (Supplementary Table 2.3), but a pattern may emerge if more strains are studied. However, we observed that *W. muriae* was found strictly in

Europe, *W. sebi* clade 3 was found in regions with temperate climates (Canada Desroches et al. (2014), S. Frasz and D. Miller pers. comm) and Finland (Jančič et al. unpublished)), and *W. sebi* clade 4 was detected in the subtropical countries (Uruguay, Micronesia, and Indonesia). However, *W. sebi* clade 1 and 2 seem to be distributed worldwide. Because of their overlapping ranges, there does not seem to be an indication of allopatric speciation, so these *Wallemia* species likely arose sympatrically or parapatrically from an ancestor population. The overlap in ranges suggests speciation may have occurred following colonization of new niches.

Wallemia sebi was suspected to cause allergies (Kolossa-Gehring et al. 2007; Desroches et al. 2014) and perhaps subcutaneous lesions (Guarro et al. 2008). We did not find any evidence of a pathogenic species or haplotype of *Wallemia*. *Wallemia sebi* DAOM 226642 produces metabolites that react to human antibodies, whereas DAOM 242570 and DAOM 242571 lack compounds that bind to human antibodies (Desroches et al. 2014); all grouped phylogenetically in *W. sebi* clade 3. *Wallemia* is rarely reported as a pathogen and there are too few strains available to reveal any pattern. Its involvement in allergy is still enigmatic and requires further study.

Wallemia species lack striking morphological differences. They are defined by their physiology, especially their abilities to tolerate and grow on ranges of water activities. We describe and provide formal species names for the clades within the WSSC in a companion study (Jančič et al. 2015), confirming the existence of the four phylogenetic species using strains from a broader range of habitats. The companion study uses the phylogenetic species hypotheses from this study to guide

phenotypic assessment resulting in the description of three new species called *W. mellicola*, *W. canadensis*, and *W. tropicalis*.

Acknowledgements

We thank K. Mwange and E. White for performing the dilution-to-extinction plating method on the samples, R. Assabgui and W. McCormick for help with sequencing, Q. Eggertson and C. Spies for advice on Bayesian phylogenetic analyses on the computer cluster, S. Bilkhu for help with Perl scripting, J. Guarro for providing us with the *W. sebi* strain from India and A. Walker and Y. Hirooka for reviewing an earlier draft.

Author contribution

HDTN and KAS conceived and designed the work. HDTN, SJ, MM, and JBT acquired the data: MM provided the *Wallemia* strains from Germany and the Netherlands, MM also provided the strains from the Zalar et al. (2005) study; SJ isolated and provided strains from Slovenia and Denmark; JBT provided the remaining *Wallemia* strains from the larger Sloan house dust study; HDTN designed primers, tested markers, generated all sequences and deposited all data in GenBank; MM, SJ and HDTN deposited *Wallemia* cultures into CBS, EXF and DAOM respectively. HDTN analyzed and interpreted the data. HDTN drafted the article. HDTN, SJ, MM, JBT, PZ, NGC and KAS critically revised the manuscript for important intellectual content.

Chapter 3: *Basidioascus* and *Geminibasidium*: a new lineage of heat resistant and xerotolerant basidiomycetes

Hai D.T. Nguyen[1,2], Nancy L. Nickerson[3], Keith A. Seifert[1,2]

[1] Department of Biology, University of Ottawa, Ottawa, Ontario, Canada K1N 6N5

[2] Biodiversity (Mycology), Eastern Cereal and Oilseed Research Centre, Agriculture and Agri-Food Canada, Ottawa, Ontario, Canada K1A 0C6

[3] P.O. Box 127, Port Williams, Nova Scotia, Canada B0P 1T0

Abstract

Using a heat treatment method, two genera of heat resistant and xerotolerant basidiomycetes were isolated from soil samples. These two genera, *Basidioascus* and *Geminibasidium* gen. nov., are morphologically similar and phylogenetically related. The genus *Basidioascus* was originally described as an ascomycete but the structures originally interpreted as single-spored asci appear to represent basidiospores. Morphologically, both genera are characterized by the lack of a fruiting body, conspicuously granular and deciduous basidia with a unique basal lateral projection, and apparently double walled basidiospores. The basidia, rather than the basidiospores, are forcibly discharged in *Basidioascus* species but not in *Geminibasidium* species. In *Geminibasidium* species, a putative basidium arises from a primary cell. These are novel forms of basidial ontogenesis previously unreported in basidiomycetes. The rDNA (SSU+5.8S+LSU) Bayesian phylogenetic analysis suggests that these fungi are distantly related to *Wallemia*, another xerotolerant basidiomycete genus commonly found in indoor environments, dried foods and natural hypersaline environments. Given the physiological similarity and phylogenetic relationships, *Basidioascus* and *Geminibasidium* are classified in a new order, Geminibasidiales, and are taxonomically assigned to the class Wallemiomycetes. Based on morphological observations and molecular phylogeny of the internal transcribed spacer (ITS), two species of *Basidioascus* (*B. undulatus* and *B. magus* sp. nov.) and two species of *Geminibasidium* (*G. donsium* sp. nov. and *G. hirsutum* sp. nov.) are described. A key to these species is provided using micromorphological and cultural characters.

Keywords

Basidiomycota, deciduous basidium, Geminibasidiaceae, Geminibasidiales, soil fungi, Wallemiomycetes

Introduction

The genus *Basidioascus* was first described by Matsushima (2001) as an ascomycete. The only species, *B. undulatus,* based on one strain, was isolated from the tropical rainforest soil on CMA (corn meal agar) in Cape Tribulation National Park, Queensland, Australia. Unfortunately, the method of isolation was not mentioned. Matsushima (2003) interpreted the fertile structures as single-spored asci, and although he did not mention it in the text, he likely interpreted the basal lateral projections as croziers. His strain of *B. undulatus* also produced a *Geotrichum*-like anamorph in culture. Given these observations, Matsushima concluded that the fungus was an ascomycete, a classification currently followed by the Dictionary of Fungi (Kirk et al. 2008) and Mycobank (Robert et al. 2013). Although the Latin description and microphotographs are precise enough to allow morphological identification of *B. undulatus*, DNA sequences and phylogenetic analysis were lacking.

During surveys for heat resistant fungi in different kinds of soil, we isolated a variety of ascomycetes and basidiomycetes from samples. These samples were collected from various provinces in Canada and from Crater Lake National Park in the United States. By definition, heat-resistant fungi can survive exposure to 75 °C for 30 min (Samson et al. 2000). Among these heat resistant fungi, we isolated

Basidioascus-like strains, including several of an apparently undescribed genus related to *Basidioascus*, which we describe below as *Geminibasidium*.

In this study, we characterized *Basidioascus* and *Geminibasidium* morphologically, physiologically and phylogenetically. We re-interpreted the structures of *B. undulatus* as those of a basidiomycete rather than as an ascomycete. Basidial and basidiospore ontogeny, and colony morphology were detailed and cardinal growth temperatures established. Also, we determined the xerotolerance of some strains using glycerol or sucrose amended media and halotolerance using media supplemented with sodium chloride. Finally, we sequenced the ribosomal operon (SSU, ITS and LSU) of *Basidioascus* and *Geminibasidium* and performed a phylogenetic analysis to determine their phylogenetic position in kingdom Fungi, and in support of the morphological species concept.

Materials and methods

Culture isolation and preservation

Cultures were isolated following the method outlined in Seifert et al. (2004). Briefly, soil samples were suspended in a 0.1% (w/v) proteose peptone solution and exposed to 75 °C for 30 min in a water bath. A 1 mL aliquot of the sample was mixed with 20 mL of molten chloramphenicol (40 mg/L) potato dextrose agar (PDA, Difco) and dispensed in 9 cm polystyrene Petri dishes in three replicates. Petri dishes were sealed and incubated upright at room temperature (approximately 22 °C) under ambient light conditions. Cultures were deposited in the Canadian

Collection of Fungal Cultures, Agriculture and Agri-Food Canada (DAOM/CCFC) and at the Centraalbureau voor Schimmelcultures, Fungal Biodiversity Centre in Utrecht, The Netherlands (CBS) (Supplementary Table 3.1).

Morphological studies

To study micromorphology, observations were made from cultures on corn meal agar (CMA, Acumedia) mounted in 85% lactic acid. Digital photographs were taken with an Evolution MP digital microscope camera on an Olympus BX50 compound microscope, using ImagePro 6.0 software (Media Cybernetics, Bethesda, Maryland). Measurements were carried out using ImagePro 6.0 with means and standard errors calculated in Microsoft Excel.

To assess colony morphology and sizes, strains were grown on 2% malt extract agar (MEA: 20 g Bacto malt extract (Difco Laboratories, Sparks, USA); 15 g agar (EMD Chemicals Inc., Gibbstown, USA); 1000 mL distilled water), dichloran 18% glycerol agar (DG18: Oxoid Ltd, Hampshire, UK) (Samson et al. 2010) and malt yeast 40% sucrose agar (M40Y: 20 g Bacto malt extract (Difco Laboratories, Sparks, USA); 5 g Bacto yeast extract (Difco Laboratories, Sparks, USA); 400 g of sucrose (EMD Chemicals Inc., Gibbstown, USA); 15 g agar (EMD Chemicals Inc., Gibbstown, USA); 1000 mL distilled water). The cultures were incubated upright at room temperature. Colony diameter was measured after one week. Photographs of the colonies were taken after two weeks using an iPhone 4S camera. To check for arthroconidial anamorphs, type strains (*B. undulatus* DAOM 241956, *B. magus* DAOM 241948, *G. donsium* DAOM 241966 and *G. hirsutum* DAOM 241969) were grown in 2% malt broth at room temperature for one week on a rotary shaker, then a 20 µL aliquot of the liquid culture was observed microscopically. To test for forcibly

discharged basidia or basidiospores, type strains (listed above) were inoculated on CMA in Petri dishes with glass slides taped to the lid. After 5 d of incubation in the upright position, the slides were checked under the microscope for structures shot from the colony onto the lid.

The SEM photomicrograph was prepared by Susan Carbyn, Paula Allan-Wojtas and Milos Kalab using standard techniques.

Physiological studies

To test xerotolerance and halotolerance, the type strains (listed above) were grown on malt yeast agar (MYA) as a basal medium (Wheeler et al. 1988), with increasing amounts of controlling solutes (NaCl, glycerol and sucrose) to achieve water activities ranging from 1.00 to 0.77. Amounts of solutes were estimated from previous studies (P. Zalar pers. comm., A. Patriarcia pers. comm., see Supplementary Table 3.2). MYA was first prepared without agar, and after addition of solutes to MYA, the pH was adjusted to 7.0 with NaOH or HCl. Then agar was added and the media were sterilized for 20 min. Strains were inoculated on the 6 cm agar polystyrene Petri dishes in three replicates for each treatment. Petri dishes were incubated upright at room temperature for 28 days. Photographs were taken using an iPhone 4S camera every 7 days. Images were imported into the program ImageJ (Schneider et al. 2012) where the colony diameter was measured in proportion to the known diameter of the Petri dish. Growth diameters were averaged and data were compiled in Microsoft Excel.

To determine the cardinal temperatures, type strains (listed above) were inoculated on MYA and M40Y in triplicate. The strains were incubated at 5 °C, 10 °C, 15 °C, 20 °C, 25 °C, 30 °C, 35 °C, 37 °C, and 40 °C for one week. Photographs

were taken using an iPhone 4S camera. Images were imported into ImageJ (Schneider et al. 2012) for diameter measurement as described above.

DNA extraction, PCR, Sequencing

The UltraClean Microbial DNA Isolation kit (MO BIO Laboratories Inc., Carlsbad, California) was used for DNA extraction following the manufacturer's instructions. To amplify the ITS region, the primer combination ITS5 and ITS4 or ITS1 and ITS4 (White et al. 1990) were used. Primers ITS1, ITS4 and ITS5 were used as sequencing primers with primers ITS2 and ITS3 as internal sequencing primers if required. The SSU region was amplified using primers NS1 and ITS2. The primers NS1, NS2, NS3, NS4, NS5 and NS8 (White et al. 1990) were used as sequencing primers for the SSU region. The LSU region was amplified using primers LR0R and LR8, with LR0R, LR3R, LR6, LR7R, LR7, and LR8 used as sequencing primers (Vilgalys and Hester 1990).

To amplify DNA, a PCR master mix consisting of 0.1 mM dNTP's, 0.08 µM forward primer, 0.08 µM reverse primer, 1X Titanium Taq buffer (Clontech, Mountain View, California), 0.5X Titanium Taq enzyme (Clontech, Mountain View, California) and 1.00 µL of DNA template mixed in sterile water totaling 10 µL per reaction was prepared. The following PCR profile was used for SSU, LSU and ITS amplifications: 95 °C for 3 min (initial denaturation), then 35 cycles at 95 °C for 1 min (denaturation), 56 °C for 45 s (annealing), 72 °C for 1.5 min (extension), followed by 72 °C for 10 min (final extension). PCR products were checked by agarose gel electrophoresis and sequenced with Big Dye Terminator (Applied Biosystems, Foster City, California).

Phylogenetic analysis

Sequences were assembled and edited using SeqMan II v8.0 (DNA Star Inc., Madison, Wyoming). BLAST analyses were performed with SSU, LSU and ITS sequences to verify their homology with other fungal SSU, LSU and ITS sequences. All sequences were deposited in GenBank (Supplementary Table 3.1). Sequences of each gene were aligned using MAFFT v5 (Katoh et al. 2005). These alignments were trimmed using BioEdit v7.2.2 (Hall 1999). Alignments were deposited in TreeBASE (www.treebase.org/treebase/), study accession no. S13396.

All molecular phylogenies were determined by Bayesian inference. To select the most appropriate model of sequence evolution, MrModeltest v2.2.6 (Nylander 2004) was applied on each gene (ITS, SSU, LSU and 5.8S) and the model was chosen according to the Akaike Information Criterion (AIC). The GTR+I+G model was selected for SSU and LSU, SYM+I+G was chosen for 5.8S and GTR+G model was adopted for ITS. Prior to Bayesian analysis, the SSU, 5.8S and LSU matrices were concatenated with Seaview v4.4.2 (Gouy et al. 2010). Bayesian inference was performed with MrBayes v3.2 (Ronquist et al. 2012). Two independent Markov Chain Monte Carlo (MCMC) runs were performed simultaneously. Each MCMC ran for 5.0×10^6 generations for the rDNA analysis and 2.0×10^6 generations for the ITS analysis, sampling every 500 generations. The first 25% of trees were discarded as burn-in, the remaining trees (15002 trees for rDNA and 6002 trees for ITS) were kept and combined into one consensus tree with 50% majority rule consensus.

Consensus trees in Newick format were imported into TreeView X (Page 1996) and exported as SVG vector graphics for figure assembly in Adobe Illustrator CS5 and Adobe Photoshop CS5.

Results

Isolation

Basidioascus strains were isolated from soils collected at Crater Lake National Park, Oregon USA, and from soils collected from Ontario, British Columbia, Alberta, Nova Scotia, and Manitoba in Canada. We isolated nine strains of *B. undulatus*, nine strains of *B. magus*, and three strains of *Basidioascus* sp. that we are not naming because we could not find distinguishing morphological characters. *Geminibasidium* species were isolated from soils collected in British Columbia and Nova Scotia, Canada. We isolated three strains of *G. donsium* and two strains of *G. hirsutum*. These fungi were found in soil from forests, grasslands and blueberry fields, many of which had been exposed to deliberate or accidental burning (Supplementary Table 3.1).

Colony size and morphology

Basidioascus undulatus grew faster than *B. magus* and *G. hirsutum* grew faster than *G. donsium*. Generally, colonies of *Basidioascus* species are white and those of *Geminibasidium* species are pink. On MEA, *B. undulatus* colonies are uniform whereas those of *B. magus* appear stellate. The convex rosette growth of *B. undulatus* differentiates it from the flat, sulcate pattern of *B. magus* on DG18. It was difficult to differentiate *B. undulatus* and *B. magus* on M40Y because both species have a flat white appearance. On MEA, *G. donsium* colonies are pink and *G. hirsutum* colonies are beige. On M40Y and DG18, it was difficult to distinguish *G. donsium* and *G. hirsutum* because both produce pink colonies. There are many slight variations in colony appearance among our strains.

Development of basidia and basidiospores

In *Basidioascus* species, a small basidium develops laterally or terminally on somatic hyphae and matures to a larger clavate basidium. Basidia are deciduous and forcibly discharge at maturity. These basidia produce symmetrical basidiospores attached by tubular sterigmata resembling those of some gasteromycetes basidia and basidiospores. The basidiospores of *B. undulatus* and *B. magus* are subglobose, brown and have a thick wavy wall. Generally, *B. undulatus* produces basidia and basidiospores larger than those of *B. magus*.

In *Geminibasidium* species, a basidium-bearing cell (primary cell) develops on terminal and lateral branches of somatic hyphae. The primary cell is attached to hyphae by a thin tubular connector (Figure 3.3P and Figure 3.5M). Over time, a basidium develops on the apical portion of the primary cell. The globose and brown basidiospores in *G. donsium* are slightly verrucose, whereas they are hirsute in *G. hirsutum*. We saw no evidence that either the basidia or basidiospores of *Geminibasidium* species were forcibly discharged.

Both *Basidioascus* and *Geminibasidium* species have conspicuously granular basidia with a basal lateral projection. The basal lateral projection refers to a small protrusion that is found near the base of the basidium in *Basidioascus* species and near the base of the basidium-bearing cell (primary cell) in *Geminibasidium* species. These basal lateral projections sometimes resemble clamp connections (Figure 3.1B and Figure 3.2D) but they are not attached to the subtending cell; they collapse as basidia mature in *Basidioascus* species, but not in *Geminibasidium* species.

Arthroconidia

Only *B. undulatus* produces an arthroconidial, *Geotrichum*-like anamorph. Arthroconidia are produced both in liquid culture and on agar. In liquid culture, arthroconidia are predominant and are perhaps analogous to a yeast form of *B. undulatus*. Type strains of *B. magus*, *G. donsium* and *G. hirsutum* did not produce arthroconidia in liquid cultures or on agar.

Phylogenetic analysis

To determine the relationships of *Basidioascus* and *Geminibasidium* in relation to other basidiomycetes, a Bayesian phylogenetic analysis with combined SSU, 5.8S, and LSU genes was performed with selected sequences from the AFTOL (Assembling the Fungal Tree of Life) project and other sequences from GenBank (Figure 3.6 and see Supplementary Table 3.3). The GenBank accession numbers for these sequences are listed in Supplementary Table 3.1. The results show that *Basidioascus* and *Geminibasidium* are related sister groups with a posterior probability of 0.93. They reside at the base of Agaricomycotina and are related to *Wallemia* on a long branch supported by a posterior probability of 1.00.

A Bayesian phylogenetic analysis of the ITS was performed to delimit species in support of our morphological observations (Figure 3.7). Full ITS sequences from *Basidioascus* and *Geminibasidium* are roughly 600 bp long. BLAST searches with our ITS sequences detected several unidentified but related soil environmental sequences and we included these in our ITS analysis. Further information on these environmental sequences can be found in Supplementary Table 3.4. Representatives from Cystofilobasidiales and Wallemiales were chosen to root the tree because they are the most closely related known groups according to our rDNA

phylogenetic analysis. The ITS phylogeny shows that both *Basidioascus* and *Geminibasidium* are monophyletic. The posterior probability at the node grouping strains of *B. magus* is 1.00, *B. undulatus* is 0.98, *G. donsium* is 1.00 and *G. hirsutum* is 0.99. The ITS tree shows a polytomous phylogenetic delimitation between *B. undulatus* and *B. magus* and a dichotomous phylogenetic delimitation between *G. donsium* and *G. hirsutum*.

The strains identified as *Basidioascus* sp. (DAOM 241960, DAOM 241965, and DAOM 241957) did not group with *B. undulatus* and *B. magus* type strains phylogenetically. Two environmental sequences from GenBank (sequences FN397319 and EU626069) form a strongly supported clade of 1.00. The environmental sequences that are phylogenetically near *Geminibasidium* make up at least 4 phylogenetic clades composed of various GenBank sequences from Italy, USA, Canada, Japan and Guyana. The sequence named Kikoku was from a fungal contaminant isolated in Japan. This contaminant was isolated from imported frozen Canadian blueberries destined for jam production (Y. Kikoku pers. comm.). This sequence groups with *G. donsium*.

Physiology

Basidioascus and *Geminibasidium* species are able to grow on low water activity media such as DG18 and M40Y. As such, they are xerotolerant like *Wallemia* species (their closest known relative). To test the xerotolerance of *Basidioascus* and *Geminibasidium* species, neutral pH MYA was mixed with varying amounts of glycerol or sucrose (Figure 3.8). The fastest colony growth occurred within the first week. Over the range of water activities tested, *Basidioascus* and *Geminibasidium* species grew faster in a_w=1.00 in the first week. However, from the

second to the fourth week, they grew better under lower water activities adjusted by glycerol and sucrose. For example, the peak growth diameter for *B. undulatus*, *B. magus*, *G. donsium* and *G. hirsutum* in a glycerol gradient occurred at a_w=0.98 after 4 weeks. The peak growth in the sucrose gradient occurred at a_w=0.95 for *B. undulatus* and *B. magus*, a_w=0.90 for *G. donsium*, and a_w=0.98 for *G. hirsutum*.

To test the halotolerance of *Basidioascus* and *Geminibasidium* species, neutral pH MYA was mixed with varying amounts of NaCl (Figure 3.8). *Basidioascus undulatus* can tolerate the most salt (up to 2.3 M or 13.5% (w/v)) whereas *B. magus* could not tolerate any salt. Both *G. donsium* and *G. hirsutum* tolerate a low amount of salt (up to 0.6 M or 3.5% (w/v)).

To test the cardinal temperatures, type cultures of *Basidioascus* and *Geminibasidium* species were grown on MYA and M40Y (Figure 3.9). Generally, *Basidioascus* and *Geminibasidium* are mesophilic. The optimum growth temperature on MYA medium for *B. undulatus* is between 25 °C and 30 °C; *B. magus* is 25 °C; *G. donsium* and *G. hirsutum* is 30 °C. The optimum growth temperature on M40Y for *B. undulatus*, *B. magus* and *G. donsium* is 30 °C while it is 37 °C in *G. hirsutum*. Interestingly, *B. undulatus*, *G. donsium* and *G. hirsutum* are all able to grow at 37 °C to some extent on MYA and M40Y.

Taxonomy

Wallemiomycetes P. Zalar, G.S. de Hoog and H.-J.Schroers, emend H.D.T. Nguyen, N.L. Nickerson and Seifert

MycoBank MB 501496

Description. Class of xerotolerant and halotolerant basidiomycetes. Basidiomata are absent; basidiospores are produced by some genera. Arthroconidial or basauxic anamorphs are produced in some species. This class is the earliest diverging lineage of Agaricomycotina based on analyses of combined SSU, 5.8S and LSU ribosomal RNA, as well as amino acid analysis of 71 protein-coding genes.

Type order. Wallemiales*.*

Notes. This description was emended by the addition of information on teleomorphs and more precise information on the phylogenetic position of Wallemiomycetes based on genome sequences.

Geminibasidiales H.D.T. Nguyen, N.L. Nickerson and Seifert ord. nov.

MycoBank MB 801330

Description. Basidiomata are absent. Basidia are produced singly or in clusters, perhaps representing incipient or vestigial fruiting bodies, arise singly from somatic hyphae or from swollen basidium bearing cells (primary cells), and have granular cellular contents. A basal lateral projection occurs either on the basidium or the swollen primary cell supporting the basidium. The basidia, or the basidia attached to the swollen primary cell, are deciduous or forcibly discharged before basidiospores begin to develop. One sterigma, or sometimes more than one sterigma, arises randomly over the apical two thirds of the surface of the detached basidium. Only one mature basidiospore develops per basidium. Basidiospores are symmetrical on sterigma, not forcibly discharged, initially hyaline, dark brown when mature, with an apparent double wall. Basidia lose their cytoplasm and sometimes collapse as basidiospores mature. Arthroconidial anamorphs are sometimes produced.

Species of the Geminibasidiales are heat resistant and xerotolerant. Analyses of combined SSU, 5.8S and LSU ribosomal RNA suggest a sister relationship to the Wallemiales and a basal phylogenetic position in the Agaricomycotina.

Type family. Geminibasidiaceae.

Geminibasidiaceae H.D.T. Nguyen, N.L. Nickerson and Seifert fam. nov.

MycoBank MB 801331

Description. Conforming to the diagnosis of the order Geminibasidiales given above.

Type genus. Geminibasidium.

Basidioascus Matsush., emend H.D.T. Nguyen, N.L. Nickerson and Seifert

MycoBank MB 28558

Description. Basidia are produced singly or in clusters, arise singly from somatic hyphae, and have granular cellular contents and a basal lateral projection. The basidia are forcibly discharged before basidiospores begin to develop. One sterigma, and in one species more than one sterigma arise randomly over the apical two thirds of the surface of the detached basidium. Only one mature basidiospore develops per basidium. Basidiospores are symmetrical on sterigma, not forcibly discharged, initially hyaline, dark brown when mature with an apparent double wall. Basidia lose their cytoplasm and sometimes collapse as basidiospores mature. Arthroconidial anamorphs are produced in one species. Species of *Basidioascus* are heat resistant and xerotolerant. Analyses of SSU, 5.8S and LSU ribosomal RNA suggest a sister relationship to *Geminibasidium*.

Etymology. Basidioascus = basidia behaving like asci.

Type species. Basidioascus undulatus.

Notes. The genus *Basidioascus* was first described by Matsushima (2001) as an ascomycete. However, it was ineffectively published on CD-ROM only. To legitimize this name, the information on the CD-ROM was subsequently published in hard copy in 2003 and distributed to the biosystematics libraries of Agriculture and Agri-Food Canada, Ottawa and CABI Bioscience, Egham, UK (S. Redhead pers. comm.). This description was emended by the morphological reinterpretation of *Basidioascus* as a basidiomycete rather than an ascomycete, information on physiological characters and the addition of phylogenetic data on its relationship with *Geminibasidium*.

Basidioascus undulatus Matsush., Matsushima Mycological Memoirs 10:98 (2003)[2001]

MycoBank MB 374219

Figure 3.1

Etymology. undulatus = basidiospores with wavy wall.

Figure 3.1. *Basidioascus undulatus* DAOM 241956 ontogenesis and colonies. A–C. Granular basidia with a basal lateral projection develop on hyphae and over time mature into a clavate basidium. D–E. The basidia then become deciduous and are detached from hyphae. F–J. One or more than one basidiospore, attached by sterigmata, develop on the basidia. K. More than one immature basidiospore can develop on a basidium, but only one basidiospore matures and the other basidiospores are aborted. K–N. Basidia lose their cytoplasm and sometimes collapse as basidiospores mature. O. Clusters of basidiospores are often seen in one-month-old cultures. P. Slender arthroconidia occur in cultures on agar. Q. Oval arthroconidia are prevalent in liquid culture. R. Colonies of *B. undulatus* on MEA, M40Y and DG18 after 2 weeks incubation at room temperature. Scale bar = 20 μm for panels A–Q.

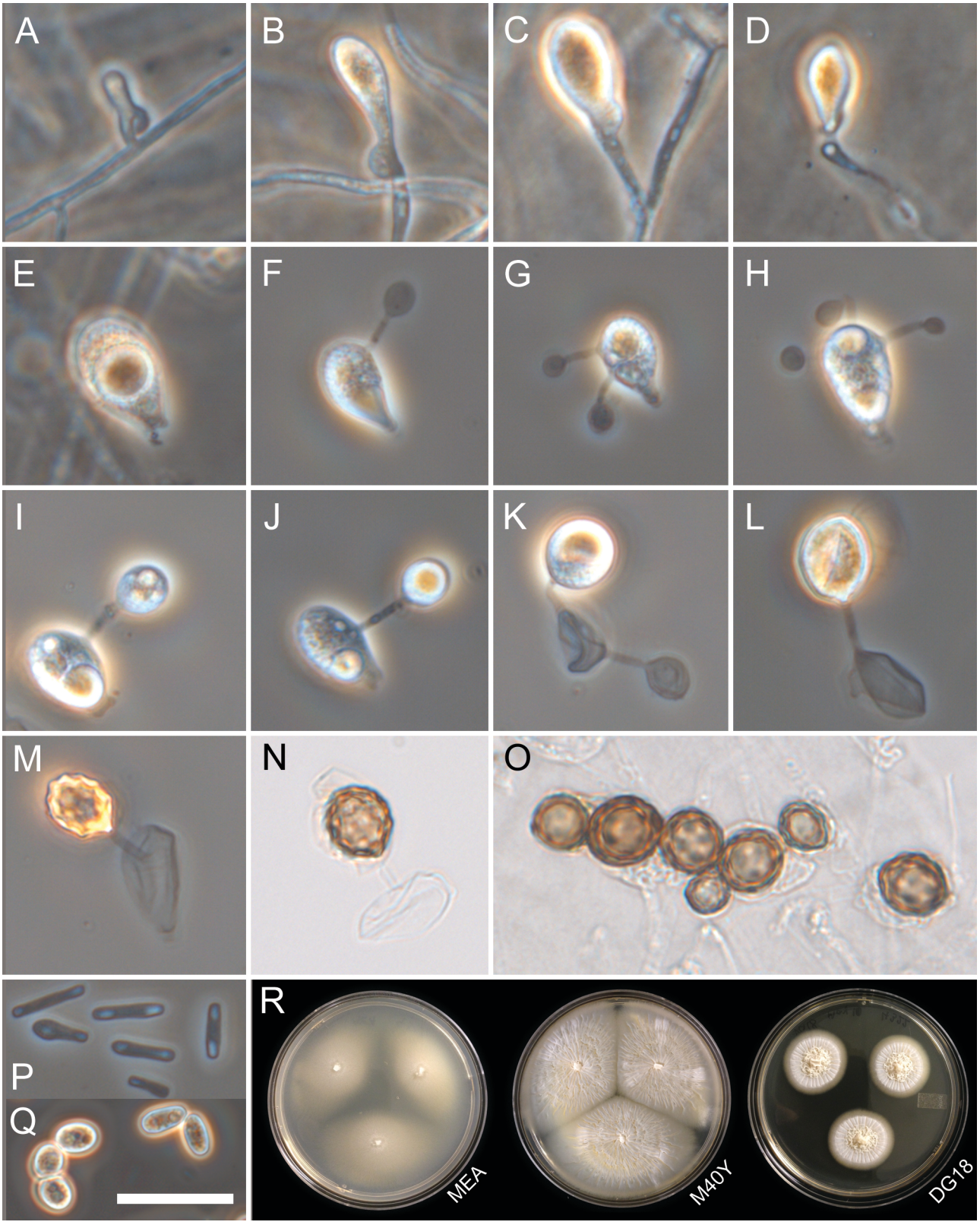
A
B
C
D
E
F
G
H
I
J
K
L
M
N
O
P
Q
R
MEA
M40Y
DG18

Description.

Colonies grow to a diameter of 2.6–3.4 cm (mean ± SE = 3.0 ± 0.1 cm) on MEA, 2.3–3.3 cm (mean ± SE = 2.9 ± 0.1 cm) on M40Y and 1.2–1.7 cm (mean ± SE = 1.4 ± 0.1 cm) on DG18 after 1 week at room temperature. The surface of the colony on CMA is glandular in texture because basidia form basidiospores on the surface of the agar. After 2 weeks on MEA: colonies are planar, uniform, white-beige with diffuse margins; on M40Y, colonies are flat and sulcate/velvet, white with diffuse margins; on DG18, colonies are convex and form a rosette pattern in the center, white, with diffuse margins.

Basidia are at first clavate on terminal and lateral branches of hyphae. Over time, basidia expand and mature into obovate basidia. Mature basidia are 12.5–17.5 × 8.0–11.0 µm (mean ± SE = 15.1 ± 0.6 × 9.6 ± 0.3 µm), deciduous, forcibly discharged, with cell contents conspicuously granular, often with a basal lateral projection that eventually collapses. Mature basidia are visible as early as three to four days.

More than one basidiospore can develop on a basidium but only one basidiospore develops to maturity and the other basidiospores are aborted. Basidia lose their cytoplasm and sometimes collapse as basidiospores mature. Basidiospores are subglobose, hyaline brown to brown, have thick, wavy, verrucose walls, 9.5–12.5 × 8.0–10.0 µm (mean ± SE = 11.1 ± 0.3 × 8.7 ± 0.2 µm). Basidiospores can be observed after seven days. In one month old cultures, clusters of basidiospores encased in a gelatinous matrix (presumed to be remnants of basidia) can be observed.

On one month old cultures on agar, arthroconidia, 6.0–12.0 × 1.5–3.0 µm (mean ± SE = 8.0 ± 0.4 × 2.1 ± 0.1 µm) usually attached in chains, are produced above the surface of the agar. In shaking malt extract broth culture, oval arthroconidia, 4.5–8.0 × 3.0–7.0 µm (mean ± SE = 6.8 ± 0.2 × 4.4 ± 0.2 µm) are produced in chains.

Epitype (designated here). *B. undulatus* DAOM 241956; dried culture on CMA (October 2012) of an isolate from soil, Manitoba, Canada; living culture deposited at Canadian Collection of Fungal Cultures in Ottawa, Canada as DAOM 241956.

Strains examined. DAOM 241956 (epitype), 241958, 241959, 241961, 241962, 241963, 241964, 242122, 229809 (Supplementary Table 3.1).

Holotype. *B. undulatus* MFC-21004; isolated from soil at Cape Tribulation National Park, Australia (Matsushima 2003).

Notes. The production of arthroconidia, presence of abortive basidiospores, and ability to grow in MYA with sodium chloride concentrations up to 2.3 M or 13.5% (w/v) are diagnostic characteristics of *B. undulatus*. Despite repeated attempts to confirm the existence of a holotype for this species, we received no response from T. Matsushima, but are aware that much of his collection was destroyed in the great Hanshin earthquake of 1995. Thus, the holotype of *B. undulatus* (MFC-21004) was not obtained for this study and probably no longer exists; however, until this can be confirmed we feel it would be inappropriate to designate Matsushima's published illustrations as lectotype, and assign our epitypification to the holotype. We initially identified our strains as *B. undulatus* because they produced arthroconidia. Strains of *B. magus* (described below) do not produce arthroconidia and therefore they cannot represent *B. undulatus* sensu Matsushima. Clamp connections are present

on some septa of *B. undulatus* according to Matsushima (2003), but we have not observed them.

Basidioascus magus H.D.T. Nguyen, N.L. Nickerson and Seifert sp. nov.

MycoBank MB 801332

Figure 3.2

Etymology. magus = wizard. The name refers to Wizard Island at Crater Lake National Park where the type strain was isolated.

Diagnosis. Colonies are white on M40Y and DG18. Sporulation occurs on CMA. Granular basidia are 9.5–14.5 × 6.5–10.5 µm, often found with a basal lateral projection, obovate or cylindrical when mature, and produce one mature basidiospore. Basidiospores are brown, 8.0–11.0 × 6.5–8.5 µm, and have wavy, verrucose, and double wall. Arthroconidia are not produced.

Description.

Colonies grow to a diameter of 1.4–2.5 cm (mean ± SE = 1.9 ± 0.1 cm) on MEA, 1.8–2.9 cm (mean ± SE = 2.3 ± 0.1 cm) on M40Y and 0.7–1.5 cm (mean ± SE = 1.1 ± 0.1 cm) on DG18 after 1 week at room temperature. The surface of the colony on CMA is glandular in texture because basidia form basidiospores on the surface of the agar. After 2 weeks on MEA: colonies are planar, stellate, white-beige, with diffuse margins; on M40Y, colonies are flat, uniform, white with diffuse margins; on DG18, colonies are flat and sulcate, white with diffuse margins.

Basidia are at first clavate on terminal and lateral branches of hyphae. Over time, basidia expand and mature into obovate or cylindrical basidia. Mature basidia are 9.5–14.5 × 6.5–10.5 µm (mean ± SE = 12.2 ± 0.7 × 7.9 ± 0.5 µm), deciduous,

forcibly discharged, with cell contents conspicuously granular, often with a basal lateral projection that eventually collapses. Mature basidia are visible after five days.

One basidiospore on a sterigma grows out from the detached basidium. Basidia lose their cytoplasm and sometimes collapse as basidiospores mature. Basidiospores are subglobose, hyaline brown to brown, and have a thick, wavy, verrucose walls, 8.0–11.0 × 6.5–8.5 µm (mean ± SE = 9.6 ± 0.4 × 7.6 ± 0.2 µm). Basidiospores can be observed after seven days. In one month old cultures, clusters of basidiospores encased in a gelatinous matrix (presumed to be remnants of basidia) can be observed.

Arthroconidia are not produced by any of the *B. magus* strains observed.

Holotype. *B. magus* DAOM 241948; dried culture on CMA (October 2012) of an isolate from soil on Wizard Island at Crater Lake National Park, Oregon, United States. (42°56'N 122°08'W, 1900 m altitude).

Strains examined. DAOM 241948 (ex-type), 241949, 241950, 241951, 241952, 241953, 242123, 241954, 241955 (Supplementary Table 3.1).

Notes. The characters that most readily differentiate *B. magus* from *B. undulatus* are the absence of arthroconidia, the absence of abortive basidiospores, and its limited ability to grow in the presence of sodium chloride.

Figure 3.2. *Basidioascus magus* DAOM 241948 ontogenesis and colonies. A–E. Granular basidia with basal lateral projection develop on hyphae and over time mature into obovate or cylindrical basidia. E–G. The basidia then become deciduous and are detached from hyphae. G–O. A single basidiospore arises from the basidium on a sterigma. K–O. Basidia lose their cytoplasm and sometimes collapse as the developing basidiospore matures. P–Q. A cluster of basidia gives rise to a cluster of basidiospores over time. R. Colonies of *B. magus* on MEA, M40Y and DG18 after 2 weeks incubation at room temperature. Scale bar = 20 µm for panels A–Q.

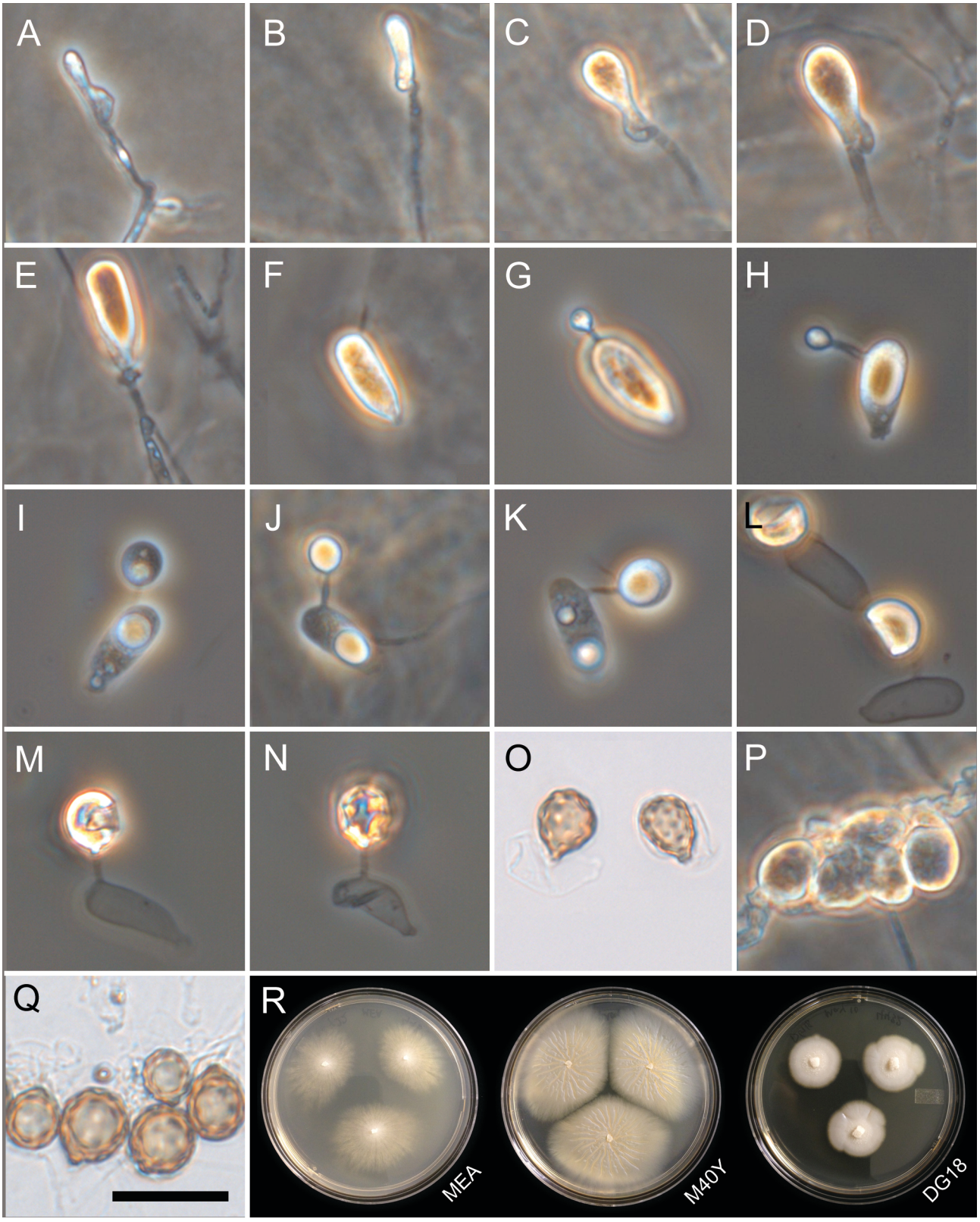
A
B
C
D
E
F
G
H
I
J
K
L
M
N
O
P
Q
R
MEA
M40Y
DG18

Geminibasidium H.D.T. Nguyen, N.L. Nickerson and Seifert gen. nov.

MycoBank MB 801333

Description. Basidia are produced singly or in clusters, arise from swollen basidium bearing cells (primary cells), and have granular cellular contents. A basal lateral projection occurs on the swollen primary cell supporting the basidium and does not collapse during maturation. The basidia attached to the primary cells are deciduous before basidiospores begin to develop. One sterigma, or in one species a series of swollen cells attached by sterigma-like connectors, arise randomly over the apical two thirds of the surface of the putative basidium. Only one mature basidiospore develops per basidium. Basidiospores are symmetrical on sterigma, not forcibly discharged, initially hyaline, brown when mature with an apparent double wall. Basidia lose their cytoplasm and sometimes collapse as basidiospores mature. Species of *Geminibasidium* are heat tolerant and xerotolerant. Analyses of SSU, 5.8S and LSU ribosomal RNA suggest a sister relationship to *Basidioascus*.

Etymology. Geminibasidium = twin basidium. The name refers to the basidium bearing cell (primary cell) and its attached basidium.

Type species. Geminibasidium donsium.

Geminibasidium donsium H.D.T. Nguyen, N.L. Nickerson and Seifert sp. nov.

MycoBank MB 801334

Figures 3.3–3.4

Etymology. donsium was named after Don Brisson who is a good friend of the first author.

Figure 3.3. *Geminibasidium donsium* DAOM 241966 ontogenesis and colonies. A–D. Granular basidium bearing cells (primary cells), with a basal lateral projection, develop on hyphae and over time become swollen and irregular. E–F. Basidia arise from the apex of the primary cells. G–L. Basidia produce a chain of swollen cells with sterigma-like connectors with the terminal swollen cell becoming a mature basidiospore. M. Mature basidiospores are brown and have slightly verrucose walls. N–O. Basidiospores in clusters can be found in one month old cultures. P. The basidium is attached to hyphae by a thin connector. Q. Colonies of *G. donsium* on MEA, M40Y and DG18 after 2 weeks incubation at room temperature. Scale bar = 20 µm for panels A–P.

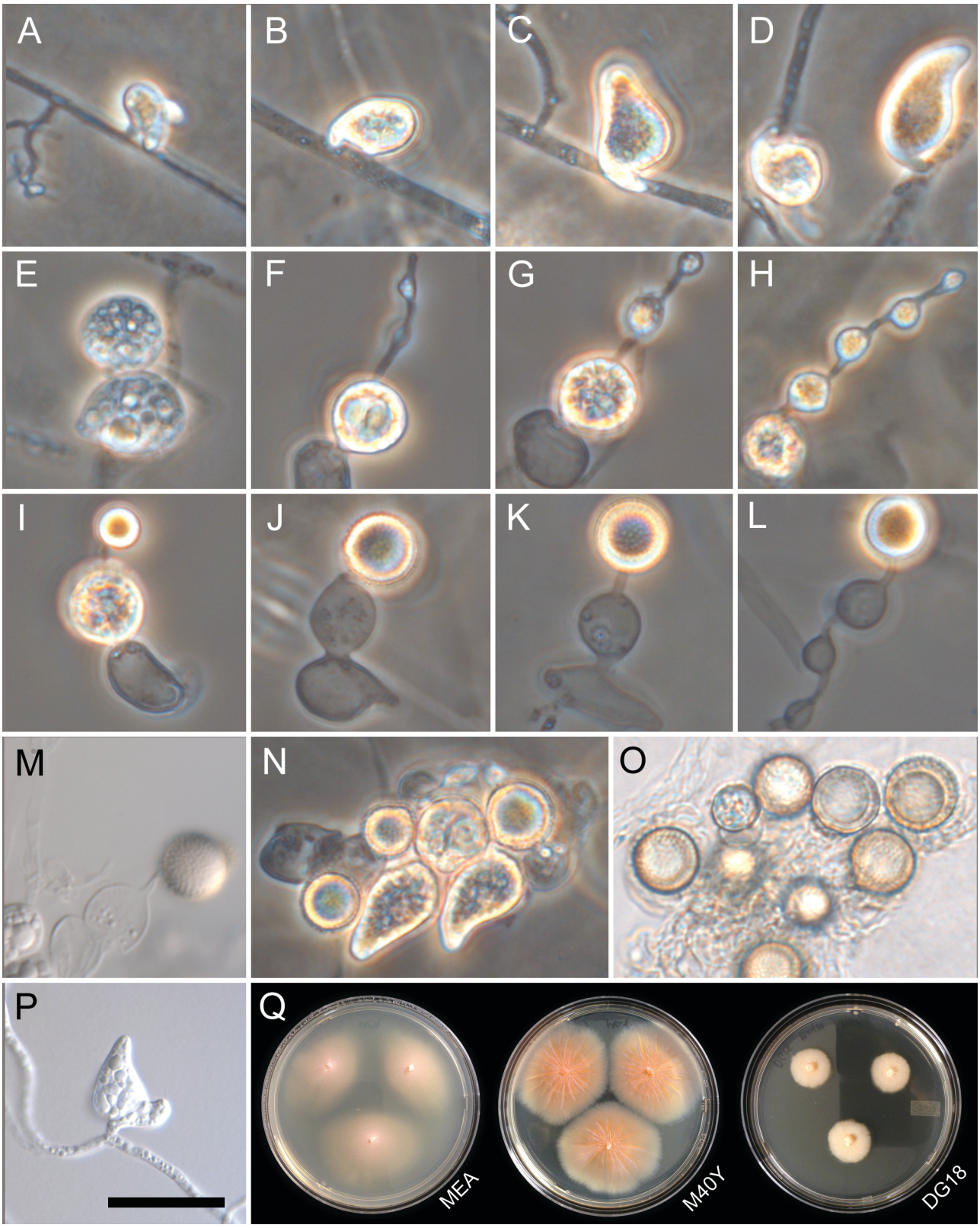
A
B
C
D
E
F
G
H
I
J
K
L
M
N
O
P
Q
MEA
M40Y
DG18

Figure 3.4. Scanning electron micrograph of *Geminibasidium donsium* DAOM 241966. S = basidiospore. B = basidium. P = primary cell. Scale bar = 10 µm.

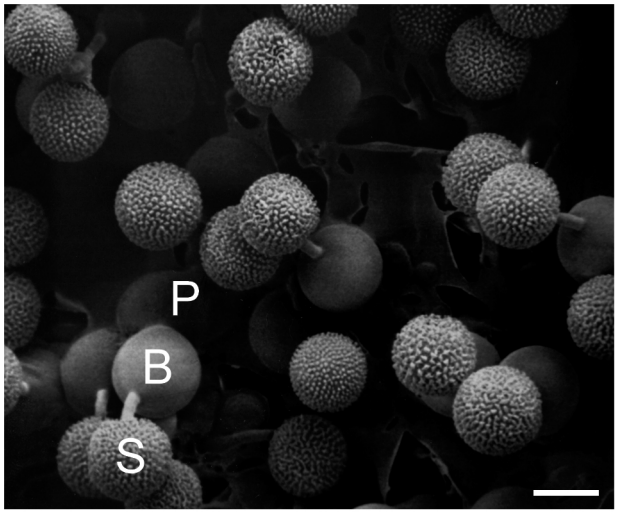
P
B
S

Diagnosis. Colonies are pink on M40Y and DG18. Sporulation occurs on CMA. Basidium bearing cells (primary cells) are 14.5–17.0 × 11.0–12.0 µm, have granular cell contents, a basal lateral projection, and are irregularly shaped when mature. During maturation, a basidium, 10.5–14.5 × 9.5–12.5 µm, arises on the apex of the primary cell. The basidium forms a series of swollen cells with sterigmata like connectors with the terminal swollen cell becoming a basidiospore. Mature basidiospores are globose, hyaline or brown, 11.0–12.0 µm in diameter, slightly verrucose, and double walled.

Description.

Colonies grow to a diameter of 2.2–2.4 cm (mean ± SE = 2.2 ± 0.1 cm) on MEA, 1.5–2.0 cm (mean ± SE = 1.8 ± 0.2 cm) on M40Y and 0.9–1.0 cm (mean ± SE = 0.9 ± 0 cm) on DG18 after 1 week at room temperature. The surface of the colony on CMA is glandular in texture because basidia form basidiospores on the surface of the agar. After 2 weeks on MEA: colonies are planar, uniform, pink with diffuse margins; on M40Y, colonies are flat, plicate, pink with diffuse margins; on DG18, colonies are flat, pink in color with diffuse or discrete margins.

Basidium bearing cells (primary cells) are at first irregularly shaped on terminal and lateral branches of hyphae. Over time, they expand and mature into swollen and irregularly shaped primary cells attached to hyphae by a thin connector. Mature primary cells are 14.5–17.0 × 11.0–12.0 µm (mean ± SE = 16.3 ± 0.8 × 11.6 ± 0.3 µm), have granular cell contents and a basal lateral projection. Primary cells are visible after four days.

After about five days, a basidium, 10.5–14.5 × 9.5–12.5 µm (mean ± SE = 12.3 ± 0.4 × 11.0 ± 0.3 µm), arises on the apex of the primary cells. The basidium

produces a series of swollen cells with sterigmata like connectors with the terminal swollen cell becoming a basidiospore. These swollen cells are granular in appearance at first but they eventually become transparent after the terminal swollen cell matures into a single basidiospore. The basidium collapses as the basidiospore matures. One-week-old basidiospores are usually hyaline and older basidiospores are usually brown. Basidiospores are globose, slightly verrucose, 11.0–12.0 µm (mean ± SE = 11.3 ± 0.3 µm) in diameter, and possess a thick double wall. Basidiospores are visible after seven days. In one month old cultures, clusters of basidiospores encased in a gelatinous matrix (presumed to be remnants of basidia) can be observed.

Holotype. *G. donsium* DAOM 241966; dried culture on CMA (October 2012) of an isolate from soil of commercial field of low bush blueberries in Sable River, Nova Scotia, Canada.

Strains examined. DAOM 241966 (ex-type), 241967, 242124 (Supplementary Table 3.1).

Notes. The characters that differentiate *G. donsium* from *G. hirsutum* are the production of a series of swollen cells with sterigma-like connectors on the basidium and the slightly verrucose appearance of mature basidiospores.

Geminibasidium hirsutum H.D.T. Nguyen, N.L. Nickerson and Seifert sp. nov.

MycoBank MB 801335

Figure 3.5

Figure 3.5. *Geminibasidium hirsutum* DAOM 241969 ontogenesis and colonies. A–C. Granular basidium bearing cell (primary cells), with a basal lateral projection, develop on hyphae and over time become swollen and irregular. D–I. Basidia arise from the apex of primary cells and produce a basidiospore on a sterigma. H–J. Basidiospores are at first smooth-walled and become hirsute over time. K–L. Basidiospores in clusters can be found in one month old cultures. M. The basidium is attached to hyphae by thin connector. N. Colonies of *G. donsium* on MEA, M40Y and DG18 after 2 weeks incubation at room temperature. Scale bar = 20 µm for panels A–M.

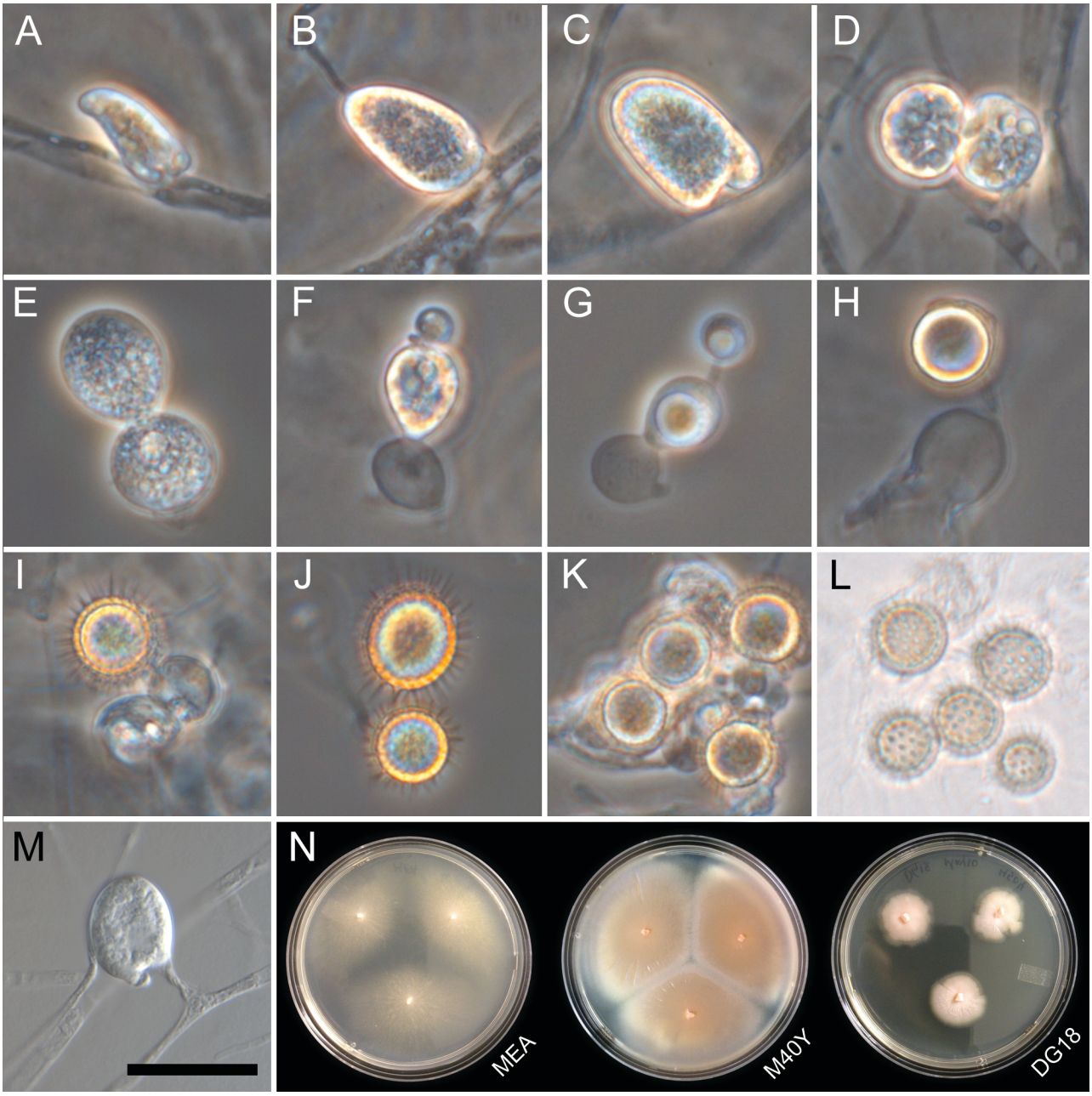
A
B
C
D
E
F
G
H
I
J
K
L
M
N
MEA
M40Y
DG18

Etymology. hirsutum = hairy. The name refers to the hirsute basidiospores.

Diagnosis. Colonies are pink on M40Y and DG18. Sporulation occurs on CMA. Basidium bearing cells (primary cells) are 14.0–20.5 × 11.5–14.0 µm, have granular cell contents, a basal lateral projection, and are irregularly shaped when mature. During maturation, a basidium, 13.5–23.5 × 11.0–17.5 µm, arises on the apex of the primary cells. One mature basidiospore on sterigma arises from the basidium. Basidiospores are globose, hyaline or brown, hirsute, 10.5–13.5 µm in diameter, and double walled.

Description.

Colonies grow to a diameter of 2.6–2.7 cm (mean ± SE = 2.7 ± 0.1 cm) on MEA, 2.5–2.7 cm (mean ± SE = 2.6 ± 0.1 cm) on M40Y and 0.8–1.5 cm (mean ± SE = 1.2 ± 0.3 cm) on DG18 after 1 week at room temperature. The surface of the colony on CMA is glandular in texture because basidia form basidiospores on the surface of the agar. After 2 weeks; on MEA, colonies are flat, uniform, white-beige or light pink-beige with diffuse margins; on M40Y, colonies are flat, smooth, pink with diffuse margins; on DG18, colonies are flat, pink in color with diffuse or discrete margins.

Basidium bearing cells (primary cells) are at first irregularly shaped on terminal and lateral branches of hyphae. Over time, they expand and mature into swollen and irregularly shaped primary cells, attached to hyphae by a thin connector. Mature primary cells are 14.0–20.5 × 11.5–14.0 µm (mean ± SE = 17.2 ± 3.4 × 12.9 ± 1.3 µm), have granular cell contents and a basal lateral projection. Primary cells are visible after four days.

After about five days, a basidium, 13.5–23.5 × 11.0–17.5 µm (mean ± SE = 18.2 ± 1.4 × 14.5 ± 0.9 µm), arises on the apex of the primary cells. The basidium produces a smooth immature basidiospore on a sterigma. The basidium collapses as the smooth basidiospore matures into a hirsute basidiospore. Basidiospores are globose (rarely subglobose), hirsute, 10.5–13.5 µm (mean ± SE = 12.0 ± 1.5 µm) in diameter, and possessing a thick double wall. Basidiospores are visible after seven days. In one month old cultures, clusters of basidiospores encased in a gelatinous matrix (presumed to be remnants of basidia) can be observed.

Holotype. *G. hirsutum* DAOM 241969; dried culture on CMA (October 2012) of an isolate from soil of a coniferous forest of mainly *Pseudotsuga* sp. with understory of *Vaccinium parvifolium* in Shingle Bolt Trail, Capilano Gorge, base of Grouse Mountain, North Vancouver, British Columbia, Canada. (49°22'N 123°05'W, 310 m altitude).

Strains examined. DAOM 241969 (ex-type), 241968 (Supplementary Table 3.1).

Notes. The characters that differentiate *G. hirsutum* from *G. donsium* are the presence of hirsute basidiospores and absence of the chain of swollen cells produced by the basidium.

Key to the species of *Basidioascus* and *Geminibasidium*

1A – Basidia forcibly discharged; sessile or arising on a cylindrical stalk, but lacking a basal, swollen (primary) cell – 2

1B – Basidia not forcibly discharged; arising from a swollen and irregularly shaped swollen (primary) cell – 3

2A – Abortive basidiospores on some basidia, arthroconidia produced – *B. undulatus*

2B – Only one basidiospore on each basidium, no arthroconidia produced – *B. magus*

3A – Basidiospores with slightly verrucose walls when mature – *G. donsium*

3B – Basidiospores with hirsute walls when mature – *G. hirsutum*

Discussion

During surveys for heat resistant fungi in soil, we isolated *Basidioascus* and *Geminibasidium* species from soil using a pasteurization-like heat treatment method. After analyzing these strains morphologically, phylogenetically and physiologically, our data support the description of two species of *Basidioascus* (*B. undulatus* and *B. magus* sp. nov.) and a novel genus, *Geminibasidium*, along with two novel species (*G. donsium* and *G. hirsutum*).

Geminibasidium and *Basidioascus* share similar ecology, physiology, and morphology but also have several differences. *Basidioascus* species form white colonies whereas *Geminibasidium* species form pink colonies. In *Geminibasidium* species, the basidium arises on a primary cell whereas in *Basidioascus* species, the

basidium matures directly on somatic hyphae. Basidiospores in *Geminibasidium* species are globose whereas they are subglobose in *Basidioascus* species. Surprisingly, the basidia of *Basidioascus* species are forcibly discharged, a unique behavior that to our knowledge does not occur elsewhere in the Basidiomycota, including the sister genus *Geminibasidium.* Given these morphological observations (Figures 3.1–3.5) and our molecular phylogeny (Figure 3.6 and Figure 3.7), we conclude that *Basidioascus* and *Geminibasidium* are distinct genera.

The topology of our rDNA phylogenetic reconstruction reflects the currently accepted taxonomic view of the basidiomycetes (McLaughlin et al. 2009). In this analysis, *Basidioascus* and *Geminibasidium* were found to be sister groups in Wallemiomycetes (Figure 3.6). Our results also show that *Wallemia* is the sister taxon to *Basidioascus* and *Geminibasidium*. The taxonomic position of *Wallemia* was uncertain (Matheny et al. 2006) until (Padamsee et al. 2012) found it is unambiguously fixed at the base of the Agaricomycotina with high certainty by phylogenetic analysis with an amino acid data set from 71 protein-coding genes.

Figure 3.6. Ribosomal phylogeny of *Basidioascus* and *Geminibasidium*. The relationship of *Basidioascus* and *Geminibasidium* to the other basidiomycetes is shown in a Bayesian phylogenetic partition analysis with the combined SSU, 5.8S, and LSU genes. Posterior probabilities are displayed at nodes of the tree.

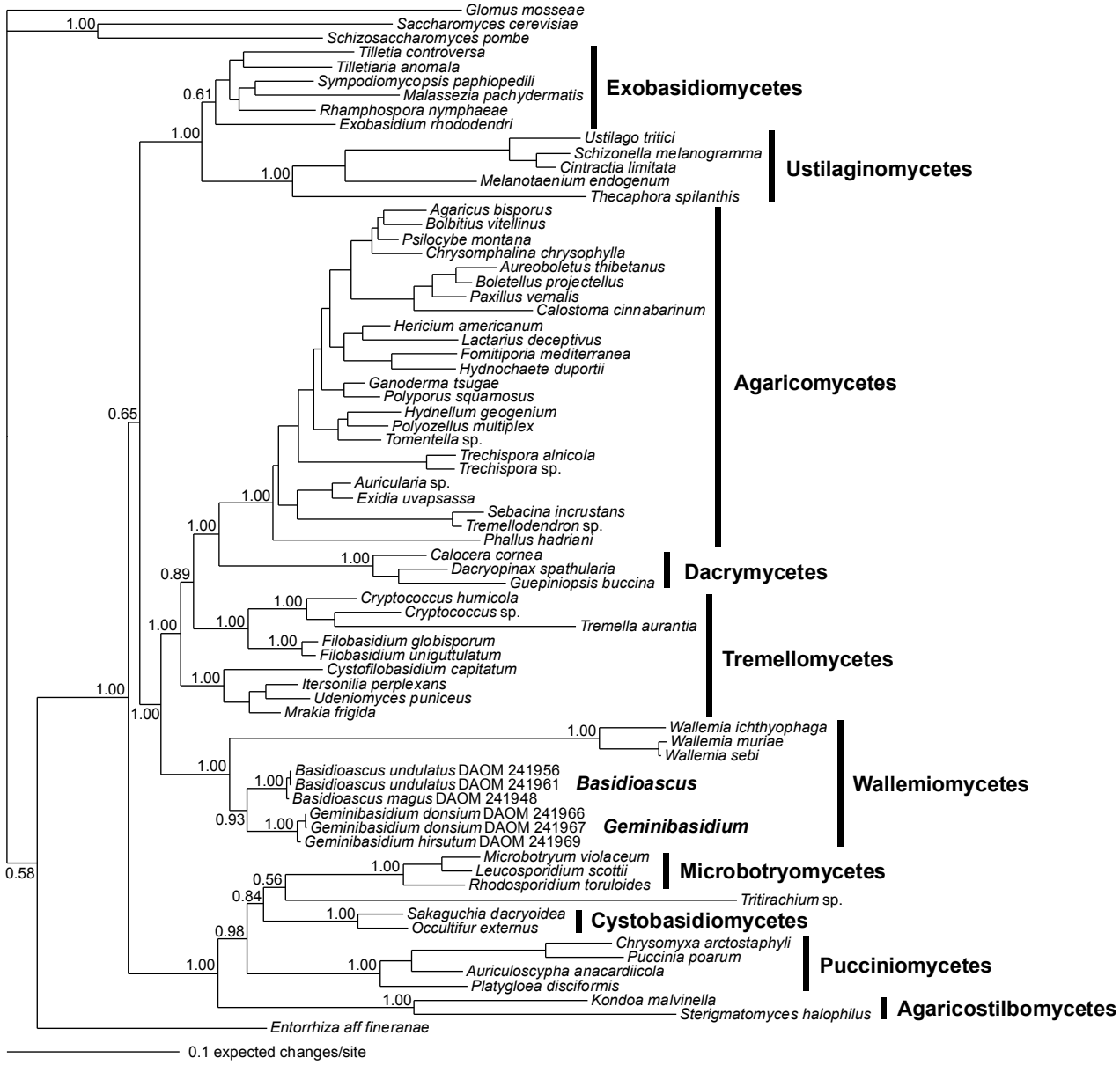
Glomus mosseae
Saccharomyces cerevisiae
Schizosaccharomyces pombe
Tilletia controversa
Tilletiaria anomala
Sympodiomycopsis paphiopedili
Malassezia pachydermatis
Rhamphospora nymphaeae
Exobasidium rhododendri
Exobasidiomycetes
Ustilago tritici
Schizonella melanogramma
Cintractia limitata
Melanotaenium endogenum
Thecaphora spilanthis
Ustilaginomycetes
Agaricus bisporus
Bolbitius vitellinus
Psilocybe montana
Chrysomphalina chrysophylla
Aureoboletus thibetanus
Boletellus projectellus
Paxillus vernalis
Calostoma cinnabarinum
Hericium americanum
Lactarius deceptivus
Fomitiporia mediterranea
Hydnochaete duportii
Ganoderma tsugae
Polyporus squamosus
Hydnellum geogenium
Polyozellus multiplex
Tomentella sp.
Trechispora alnicola
Trechispora sp.
Auricularia sp.
Exidia uvapsassa
Sebacina incrustans
Tremellodendron sp.
Phallus hadriani
Agaricomycetes
Calocera cornea
Dacryopinax spathularia
Guepiniopsis buccina
Dacrymycetes
Cryptococcus humicola
Cryptococcus sp.
Tremella aurantia
Filobasidium globisporum
Filobasidium uniguttulatum
Cystofilobasidium capitatum
Itersonilia perplexans
Udeniomyces puniceus
Mrakia frigida
Tremellomycetes
Wallemia ichthyophaga
Wallemia muriae
Wallemia sebi
Basidioascus undulatus DAOM 241956
Basidioascus undulatus DAOM 241961
Basidioascus magus DAOM 241948
Basidioascus
Geminibasidium donsium DAOM 241966
Geminibasidium donsium DAOM 241967
Geminibasidium hirsutum DAOM 241969
Geminibasidium
Wallemiomycetes
Microbotryum violaceum
Leucosporidium scottii
Rhodosporidium toruloides
Microbotryomycetes
Tritirachium sp.
Sakaguchia dacryoidea
Occultifur externus
Cystobasidiomycetes
Chrysomyxa arctostaphyli
Puccinia poarum
Auriculoscypha anacardiicola
Platygloea disciformis
Pucciniomycetes
Kondoa malvinella
Sterigmatomyces halophilus
Agaricostilbomycetes
Entorrhiza aff fineranae
0.1 expected changes/site

Figure 3.7. Phylogenetic species delimitation of *Basidioascus* and *Geminibasidium* species using ITS. A Bayesian phylogenetic analysis was performed and posterior probabilities are displayed at nodes of the tree. Environmental ITS sequences from GenBank were also included. Sequences marked with HT denote the holotype strain whereas ET indicates the epitype strain. The sequence named Kikoku came from a fungal contaminant. This fungal contaminant was isolated from imported frozen Canadian blueberries destined for jam production in Japan (Y. Kikoku pers. comm.).

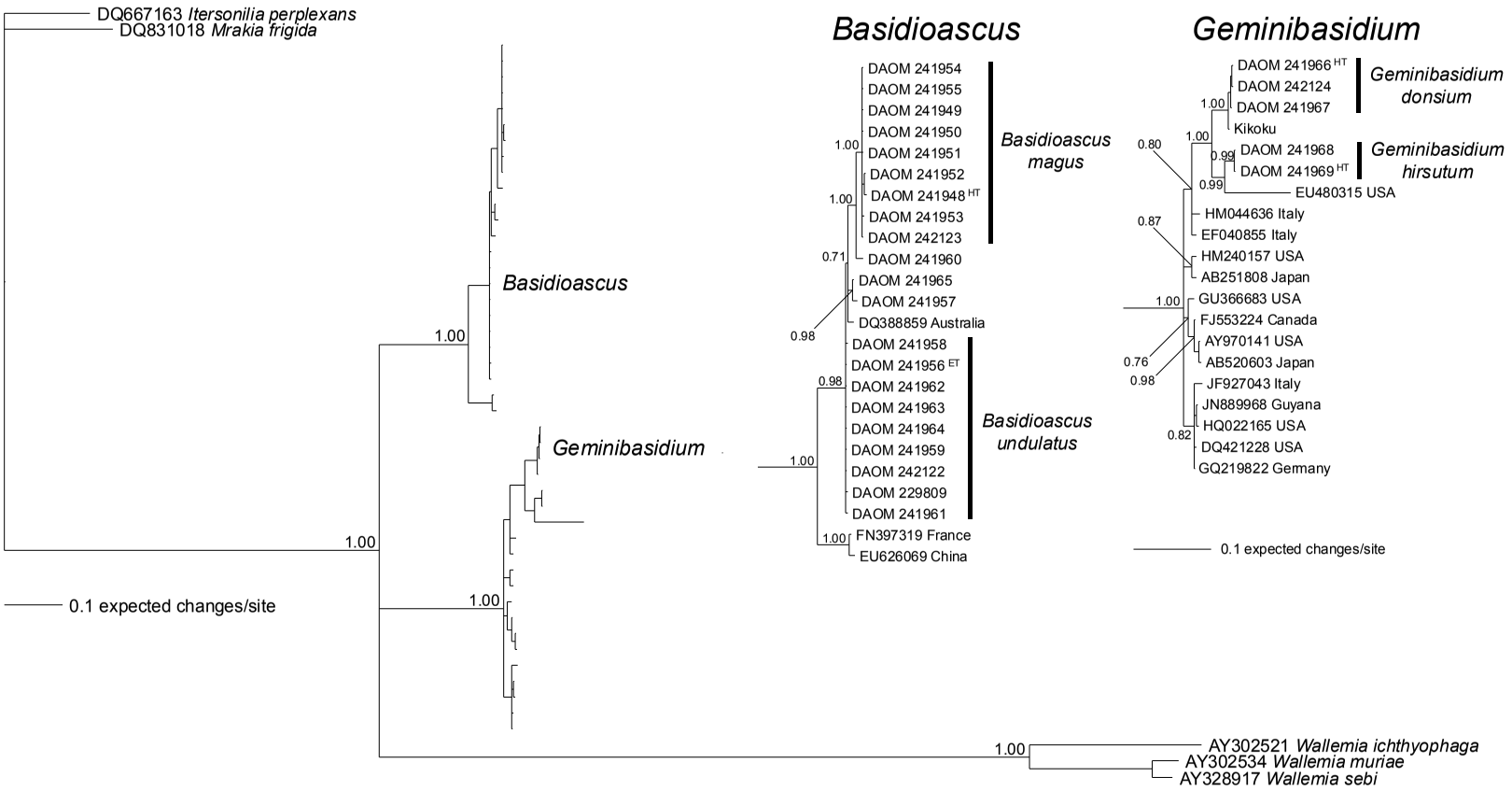
DQ667163 Itersonilia perplexans
DQ831018 Mrakia frigida
Basidioascus
Geminibasidium
1.00
1.00
1.00
0.1 expected changes/site
AY302521 Wallemia ichthyophaga
AY302534 Wallemia muriae
AY328917 Wallemia sebi
Basidioascus
DAOM 241954
DAOM 241955
DAOM 241949
DAOM 241950
DAOM 241951
DAOM 241952
DAOM 241948 HT
DAOM 241953
DAOM 242123
DAOM 241960
DAOM 241965
DAOM 241957
DQ388859 Australia
DAOM 241958
DAOM 241956 ET
DAOM 241962
DAOM 241963
DAOM 241964
DAOM 241959
DAOM 242122
DAOM 229809
DAOM 241961
FN397319 France
EU626069 China
Basidioascus magus
Basidioascus undulatus
1.00
0.71
0.98
0.98
1.00
1.00
Geminibasidium
DAOM 241966 HT
DAOM 242124
DAOM 241967
Kikoku
DAOM 241968
DAOM 241969 HT
EU480315 USA
HM044636 Italy
EF040855 Italy
HM240157 USA
AB251808 Japan
GU366683 USA
FJ553224 Canada
AY970141 USA
AB520603 Japan
JF927043 Italy
JN889968 Guyana
HQ022165 USA
DQ421228 USA
GQ219822 Germany
Geminibasidium donsium
Geminibasidium hirsutum
1.00
0.80
1.00
0.99
0.99
0.87
1.00
0.76
0.98
0.82
0.1 expected changes/site

The phylogenetic placement of *Basidioascus* and *Geminibasidium* in the Basidiomycota led us to interpret their characters in the context of basidiomycete morphology. In this paper, the structures referred to as basidia and basidiospores are putatively identified as such. We plan detailed follow-up studies of the karyology and ultrastructure of these fungi (see Chapter 4). Basidia in *Basidioascus* species resemble those of gasteroid Agaricomycetes such as *Secotium agaricoides* and *Lycoperdon candidum* (Coker and Couch 1974). In common with the gasteroid Agaricomycetes, the basidiospores of *Basidioascus* basidia are not actively discharged. The gasteroid morphological character is polyphyletic in the Agaricomycetes (Binder and Bresinsky 2002). Although similar, basidia from many gasteroid fungi are more elongated than those of *Basidioascus* species, perhaps reflecting the evolution of the gasteroid fungi from the typically elongated clavate basidia of the Agaricales. Our rDNA data (Figure 3.6) suggest that *Basidioascus* species are only distantly related to the Agaricomycetes. In *Geminibasidium* species, basidium-bearing cells (primary cells) give rise to basidia. This peculiar basidium arrangement does not resemble that of any other known fungi. As an aside, we note the striking similarity of the simple basidial structures of *Basidioascus* and *Geminibasidium* with the sporangia and sub-sporangial swellings of the chytrid *Phlyctochytrium aureliae* as illustrated by Letcher et al. (2012).

The basidia in *Basidioascus* and *Geminibasidium* species have a basal lateral projection. The origin and function of this structure are unknown. As basidia mature, the basal lateral projection in *Basidioascus* species collapses but not that of *Geminibasidium* species. Basidia with collapsed basal lateral projections were found on the Petri dish lids above colonies of *Basidioascus* species. However,

basidia were not found on the Petri dish lids above *Geminibasidium* species. We speculate that the collapse of this projection is involved in the forcible discharge of the basidia in *Basidioascus* species.

Both *Geminibasidium* and *Basidioascus* have double-walled basidiospores that are not themselves actively discharged. The double-walled basidiospores, which can be hirsute or verrucose, resemble those of gasteroid species of *Lycoperdon* and *Scleroderma* (Coker and Couch 1974), but also those of basidiomycetes with actively discharged basidiospores such as species of *Ganoderma* (Hong and Jung 2004). In older cultures, double-walled basidiospores often cluster together. Perhaps these clusters are immature or degenerated basidiomes, a cultural expression of what might be a more developed structure in nature. We speculate that the double wall adaptation and clustering helps in resisting heat. The outer wall of the spore may provide an additional protective layer. Clustering also decreases exposed surface area and spores in the center of the cluster could be further shielded from heat. The basidiospores in *G. hirsutum* are hirsute and this adaptation may help sticking to an animal or insect vector for spore dispersal or could be an additional way for spores to cluster together for increased protection.

The majority of basidiomycetes in the Agaricales, Pucciniales, and Tremellales have basidia that produce four meiotic basidiospores. Some basidiomycetes produce other numbers (e.g. the tuning fork basidium in *Dacrymyces* with two basidiospores, and *Sistotrema* species with eight). Each basidium in *Basidioascus* and *Geminibasidium* species only produces one mature basidiospore. The adaptive benefits of this, if any, are uncertain. Perhaps CMA is

not the ideal medium to observe ontogenesis because *B. undulatus* produces abortive basidiospores and *G. donsium* can produce a series of swollen cells (which may be interpreted as immature basidiospores) before the terminal mature basidiospore. Therefore, the production of one basidiospore may be an artifact of growth in culture.

Basidioascus and *Geminibasidium* species share other common characters with *Wallemia*. They are commonly xerotolerant, have similar optimal growth temperature, are found in soil and lack a basidiocarp. *Wallemia* is mostly isolated from indoor environments, dried and salty foods but can also be isolated from soil (Zalar et al. 2005; Zajc et al. 2011). However, they differ in ontogenesis, morphology, and heat resistance. In *Wallemia*, conidia develop basipetally (Padamsee et al. 2012) in a unique pattern known as basauxic conidiogenesis (Zalar et al. 2005). Furthermore, *Wallemia* is not heat resistant (Vytrasova et al. 2002).

Given all these unusual characters, we suggest the placement of *Basidioascus* and *Geminibasidium* in a novel family Geminibasidiaceae within a novel order Geminibasidiales. As well, we propose that Geminibasidiales tentatively be placed under the class Wallemiomycetes. Class level assignment based on the septal pore ultrastructure would provide conclusive evidence for this higher taxonomic classification (Chapter 4).

Ecology and physiology

Basidioascus and *Geminibasidium* species were isolated from soil of forests, grasslands and blueberry fields (Supplementary Table 3.1) suggesting that they are common and have been previously overlooked. These soils were sometimes

accidentally or intentionally burned. There are very few published studies dealing with basidiomycetes recovered in heat-treated or burned soils (Bollen 1969, 1974; Izzo et al. 2006). The only basidiomycetes reported to be recovered after heat treatment of soils were *Tephrocybe* sp. (Bollen 1974), *Coprinus fimetarius* (Bollen 1969), and *Rhizopogon olivaceotinctus* (Izzo et al. 2006). Our study adds *Basidioascus* and *Geminibasidium* species to the list of heat resistant basidiomycetes.

Our ITS analysis show that there remain undescribed genera or species related to *Basidioascus* and *Geminibasidium* (Figure 3.7). Location data in the environmental sequences suggest that these fungi are widely distributed in soil around the world. Additional soil sampling will likely help isolate these environmental taxa now that a method of isolation for these fungi is established. The environmental sequences FN397319 from France and EU626069 from China form an additional well-supported clade and may represent a yet to be described genus or species of *Basidioascus*. The environmental sequences near *Geminibasidium* species form four additional clades with moderate node support that could represent additional undescribed species of *Geminibasidium*. Many of the studies (see citations in Supplementary Table 3.4) that generated these environmental sequences focused on ectomycorrhizal communities. One environmental ITS sequence was reported to be from “ectomycorrhized root tips” in the GenBank (HM044636, otherwise unpublished) record. This ITS sequence is closely related to *Geminibasidium* strains found in our study (Figure 3.7). If this information is accurate, *Geminibasidium* or a *Geminibasidium*-like fungus may be ectomycorrhizal.

Xerophilic fungi grow at water activities below 0.85 under at least one set of environmental conditions (Pitt 1975). Most ascomycetes are able to tolerate water activities below a_w=0.90 (Zak and Wildman 2004). Xerotolerance is presently considered a rare character in the basidiomycetes (Zak and Wildman 2004; Zalar et al. 2005). All *Basidioascus* and *Geminibasidium* strains are able to grow on low water activity media such as M40Y and DG18. Our data show that they can also grow below a_w=0.85 (Figure 3.8), the threshold defining a xerophilic fungus, but they grow better at slightly higher water activity. Thus, we consider them as xerotolerant rather than xerophilic. The average NaCl concentration of seawater is 0.5 M (about 3.0%). *Basidioascus undulatus*, *G. donsium* and *G. hirsutum* are able to grow above this concentration suggesting these fungi could live in the ocean as well as in normal or salty soils. Soil is probably their primary habitat because most of the environmental sequences from GenBank are from soil and we isolated them from soil in our study.

Figure 3.8. Growth of *Basidioascus* and *Geminibasidium* type strains in water activities ranging from 1.00 to 0.77 approximately over 28 days. Diameter (mm) is shown on the y-axis and water activity (a_w) is shown on the x-axis. Water activity in the media was lowered by addition of glycerol, sodium chloride and sucrose.

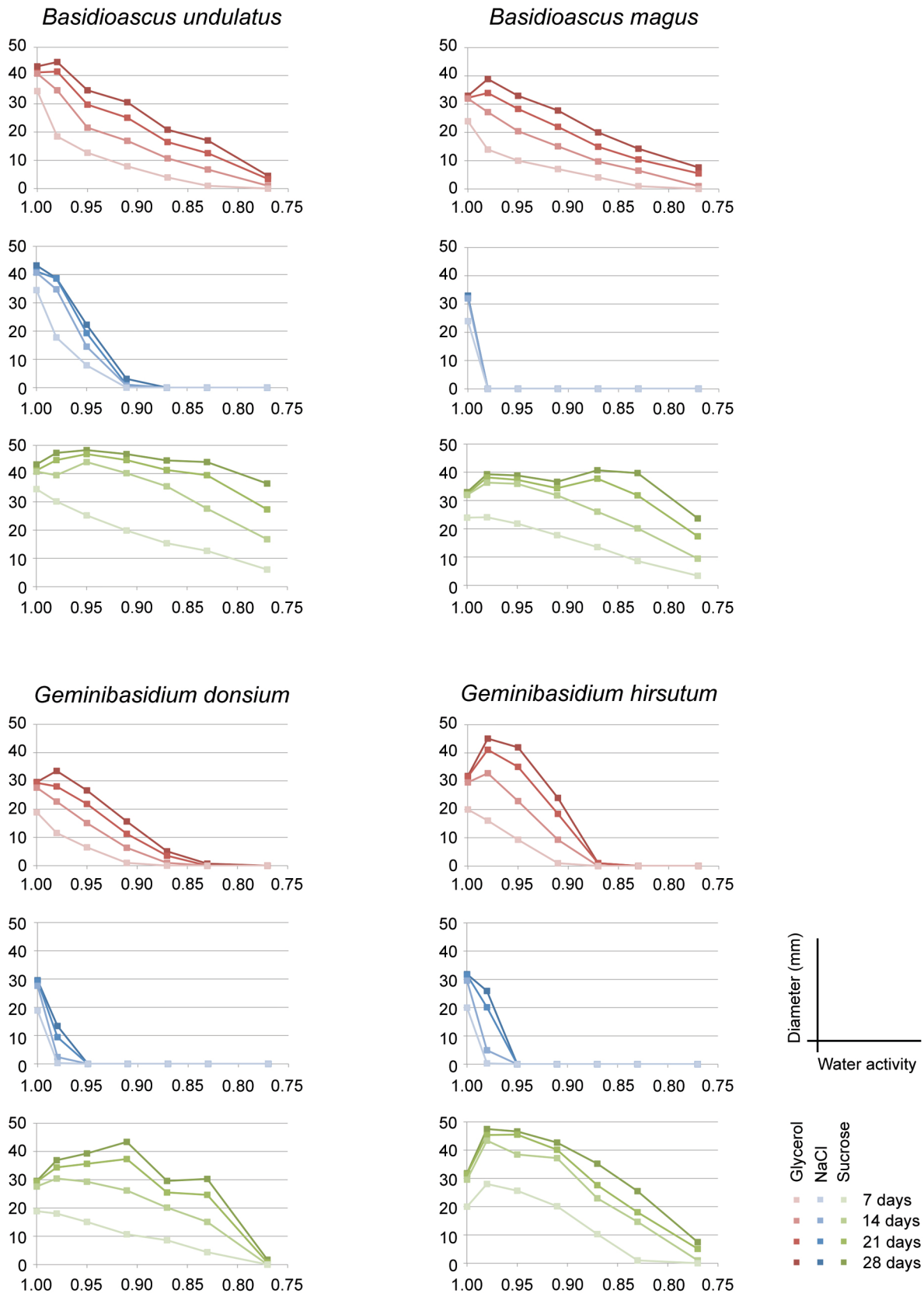
Basidioascus undulatus
Basidioascus magus
Geminibasidium donsium
Geminibasidium hirsutum
50
40
30
20
10
0
1.00 0.95 0.90 0.85 0.80 0.75
Diameter (mm)
Water activity
Glycerol
NaCl
Sucrose
7 days
14 days
21 days
28 days

Figure 3.9. Average growth of *Basidioascus* and *Geminibasidium* at temperatures of 5 °C to 40 °C after 7 days on MYA and M40Y media.

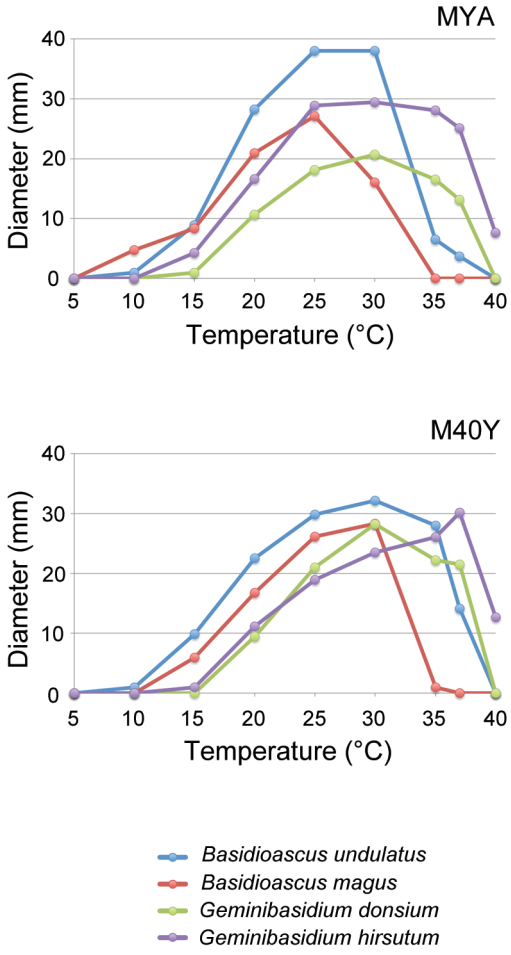
MYA
Diameter (mm)
0
10
20
30
40
5
10
15
20
25
30
35
40
Temperature (°C)
M40Y
Diameter (mm)
0
10
20
30
40
5
10
15
20
25
30
35
40
Temperature (°C)
Basidioascus undulatus
Basidioascus magus
Geminibasidium donsium
Geminibasidium hirsutum

Acknowledgments

We would like to thank the collectors of soil samples (G.P. White, R.J. Bandoni, A.K. Davis, H. Veldhuis, R.J. Davies, R. Hunt, J. Unruh, A. Olson, H. Douwes, S.P. Vander Kloet, M. Trappe), various people for discussions of this project (D. Begerow, S.A. Redhead, J. Spatafora, M.C. Aime, Y. Kikoku, A. Patriarcia, P. Zalar, D. Brisson) and technical support (R.J. Davies, G. Louis-Seize). We thank Susan Carbyn, Paula Allan-Wojtas and Milos Kalab for providing the SEM micrograph. This research was supported through funding from the Ontario Graduate Scholarship, University of Ottawa Excellence Scholarship and the Queen Elizabeth II Science and Technology Scholarship.

Author contribution

HDTN and KAS conceived and designed the work. HDTN and NLN acquired the data: NLN contributed all strains of *Basidioascus* & *Geminibasidium*, except those from Crater Lake National Park which were isolated by HDTN; HDTN deposited all cultures in DAOM; HDTN performed all morphological and physiological work; HDTN generated all sequences and deposited all data in GenBank; HDTN performed all phylogenetic analyses. HDTN analyzed and interpreted the data. HDTN drafted the article. HDTN, KAS and NLN critically revised the manuscript for important intellectual content.

Chapter 4: *Basidioascus undulatus*: genome, origins and sexuality

Hai D.T. Nguyen[1,2], Denise Chabot[3], Yuuri Hirooka[1,2], Robert W. Roberson[4], Keith A. Seifert[1,2]

[1] Department of Biology, Faculty of Science, University of Ottawa, Ottawa, Ontario, Canada

[2] Biodiversity (Mycology), Eastern Cereal and Oilseed Research Centre, Agriculture and Agri-Food Canada, Ottawa, Ontario, Canada

[3] Microscopy Centre, Eastern Cereal and Oilseed Research Centre, Agriculture and Agri-Food Canada, Ottawa, Ontario, Canada

[4] School of Life Sciences, Arizona State University, Tempe, AZ 85287-1601, United States

Abstract

Basidioascus undulatus is a soil basidiomycete belonging to the order Geminibasidiales. The taxonomic status of the Geminibasidiales is unclear because originally it was only tentatively classified in the class Wallemiomycetes. The fungi in the Geminibasidiales have an ambiguously defined sexual cycle. In this study, we sequenced the genome of *B. undulatus* to help us gain insight into its sexuality and evolutionary origins. The assembled genome was around 32 Mb in size, had an average nucleotide-wise coverage of 28X, and contained 6123 predicted genes. Previous morphological descriptions of *B. undulatus* relied on interpretation of putative sexual structures. In this study, nuclear staining and confocal microscopy showed meiosis occurring in basidia and genome analysis confirmed the existence of genes involved in meiosis and mating. Using 35 protein-coding genes extracted from genomic information, phylogenomic and molecular dating analyses confirmed that *B. undulatus* indeed belongs to a lineage distantly related to *Wallemia* while retaining a basal position in the Agaricomycotina. These results, combined with differences in septal pore morphology, led us to move the Geminibasidiales out of the Wallemiomycetes and into the Geminibasidiomycetes cl. nov. Finally, the concept of Agaricomycotina was emended to include both the classes Wallemiomycetes and Geminibasidiomycetes.

Keywords

Agaricomycotina; Geminibasidiomycetes; Wallemiomycetes

Introduction

Using morphological characters, Matsushima (2003) described the species *Basidioascus undulatus* as the only species in the genus *Basidioascus* based on only one strain that was isolated from the tropical rainforest soil in Cape Tribulation National Park, Queensland, Australia. Matsushima (2003) photographed fertile structures of *B. undulatus*, which he interpreted as asci giving rise to ascospores, bearing hooks that might be either croziers or clamps. The genus was named *Basidioascus* for "basidia like asci" and the species epithet *undulatus* was given to represent "ascospores with a wavy wall" (Matsushima 2003). Also, *B. undulatus* produced a *Geotrichum*-like anamorph in culture, characterized by chains of aseptate arthroconidia. A different genus and species name used to be given to the sexual and asexual morph of the same fungus until the Amsterdam declaration (Hawksworth et al. 2011), which proposed that all fungi should only have one name. *Basidioascus undulatus* was assumed to be a species of *Geotrichum* (a genus name used to describe an asexual morph) exhibiting a sexual state distinct from *Galactomyces* or *Dipodascus* (names used to describe sexual morphs). These genera are classified in Saccharomycetes (Ascomycota). As a consequence, MycoBank (Robert et al. 2013) and the Dictionary of the Fungi (Kirk et al. 2008) classified *B. undulatus* in the Saccharomycetes.

During a survey of heat resistant fungi in Canadian soils, Nguyen et al. (2013) isolated nine additional strains of *B. undulatus*, and a second species of *Basidioascus* given the name *B. magus*. A third yeast-like species, *B. persicus*, was recently described from soil in Iran (Nasr et al. 2014). Soil appears to be the main

habitat for *Basidioascus* species and their distribution is probably broad. However, their ecological role is currently unknown, but they are presumably saprobic like most soil inhabiting fungi (Domsch et al. 1993).

Surprisingly, phylogenetic analyses with rDNA sequences showed that *Basidioascus* was related to the Wallemiomycetes (Basidiomycota) rather than the Saccharomycetes (Ascomycota) (Nguyen et al. 2013). This finding initiated a revision of its taxonomy and a re-interpretation of its morphology as a basidiomycete (Nguyen et al. 2013). The species of *Basidioascus* and species of its sister genus *Geminibasidium* (*G. donsium* and *G. hirsutum*) were classified in the new order Geminibasidiales (Nguyen et al. 2013). The Geminibasidiales is a phylogenetic sister group to the Wallemiales and was placed tentatively under the class Wallemiomycetes (Nguyen et al. 2013). The Wallemiales is currently composed of a single genus *Wallemia* with 6 species (*W. sebi*, *W. muriae*, *W. ichthyophaga*, and three new species) (Jančič et al. 2015; Zalar et al. 2005). The phylogenetic placement of the Wallemiomycetes in the fungal kingdom was at first ambiguous (Matheny et al. 2006) because few coding protein genes were used in phylogenetic analyses. However, a few recent studies, through phylogenomic analyses with a large number of protein coding genes, demonstrated that this lineage was fixed at the base of the Agaricomycotina (Padamsee et al. 2012; Zajc et al. 2013).

The first eukaryotic genome sequenced belonged to the yeast *Saccharomyces cerevisiae* (Goffeau et al. 1996). With the decreasing costs of next generation sequencing technologies, mycology is experiencing an explosion of fungal genomes, exemplified by the 1000 fungal genomes initiative (http://1000.fungalgenomes.org/home/) and other independent efforts.

In this study, we release the first version of the *B. undulatus* genome. We address details of sexuality and classification of *Basidioascus* that were previously unsolved by Nguyen et al. (2013) using a combined approach of microscopic techniques and genomic information. Our first objective was to gain further insight into the sexuality of *B. undulatus* because the structures referred to as basidia and basidiospores were only putatively identified as such (Nguyen et al. 2013). We sequenced the genome of *B. undulatus* and looked for the presence of genes involved in meiosis and mating. Further, we performed nuclear staining on these presumed sexual structures and observed them with laser confocal microscopy to support our genomic findings. Our second objective was to resolve the tentative placement of the Geminibasidiales in the Wallemiomycetes. We extracted a set of amino acid sequences from 35 single copy genes from the *B. undulatus* genome. Using this data, we performed phylogenomic analysis to verify its relationship to *Wallemia* species with sequenced genomes (*W. sebi and W. ichthyophaga*) and other fungi with sequenced genomes. We performed a molecular clock analysis to date the divergence of *B. undulatus* from *Wallemia* species and other fungi. Septal pore morphology traditionally played a large role in basidiomycete systematics and is relevant for class rank classification, particularly in lineages of Agaricomycotina (van Driel et al. 2009). We imaged the septal pore of *B. undulatus*, *G. donsium* and *W. sebi* using transmission electron microscopy. Using this combined approach, the higher classification of the Geminibasidiales was resolved.

Materials and methods

Growth, DNA extraction and sequencing

The ex-type strain of *Basidioascus undulatus* (DAOM 241956) was inoculated in 2% malt extract broth in an Erlenmeyer flask on an orbital shaker at 25 °C for 2 weeks. The broth culture was transferred to two 50 mL Falcon tubes and centrifuged at 10000 × g for 5 min. The liquid was decanted, leaving only the fungal tissue. The fungal tissue was frozen in liquid nitrogen and crushed with a sterile pestle. DNA was extracted with the OmniPrep kit (G-Biosciences, St. Louis, USA) following manufacturer's instructions. DNA quality and quantity were verified with Qbit (Life Technologies, Burlington, Canada). Whole-genome sequencing (101 base pairs (bp) paired-end) was performed on an Illumina HiSeq 2500 with TrueSeq V3 chemistry at the National Research Council Canada in Saskatoon, Saskatchewan, Canada.

Genome assembly and annotation

The quality of the reads was checked with the program FastQC v0.10.1 (http://www.bioinformatics.babraham.ac.uk/projects/fastqc/). Using fastx_trimmer (part of the FASTX-Toolkit 0.0.13 (http://hannonlab.cshl.edu/fastx_toolkit/)), 8 bases from the 5' end were trimmed to yield reads of 93 bp in length of higher quality. *De novo* assembly was performed using SPAdes 3.0 (Bankevich et al. 2012) with BayesHammer (Nikolenko et al. 2013) error correction and mismatch correction enabled (parameters: --careful and k=21, 31, 41, 51, 61, 71, 81, 91). Final contigs were assembled into scaffolds with SSPACE v2.0 (Boetzer et al. 2011) (parameters: -x 1 -m 45 -o 10 -t 0 -r 0.7 -k 5 -a 0.7 -n 10 -z 2000 -T 16 -p 1) and contigs shorter

than 2000 bp were discarded. Assembly statistics were generated with QUAST v2.3 (Gurevich et al. 2013). The assembly was checked by aligning the corrected reads onto the scaffolds using Bowtie2 v2.1.0 (Langmead and Salzberg 2012). Alignments produced by Bowtie2 in SAM format were converted to sorted BAM format by SAMtools v0.1.19 (Li et al. 2009) and statistics for coverage were generated with Qualimap v0.8.1 (Garcia-Alcalde et al. 2012). To benchmark the completeness of our genome assembly, CEGMA v2.5 (Parra et al. 2007) was run on the scaffolds to detect the percentage of conserved eukaryotic genes (CEG's).

Genome annotation was performed following established guidelines (Haas et al. 2011). Repeats in scaffold sequences were masked with RepeatMasker v4.0.5 (http://www.repeatmasker.org) (parameters: -no_is -species fungi) using the Repbase libraries (Feb 3, 2014 release) (http://www.girinst.org/). The masked scaffolds were used as input for the MAKER2 v2.10 (Holt and Yandell 2011) genome annotation pipeline. In the MAKER2 pipeline, the GeneMark-ES v2.3e (Borodovsky and Lomsadze 2011) *ab initio* gene prediction tool was enabled and the NCBI RefSeq protein (Mar 13, 2014 release) sequences were aligned to the genome using exonerate v2.2.0 (Slater and Birney 2005). Predicted gene models exhibiting strong evidence by exon alignment were exported as protein sequences and coding nucleotide sequences (CDS). Predicted gene models lacking evidence from exon alignment were discarded in downstream analyses. To determine function, the protein sequences were used as input for InterProScan 5RC6 (Jones et al. 2014) (parameters: -dp -f -t p -iprlookup -pa -goterms) and were also compared to the manually curated protein data set from UniProt/Swiss-Prot (downloaded May 23, 2014) by blastp v2.2.28+. The results in XML format from blastp v2.2.28+ and

InterProScan were loaded into Blast2GO v2.7.1 (Conesa et al. 2005) and merged to create an annotation table. The gene models with BLAST hits having e-value of less than $1.0E^{-100}$ and mean similarity hit of ≥ 70% were assumed to be orthologs and they were given names following recommended conventions (http://www.uniprot.org/docs/proknameprot). All annotations are summarized in Supplementary File 4.5. Ribosomal RNA's were predicted by RNAmmer v1.2 (Lagesen et al. 2007). Data files are publicly available at NCBI (Genome Accession No. JTLS00000000 version JTLS01000000; BioProject Accession No. PRJNA247992) and as supplementary materials (Supplementary Files 4.1–4.4).

Confocal laser scanning microscopy

To study nuclear behavior and to look for indicators of meiosis, *B. undulatus* DAOM 241956 was grown on corn meal agar (CMA, Acumedia Manufacturers, Inc., Lansing, USA) for 1 week and mounted in DNA stains: DAPI-Fluoromount-G (EMS, Hatfield, PA, USA) or SYTO-9 (25 μM) (Life Technologies Inc., Burlington, ON, Canada). Samples were visualized under confocal laser scanning microscopy LSM 510 DUO (Carl Zeiss MicroImaging, Göttingen, Germany) with a Plan-Apochromat 40X/1.4 Oil DIC objective and electronic zoom 4. An excitation diode laser (405 nm) and emission Long Pass (420 nm) were used for DAPI. An excitation Argon laser (488 nm) and emission light (505–550 nm) were used for SYTO-9. Images were captured using ZEN 2009 Imaging Software (Carl Zeiss MicroImaging, Göttingen, Germany).

Identification of meiosis and mating genes

BLAST was used for finding the *B. undulatus* mating and meiosis genes. The protein sequences predicted from evidence supported gene models, determined above, were formatted into a local BLAST database with makeblastdb v2.2.28+.

Genes involved in meiosis in *Saccharomyces cerevisiae* and *Cryptococcus neoformans*, determined previously (Halary et al. 2011), were chosen as input queries (e-value cut off < $1.0E^{-05}$) for the *B. undulatus* protein BLAST database using blastp v2.2.28+. *Saccharomyces cerevisiae* and *C. neoformans* were chosen because they are well studied genetically and all meiosis-specific proteins are present (Halary et al. 2011). The results are summarized in Supplementary Table 4.4. The *B. undulatus* genes with the best BLAST hit to a given query sequence of *S. cerevisiae* and/or *C. neoformans* were added as annotations in Supplementary File 4.5.

Mating genes were located with the protein domains identified by InterProScan, and by blastp v2.2.28+ using known mating genes in *Saccharomyces cerevisiae* as blastp input queries (e-value cut off < $1.0E^{-05}$). The results are summarized in Supplementary Table 4.5 and are also included in the annotations in Supplementary File 4.5.

Phylogenomics and molecular dating

Protein sequences of selected fungi (*Pyronema confluens* CBS 100304, *Neurospora crassa* OR74A v2.0*, Cryptococcus neoformans* var *neoformans* JEC21, *Ustilago maydis*, *Malassezia globosa*, *Penicillium chrysogenum* Wisconsin 54-1255, *Coccidioides immitis* RS, *Tuber melanosporum*, *Coprinopsis cinerea*, *Trichoderma atroviride* v2.0, *Sclerotinia sclerotiorum* v1.0, *Arthrobotrys oligospora* ATCC 24927,

Puccinia striiformis f. sp. *tritici* PST-130, *Wallemia sebi* v1.0, *Auricularia subglabra* v2.0, *Dacryopinax* sp. DJM 731 SSP1 v1.0, *Fomitopsis pinicola* FP-58527 SS1 v3.0, *Fomitiporia mediterranea* v1.0, *Tremella mesenterica* Fries v1.0, *Agaricus bisporus* var *bisporus* (H97) v2.0, *Botrytis cinerea* v1.0, *Alternaria brassicicola*, *Taphrina deformans*, *Wallemia ichthyophaga* EXF-994, *Monacrosporium haptotylum* CBS 200.50, *Rhizophagus irregularis* DAOM 181602 v1.0, *Mixia osmundae* IAM 14324 v1.0, *Tilletiaria anomala*, *Aureobasidium pullulans* var. *pullulans* EXF-150, *Saccharomyces cerevisiae* S288C) (see Supplementary Table 4.1 for more details) were downloaded from the JGI MycoCosm portal (Grigoriev et al. 2014) and formatted into separate BLAST databases with makeblastdb v2.2.28+. The 246 reliable single copy ortholog protein data set from FUNYbase (Marthey et al. 2008) was downloaded. Only protein sequences coming from nuclear genes yielding a topological score of > 90% (Marthey et al. 2008) were considered for our phylogenomic analysis (Supplementary Table 4.2). These protein sequences were used as blastp v2.2.28+ search queries (e-value threshold < $1.0E^{-05}$) against the protein databases built from the JGI MycoCosm downloaded data described above. Protein sequences were aligned with T-Coffee v10.00.r1613 (Notredame et al. 2000) (parameters: t_coffee sequence.fasta -output score_ascii, aln) and poorly aligned regions and columns containing gaps were automatically discarded (parameters: t_coffee -other_pg seq_reformat -in sequence.aln -struc_in sequence.score_ascii -struc_in_f number_aln -action +use_cons +keep '[8-9]' +rm_gap 1 > sequence.best.aln). The alignments were concatenated and converted to PHYLIP format with SeaView v4.5.3 (Gouy et al. 2010). Three independent phylogenomic analyses were performed with the parallelized version of PhyloBayes 3 (pb_mpi

v1.4) (Lartillot et al. 2013; Lartillot et al. 2009) using the CATGTR model. Analyses were stopped when convergence was attained (effective size > 100 and maxdiff < 0.1 determined with the programs bpcomp (parameters: -x 1000 50 run1 run2 run3) and tracecomp (parameters: -x 1000 run1 run2 run3), which are part of pb_mpi software package). A lognormal 'relaxed clock' molecular dating analysis was performed with the non-parallelized version of PhyloBayes 3 (pb v3.2e) with a birth-death prior using the tree topology generated from the converged Bayesian analysis above (parameters: -d combined.phy -T bpcomp.con.tre -r outgroup.txt -cal calib.txt -ln -bd md1). *Rhizophagus irregularis* (Glomeromycota) was specified as the outgroup. Date constraints previously determined (Supplementary Table 4.3) were used as calibrations (Berbee and Taylor 2010; Prieto and Wedin 2013; Taylor and Berbee 2006; Hibbett et al. 1997; Smith et al. 2004). Chronograms and statistics were obtained with readdiv (parameters: -x 1000 50 md1), which is part of PhyloBayes 3.

Transmission electron microscopy

Actively growing hyphae of *B. undulatus* DAOM 241956, *G. donsium* DAOM 241966, and *W. sebi* CBS 633.66 were prepared for transmission electron microscopy using cryo-preparation methods. Hyphae were grown on thin, sterile, deionized dialysis membrane segments overlaying appropriate media at 23 ºC. The leading edge of growing mycelia and supporting membranes were trimmed with a sharp razor blade to approximately 5 × 5 mm and after 30–40 min (time to recover from trimming) were removed from the agar surface and immediately cryo-fixed by rapid plunging into liquid propane cooled to –186ºC with liquid nitrogen (McDaniel

and Roberson 2000; Roberson and Fuller 1988; Hoch 1986). After rapid freezing, the samples were freeze substituted in 1% glutaraldehyde (w/v) and 1% tannic acid (w/v) in anhydrous acetone at −85 °C for 72 h. After washing in cold acetone (−85 °C), the samples were warmed slowly to room temperature in 1% OsO_4 (w/v) in acetone, washed in acetone, and infiltrated and flat embedded on glass slides in Spurr's resin (Spurr 1969). Using phase contrast optics (100X), we examined the slides for well-preserved hyphae and mounted the selected cells on resin blocks (Howard and O'Donnell 1987) then hand-trimmed them. Selected hyphae were sectioned using a Leica Ultracut R ultramicrotome (Leica Microsystems Inc., Bannockburn, IL, USA), collected on copper grids, and post-stained for 10 min in 2% uranyl acetate in 50% ethanol and for 5 min in Sato's lead citrate (Hanaichi et al. 1986). Sections were then examined using a JEOL 1200EX (JEOL Ltd., Tokyo, Japan) transmission electron microscope equipped with a SIA L3C CCD camera (SIA Inc., Duluth, GA, USA). Measurements from captured images were made with ImageJ (Schneider et al. 2012).

Results

Genome sequencing, assembly and annotation

Short-read Illumina sequencing generated approximately 12 million paired end reads (6 million reads in the forward (R1) direction and 6 million reads in the reverse (R2) direction) of 101 bp in length each. After trimming to 93 bp, about 1.1 Gb of data was assembled *de novo* to yield a genome assembly size of about 32 Mb. The GC content in *B. undulatus* was 58%. The final assembly contained 2992 scaffolds and the longest scaffold was 97 Kb. The nucleotide-wise coverage varied for each scaffold but it was 28X on average. The N50 statistic was 15 Kb. According to CEGMA, 81% and 88% of complete and partial CEG's, were detected respectively.

A total of 13935 gene models were detected *ab initio* using GeneMark-ES but only 6123 gene models were supported by evidence from protein alignment to the NCBI RefSeq fungal protein data. We kept the set of 6123 gene models with evidence for further manual annotation and used it in downstream analyses (Supplementary File 4.5). Only 3681 of these (60%) were considered complete because they contained a start and stop codon while the remaining 2442 (40%) lacked either a start codon, a stop codon, or both.

Table 4.1. Genome assembly and annotation statistics of *B. undulatus* compared to *W. sebi* and *W. ichthyophaga*.

Descriptive statistic	*B. undulatus*	*W. sebi*	*W. ichthyophaga*
Genome assembly			
Sequencing platform	Illumina Hi-Seq	Illumina Hi-Seq & 454	Illumina Hi-Seq
Total number of reads	12 Million[a]	–	–
Read length after trimming	93 bp	–	–
Data size	1.1 Gb	–	3.7 Gb
Assembly size	32 Mb[c]	9.8 Mb	9.6 Mb
Estimated Percent GC	58%[c]	40%	45%
Mean nucleotide-wise coverage	28X[b]	71X	>270X
Number of Scaffolds	2992[c]	56	82
Longest scaffold size	97 Kb[c]	900 Kb	790 Kb
N50	15 Kb[c]	340 Kb	440 Kb
Genome annotation			
Percent core eukaryotic genes detected	88%[d]	–	–
All predicted gene models	13935[e]	5284	4863
Evidence supported gene models	6123[e]	–	–
Complete gene models	3681	–	–

Statistics were found by the following programs: [a]FastQC, [b]qualimap,[c]QUAST, [d]CEGMA, [e]MAKER

Meiosis and meiosis specific genes

To determine whether the putative sexual structures identified by Nguyen et al. (2013) represented the teleomorph, we followed the fungus's ontogeny and performed nuclear staining (Figure 4.1). Three nuclear divisions normally occur during basidiospore maturation: meiosis I, meiosis II, followed by four different patterns of post-meiotic mitosis (Duncan and Galbraith 1972). We observed dikaryotic nuclei in the basidia (Figure 4.1A), karyogamy (Figure 4.1B), anaphase I (Figure 4.1C), and the telophase I stage where the basal lateral projection was collapsed (Figure 4.1D). Four nuclei from telophase II (Figure 4.1E) were seen in non-ejected and ejected basidia as well (Figure 4.1F). The migration of a nucleus through the sterigma (Figure 4.1G) into the basidiospore (Figure 4.1H) was

observed as the basidiospore matured. There were three remaining nuclei in the collapsing basidium (Figure 4.1I) and they eventually degenerated at a later stage where the basidium completely collapsed (Figure 4.1J). Whole arthroconidia became stained instead of just their nuclei when DAPI was used. Although their nuclei could not be observed using DAPI, a single nucleus could be spotted in each arthroconidium using SYTO-9 instead (Figure 4.1K–L).

Our microscopic observations are correlated with our analysis of the genome to detect meiosis genes (Supplementary Table 4.4). All meiosis-specific genes, as defined in (Malik et al. 2008; Halary et al. 2011), were found in the genome.

Mating genes

We looked for mating genes such as ones encoding for homeodomain proteins, G-protein coupled pheromone receptor, high mobility group (HMG) DNA binding proteins, mitogen-activated protein kinases (MAPK, MAPKK, MAPKKK) and the subunits of the trimeric GTPase protein (Gα, Gβ, Gγ) (James et al. 2013). We followed the *S. cerevisiae* standard for gene names. Most of the mating response genes and the pheromone processing genes (see Supplementary Table 4.5 for details) were detected in the *B. undulatus* genome. All of the detected mating genes were located on different scaffolds except for *KSS*1 and *FUS*3, which were located on scaffold 2837. The presence of most mating genes suggests that a mating type locus exists but its structure and gene order could not be determined because our assembled genome is too fragmented.

Figure 4.1. *Basidioascus undulatus* DAOM 241956 sexual and asexual structures stained with DAPI and SYTO-9. A. Dikaryotic basidium (2 nuclei). B. Karyogamy. C. Anaphase I. D. Telophase I and collapsed basal lateral projection. E. Telophase II (4 nuclei). F. Ejected basidium (4 nuclei). G–H. Maturation of a basidiospore on a basidium and the migration of a nucleus through the sterigma and into the basidiospore. I. Collapsing basidium with the three remaining nuclei. J. A totally collapsed basidium and probably one nucleus inside the mature basidiospore. K–L. Single nuclei inside arthroconidia stained with SYTO-9. Scale bar = 5 µm.

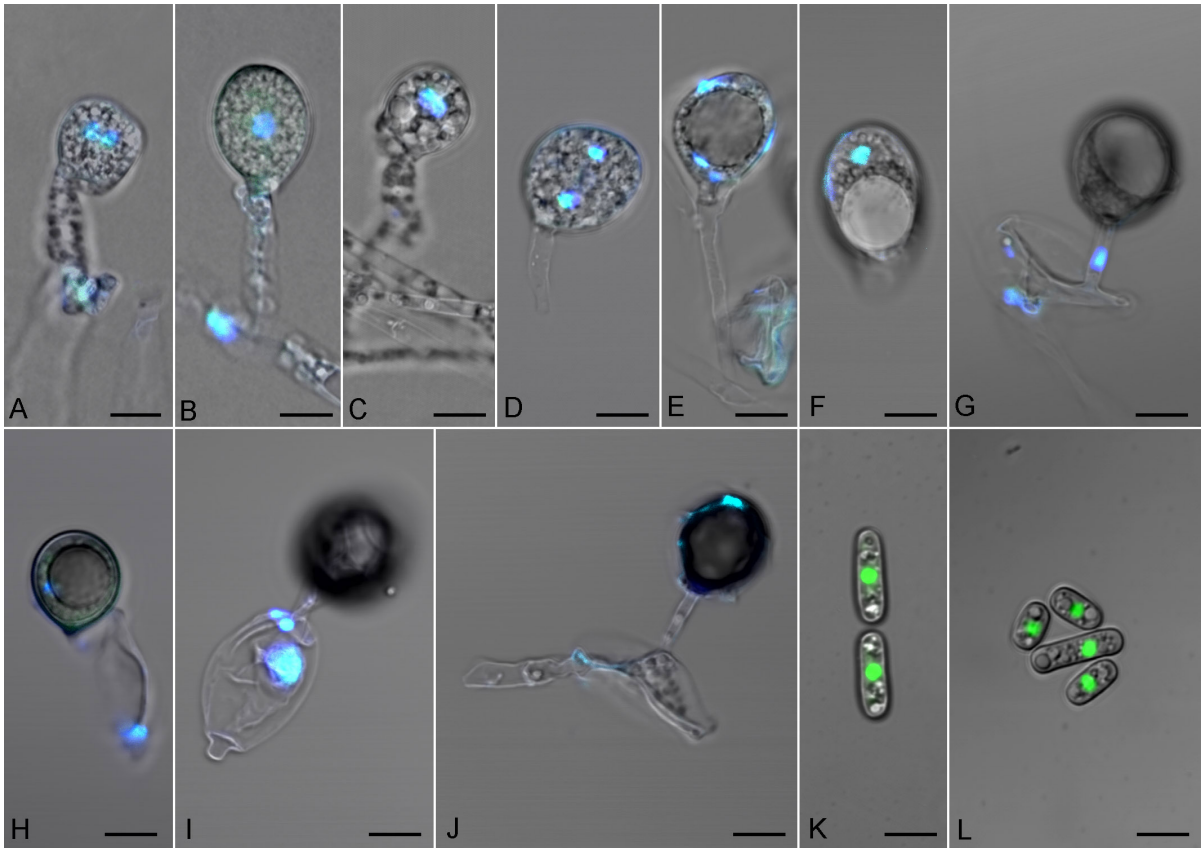
A
B
C
D
E
F
G
H
I
J
K
L

Septal pore morphology

We imaged the septal pores of *W. sebi*, *B. undulatus* and *G. donsium*, all currently classified in the Wallemiomycetes, using identical fixation methods to strengthen comparisons (Figure 4.2). *Basidioascus undulatus, G. donsium* and *W. sebi* all have a dolipore septum characteristic of the Agaricomycotina. The pore swelling of *B. undulatus* and *G. donsium* is electron dense but is not so in *W. sebi*. The adseptal tubular extensions that arise from sheets of endoplasmic reticulum in *W. sebi* were obvious (Figure 4.2E–F) but they were either absent or unclear in *B. undulatus* (Figure 4.2A–B) and *G. donsium* (Figure 4.2C–D). Electron-dense regions were observed near the septal pore in all three fungi but this area was denser in *W. sebi* than in *B. undulatus* and *G. donsium*. An electron-dense septal pore occlusion extending across the septal pore was observed in all three fungi. This occlusion was non-membranous in *W. sebi*, which agrees with previously published findings (Padamsee et al. 2012; Terracina 1974) and the *W. sebi* data on the AFTOL Structural and Biochemical Database (Celio et al. 2006). The septal pore occlusion in *B. undulatus* and *G. donsium* had a membrane making it more clearly defined than that of *W. sebi*. Furthermore, this occlusion was almost two times wider in *B. undulatus* (mean 0.114 µm) and *G. donsium* (mean 0.118 µm) than in *W. sebi* (0.064 µm). Also, the septal pore of *W. sebi* had striations that appeared to be fine fibrils vertically arranged at the pore opening but these were absent in *B. undulatus* and *G. donsium*. We did not see a septal pore cap in our sections of *W. sebi*, *B. undulatus* and *G. donsium*.

Figure 4.2. Transmission electron micrographs showing septal pore morphology. A–B. *Basidioascus undulatus* DAOM 241956 ex-type. C–D. *Geminibasidium donsium* DAOM 241966 ex-type. E–F. *Wallemia sebi* CBS 633.66.

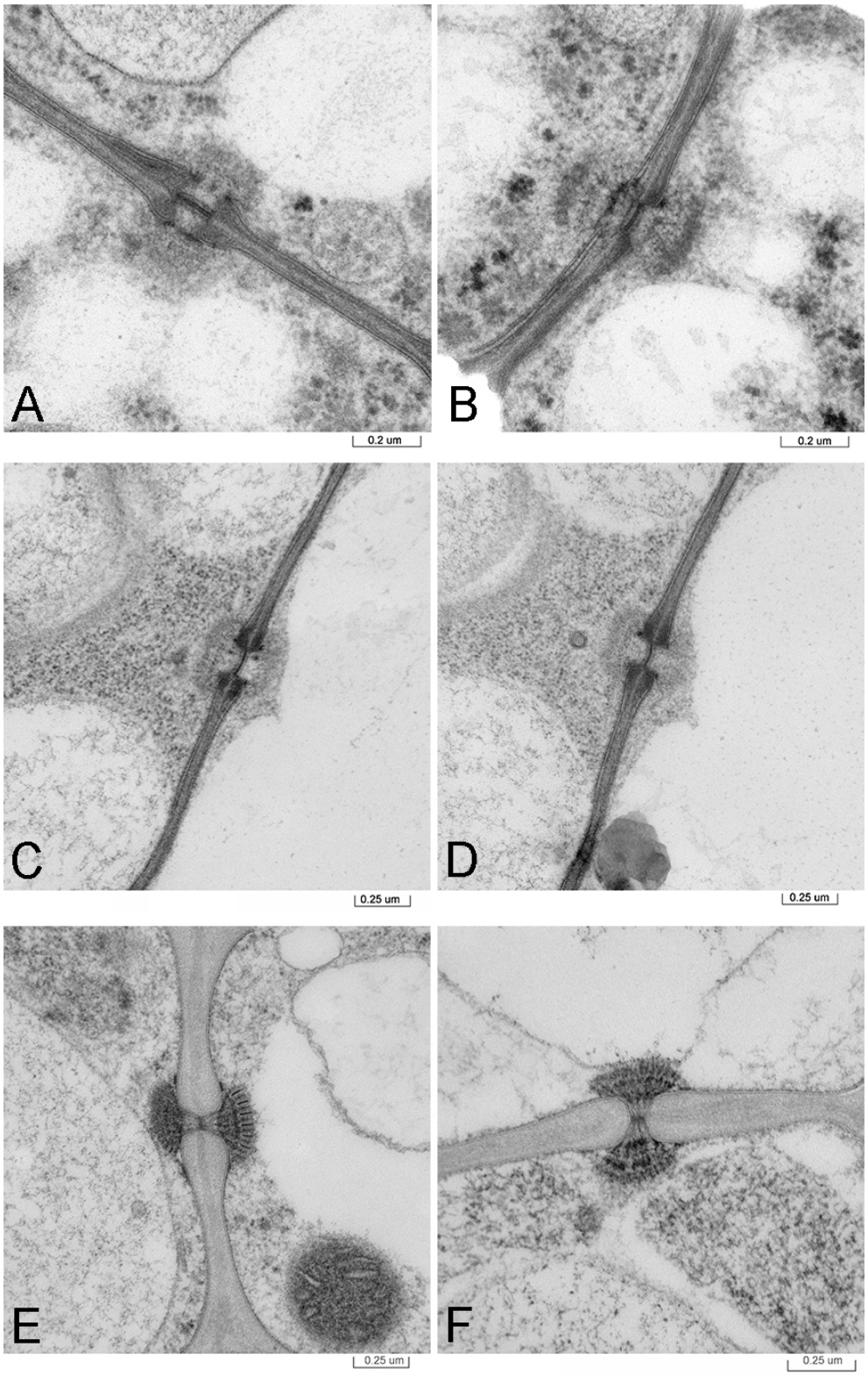
A
0.2 um
B
0.2 um
C
0.25 um
D
0.25 um
E
0.25 um
F
0.25 um

Phylogenomic analysis and molecular dating

Because *Basidioascus* is currently classified in the Wallemiomycetes, and the phylogenetic position of the fungi classified in this class is unstable in different analyses as a result of sparse taxon sampling, low gene sampling and conflicts in certain genealogies (Matheny et al. 2006; Zalar et al. 2005), we performed a phylogenomic analysis using protein sequences from 35 single copy protein-coding genes to study its phylogenetic position in a more robust fashion (Figure 4.3A). Our results were similar to those obtained from the rDNA phylogenetic analysis in Nguyen et al. (2013), showing *Basidioacus* as a distant lineage to *Wallemia*, with a posterior probability of 1.00.

We dated the divergence of *Basidioascus* from other lineages using some reliable fossil data of basidiomycetes (Hibbett et al. 1997; Smith et al. 2004) and the latest calculated calibration points (Berbee and Taylor 2010; Prieto and Wedin 2013) (Figure 4.3B). Under our assumptions, the split between *B. undulatus* and *Wallemia* was estimated at 250±29 Mya. The split between *W. sebi* and *W. ichthyophaga* was 33±6 Mya.

Figure 4.3. Phylogenetic trees resulting from phylogenomic analysis and molecular dating. A. Consensus topology and branch lengths from analyses of concatenated amino acid sequences from 35 single copy genes. There was a total of 10129 data columns. Gapped and poorly aligned sites were removed. Analyses were performed with the CATGTR model. Posterior probabilities are shown at nodes of the tree. Scale bar indicates expected changes per site. B. Chronogram resulting from a lognormal relaxed molecular clock analysis with the birth-death prior. The mean divergence time with standard error are shown at each node. Circled nodes were pre-calibrated before the analysis. The paleontological periods, in million years ago (Mya), are shown as a scale at the bottom. *Rhizophagus irregularis* (Glomeromycota) was used as the outgroup.

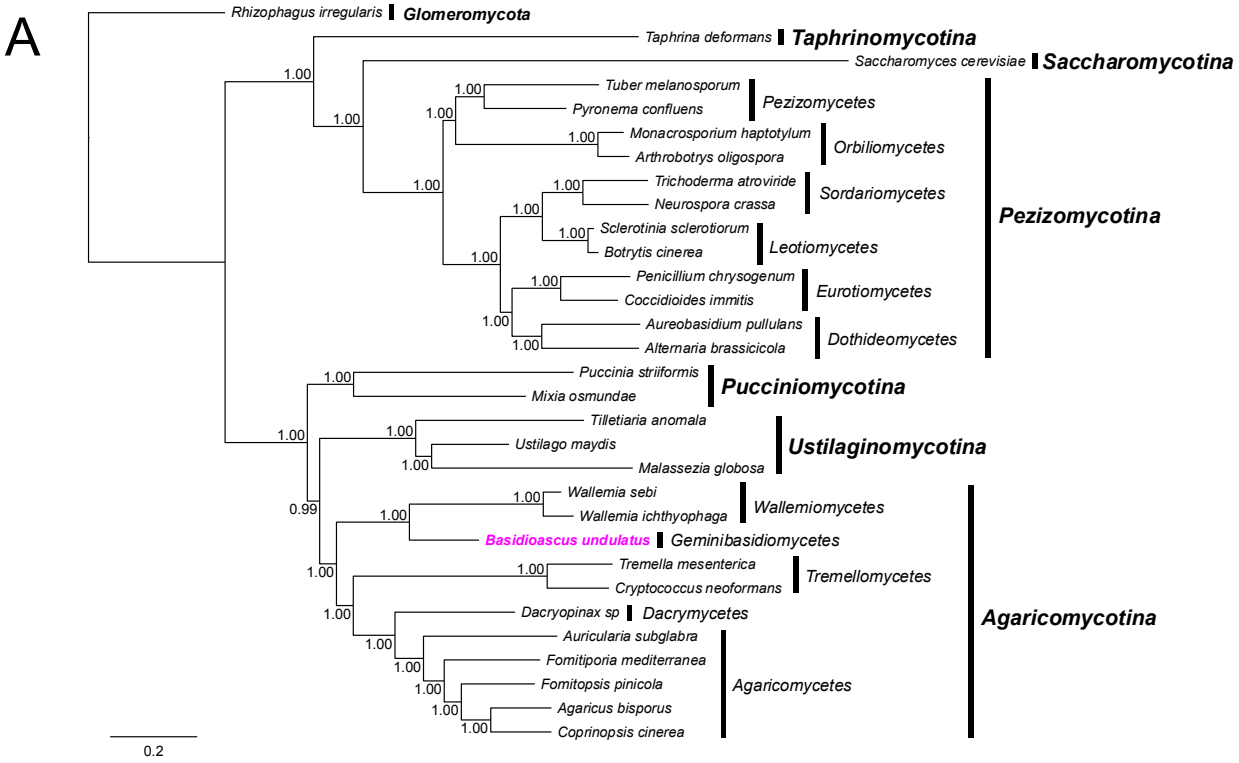
A
Rhizophagus irregularis
Glomeromycota
Taphrina deformans
Taphrinomycotina
Saccharomyces cerevisiae
Saccharomycotina
Tuber melanosporum
Pyronema confluens
Pezizomycetes
Monacrosporium haptotylum
Arthrobotrys oligospora
Orbiliomycetes
Trichoderma atroviride
Neurospora crassa
Sordariomycetes
Sclerotinia sclerotiorum
Botrytis cinerea
Leotiomycetes
Penicillium chrysogenum
Coccidioides immitis
Eurotiomycetes
Aureobasidium pullulans
Alternaria brassicicola
Dothideomycetes
Pezizomycotina
Puccinia striiformis
Mixia osmundae
Pucciniomycotina
Tilletiaria anomala
Ustilago maydis
Malassezia globosa
Ustilaginomycotina
Wallemia sebi
Wallemia ichthyophaga
Wallemiomycetes
Basidioascus undulatus
Geminibasidiomycetes
Tremella mesenterica
Cryptococcus neoformans
Tremellomycetes
Dacryopinax sp
Dacrymycetes
Auricularia subglabra
Fomitiporia mediterranea
Fomitopsis pinicola
Agaricus bisporus
Coprinopsis cinerea
Agaricomycetes
Agaricomycotina
0.2

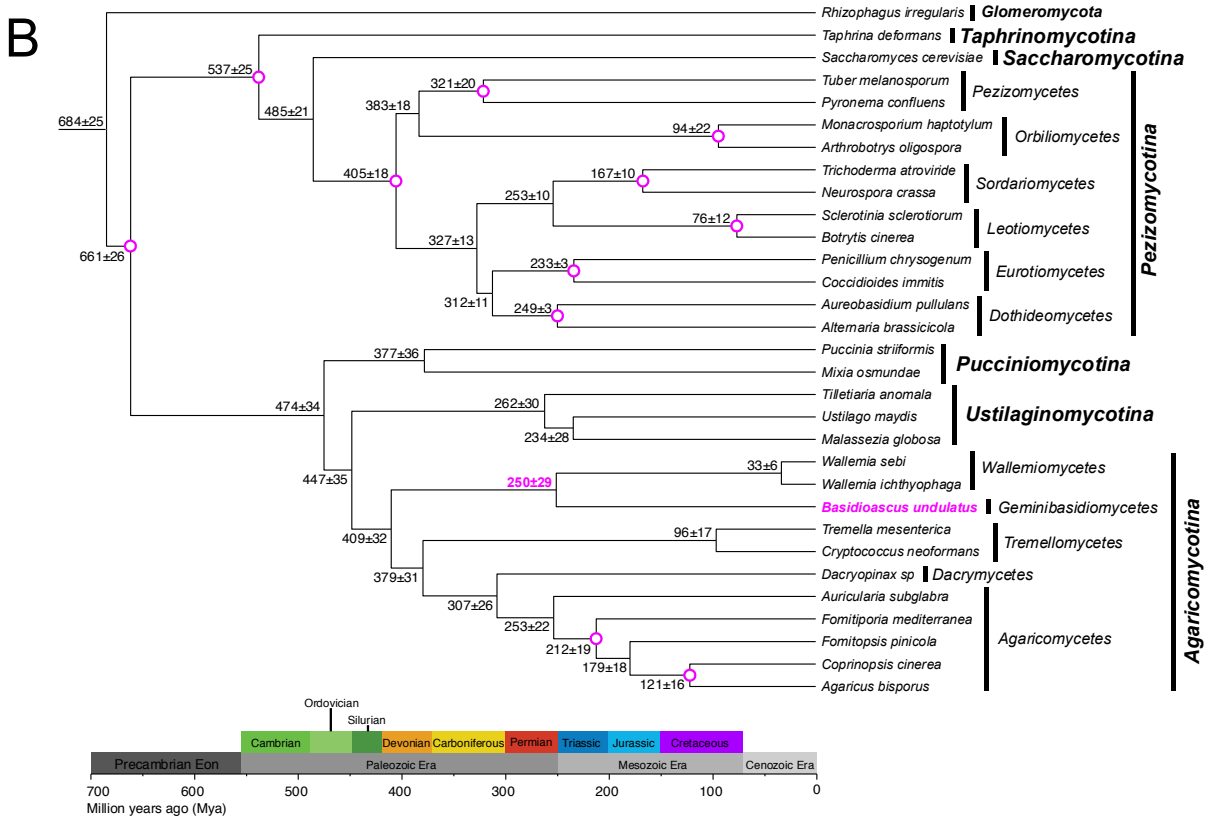
B
Rhizophagus irregularis
Glomeromycota
Taphrina deformans
Taphrinomycotina
Saccharomyces cerevisiae
Saccharomycotina
Tuber melanosporum
Pyronema confluens
Pezizomycetes
Monacrosporium haptotylum
Arthrobotrys oligospora
Orbiliomycetes
Trichoderma atroviride
Neurospora crassa
Sordariomycetes
Sclerotinia sclerotiorum
Botrytis cinerea
Leotiomycetes
Penicillium chrysogenum
Coccidioides immitis
Eurotiomycetes
Aureobasidium pullulans
Alternaria brassicicola
Dothideomycetes
Pezizomycotina
Puccinia striiformis
Mixia osmundae
Pucciniomycotina
Tilletiaria anomala
Ustilago maydis
Malassezia globosa
Ustilaginomycotina
Wallemia sebi
Wallemia ichthyophaga
Wallemiomycetes
Basidioascus undulatus
Geminibasidiomycetes
Tremella mesenterica
Cryptococcus neoformans
Tremellomycetes
Dacryopinax sp
Dacrymycetes
Auricularia subglabra
Fomitiporia mediterranea
Fomitopsis pinicola
Coprinopsis cinerea
Agaricus bisporus
Agaricomycetes
Agaricomycotina
537±25
321±20
383±18
485±21
684±25
94±22
405±18
167±10
253±10
76±12
327±13
661±26
233±3
312±11
249±3
377±36
474±34
262±30
234±28
33±6
447±35
250±29
409±32
96±17
379±31
307±26
253±22
212±19
179±18
121±16
Ordovician
Silurian
Cambrian
Devonian
Carboniferous
Permian
Triassic
Jurassic
Cretaceous
Precambrian Eon
Paleozoic Era
Mesozoic Era
Cenozoic Era
700
600
500
400
300
200
100
0
Million years ago (Mya)

Discussion

Genome sequencing and annotation

Basidioascus undulatus is the first fungus in the Geminibasidiales with a sequenced genome. The 1.1 Gb of sequence data gave a nucleotide-wise coverage of 28X and a final assembly that contained 2992 scaffolds, which is similar in coverage to other recent whole genome sequencing studies (Sims et al. 2014). *Wallemia sebi* and *W. ichthyophaga* were the closest known relatives to *B. undulatus*. Despite being considered close relatives previously, the genome assembly size of *B. undulatus* (32 Mb) was larger than *W. sebi* (9.8 Mb) (Padamsee et al. 2012) and *W. ichthyophaga* (9.6 Mb) (Zajc et al. 2013). Also, the GC content of *B. undulatus* was higher (58%) compared to *W. sebi* (40%) (Padamsee et al. 2012) and *W. ichthyophaga* (45%) (Zajc et al. 2013) (Table 4.1). Based on these results, they should be considered relatively distantly related.

The N50 value is often used in genome assembly to assess completeness. This statistic is more informative when genome assemblies of closely related species are compared, especially where a complete reference genome of that species was assembled to the chromosome level. Given that we lacked a genome of a closely related species to assess completeness with N50, we also evaluated the presence of core eukaryotic genes (CEG's) in our genome assembly. We were able to detect 88% of partial CEG's. We assumed that downstream annotation with this genome assembly should, in theory, reveal close to the same proportion of the true number of genes contained in *B. undulatus.* In this case, the percentage of observed CEG's is more useful at assessing completeness than N50. Most draft

fungal genomes are not assembled into chromosomes by analyses and it would be more informative for genomic studies to report the percentage of observed CEG's in addition to the N50 statistic as was done by van der Nest et al. (2014).

Many gene prediction tools are available, but the gene prediction tool GeneMark-ES was selected because it was shown previously to be accurate at detecting genes in fungal genomes (Ter-Hovhannisyan et al. 2008). GeneMark-ES considers branch point sequences in the intron model, which guides lariat formation during splicing, providing greater accuracy at locating intron boundaries. Because RNA data was not acquired in our study, we chose to use GeneMark-ES, which does not require RNA data for algorithm training. Genome annotation based on genome sequence alone has limitations. The first is that without RNA data, coding sequence (CDS) predictions cannot be validated and genes from splice sites that use donor and acceptor sequences other than the canonical GT-AG introns cannot be predicted. The frequencies of the non-canonical GC-AG introns are 1.0-1.2% in some Ascomycetes (Rep et al. 2006) and could be as high as 3% in Basidiomycetes (Misiek and Hoffmeister 2008). To compensate for the absence of RNA data, the fungal NCBI RefSeq protein sequence data set (Mar 13, 2014 release), which contains curated protein sequences from completed fungal genome projects, was aligned to our *B. undulatus* genome using exonerate. Exonerate is an advanced alignment tool that can align protein sequences to a genome and will allow introns in the alignment, frameshifts, and exon phase changes when a codon is split by an intron. This approach should help validate most of the conserved genes without RNA sequence data but will not help in the discovery of novel genes. In the MAKER2 pipeline, aligning protein sequences to predicted genes on the genome

generates ‘evidence’ expressed as the exon AED (eAED) score. The eAED score is a metric that measures how a predicted gene determined from GeneMark-ES agrees with the protein alignment evidence from exonerate while accounting for protein reading frames shifts. This score is helpful for assessing annotation quality of a predicted gene (Eilbeck et al. 2009). Overall, 13935 genes were predicted by GeneMark-ES but only 6123 of those genes were supported by protein alignment evidence. For each of the 6123 predicted genes, we made further functional annotation with a BLAST search against the UniProt/Swiss-Prot manually curated data set and an InterProScan analysis. Using this information, 452 genes were manually annotated with confidence (see Supplementary File 4.5). Future releases of the *B. undulatus* genome with RNA sequence data would increase the number of annotated genes and allow discovery and validation of completely novel genes or splice variants.

Meiosis

We used genomic information in combination with confocal microscopy to gain further understanding of sexuality in *B. undulatus*. Fungal taxonomists infer function of meiosporangia in newly discovered fungi based on morphological similarities to proven meiosporangia in similar or related fungi. Proof of meiosis by nuclear staining is not usually required. In our case, *B. undulatus* is different morphologically, ontogenetically and phylogenetically from known basidiomycetes and it was difficult to assess whether previous morphological interpretations (Nguyen et al. 2013) were correct without nuclear staining experiments. It was suggested previously that the clavate structures found on somatic hyphae were basidia (Nguyen et al. 2013). These basidia were deciduous, forcibly discharged,

and had a basal lateral projection that eventually collapsed. Sterigmata grew on the basidium and basidiospores developed at the tip of each sterigma. To verify these interpretations, we visualized these putative sexual structures with nuclear staining and confocal microscopy. Our observations suggested that meiosis occurred in the clavate structures (Figure 4.1) providing the evidence for previous interpretation of them as basidia. Post-meiotic mitosis in the basidium was not seen but it was difficult to visualize nuclei in the mature basidiospores. Although we saw evidence of meiosis with microscopy, we also confirmed the presence of meiosis genes in the genome (Supplementary Table 4.4). We did not detect *HOP*2 among the 10 meiosis specific genes. The *HOP*2 gene product is involved in preventing synapsis between non-homologous chromosomes during meiotic double-strand break repair (Malik et al. 2008). The function of *HOP*2 could be served by another unknown gene or gene product or perhaps our genome assembly was not complete enough to detect it. With 88% of CEG's detected, about 1 out of every 10 genes would not be detected during the annotation procedure.

Basidioascus undulatus produced cells attached in chains, which are presumed to be arthroconidia (Nguyen et al. 2013). Arthroconidia were indeed single nucleated (Figure 4.1K–L) and therefore represent the anamorph of *B. undulatus*. Given these results, *B. undulatus* indeed exhibits both the teleomorph and anamorph in culture.

Mating

The genes located at the MAT locus orchestrate the fungal mating process and determines the sex of individuals (Lee et al. 2010). In the fungal kingdom, mating is most comprehensively studied in *S. cerevisiae*. Therefore, we used what

is known about mating in *S. cerevisiae* as a model to guide our interpretations of mating genes in the *B. undulatus* genome.

Homeodomain (HD) transcription factors control the expression of pheromone and pheromone receptor genes. Normally, dimerization occurs between two paralogous HD transcription factors, HD1 and HD2, to form HD1-HD2 complex. In *U. maydis*, this is called the bE/bW heterodimer and in *S. cerevisiae* it is called the a1/α2 complex (Lee et al. 2010). We identified the HD1 (8946F71C4C) and HD2 (AF24C22F02) proteins in *B. undulatus*.

Pheromone production and processing are also important in mating. All orthologs for pheromone processing (*KEX*1, *KEX*2, *STE*13, *RAM*1, *RAM*2, *STE*14, *AXL*11, *STE*6) were detected in *B. undulatus* except for the *RCE*1/*STE*24 genes responsible for cleavage (Supplementary Table 4.5). Perhaps the cleavage step is the function of another protein, is unnecessary, or was simply undetected with our current genome assembly.

Upon release into the environment, pheromones must bind to pheromone receptors to initiate a signaling cascade involving the mitogen-activated protein kinase (MAPK) pathway to turn on mating genes (Jones and Bennett 2011). MAPK pathways regulate the activity of high mobility group (HMG) DNA binding proteins, which are transcription factors regulating pheromone responsive genes in the MAT loci (Hartmann et al. 1996). Most of the mating response genes were detected (*STE*3, *KSS*1, *FUS*3, *STE*7, *STE*11, *GPA*1, *STE*4, *STE*20) (Supplementary Table 4.5) except the G-protein γ subunit (*STE*18), the transcription factor *STE*12, the coordinator of MAPK pathway *STE*5, and the cell cycle control *FAR*1 protein. We

identified four HMG DNA binding proteins (B013112742, C8B77D01D8, C1AD40EA22, and 9CC40B0A26).

We were unable to isolate single arthroconidia or successfully germinate basidiospores so mating tests were not possible. Thus, it is unknown whether *B. undulatus* is homothallic or heterothallic. *Wallemia sebi* apparently has a bipolar mating system (Padamsee et al. 2012) but no discernible mating type locus could be identified in the genome of *W. ichthyophaga* (Zajc et al. 2013). Our genome assembly was too fragmented to determine the structure of the mating type locus conclusively and therefore the mating system in *B. undulatus* remains uncharacterized until more sequencing is done. The detection of a near complete cellular machinery for the mating response, pheromone processing, and meiosis suggests that *B. undulatus* is capable of outcrossing. However, future experiments with gene knockout mutants will be needed to validate these identified genes.

Higher classification and divergence of the Geminibasidiales

Basidioascus undulatus and *G. donsium* are classified in the Geminibasidiales, a sister order to the Wallemiales. The Geminibasidiales was placed tentatively in the class Wallemiomycetes (Nguyen et al. 2013). The main reason for this inconclusive placement, at that time, was the absence of septal pore ultrastructure data and the fact that only ribosomal genes could be used to make a phylogenetic analysis with enough taxon sampling to reach a conclusion. More genomes are available now and phylogenomic analysis with protein coding genes is more feasible and informative.

Our phylogenomic analysis shows the same relationships previously determined with rDNA, where *Wallemia* and *Basidioascus* are distantly related sister

groups that occupy a basal phylogenetic position in the Agaricomycotina (Figure 4.3A). The distance of this relationship is also reflected in differences in GC content and genome size between *B. undulatus* and *Wallemia* discussed above. According to the sampling and assumptions made in our analyses, molecular dating suggests that the split between *B. undulatus* and *W. sebi* occurred 250 Mya (Figure 4.3B), which is around the same time that the Sordariomycetes split from the Leotiomycetes (253 Mya) and the Exobasidiomycetes split from the Ustilaginomycetes and Malasseziomycetes (262 Mya). If this is accurate, it means *Wallemia* and *B. undulatus* shared a common ancestor until a divergence event occurred between the Permian and Triassic period when the Earth was hot and dry in some places (Kidder and Worsley 2004). Interestingly, it was during this period that Earth experienced its most severe extinction event (Sahney and Benton 2008). Species of the Geminibasidiales are heat resistant (Nguyen et al. 2013) while species of *Wallemia* are not heat resistant (Vytrasova et al. 2002). Perhaps the Geminibasidiales split from Wallemiales when their ability to adapt to a hot climate gave them a competitive ecological advantage. The split between *W. sebi* and *W. ichthyophaga* was 33±6 Mya. This estimate differs from previous analyses that indicate a 11.9 Mya split (Zajc et al. 2013), although different methods, taxon sampling and calibrations were used for that molecular dating analysis. These should be considered rough estimates because the fungal fossil record is rather limited and many studies obtained radically different age estimates for the same divergence events (Lücking et al. 2009).

Before sequence data began to dominate fungal systematics, morphological characters of the septa and septal pore caps were important for classifying fungi at a

class or higher taxonomic level (Khan and Kimbrough 1982; Oberwinkler and Bandoni 1982; Müller et al. 2000; van Driel et al. 2009) and septal pore morphology is still considered essential for delimiting classes in the Basidiomycota. However, the overall septal pore morphologies of *B. undulatus* and *G. donsium* are similar and there are significant differences when compared to *W. sebi* (described in results section and depicted in Figure 4.2). The septal pore cap is probably not a reliable or practical feature for classification of *Wallemia*, *Basidioascus* and *Geminibasidium* because it is sometimes present or absent in *Wallemia* (Padamsee et al. 2012; D.J. McLaughlin pers. comm.) and was not seen in *B. undulatus* or *G. donsium*.

Given the results obtained from phylogenomics analysis, molecular dating, and septal pore ultrastructure, we propose to classify the Geminibasidiales in a new class Geminibasidiomycetes. Although *Geminibasidium* could not be included in the phylogenomic analysis and molecular dating because its genome is not yet sequenced, we are confident from previous rDNA phylogenetic analysis (Nguyen et al. 2013), morphological characters, and similarities in the septal pore morphology (Figure 4.2) that *Geminibasidium* will remain a close sister group to *Basidioascus*. Previous phylogenies position the Wallemiomycetes at the base of Basidiomycota (Zalar et al. 2005; Matheny et al. 2006), as a sister group to or as the earliest diverging lineage of the Agaricomycotina (Padamsee et al. 2012; Zajc et al. 2013; Nguyen et al. 2013). The classification for the Wallemiomycetes is shown as *incertae sedis* in the Basidiomycota in the NCBI Taxonomy (Federhen 2012), MycoBank (Robert et al. 2013), and the Encyclopedia of Life (http://www.eol.org). In the taxonomy section below, we emend the description of the subphylum Agaricomycotina to include the classes Geminibasidiomycetes and

Wallemiomycetes along with the Agaricomycetes, Tremellomycetes and Dacrymycetes, which are well delimited classes of the Agaricomycotina (Hibbett 2006). By formally connecting the basal Geminibasidiomycetes and Wallemiomycetes to the Agaricomycotina, we eliminate the uncertain status of these taxa. The subphylum name Wallemiomycotina was effectively published recently to accommodate *Wallemia* (Doweld 2014). There was no discussion of the rationale behind this proposal and we consider it unnecessary to include the Wallemiomycetes (with or without the Geminibasidiomycetes) in its own subphylum.

Taxonomy

Agaricomycotina Doweld Prosyllabus LXXVII (2001)

Homonym. Agaricomycotina R. Bauer, Begerow, J. P. Samp., M. Weiß & Oberw., Mycol. Progr. 5: 45 (2006).

MycoBank MB 560553

Description. Members of the Basidiomycota that have a cell wall carbohydrate composition with dominance of glucose and presence of xylose and having a type B secondary structure of the 5S RNA (Bauer et al. 2006). Fungi that belong to this subphylum are classified in the classes Agaricomycetes, Dacrymycetes, Tremellomycetes, Wallemiomycetes or Geminibasidiomycetes.

Notes. Although Agaricomycotina Dowell (2001) is the oldest name, the actual concept of Agaricomycotina by Bauer et al. (2006) (Hymenomycetes sensu Swann and Taylor (1995)) is widely used today by mycologists. We modified it only to explicitly state all of the accepted classes within the Agaricomycotina. The cell wall

of *B. persicus* was composed mostly of glucose and xylose (Nasr et al. 2014) and assuming that this is the same for other species of *Basidioascus* and *Geminibasidium*, this placement for the Geminibasidiomycetes is appropriate. The cell wall carbohydrate composition of *Wallemia* species is unknown.

Wallemiomycetes P. Zalar, G.S. de Hoog and H.-J. Schroers

MycoBank MB 501496

Description. Class of xerophilic basidiomycetes belonging to the subphylum Agaricomycotina. These fungi produce basauxic anamorphs and do not produce basidiomata in culture. Species have dolipore septa with adseptal tubular extensions that arise from sheets of endoplasmic reticulum that form the septal pore cap. The septal pore cap is sometimes absent. The septal pore has an electron-dense non-membranous septal pore occlusion and striations that are oriented vertically.

Type order. Wallemiales.

Notes. This description is altered to exclude characters of the Geminibasidiales previously added to the concept of Wallemiomycetes by Nguyen et al. (2013). Information about the septal pore morphology was added, as detailed in Padamsee et al. (2012).

Geminibasidiomycetes H.D.T. Nguyen & Seifert, cl. nov.

MycoBank MB 811680

Description. Class of xerotolerant basidiomycetes belonging to the subphylum Agaricomycotina. Basidiomata are not produced in culture. Basidia arise from

somatic hyphae or from swollen basidium bearing cells (primary cells) with a basal lateral projection occurring either on the basidium or the swollen primary cell. Basidiospores are symmetrical on sterigma, not forcibly discharged, and brown at maturity. Some species are heat resistant. Arthroconidial and/or yeast-like anamorphs are sometimes produced. Species have a dolipore septum that is electron-dense at the pore swelling with an electron-dense membranous septal pore occlusion.

Type order. Geminibasidiales.

Acknowledgments

We thank: A. Pelin and Z. Adam for discussions on genome assembly, M. Li for advice on genome annotation with MAKER2, C. Lowe for guidance on doing phylogenic analyses with PhyloBayes, K. Bradnam for running CEGMA, C. Grace and K. Fisher for help with TEM, J. Cullis for reviewing an early draft of the manuscript, the staff at the DNA Technologies Laboratory at the National Research Council Canada in Saskatoon for performing library construction and Illumina sequencing.

Author contribution

HDTN conceived and designed the work. HDTN, DC and YH acquired the data: HDTN and DC performed confocal microscopy; YH helped with mating tests; the acknowledged students of RWR performed transmission electron microscopy; HDTN sequenced, assembled, and annotated the genome. HDTN analyzed and interpreted the data. HDTN drafted the article. HDTN, DC, YH, RWR and KAS critically revised the manuscript for important intellectual content.

Chapter 5: Conclusions

Hai D.T. Nguyen[1,2]

[1] Department of Biology, Faculty of Science, University of Ottawa, Ottawa, Ontario, Canada

[2] Biodiversity (Mycology), Eastern Cereal and Oilseed Research Centre, Agriculture and Agri-Food Canada, Ottawa, Ontario, Canada

There is a lot of interest in *Wallemia* because of its ubiquity in human indoor environments and its potential roles in human allergy and food spoilage. This journey began with a survey of indoor *Wallemia* species. DNA sequencing and phylogenetic analyses led to the characterization of four phylogenetic species within the *Wallemia sebi* species complex (WSSC).

The phylogenetic species hypothesis served as a guide for the phenotypic characterization of *W. sebi* strains from a wide range of substrates, climates and geographical locations in a companion study (Jančič et al. 2015). The phenotypic characterization involved measurements of conidial size, xerotolerance, halotolerance, chaotolerance, growth temperatures, extracellular enzyme activity, and secondary metabolite patterns. Although the companion study was not included in the body of my thesis, it was crafted in close collaboration with S. Jančič in Slovenia. I sequenced ITS, *RPB*2, *RPB*1, *MCM*7, *TSR*1 genes for the strains in that study and performed phylogenetic analyses (Figure 5.1) while S. Jančič carried out the phenotypic characterization and sequenced *HAL*2 as an additional gene. The phylogenetic analyses in that paper again confirmed the four phylogenetic species in the WSSC. Combined with phenotypic, biochemical, physiological characters, we divided the complex. The 'true' *W. sebi* was re-defined and three new species of *Wallemia* called *W. mellicola*, *W. tropocalis* and *W. canadensis* were formally described.

Figure 5.1. Midpoint rooted majority rule consensus Bayesian tree inferred from combined sequences. The tree from six aligned loci (ITS, *RPB*2, *RPB*1, *MCM*7, *TSR*1, *HAL*2) provides a resolved structure of the WSSC. Bayesian posterior probabilities are displayed at the nodes of the tree. Labels provide information on strain number and origin. Red T = ex-type strains; red NT = ex-neotype strain; bold = strains included in physiological and morphological studies, and for the determination of extracellular enzyme activities; underlined = strains included in studies of secondary metabolites. Scale bar = expected changes per site. Figure taken from Jančič et al. (2015).

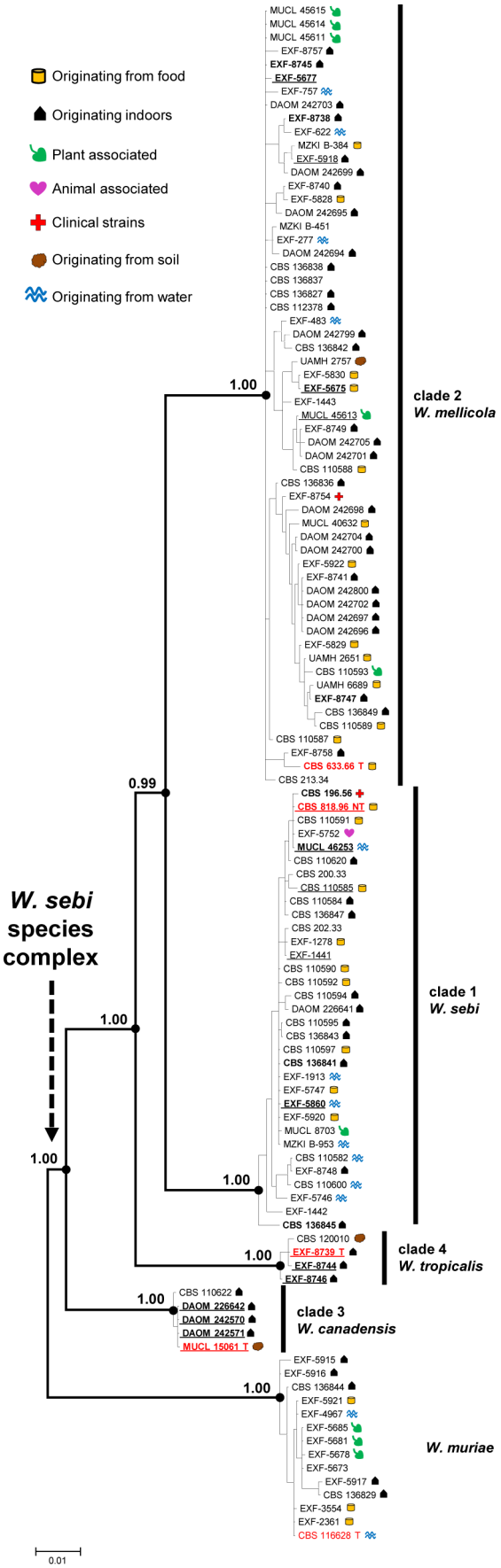
Originating from food
Originating indoors
Plant associated
Animal associated
Clinical strains
Originating from soil
Originating from water
W. sebi species complex
clade 2
W. mellicola
clade 1
W. sebi
clade 4
W. tropicalis
clade 3
W. canadensis
W. muriae
1.00
0.99
1.00
1.00
1.00
1.00
1.00
0.01

A survey of heat resistant fungi in soils coincidentally resulted in the discovery of a new lineage of fungi related to *Wallemia*. This new lineage included a previously described genus *Basidioascus* and a newly recognized sister genus given the name *Geminibasidium*. Part of the morphological life cycle of these fungi was observed for the first time. Although related to *Wallemia*, these fungi are very different morphologically and phylogenetically. Thus, these fungi were classified in a newly erected order called Geminibasidiales.

An in-depth study of the sexuality and origins of *Basidioascus undulatus* using genomic analyses, confocal microscopy and transmission electron microscopy was carried out in the last chapter of the thesis. Using nuclear staining and confocal microscopy, meiosis was observed in the structures putatively identified as the sexual structures of the fungus. The meiosis and mating type genes were detected in the genome by BLAST searches and by analyses of protein domains. Phylogenomic analysis was performed to assess its relationship to *Wallemia* species and molecular clock analysis was done in attempt to date the divergence of *B. undulatus* from *Wallemia* species. These results confirm a sister relationship but a distant one. Using transmission electron microscopy, the septal pore of *B. undulatus*, *G. donsium* were shown to be similar to each other but different than *W. sebi.* These results led to the creation of a new class Geminibasidiomycetes to accommodate these related fungi.

Fungal taxonomy is concerned with the characterization of fungal biodiversity on Earth. Overall, this work contributed to that effort and resulted in the characterization of additional species of *Wallemia* and the characterization of an

entire class of fungi, related to the Wallemiomycetes, called the Geminibasidiomycetes.

Future directions

This work opens the doors to new and exciting studies that are either currently ongoing or that could be undertaken in the future.

The distribution and ecological niches where *Wallemia* species might be found remain unexplored. A few research groups found new species of *Wallemia* outside of the WSSC and are describing them (M.C. Aime and S. Jančič pers. comm.). Fungi can associate with plants in a mutualistic or pathogenic relationship. *Wallemia muriae* and *W. mellicola* were found on plants in Slovenia and Cuba respectively (Jančič et al. 2015). This is unusual and somewhat unexpected because these fungi are not normally thought of as plant associated or part of the phylloplane. However, it could be because mycologists never thought to look for *Wallemia* on plants. Thus, *Wallemia*'s relationship with plants, whether mutualistic or pathogenic, could be interesting to study further.

The genome sequencing of *W. sebi* CBS 633.66 clade 2 (described as *W. mellicola* in Jančič et al. (2015)) revealed a full set of meiosis genes and a characterized bipolar mating type locus (Padamsee et al. 2012). Although these genes are presumed to be functional, *Wallemia* species have never been observed to mate and form sexual structures. Hence, it is thought that cryptic sexuality is occurring in *Wallemia*. Before the WSSC was resolved, it would be difficult to attempt mating tests because all strains would have been identified as *W. sebi*.

Now that the phylospecies in the WSSC are properly delineated, one could use this information to both accurately identify species and assign mating types to all strains. Doing this removes two variables from mating experiments leading to increased experimental efficiency. A mating test could be set up to induce the production of the sexual morph of *Wallemia* in culture. If successful, we could potentially see a new type of basidia. However, this assumes that the phylospecies of the WSSC are actually separate biological species.

The ecological roles of *Geminibasidium* are not known. One GenBank record of an undescribed species of *Geminibasidium* (accession number HM044636) lists the isolation source as “ectomycorrhized root tips”. Furthermore, *Geminibasidium* species were isolated from soils that were accidentally or intentionally burned (Chapter 3) and were found to be more abundant in burned forest soils in metagenomic studies (E. Cardenas Poire pers. comm.), which could be further clues to reveal the ecological role of *Geminibasidium.* Taken together, perhaps *Geminibasidium* plays a role as an ectomycorrhizae in the forest regeneration cycle after natural fires. Burnt soil was found to stimulate seedling growth significantly because of changes in nutrient and ectomycorrhizae (Launonen et al. 1999).

Many heat resistant moulds grow on Canadian blueberries (Jackson et al. 1996; Kikoku et al. 2008). In 1990, there was a large recall of shelf-stable products made from Canadian blueberries by German manufacturers because of spoilage caused by the fungus *Byssochlamys fulva* (Jackson et al. 1996). *Geminibasidium donsium* was found as a contaminant in imported Canadian frozen blueberries destined for jam production in Japan (Y. Kikoku pers. comm.). An effective pasteurization protocol was found to remove *G. donsium* during the jam production

process (Kikoku et al. 2014). However, frozen blueberries are also consumed raw so future studies could investigate whether *G. donsium* produces any harmful, or beneficial, metabolites that can affect human health.

Fungi protect themselves against heat, drought and other stresses by accumulating solutes (Wyatt et al. 2013). Glycerol accumulates in *Wallemia* upon exposure to a xeric environment (Lenassi et al. 2011). Mannitol and trehalose are solutes that accumulate in *Aureobasidium* upon heat stress (Managbanag and Torzilli 2002). Exposure to heat causes the upregulation of small heat shock proteins in *Saccharomyces cerevisiae* (Haslbeck et al. 2004) and the basidiomycete *Pisolithus* (Ferreira et al. 2005). The potential genetic mechanisms that confer heat resistance and xerotolerance in *Geminibasidium* and *Basidioascus* remain to be explored further. Being related to the Wallemiomycetes, glycerol accumulation is probably a key mechanism for xerotolerance in species of the Geminibasidiomycetes. *Wallemia* is not heat resistant. Given that the Geminibasidiomycetes are not closely related to other heat resistant basidomycetes, their heat resistance properties could involve novel and uncharacterized biochemical pathways. However, these speculations will have to be confirmed with further genetic studies. The *B. undulatus* genome presented in Chapter 4 could serve as a starting point in the planning and design of these studies.

Basidiomycetes have evolved many different basidial types (discussed in Chapter 1). The basidium of *Geminibasidium* arises from a swollen cell called the primary cell. *Basidioascus* has a unique dispersal method in that the entire basidium is forcibly ejected rather than just the basidiospore. These are considered a new basidial type to be added to our knowledge of basidia diversity (Figure 5.2).

Forcible ejection of spores is an important mechanism for dispersal. The mechanism for this basidial ejection in *Basidioascus* is unknown. In other fungi, spore ejection involves the coalescence of the Buller's drop with an abrupt change in the center of mass. This was recently captured with a high-speed camera (Pringle et al. 2005). One could perform a similar experiment with a high-speed or an ultra fast camera to study the mechanism of basidia ejection in *Basidioascus*.

Current research efforts on the Wallemiomycetes and Geminibasidiomycetes remain on a fundamental level. The economic impact of these fungi is so far unknown. Given their extremophilic nature and isolated evolutionary position in the fungal kingdom, there is potential for discovery of new species, unusual ecological roles, previously unknown dispersal mechanisms, unique stress tolerance genes, and perhaps useful biochemical compounds, enzymes and antibiotics.

Figure 5.2. Existing basidial types and new basidial types discovered in this thesis. A. *Puccinia* basidium germinating from a teliospore. B. *Ustilago* basidium germinating from a teliospore. C. Typical basidium of fungi in the Auriculariales. D. *Tremella* basidium. E. *Dacrymyces* forked basidium. F. Typical basidium of fungi in the Agaricales. G. A forcibly ejected basidium with an immature basidiospore from *Basidioascus* species. H. The primary cell, basidium and basidiospore of *Geminibasidium* species. Figures A–F were after (Begerow et al. 2014; Crous et al. 2009).

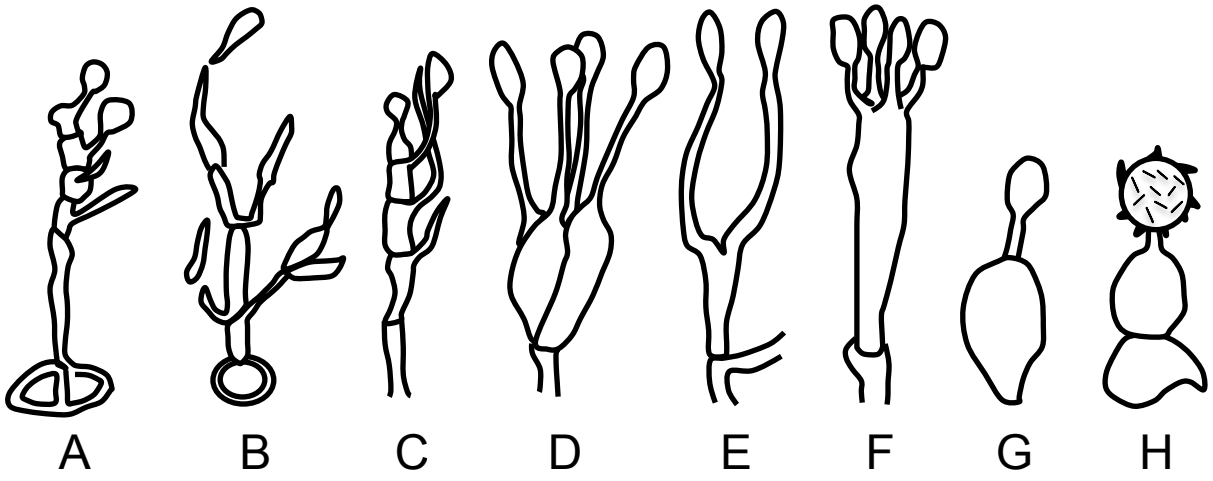
A
B
C
D
E
F
G
H

References

Aguileta G, Marthey S, Chiapello H, Lebrun MH, Rodolphe F, Fournier E, Gendrault-Jacquemard A, Giraud T (2008) Assessing the performance of single-copy genes for recovering robust phylogenies. Systematic Biology 57 (4):613-627. doi:10.1080/10635150802306527

Aime MC, Matheny PB, Henk DA, Frieders EM, Nilsson RH, Piepenbring M, McLaughlin DJ, Szabo LJ, Begerow D, Sampaio JP, Bauer R, Weiss M, Oberwinkler F, Hibbett D (2006) An overview of the higher level classification of Pucciniomycotina based on combined analyses of nuclear large and small subunit rDNA sequences. Mycologia 98 (6):896-905

Aime MC, Toome M, Mclaughlin DJ (2014) Pucciniomycotina. In:McLaughlin D, Spatafora J (eds) Systematics and Evolution (Part A). The Mycota. Springer

Amend AS, Seifert KA, Samson R, Bruns TD (2010) Indoor fungal composition is geographically patterned and more diverse in temperate zones than in the tropics. Proceedings of the National Academy of Sciences of the United States of America 107 (31):13748-13753. doi:10.1073/pnas.1000454107

Amselem J, Cuomo CA, van Kan JA, Viaud M, Benito EP, Couloux A, Coutinho PM, de Vries RP, Dyer PS, Fillinger S, Fournier E, Gout L, Hahn M, Kohn L, Lapalu N, Plummer KM, Pradier JM, Quevillon E, Sharon A, Simon A, ten Have A, Tudzynski B, Tudzynski P, Wincker P, Andrew M, Anthouard V, Beever RE, Beffa R, Benoit I, Bouzid O, Brault B, Chen Z, Choquer M, Collemare J, Cotton P, Danchin EG, Da Silva C, Gautier A, Giraud C, Giraud T, Gonzalez C, Grossetete S, Guldener U, Henrissat B, Howlett BJ, Kodira C, Kretschmer M, Lappartient A, Leroch M, Levis C, Mauceli E, Neuveglise C, Oeser B, Pearson M, Poulain J, Poussereau N, Quesneville H, Rascle C, Schumacher J, Segurens B, Sexton A, Silva E, Sirven C, Soanes DM, Talbot NJ, Templeton M, Yandava C, Yarden O, Zeng Q, Rollins JA, Lebrun MH, Dickman M (2011) Genomic analysis of the necrotrophic fungal pathogens *Sclerotinia sclerotiorum* and *Botrytis cinerea*. PLoS Genetics 7 (8):e1002230. doi:10.1371/journal.pgen.1002230

Auvrey M (1909) A propos d'une nouvelle mycose observée chez l'homme. Suppuration cervicale due à *Hemispora stellata*. Bulletin et mémoires de la Société des chirurgiens de Paris 20:686

Baldauf SL, Doolittle WF (1997) Origin and evolution of the slime molds (Mycetozoa). Proceedings of the National Academy of Sciences of the United States of America 94 (22):12007-12012

Baldauf SL, Palmer JD (1993) Animals and fungi are each other's closest relatives: congruent evidence from multiple proteins. Proceedings of the National Academy of Sciences of the United States of America 90 (24):11558-11562

Baldauf SL, Roger AJ, Wenk-Siefert I, Doolittle WF (2000) A kingdom-level phylogeny of eukaryotes based on combined protein data. Science 290 (5493):972-977

Bankevich A, Nurk S, Antipov D, Gurevich AA, Dvorkin M, Kulikov AS, Lesin VM, Nikolenko SI, Pham S, Prjibelski AD, Pyshkin AV, Sirotkin AV, Vyahhi N,

Tesler G, Alekseyev MA, Pevzner PA (2012) SPAdes: a new genome assembly algorithm and its applications to single-cell sequencing. Journal of Computational Biology 19 (5):455-477. doi:10.1089/cmb.2012.0021
Bartnicki-Garcia S (1968) Cell wall chemistry, morphogenesis, and taxonomy of fungi. Annual Review of Microbiology 22:87-108. doi:10.1146/annurev.mi.22.100168.000511
Bass D, Richards TA (2011) Three reasons to re-evaluate fungal diversity 'on Earth and in the ocean'. Fungal Biology Reviews 25:159-164. doi:10.1016/j.fbr.2011.10.003
Bauer R, Begerow B, Sampaio JP, Weiss M, Oberwinkler F (2006) The simple-septate basidiomycetes: a synopsis. Mycological Progress 5 (1):41-66. doi:10.1007/s11557-006-0502-0
Begerow B, Schafer AM, Kellner R, Yurkov A, Kemler M, Oberwinkler F, Bauer R (2014) Ustilaginomycotina. In:McLaughlin D, Spatafora J (eds) Systematics and Evolution (Part A). The Mycota. Springer
Begerow D, Stoll M, Bauer R (2006) A phylogenetic hypothesis of Ustilaginomycotina based on multiple gene analyses and morphological data. Mycologia 98 (6):906-916
Berbee ML, Taylor JW (2010) Dating the molecular clock in fungi – how close are we? Fungal Biology Reviews 24:1-16. doi:10.1016/j.fbr.2010.03.001
Beurmann L, de Clair M, Gourgerot H (1909) Une nouvelle mycose, l'hemisporose de la verge. Bulletins et mémoires de la Société médicale des hôpitaux de Paris 3:911-917
Binder M, Bresinsky A (2002) Derivation of a polymorphic lineage of Gasteromycetes from boletoid ancestors. Mycologia 94 (1):85-98
Boetzer M, Henkel CV, Jansen HJ, Butler D, Pirovano W (2011) Scaffolding pre-assembled contigs using SSPACE. Bioinformatics 27 (4):578-579. doi:10.1093/bioinformatics/btq683
Bollen GJ (1969) The selective effect of heat treatment on the microflora of a greenhouse soil. Netherlands Journal of Plant Pathology 75:157-163. doi:10.1007/BF02137211
Bollen GJ (1974) Fungal recolonization of heat-treated glasshouse soils. Agro-Ecosystems 1:139-155. doi:10.1016/0304-3746(74)90022-5
Borodovsky M, Lomsadze A (2011) Eukaryotic gene prediction using GeneMark.hmm-E and GeneMark-ES. Current protocols in bioinformatics Chapter 4:Unit 4 6 1-10. doi:10.1002/0471250953.bi0406s35
Botic T, Kuncic MK, Sepcic K, Knez Z, Gunde-Cimerman N (2012) Salt induces biosynthesis of hemolytically active compounds in the xerotolerant food-borne fungus *Wallemia sebi*. FEMS microbiology letters 326 (1):40-46. doi:10.1111/j.1574-6968.2011.02428.x
Bouckaert R, Heled J, Kuhnert D, Vaughan T, Wu CH, Xie D, Suchard MA, Rambaut A, Drummond AJ (2014) BEAST 2: a software platform for Bayesian evolutionary analysis. PLoS Computational Biology 10 (4):e1003537. doi:10.1371/journal.pcbi.1003537
Bruns TD, Vilgalys R, Barns SM, Gonzalez D, Hibbett DS, Lane DJ, Simon L, Stickel S, Szaro TM, Weisburg WG, et al. (1992) Evolutionary relationships within the

fungi: analyses of nuclear small subunit rRNA sequences. Molecular Phylogenetics and Evolution 1 (3):231-241
Bruns TD, White TJ, Taylor JW (1991) Fungal Molecular Systematics. Annual Review of Ecology and Systematics 22:525-564
Buee M, Reich M, Murat C, Morin E, Nilsson RH, Uroz S, Martin F (2009) 454 Pyrosequencing analyses of forest soils reveal an unexpectedly high fungal diversity. The New Phytologist 184 (2):449-456. doi:10.1111/j.1469-8137.2009.03003.x
Cantu D, Govindarajulu M, Kozik A, Wang M, Chen X, Kojima KK, Jurka J, Michelmore RW, Dubcovsky J (2011) Next generation sequencing provides rapid access to the genome of *Puccinia striiformis* f. sp. *tritici*, the causal agent of wheat stripe rust. PLoS One 6 (8):e24230. doi:10.1371/journal.pone.0024230
Celio GJ, Padamsee M, Dentinger BT, Bauer R, McLaughlin DJ (2006) Assembling the Fungal Tree of Life: constructing the structural and biochemical database. Mycologia 98 (6):850-859
Cisse OH, Almeida JM, Fonseca A, Kumar AA, Salojarvi J, Overmyer K, Hauser PM, Pagni M (2013) Genome sequencing of the plant pathogen *Taphrina deformans*, the causal agent of peach leaf curl. mBio 4 (3):e00055-00013. doi:10.1128/mBio.00055-13
Coker WC, Couch JN (1974) The gasteromycetes of the Eastern United States and Canada. Dover Publications, New York
Cole GT, Samson RA (1979) Development of Basauxic Conidiogenous Cells. Patterns of Development in Conidial Fungi. Pitman, p 103
Conesa A, Gotz S, Garcia-Gomez JM, Terol J, Talon M, Robles M (2005) Blast2GO: a universal tool for annotation, visualization and analysis in functional genomics research. Bioinformatics 21 (18):3674-3676. doi:10.1093/bioinformatics/bti610
Crous PW, Verkley GJM, Groenewald JZ, Samson RA (2009) Division Basidiomycota. In:Crous PW, Samson RA (eds) Fungal Biodiversity. CBS-KNAW Fungal Biodiversity Centre, Utrecht, pp 199-205
Darriba D, Taboada GL, Doallo R, Posada D (2012) jModelTest 2: more models, new heuristics and parallel computing. Nature Methods 9 (8):772. doi:10.1038/nmeth.2109
Desroches TC, McMullin DR, Miller JD (2014) Extrolites of *Wallemia sebi*, a very common fungus in the built environment. Indoor Air 24 (5):533-542. doi:10.1111/ina.12100
Dettman JR, Jacobson DJ, Taylor JW (2003) A multilocus genealogical approach to phylogenetic species recognition in the model eukaryote *Neurospora*. Evolution 57 (12):2703-2720
Domsch KH, Gams W, Anderson T-H (1993) Compendium of Soil Fungi. Lubrecht & Cramer Ltd, Eching
Doweld A (2001) *Prosyllabus tracheophytorum*: Tentamen systematis plantarum vascularium (Tracheophyta). Geos, Moscow
Doweld A (2014) Wallemiomycotina. Index Fungorum 73:1

Duncan EG, Galbraith MH (1972) Post-meiotic events in the Homobasidiomycetidae. Transactions of the British Mycological Society 58 (3):387-392. doi:10.1016/S0007-1536(72)80088-3
Edgar RC (2004) MUSCLE: multiple sequence alignment with high accuracy and high throughput. Nucleic Acids Research 32 (5):1792-1797. doi:10.1093/nar/gkh340
Eilbeck K, Moore B, Holt C, Yandell M (2009) Quantitative measures for the management and comparison of annotated genomes. BMC Bioinformatics 10:67. doi:10.1186/1471-2105-10-67
Engelhart S, Exner M (2002) Short-term versus long-term filter cassette sampling for viable fungi in indoor air: comparative performance of the Sartorius MD8 and the GSP sampler. International Journal of Hygiene and Environmental Health 205 (6):443-451. doi:10.1078/1438-4639-00183
Federhen S (2012) The NCBI Taxonomy database. Nucleic Acids Research 40 (Database issue):D136-143. doi:10.1093/nar/gkr1178
Felsenstein J (1981) Evolutionary trees from DNA sequences: a maximum likelihood approach. Journal of Molecular Evolution 17 (6):368-376
Felsenstein J (1985) Confidence limits on phylogenies: an approach using the bootstrap. Evolution 39:783-791
Ferreira AS, Totola MR, Kasuya MCM, Araujo EF, Borges AC (2005) Small heat shock proteins in the development of thermotolerance in *Pisolithus* sp. Journal of Thermal Biology 30 (8):595-602
Fitch WM (1971) Toward defining the course of evolution: minimum change for a specific tree topology. Systematic Zoology 20 (4):406-416
Fitch WM (1986) An estimation of the number of invariable sites is necessary for the accurate estimation of the number of nucleotide substitutions since a common ancestor. In:Gershowitz H, Rucknagel DL, Tashian RE (eds) Evolutionary perspectives and the new genetics. Alan R. Liss Inc., New York, pp 149-159
Floudas D, Binder M, Riley R, Barry K, Blanchette RA, Henrissat B, Martinez AT, Otillar R, Spatafora JW, Yadav JS, Aerts A, Benoit I, Boyd A, Carlson A, Copeland A, Coutinho PM, de Vries RP, Ferreira P, Findley K, Foster B, Gaskell J, Glotzer D, Gorecki P, Heitman J, Hesse C, Hori C, Igarashi K, Jurgens JA, Kallen N, Kersten P, Kohler A, Kues U, Kumar TK, Kuo A, LaButti K, Larrondo LF, Lindquist E, Ling A, Lombard V, Lucas S, Lundell T, Martin R, McLaughlin DJ, Morgenstern I, Morin E, Murat C, Nagy LG, Nolan M, Ohm RA, Patyshakuliyeva A, Rokas A, Ruiz-Duenas FJ, Sabat G, Salamov A, Samejima M, Schmutz J, Slot JC, St John F, Stenlid J, Sun H, Sun S, Syed K, Tsang A, Wiebenga A, Young D, Pisabarro A, Eastwood DC, Martin F, Cullen D, Grigoriev IV, Hibbett DS (2012) The Paleozoic origin of enzymatic lignin decomposition reconstructed from 31 fungal genomes. Science 336 (6089):1715-1719. doi:10.1126/science.1221748
Frank M, Kingston E, Jeffery JC, Moss MO, Murray M, Simpson TJ, Sutherland A (1999) Walleminol and Walleminone: novel caryophyllenes from the toxigenic fungus *Wallemia sebi*. Tetrahedron Letters 40:133-136

Gadberry MD, Malcomber ST, Doust AN, Kellogg EA (2005) Primaclade--a flexible tool to find conserved PCR primers across multiple species. Bioinformatics 21 (7):1263-1264. doi:10.1093/bioinformatics/bti134

Galagan JE, Calvo SE, Borkovich KA, Selker EU, Read ND, Jaffe D, FitzHugh W, Ma LJ, Smirnov S, Purcell S, Rehman B, Elkins T, Engels R, Wang S, Nielsen CB, Butler J, Endrizzi M, Qui D, Ianakiev P, Bell-Pedersen D, Nelson MA, Werner-Washburne M, Selitrennikoff CP, Kinsey JA, Braun EL, Zelter A, Schulte U, Kothe GO, Jedd G, Mewes W, Staben C, Marcotte E, Greenberg D, Roy A, Foley K, Naylor J, Stange-Thomann N, Barrett R, Gnerre S, Kamal M, Kamvysselis M, Mauceli E, Bielke C, Rudd S, Frishman D, Krystofova S, Rasmussen C, Metzenberg RL, Perkins DD, Kroken S, Cogoni C, Macino G, Catcheside D, Li W, Pratt RJ, Osmani SA, DeSouza CP, Glass L, Orbach MJ, Berglund JA, Voelker R, Yarden O, Plamann M, Seiler S, Dunlap J, Radford A, Aramayo R, Natvig DO, Alex LA, Mannhaupt G, Ebbole DJ, Freitag M, Paulsen I, Sachs MS, Lander ES, Nusbaum C, Birren B (2003) The genome sequence of the filamentous fungus *Neurospora crassa*. Nature 422 (6934):859-868. doi:10.1038/nature01554

Ganley AR, Kobayashi T (2007) Highly efficient concerted evolution in the ribosomal DNA repeats: total rDNA repeat variation revealed by whole-genome shotgun sequence data. Genome Research 17 (2):184-191. doi:10.1101/gr.5457707

Garcia-Alcalde F, Okonechnikov K, Carbonell J, Cruz LM, Gotz S, Tarazona S, Dopazo J, Meyer TF, Conesa A (2012) Qualimap: evaluating next-generation sequencing alignment data. Bioinformatics 28 (20):2678-2679. doi:10.1093/bioinformatics/bts503

Goffeau A, Barrell BG, Bussey H, Davis RW, Dujon B, Feldmann H, Galibert F, Hoheisel JD, Jacq C, Johnston M, Louis EJ, Mewes HW, Murakami Y, Philippsen P, Tettelin H, Oliver SG (1996) Life with 6000 genes. Science 274 (5287):546, 563-567

Gostincar C, Ohm RA, Kogej T, Sonjak S, Turk M, Zajc J, Zalar P, Grube M, Sun H, Han J, Sharma A, Chiniquy J, Ngan CY, Lipzen A, Barry K, Grigoriev IV, Gunde-Cimerman N (2014) Genome sequencing of four *Aureobasidium pullulans* varieties: biotechnological potential, stress tolerance, and description of new species. BMC Genomics 15:549. doi:10.1186/1471-2164-15-549

Gouy M, Guindon S, Gascuel O (2010) SeaView version 4: A multiplatform graphical user interface for sequence alignment and phylogenetic tree building. Molecular Biology and Evolution 27 (2):221-224. doi:10.1093/molbev/msp259

Grigoriev IV, Nikitin R, Haridas S, Kuo A, Ohm R, Otillar R, Riley R, Salamov A, Zhao X, Korzeniewski F, Smirnova T, Nordberg H, Dubchak I, Shabalov I (2014) MycoCosm portal: gearing up for 1000 fungal genomes. Nucleic Acids Research 42 (Database issue):D699-704. doi:10.1093/nar/gkt1183

Guarro J, Gugnani HC, Sood N, Batra R, Mayayo E, Gene J, Kakkar S (2008) Subcutaneous phaeohyphomycosis caused by *Wallemia sebi* in an immunocompetent host. Journal of Clinical Microbiology 46 (3):1129-1131. doi:10.1128/JCM.01920-07

Guindon S, Gascuel O (2003) A simple, fast, and accurate algorithm to estimate large phylogenies by maximum likelihood. Systematic Biology 52 (5):696-704

Gurevich A, Saveliev V, Vyahhi N, Tesler G (2013) QUAST: quality assessment tool for genome assemblies. Bioinformatics 29 (8):1072-1075. doi:10.1093/bioinformatics/btt086
Haas BJ, Zeng Q, Pearson MD, Cuomo CA, Wortman JR (2011) Approaches to Fungal Genome Annotation. Mycology 2 (3):118-141. doi:10.1080/21501203.2011.606851
Halary S, Malik SB, Lildhar L, Slamovits CH, Hijri M, Corradi N (2011) Conserved meiotic machinery in *Glomus* spp., a putatively ancient asexual fungal lineage. Genome biology and evolution 3:950-958. doi:10.1093/gbe/evr089
Hall TA (1999) BioEdit: a user-friendly biological sequence alignment editor and analysis program for Windows 95/98/NT. Paper presented at the Nucleic Acids Symposium Series
Hanaichi T, Sato T, Iwamoto T, Malavasi-Yamashiro J, Hoshino M, Mizuno N (1986) A stable lead by modification of Sato's method. Journal of Electron Microscopy 35 (3):304-306
Hartmann HA, Kahmann R, Bolker M (1996) The pheromone response factor coordinates filamentous growth and pathogenicity in *Ustilago maydis*. The EMBO Journal 15 (7):1632-1641
Haslbeck M, Braun N, Stromer T, Richter B, Model N, Weinkauf S, Buchner J (2004) Hsp42 is the general small heat shock protein in the cytosol of Saccharomyces cerevisiae. The EMBO Journal 23 (3):638-649. doi:10.1038/sj.emboj.7600080
Hawksworth DL (1991) The fungal dimension of biodiversity: magnitude, significance and conservation. Mycological Research 95 (641-655)
Hawksworth DL (2001) The magnitude of fungal diversity: the 1.5 million species estimate revisited. Mycological Research 105:1422-1432
Hawksworth DL, Crous PW, Redhead SA, Reynolds DR, Samson RA, Seifert KA, Taylor JW, Wingfield MJ, Abaci O, Aime C, Asan A, Bai FY, de Beer ZW, Begerow D, Berikten D, Boekhout T, Buchanan PK, Burgess T, Buzina W, Cai L, Cannon PF, Crane JL, Damm U, Daniel HM, van Diepeningen AD, Druzhinina I, Dyer PS, Eberhardt U, Fell JW, Frisvad JC, Geiser DM, Geml J, Glienke C, Grafenhan T, Groenewald JZ, Groenewald M, de Gruyter J, Gueho-Kellermann E, Guo LD, Hibbett DS, Hong SB, de Hoog GS, Houbraken J, Huhndorf SM, Hyde KD, Ismail A, Johnston PR, Kadaifciler DG, Kirk PM, Koljalg U, Kurtzman CP, Lagneau PE, Levesque CA, Liu X, Lombard L, Meyer W, Miller A, Minter DW, Najafzadeh MJ, Norvell L, Ozerskaya SM, Ozic R, Pennycook SR, Peterson SW, Pettersson OV, Quaedvlieg W, Robert VA, Ruibal C, Schnurer J, Schroers HJ, Shivas R, Slippers B, Spierenburg H, Takashima M, Taskin E, Thines M, Thrane U, Uztan AH, van Raak M, Varga J, Vasco A, Verkley G, Videira SI, de Vries RP, Weir BS, Yilmaz N, Yurkov A, Zhang N (2011) The amsterdam declaration on fungal nomenclature. IMA Fungus 2 (1):105-112. doi:10.5598/imafungus.2011.02.01.14
Hebert PD, Cywinska A, Ball SL, deWaard JR (2003) Biological identifications through DNA barcodes. Proceedings Biological sciences / The Royal Society 270 (1512):313-321. doi:10.1098/rspb.2002.2218

Heled J, Drummond AJ (2010) Bayesian inference of species trees from multilocus data. Molecular Biology and Evolution 27 (3):570-580. doi:10.1093/molbev/msp274
Henk DA, Eagle CE, Brown K, Van Den Berg MA, Dyer PS, Peterson SW, Fisher MC (2011) Speciation despite globally overlapping distributions in *Penicillium chrysogenum*: the population genetics of Alexander Fleming's lucky fungus. Molecular Ecology 20 (20):4288-4301. doi:10.1111/j.1365-294X.2011.05244.x
Hibbett D, Grimaldi D, Donoghue M (1997) Fossil mushrooms from Miocene and Cretaceous ambers and the evolution of Homobasidiomycetes. American Journal of Botany 84 (7):981-991
Hibbett DS (2006) A phylogenetic overview of the Agaricomycotina. Mycologia 98 (6):917-925
Hibbett DS, Bauer R, Binder M, Giachini AJ, Hosaka K, Justo A, Larsson E, Larsson KH, Lawrey JD, Miettinen O, Nagy LG, Nilsson RH, Weiss M, Thorn RG (2014) Agaricomycetes. In:McLaughlin D, Spatafora J (eds) Systematics and Evolution (Part A). The Mycota. Springer
Hill ST (1974) Conidium ontogeny in the xerophilic fungus *Wallemia sebi*. Journal of Stored Products Research 10:209-210. doi:10.1016/0022-474X(74)90008-3
Hoch HC (1986) Freeze-substitution of fungi. In:Aldrich HC, Todd WJ (eds) Ultrastructure techniques for microorganisms. Plenum Press, New York, pp 183-212
Holt C, Yandell M (2011) MAKER2: an annotation pipeline and genome-database management tool for second-generation genome projects. BMC Bioinformatics 12:491. doi:10.1186/1471-2105-12-491
Hong SG, Jung HS (2004) Phylogenetic analysis of Ganoderma based on nearly complete mitochondrial small-subunit ribosomal DNA sequences. Mycologia 96 (4):742-755
Hovmoller R, Knowles LL, Kubatko LS (2013) Effects of missing data on species tree estimation under the coalescent. Molecular phylogenetics and evolution 69 (3):1057-1062. doi:10.1016/j.ympev.2013.06.004
Howard RJ, O'Donnell KL (1987) Freeze substitution of fungi for cytological analysis. Experimental Mycology 11:250-269. doi:10.1016/0147-5975(87)90014-4
Izzo A, Canright M, Bruns TD (2006) The effects of heat treatments on ectomycorrhizal resistant propagules and their ability to colonize bioassay seedlings. Mycological Research 110:196-202. doi:10.1016/j.mycres.2005.08.010
Jackson ED, Ells TC, Hughes TJ, Renderos W, Bell CR (1996) The incidence, source and significance of heat resistant moulds in fresh and freeze-processed wild lowbush blueberries. Agriculture and Agri-Food Canada, Kentville, Nova Scotia, Canada
James TY, Sun S, Li W, Heitman J, Kuo HC, Lee YH, Asiegbu FO, Olson A (2013) Polyporales genomes reveal the genetic architecture underlying tetrapolar and bipolar mating systems. Mycologia 105 (6):1374-1390. doi:10.3852/13-162

Jančič S, Nguyen HDT, Frisvad JC, Zalar P, Schroers HJ, Seifert KA, Gunde-Cimerman N (2015) A taxonomic revision of the *Wallemia sebi* species complex. PLoS One. Accepted with minor revisions.

Jia F, Lo N, Ho SY (2014) The impact of modelling rate heterogeneity among sites on phylogenetic estimates of intraspecific evolutionary rates and timescales. PLoS One 9 (5):e95722. doi:10.1371/journal.pone.0095722

Johan-Olsen O (1887) Om sop på klipfisk den såkaldte mid. Christiania Videnskabs-Selskabs Forhandlinger 12:1-20

Jones P, Binns D, Chang HY, Fraser M, Li W, McAnulla C, McWilliam H, Maslen J, Mitchell A, Nuka G, Pesseat S, Quinn AF, Sangrador-Vegas A, Scheremetjew M, Yong SY, Lopez R, Hunter S (2014) InterProScan 5: genome-scale protein function classification. Bioinformatics 30 (9):1236-1240. doi:10.1093/bioinformatics/btu031

Jones SK, Jr., Bennett RJ (2011) Fungal mating pheromones: choreographing the dating game. Fungal Genetics and Biology 48 (7):668-676. doi:10.1016/j.fgb.2011.04.001

Joslyn DJ, Boucias DG (1981) Isozyme differentiation among three pathotypes of the entomogenous fungus Nomuraea rileyi. Canadian Journal of Microbiology 27 (3):364-366

Jukes TH, Cantor CR (1969) Evolution of Protein Molecules. Academic Press, New York

Jumpponen A, Jones KL (2009) Massively parallel 454 sequencing indicates hyperdiverse fungal communities in temperate Quercus macrocarpa phyllosphere. The New Phytologist 184 (2):438-448. doi:10.1111/j.1469-8137.2009.02990.x

Kamper J, Kahmann R, Bolker M, Ma LJ, Brefort T, Saville BJ, Banuett F, Kronstad JW, Gold SE, Muller O, Perlin MH, Wosten HA, de Vries R, Ruiz-Herrera J, Reynaga-Pena CG, Snetselaar K, McCann M, Perez-Martin J, Feldbrugge M, Basse CW, Steinberg G, Ibeas JI, Holloman W, Guzman P, Farman M, Stajich JE, Sentandreu R, Gonzalez-Prieto JM, Kennell JC, Molina L, Schirawski J, Mendoza-Mendoza A, Greilinger D, Munch K, Rossel N, Scherer M, Vranes M, Ladendorf O, Vincon V, Fuchs U, Sandrock B, Meng S, Ho EC, Cahill MJ, Boyce KJ, Klose J, Klosterman SJ, Deelstra HJ, Ortiz-Castellanos L, Li W, Sanchez-Alonso P, Schreier PH, Hauser-Hahn I, Vaupel M, Koopmann E, Friedrich G, Voss H, Schluter T, Margolis J, Platt D, Swimmer C, Gnirke A, Chen F, Vysotskaia V, Mannhaupt G, Guldener U, Munsterkotter M, Haase D, Oesterheld M, Mewes HW, Mauceli EW, DeCaprio D, Wade CM, Butler J, Young S, Jaffe DB, Calvo S, Nusbaum C, Galagan J, Birren BW (2006) Insights from the genome of the biotrophic fungal plant pathogen *Ustilago maydis*. Nature 444 (7115):97-101. doi:10.1038/nature05248

Katoh K, Kuma K, Toh H, Miyata T (2005) MAFFT version 5: improvement in accuracy of multiple sequence alignment. Nucleic Acids Research 33 (2):511-518. doi:10.1093/nar/gki198

Katoh K, Standley DM (2013) MAFFT multiple sequence alignment software version 7: improvements in performance and usability. Molecular Biology and Evolution 30 (4):772-780. doi:10.1093/molbev/mst010

Kendrick B (2001) The Fifth Kingdom. Focus Publishing/R. Pullins Co., Newburyport
Khan SR, Kimbrough JW (1982) A reevaluation of the basidiomycetes based upon septal and basidial structures. Mycotaxon 15:103-120
Kidder DL, Worsley TR (2004) Causes and consequences of extreme Permo-Triassic warming to globally equable climate and relation to the Permo-Triassic extinction and recovery. Palaeogeography, Palaeoclimatology, Palaeoecology 203:207-237. doi:10.1016/S0031-0182(03)00667-9
Kikoku Y, Tagashira N, Nakano H (2008) Heat resistance of fungi isolated from frozen blueberries. Journal of Food Protection 71 (10):2030-2035
Kikoku Y, Yamane K, Nakagawa H (2014) Heat resistance of *Leohumicola verrucosa* and *Geminibasidium donsium* isolated from Canadian frozen blueberries. IUMS, Montreal.
Kingman JFC (1982) The coalescent. Stochastic Processes and Their Applications 13 (3):235-248
Kirk PM, Cannon PF, Minter DW, Stalpers JA (2008) Dictionary of the Fungi. 10th edn. CABI Publishing, Wallingford
Kolossa-Gehring M, Becker K, Conrad A, Ludecke A, Riedel S, Seiwert M, Schulz C, Szewzyk R (2007) German Environmental Survey for Children (GerES IV)--first results. International Journal of Hygiene and Environmental Health 210 (5):535-540. doi:10.1016/j.ijheh.2007.07.018
Koressaar T, Remm M (2007) Enhancements and modifications of primer design program Primer3. Bioinformatics 23 (10):1289-1291. doi:10.1093/bioinformatics/btm091
Kubicek CP, Herrera-Estrella A, Seidl-Seiboth V, Martinez DA, Druzhinina IS, Thon M, Zeilinger S, Casas-Flores S, Horwitz BA, Mukherjee PK, Mukherjee M, Kredics L, Alcaraz LD, Aerts A, Antal Z, Atanasova L, Cervantes-Badillo MG, Challacombe J, Chertkov O, McCluskey K, Coulpier F, Deshpande N, von Dohren H, Ebbole DJ, Esquivel-Naranjo EU, Fekete E, Flipphi M, Glaser F, Gomez-Rodriguez EY, Gruber S, Han C, Henrissat B, Hermosa R, Hernandez-Onate M, Karaffa L, Kosti I, Le Crom S, Lindquist E, Lucas S, Lubeck M, Lubeck PS, Margeot A, Metz B, Misra M, Nevalainen H, Omann M, Packer N, Perrone G, Uresti-Rivera EE, Salamov A, Schmoll M, Seiboth B, Shapiro H, Sukno S, Tamayo-Ramos JA, Tisch D, Wiest A, Wilkinson HH, Zhang M, Coutinho PM, Kenerley CM, Monte E, Baker SE, Grigoriev IV (2011) Comparative genome sequence analysis underscores mycoparasitism as the ancestral life style of *Trichoderma*. Genome Biology 12 (4):R40. doi:10.1186/gb-2011-12-4-r40
Kues U (2000) Life history and developmental processes in the basidiomycete *Coprinus cinereus*. Microbiology and Molecular Biology Reviews 64 (2):316-353
Kurtzman C, Fell JW, Boekhout T (2011) The Yeasts: A Taxonomic Study. 5th edn. Elsevier
Lagesen K, Hallin P, Rodland EA, Staerfeldt HH, Rognes T, Ussery DW (2007) RNAmmer: consistent and rapid annotation of ribosomal RNA genes. Nucleic Acids Research 35 (9):3100-3108. doi:10.1093/nar/gkm160
Langmead B, Salzberg SL (2012) Fast gapped-read alignment with Bowtie 2. Nature methods 9 (4):357-359. doi:10.1038/nmeth.1923

Lappalainen MH, Hyvarinen A, Hirvonen MR, Rintala H, Roivainen J, Renz H, Pfefferle PI, Nevalainen A, Roponen M, Pekkanen J (2012) High indoor microbial levels are associated with reduced Th1 cytokine secretion capacity in infancy. International Archives of Allergy and Immunology 159 (2):194-203. doi:10.1159/000335596

Lappalainen S, Pasanen AL, Reiman M, Kalliokoski P (1998) Serum IgG antibodies against *Wallemia sebi* and *Fusarium* species in Finnish farmers. Annals of Allergy, Asthma & Immunology 81 (6):585-592. doi:10.1016/S1081-1206(10)62710-X

Lartillot N, Lepage T, Blanquart S (2009) PhyloBayes 3: a Bayesian software package for phylogenetic reconstruction and molecular dating. Bioinformatics 25 (17):2286-2288. doi:10.1093/bioinformatics/btp368

Lartillot N, Rodrigue N, Stubbs D, Richer J (2013) PhyloBayes MPI: phylogenetic reconstruction with infinite mixtures of profiles in a parallel environment. Systematic Biology 62 (4):611-615. doi:10.1093/sysbio/syt022

Launonen TM, Ashton DH, Keane PJ (1999) The effect of regeneration burns on the growth, nutrient acquisition and mycorrhizae of *Eucalyptus regnans* F. Muell. (mountain ash) seedlings. Plant and Soil 210 (2):273-283

Leavitt SD, Johnson LA, Goward T, St Clair LL (2011) Species delimitation in taxonomically difficult lichen-forming fungi: an example from morphologically and chemically diverse *Xanthoparmelia* (Parmeliaceae) in North America. Molecular Phylogenetics and Evolution 60 (3):317-332. doi:10.1016/j.ympev.2011.05.012

Lee SC, Ni M, Li W, Shertz C, Heitman J (2010) The evolution of sex: a perspective from the fungal kingdom. Microbiology and Molecular Biology Reviews 74 (2):298-340. doi:10.1128/MMBR.00005-10

Lenassi M, Zajc J, Gostincar C, Gorjan A, Gunde-Cimerman N, Plemenitas A (2011) Adaptation of the glycerol-3-phosphate dehydrogenase Gpd1 to high salinities in the extremely halotolerant Hortaea werneckii and halophilic *Wallemia ichthyophaga*. Fungal Biology 115 (10):959-970. doi:10.1016/j.funbio.2011.04.001

Letcher PM, Powell MJ, Picard KT (2012) Zoospore ultrastructure and phylogenetic position of *Phlyctochytrium aureliae* Ajello is revealed (Chytridiaceae, Chytridiales, Chytridiomycota). Mycologia 104 (2):410-418. doi:10.3852/11-153

Li DW, Yang CS (2004) Fungal contamination as a major contributor to sick building syndrome. Advances in Applied Microbiology 55:31-112. doi:10.1016/S0065-2164(04)55002-5

Li H, Handsaker B, Wysoker A, Fennell T, Ruan J, Homer N, Marth G, Abecasis G, Durbin R, Genome Project Data Processing S (2009) The Sequence Alignment/Map format and SAMtools. Bioinformatics 25 (16):2078-2079. doi:10.1093/bioinformatics/btp352

Lindner DL, Banik MT (2011) Intragenomic variation in the ITS rDNA region obscures phylogenetic relationships and inflates estimates of operational taxonomic units in genus *Laetiporus*. Mycologia 103 (4):731-740. doi:10.3852/10-331

Loftus BJ, Fung E, Roncaglia P, Rowley D, Amedeo P, Bruno D, Vamathevan J, Miranda M, Anderson IJ, Fraser JA, Allen JE, Bosdet IE, Brent MR, Chiu R, Doering TL, Donlin MJ, D'Souza CA, Fox DS, Grinberg V, Fu J, Fukushima M, Haas BJ, Huang JC, Janbon G, Jones SJ, Koo HL, Krzywinski MI, Kwon-Chung JK, Lengeler KB, Maiti R, Marra MA, Marra RE, Mathewson CA, Mitchell TG, Pertea M, Riggs FR, Salzberg SL, Schein JE, Shvartsbeyn A, Shin H, Shumway M, Specht CA, Suh BB, Tenney A, Utterback TR, Wickes BL, Wortman JR, Wye NH, Kronstad JW, Lodge JK, Heitman J, Davis RW, Fraser CM, Hyman RW (2005) The genome of the basidiomycetous yeast and human pathogen *Cryptococcus neoformans*. Science 307 (5713):1321-1324. doi:10.1126/science.1103773

Lücking R, Huhndorf S, Pfister DH, Plata ER, Lumbsch HT (2009) Fungi evolved right on track. Mycologia 101 (6):810-822

Madelin MF, Dorabjee S (1974) Conidium ontogeny in *Wallemia sebi*. Transactions of the British Mycological Society 63 (1):121-130. doi:10.1016/S0007-1536(74)80143-9

Maleszka R, Clark-Walker GD (1993) Yeasts have a four-fold variation in ribosomal DNA copy number. Yeast 9 (1):53-58. doi:10.1002/yea.320090107

Malik SB, Pightling AW, Stefaniak LM, Schurko AM, Logsdon JM, Jr. (2008) An expanded inventory of conserved meiotic genes provides evidence for sex in Trichomonas vaginalis. PLoS One 3 (8):e2879. doi:10.1371/journal.pone.0002879

Managbanag JR, Torzilli AP (2002) An analysis of trehalose, glycerol, and mannitol accumulation during heat and salt stress in a salt marsh isolate of Aureobasidium pullulans. Mycologia 94 (3):384-391

Marthey S, Aguileta G, Rodolphe F, Gendrault A, Giraud T, Fournier E, Lopez-Villavicencio M, Gautier A, Lebrun MH, Chiapello H (2008) FUNYBASE: a FUNgal phYlogenomic dataBASE. BMC Bioinformatics 9:456. doi:10.1186/1471-2105-9-456

Martin F, Kohler A, Murat C, Balestrini R, Coutinho PM, Jaillon O, Montanini B, Morin E, Noel B, Percudani R, Porcel B, Rubini A, Amicucci A, Amselem J, Anthouard V, Arcioni S, Artiguenave F, Aury JM, Ballario P, Bolchi A, Brenna A, Brun A, Buee M, Cantarel B, Chevalier G, Couloux A, Da Silva C, Denoeud F, Duplessis S, Ghignone S, Hilselberger B, Iotti M, Marcais B, Mello A, Miranda M, Pacioni G, Quesneville H, Riccioni C, Ruotolo R, Splivallo R, Stocchi V, Tisserant E, Viscomi AR, Zambonelli A, Zampieri E, Henrissat B, Lebrun MH, Paolocci F, Bonfante P, Ottonello S, Wincker P (2010) Perigord black truffle genome uncovers evolutionary origins and mechanisms of symbiosis. Nature 464 (7291):1033-1038. doi:10.1038/nature08867

Matheny PB (2005) Improving phylogenetic inference of mushrooms with *RPB*1 and *RPB*2 nucleotide sequences (*Inocybe*; Agaricales). Molecular Phylogenetics and Evolution 35 (1):1-20. doi:10.1016/j.ympev.2004.11.014

Matheny PB, Gossmann JA, Zalar P, Kumar TK, Hibbett DS (2006) Resolving the phylogenetic position of the Wallemiomycetes: an enigmatic major lineage of Basidiomycota. Canadian Journal of Botany 84 (12):1794-1805. doi:10.1139/b06-128

Matheny PB, Liu YJ, Ammirati JF, Hall BD (2002) Using *RPB*1 sequences to improve phylogenetic inference among mushrooms (*Inocybe*, Agaricales). American Journal of Botany 89 (4):688-698. doi:10.3732/ajb.89.4.688

Matheny PB, Wang Z, Binder M, Curtis JM, Lim YW, Nilsson RH, Hughes KW, Hofstetter V, Ammirati JF, Schoch CL, Langer E, Langer G, McLaughlin DJ, Wilson AW, Froslev T, Ge ZW, Kerrigan RW, Slot JC, Yang ZL, Baroni TJ, Fischer M, Hosaka K, Matsuura K, Seidl MT, Vauras J, Hibbett DS (2007) Contributions of *RPB2* and *TEF*1 to the phylogeny of mushrooms and allies (Basidiomycota, Fungi). Molecular Phylogenetics and Evolution 43 (2):430-451. doi:10.1016/j.ympev.2006.08.024

Matsushima T (2001) Matsushima Mycological Memoirs Vol. 10 (CD-ROM)

Matsushima T (2003) *Basidioascus* gen. nov. Matsushima Mycological Memoirs 10:98-104

McDaniel DP, Roberson RW (2000) Intracellular motility and mechanisms of control during hyphal tip growth in *Allomyces*. Fungal Genetics and Biology 31:223-234

McLaughlin DJ, Hibbett DS, Lutzoni F, Spatafora JW, Vilgalys R (2009) The search for the fungal tree of life. Trends in Microbiology 17 (11):488-497. doi:10.1016/j.tim.2009.08.001

Meerupati T, Andersson KM, Friman E, Kumar D, Tunlid A, Ahren D (2013) Genomic mechanisms accounting for the adaptation to parasitism in nematode-trapping fungi. PLoS Genetics 9 (11):e1003909. doi:10.1371/journal.pgen.1003909

Misiek M, Hoffmeister D (2008) Processing sites involved in intron splicing of *Armillaria* natural product genes. Mycological Research 112:216-224. doi:10.1016/j.mycres.2007.10.011

Moore RT (1986) A note on *Wallemia sebi*. Antonie van Leeuwenhoek 52 (2):183-187

Moore RT (1996) The Dolipore/Parenthesome Septum in Modern Taxonomy. In:Sneh B, Jabaji-Hare S, Neate S, Dijst G (eds) *Rhizoctonia* species: taxonomy, molecular biology, ecology, pathology and disease control. Springer, pp 13-35. doi:10.1007/978-94-017-2901-7

Morey M, Fernandez-Marmiesse A, Castineiras D, Fraga JM, Couce ML, Cocho JA (2013) A glimpse into past, present, and future DNA sequencing. Molecular genetics and metabolism 110 (1-2):3-24. doi:10.1016/j.ymgme.2013.04.024

Morin E, Kohler A, Baker AR, Foulongne-Oriol M, Lombard V, Nagy LG, Ohm RA, Patyshakuliyeva A, Brun A, Aerts AL, Bailey AM, Billette C, Coutinho PM, Deakin G, Doddapaneni H, Floudas D, Grimwood J, Hilden K, Kues U, Labutti KM, Lapidus A, Lindquist EA, Lucas SM, Murat C, Riley RW, Salamov AA, Schmutz J, Subramanian V, Wosten HA, Xu J, Eastwood DC, Foster GD, Sonnenberg AS, Cullen D, de Vries RP, Lundell T, Hibbett DS, Henrissat B, Burton KS, Kerrigan RW, Challen MP, Grigoriev IV, Martin F (2012) Genome sequence of the button mushroom *Agaricus bisporus* reveals mechanisms governing adaptation to a humic-rich ecological niche. Proceedings of the National Academy of Sciences of the United States of America 109 (43):17501-17506. doi:10.1073/pnas.1206847109

Muller HJ (1964) The Relation of Recombination to Mutational Advance. Mutation Research 106:2-9
Müller WH, Stalpers JA, van Aelst AC, de Jong MDM, van der Krift TP, Boekhout T (2000) The taxonomic position of *Asterodon*, *Asterostroma* and *Coltricia* inferred from the septal pore cap ultrastructure. Mycological Research 104 (12):1485-1492. doi:10.1017/S0953756200002677
Nakayama K, Morimoto K (2009) [Risk factor for lifestyle and way of living for symptoms of sick building syndrome: epidemiological survey in Japan]. Japanese Journal of Hygiene 64 (3):689-698
Nasr S, Soudi MR, Nasrabadi SM, Nikou MM, Salmanian AH, Nguyen HD (2014) *Basidioascus persicus* sp. nov., a yeast-like species of the order Geminibasidiales isolated from soil. International Journal of Systematic and Evolutionary Microbiology 64:3046-3052. doi:10.1099/ijs.0.062380-0
Nguyen HDT, Nickerson NL, Seifert KA (2013) *Basidioascus* and *Geminibasidium*: a new lineage of heat-resistant and xerotolerant basidiomycetes. Mycologia 105 (5):1231-1250. doi:10.3852/12-351
Ni M, Feretzaki M, Sun S, Wang X, Heitman J (2011) Sex in fungi. Annual Review of Genetics 45:405-430. doi:10.1146/annurev-genet-110410-132536
Nikolenko SI, Korobeynikov AI, Alekseyev MA (2013) BayesHammer: Bayesian clustering for error correction in single-cell sequencing. BMC Genomics 14 Suppl 1:S7. doi:10.1186/1471-2164-14-S1-S7
Noble SM, Johnson AD (2007) Genetics of *Candida albicans*, a diploid human fungal pathogen. Annual Review of Genetics 41:193-211. doi:10.1146/annurev.genet.41.042007.170146
Nonnenmann MW, Coronado G, Thompson B, Griffith WC, Hanson JD, Vesper S, Faustman EM (2012) Utilizing pyrosequencing and quantitative PCR to characterize fungal populations among house dust samples. Journal of Environmental Monitoring 14 (8):2038-2043. doi:10.1039/c2em30229b
Notredame C, Higgins DG, Heringa J (2000) T-Coffee: A novel method for fast and accurate multiple sequence alignment. Journal of Molecular Biology 302 (1):205-217. doi:10.1006/jmbi.2000.4042
Nylander JAA (2004) MrModeltest v2.
O'Brien HE, Parrent JL, Jackson JA, Moncalvo JM, Vilgalys R (2005) Fungal community analysis by large-scale sequencing of environmental samples. Applied and Environmental Microbiology 71 (9):5544-5550. doi:10.1128/AEM.71.9.5544-5550.2005
O'Donnell K, Sutton DA, Fothergill A, McCarthy D, Rinaldi MG, Brandt ME, Zhang N, Geiser DM (2008) Molecular phylogenetic diversity, multilocus haplotype nomenclature, and in vitro antifungal resistance within the *Fusarium solani* species complex. Journal of Clinical Microbiology 46 (8):2477-2490. doi:10.1128/JCM.02371-07
Oberwinkler F (2014) Dacrymycetes. In:McLaughlin D, Spatafora J (eds) Systematics and Evolution (Part A). The Mycota. Springer,
Oberwinkler F, Bandoni RJ (1982) A taxonomic survey of the gasteroid, auricularioid Heterobasidiomycetes. Canadian Journal of Botany 60 (9):1726-1750. doi:10.1139/b82-221

Ohm RA, Feau N, Henrissat B, Schoch CL, Horwitz BA, Barry KW, Condon BJ, Copeland AC, Dhillon B, Glaser F, Hesse CN, Kosti I, LaButti K, Lindquist EA, Lucas S, Salamov AA, Bradshaw RE, Ciuffetti L, Hamelin RC, Kema GH, Lawrence C, Scott JA, Spatafora JW, Turgeon BG, de Wit PJ, Zhong S, Goodwin SB, Grigoriev IV (2012) Diverse lifestyles and strategies of plant pathogenesis encoded in the genomes of eighteen Dothideomycetes fungi. PLoS Pathogens 8 (12):e1003037. doi:10.1371/journal.ppat.1003037

Padamsee M, Kumar TK, Riley R, Binder M, Boyd A, Calvo AM, Furukawa K, Hesse C, Hohmann S, James TY, LaButti K, Lapidus A, Lindquist E, Lucas S, Miller K, Shantappa S, Grigoriev IV, Hibbett DS, McLaughlin DJ, Spatafora JW, Aime MC (2012) The genome of the xerotolerant mold *Wallemia sebi* reveals adaptations to osmotic stress and suggests cryptic sexual reproduction. Fungal Genetics and Biology 49 (3):217-226. doi:10.1016/j.fgb.2012.01.007

Page RD (1996) TreeView: an application to display phylogenetic trees on personal computers. Computer Applications in the Biosciences 12 (4):357-358

Parra G, Bradnam K, Korf I (2007) CEGMA: a pipeline to accurately annotate core genes in eukaryotic genomes. Bioinformatics 23 (9):1061-1067. doi:10.1093/bioinformatics/btm071

Peng XP, Wang Y, Liu PP, Hong K, Chen H, Yin X, Zhu WM (2011) Aromatic compounds from the halotolerant fungal strain of *Wallemia sebi* PXP-89 in a hypersaline medium. Archives of Pharmacal Research 34 (6):907-912. doi:10.1007/s12272-011-0607-0

Pevzner PA, Tang H, Waterman MS (2001) An Eulerian path approach to DNA fragment assembly. Proceedings of the National Academy of Sciences of the United States of America 98 (17):9748-9753. doi:10.1073/pnas.171285098

Pieckova E, Jesenska Z (1999) Microscopic fungi in dwellings and their health implications in humans. Annals of Agricultural and Environmental Medicine 6 (1):1-11

Pitt JI (1973) An appraisal of identification methods for *Penicillium* species: novel taxonomic criteria based on temperature and water relations. Mycologia 65 (5):1135-1157

Pitt JI (1975) Xerophilic fungi and the spoilage of foods of plant origin. In:Duckworth RB (ed) Water Relations of Foods. Academic Press, London, pp 273-307

Posada D (2004) COLLAPSE v1.2.

Prieto M, Wedin M (2013) Dating the diversification of the major lineages of Ascomycota (Fungi). PLoS One 8 (6):e65576. doi:10.1371/journal.pone.0065576

Pringle A, Patek SN, Fischer M, Stolze J, Money NP (2005) The captured launch of a ballistospore. Mycologia 97 (4):866-871

Rannala B, Yang Z (2003) Bayes estimation of species divergence times and ancestral population sizes using DNA sequences from multiple loci. Genetics 164 (4):1645-1656

Reboux G, Piarroux R, Mauny F, Madroszyk A, Millon L, Bardonnet K, Dalphin JC (2001) Role of molds in farmer's lung disease in Eastern France. American Journal of Respiratory and Critical Care Medicine 163 (7):1534-1539. doi:10.1164/ajrccm.163.7.2006077

Ren P, Jankun TM, Leaderer BP (1999) Comparisons of seasonal fungal prevalence in indoor and outdoor air and in house dusts of dwellings in one Northeast American county. Journal of Exposure Analysis and Environmental Epidemiology 9 (6):560-568
Rep M, Duyvesteijn RG, Gale L, Usgaard T, Cornelissen BJ, Ma LJ, Ward TJ (2006) The presence of GC-AG introns in *Neurospora crassa* and other euascomycetes determined from analyses of complete genomes: implications for automated gene prediction. Genomics 87 (3):338-347. doi:10.1016/j.ygeno.2005.11.014
Roberson RW, Fuller MS (1988) Ultrastructural aspects of the hyphal tip of *Sclerotium rolfsii* preserved by freeze substitution. Protoplasma 146:143-149
Robert V, Vu D, Amor AB, van de Wiele N, Brouwer C, Jabas B, Szoke S, Dridi A, Triki M, Ben Daoud S, Chouchen O, Vaas L, de Cock A, Stalpers JA, Stalpers D, Verkley GJ, Groenewald M, Dos Santos FB, Stegehuis G, Li W, Wu L, Zhang R, Ma J, Zhou M, Gorjon SP, Eurwilaichitr L, Ingsriswang S, Hansen K, Schoch C, Robbertse B, Irinyi L, Meyer W, Cardinali G, Hawksworth DL, Taylor JW, Crous PW (2013) MycoBank gearing up for new horizons. IMA Fungus 4 (2):371-379. doi:10.5598/imafungus.2013.04.02.16
Ronquist F, Huelsenbeck JP (2003) MrBayes 3: Bayesian phylogenetic inference under mixed models. Bioinformatics 19 (12):1572-1574
Ronquist F, Teslenko M, van der Mark P, Ayres DL, Darling A, Hohna S, Larget B, Liu L, Suchard MA, Huelsenbeck JP (2012) MrBayes 3.2: efficient Bayesian phylogenetic inference and model choice across a large model space. Systematic Biology 61 (3):539-542. doi:10.1093/sysbio/sys029
Roussel S, Reboux G, Dalphin JC, Bardonnet K, Millon L, Piarroux R (2004) Microbiological evolution of hay and relapse in patients with farmer's lung. Occupational and Environmental Medicine 61 (1):e3
Sahney S, Benton MJ (2008) Recovery from the most profound mass extinction of all time. Proceedings Biological sciences / The Royal Society 275 (1636):759-765. doi:10.1098/rspb.2007.1370
Saitou N, Nei M (1987) The neighbor-joining method: a new method for reconstructing phylogenetic trees. Molecular Biology and Evolution 4 (4):406-425
Sakamoto T, Urisu A, Yamada M, Matsuda Y, Tanaka K, Torii S (1989) Studies on the osmophilic fungus *Wallemia sebi* as an allergen evaluated by skin prick test and radioallergosorbent test. International Archives of Allergy and Applied Immunology 90 (4):368-372
Samson RA, Hoekstra ES, Frisvad JC, Filtenborg O (2000) Introduction to food-borne fungi. CBS-KNAW Fungal Biodiversity Centre, Utrecht
Samson RA, Houbraken J, Thrane U, Frisvad JC, Andersen B (2010) Food and Indoor Fungi. CBS Laboratory Manual, Series 2. CBS-KNAW Fungal Biodiversity Centre, Utrecht
Schmitt I, Crespo A, Divakar PK, Fankhauser JD, Herman-Sackett E, Kalb K, Nelsen MP, Nelson NA, Rivas-Plata E, Shimp AD, Widhelm T, Lumbsch HT (2009) New primers for promising single-copy genes in fungal phylogenetics and systematics. Persoonia 23:35-40. doi:10.3767/003158509X470602

Schneider CA, Rasband WS, Eliceiri KW (2012) NIH Image to ImageJ: 25 years of image analysis. Nature Methods 9 (7):671-675
Schoch CL, Seifert KA, Huhndorf S, Robert V, Spouge JL, Levesque CA, Chen W, Fungal Barcoding C, Fungal Barcoding Consortium Author L (2012) Nuclear ribosomal internal transcribed spacer (ITS) region as a universal DNA barcode marker for Fungi. Proceedings of the National Academy of Sciences of the United States of America 109 (16):6241-6246. doi:10.1073/pnas.1117018109
Schwarz GE (1978) Estimating the dimension of a model. Annals of Statistics 6 (2):461-464
Seifert KA, Nickerson NL, Corlett M, Jackson ED, Louis-Seize G, Davies RJ (2004) *Devriesia*, a new hyphomycete genus to accommodate heat-resistant, cladosporium-like fungi. Canadian Journal of Botany 82:914-926. doi:10.1139/B04-070
Sennekamp J, Joest M, Sander I, Engelhart S, Raulf-Heimsoth M (2012) [Farmer's lung antigens in Germany]. Pneumologie 66 (5):297-301. doi:10.1055/s-0031-1291676
Sharpton TJ, Stajich JE, Rounsley SD, Gardner MJ, Wortman JR, Jordar VS, Maiti R, Kodira CD, Neafsey DE, Zeng Q, Hung CY, McMahan C, Muszewska A, Grynberg M, Mandel MA, Kellner EM, Barker BM, Galgiani JN, Orbach MJ, Kirkland TN, Cole GT, Henn MR, Birren BW, Taylor JW (2009) Comparative genomic analyses of the human fungal pathogens *Coccidioides* and their relatives. Genome Research 19 (10):1722-1731. doi:10.1101/gr.087551.108
Simon UK, Weiss M (2008) Intragenomic variation of fungal ribosomal genes is higher than previously thought. Molecular Biology and Evolution 25 (11):2251-2254. doi:10.1093/molbev/msn188
Sims D, Sudbery I, Ilott NE, Heger A, Ponting CP (2014) Sequencing depth and coverage: key considerations in genomic analyses. Nature Reviews Genetics 15 (2):121-132. doi:10.1038/nrg3642
Singh RP, Hodson DP, Huerta-Espino J, Jin Y, Bhavani S, Njau P, Herrera-Foessel S, Singh PK, Singh S, Govindan V (2011) The emergence of Ug99 races of the stem rust fungus is a threat to world wheat production. Annual Review of Phytopathology 49:465-481. doi:10.1146/annurev-phyto-072910-095423
Slater GS, Birney E (2005) Automated generation of heuristics for biological sequence comparison. BMC Bioinformatics 6:31. doi:10.1186/1471-2105-6-31
Smith SY, Currah RS, Stockey RA (2004) Cretaceous and Eocene poroid hymenophores from Vancouver Island, British Columbia. Mycologia 96 (1):180-186
Spurr AR (1969) A low-viscosity epoxy resin embedding medium for electron microscopy. Journal of Ultrastructure Research 26 (1):31-43
Staats M, van Kan JA (2012) Genome update of *Botrytis cinerea* strains B05.10 and T4. Eukaryotic Cell 11 (11):1413-1414. doi:10.1128/EC.00164-12
Stajich JE, Wilke SK, Ahren D, Au CH, Birren BW, Borodovsky M, Burns C, Canback B, Casselton LA, Cheng CK, Deng J, Dietrich FS, Fargo DC, Farman ML, Gathman AC, Goldberg J, Guigo R, Hoegger PJ, Hooker JB, Huggins A, James TY, Kamada T, Kilaru S, Kodira C, Kues U, Kupfer D,

Kwan HS, Lomsadze A, Li W, Lilly WW, Ma LJ, Mackey AJ, Manning G, Martin F, Muraguchi H, Natvig DO, Palmerini H, Ramesh MA, Rehmeyer CJ, Roe BA, Shenoy N, Stanke M, Ter-Hovhannisyan V, Tunlid A, Velagapudi R, Vision TJ, Zeng Q, Zolan ME, Pukkila PJ (2010) Insights into evolution of multicellular fungi from the assembled chromosomes of the mushroom *Coprinopsis cinerea* (*Coprinus cinereus*). Proceedings of the National Academy of Sciences of the United States of America 107 (26):11889-11894. doi:10.1073/pnas.1003391107

Stamatakis A (2006) RAxML-VI-HPC: maximum likelihood-based phylogenetic analyses with thousands of taxa and mixed models. Bioinformatics 22 (21):2688-2690. doi:10.1093/bioinformatics/btl446

Stamatakis A (2014) RAxML version 8: a tool for phylogenetic analysis and post-analysis of large phylogenies. Bioinformatics 30 (9):1312-1313. doi:10.1093/bioinformatics/btu033

Swann EC, Taylor JW (1995) Phylogenetic perspectives on basidiomycete systematics: evidence from the 18s rRNA gene. Canadian Journal of Botany 73 (S1):862-868. doi:10.1139/b95-332

Swofford DL (2002) PAUP* 4.0b: phylogenetic analysis using parsimony (*and other methods). Sinauer Associates, Sunderland, Massachusetts

Takahashi I, Maruta R, Ando K, Yoshida M, Iwasaki T, Kanazawa J, Okabe M, Tamaoki T (1993) UCA1064-B, a new antitumor antibiotic isolated from *Wallemia sebi*: production, isolation and structural determination. The Journal of Antibiotics 46 (8):1312-1314

Takahashi T (1997) Airborne fungal colony-forming units in outdoor and indoor environments in Yokohama, Japan. Mycopathologia 139 (1):23-33

Tamura K, Peterson D, Peterson N, Stecher G, Nei M, Kumar S (2011) MEGA5: molecular evolutionary genetics analysis using maximum likelihood, evolutionary distance, and maximum parsimony methods. Molecular Biology and Evolution 28 (10):2731-2739. doi:10.1093/molbev/msr121

Taylor JW, Berbee ML (2006) Dating divergences in the Fungal Tree of Life: review and new analyses. Mycologia 98 (6):838-849

Taylor JW, Jacobson DJ, Kroken S, Kasuga T, Geiser DM, Hibbett DS, Fisher MC (2000) Phylogenetic species recognition and species concepts in fungi. Fungal Genetics and Biology 31 (1):21-32. doi:10.1006/fgbi.2000.1228

Ter-Hovhannisyan V, Lomsadze A, Chernoff YO, Borodovsky M (2008) Gene prediction in novel fungal genomes using an *ab initio* algorithm with unsupervised training. Genome Research 18 (12):1979-1990. doi:10.1101/gr.081612.108

Terracina FC (1974) Fine structure of the septum in *Wallemia sebi*. Canadian Journal of Botany 52:2587-2590

Tisserant E, Malbreil M, Kuo A, Kohler A, Symeonidi A, Balestrini R, Charron P, Duensing N, Frei dit Frey N, Gianinazzi-Pearson V, Gilbert LB, Handa Y, Herr JR, Hijri M, Koul R, Kawaguchi M, Krajinski F, Lammers PJ, Masclaux FG, Murat C, Morin E, Ndikumana S, Pagni M, Petitpierre D, Requena N, Rosikiewicz P, Riley R, Saito K, San Clemente H, Shapiro H, van Tuinen D, Becard G, Bonfante P, Paszkowski U, Shachar-Hill YY, Tuskan GA, Young JP, Sanders IR, Henrissat B, Rensing SA, Grigoriev IV, Corradi N, Roux C,

Martin F (2013) Genome of an arbuscular mycorrhizal fungus provides insight into the oldest plant symbiosis. Proceedings of the National Academy of Sciences of the United States of America 110 (50):20117-20122. doi:10.1073/pnas.1313452110

Toome M, Kuo A, Henrissat B, Lipzen A, Tritt A, Yoshinaga Y, Zane M, Barry K, Grigoriev IV, Spatafora JW, Aime MC (2014a) Draft Genome Sequence of a Rare Smut Relative, *Tilletiaria anomala* UBC 951. Genome Announcements 2 (3). doi:10.1128/genomeA.00539-14

Toome M, Ohm RA, Riley RW, James TY, Lazarus KL, Henrissat B, Albu S, Boyd A, Chow J, Clum A, Heller G, Lipzen A, Nolan M, Sandor L, Zvenigorodsky N, Grigoriev IV, Spatafora JW, Aime MC (2014b) Genome sequencing provides insight into the reproductive biology, nutritional mode and ploidy of the fern pathogen *Mixia osmundae*. The New Phytologist 202 (2):554-564. doi:10.1111/nph.12653

Traeger S, Altegoer F, Freitag M, Gabaldon T, Kempken F, Kumar A, Marcet-Houben M, Poggeler S, Stajich JE, Nowrousian M (2013) The genome and development-dependent transcriptomes of *Pyronema confluens*: a window into fungal evolution. PLoS Genetics 9 (9):e1003820. doi:10.1371/journal.pgen.1003820

Tulasne L, Tulasne C (1847) Memoire sur les Ustilaginees comparees Uredinees. Annales des Sciences Naturelles; Botanique 3:12-127

Untergasser A, Cutcutache I, Koressaar T, Ye J, Faircloth BC, Remm M, Rozen SG (2012) Primer3--new capabilities and interfaces. Nucleic Acids Research 40 (15):e115. doi:10.1093/nar/gks596

van den Berg MA, Albang R, Albermann K, Badger JH, Daran JM, Driessen AJ, Garcia-Estrada C, Fedorova ND, Harris DM, Heijne WH, Joardar V, Kiel JA, Kovalchuk A, Martin JF, Nierman WC, Nijland JG, Pronk JT, Roubos JA, van der Klei IJ, van Peij NN, Veenhuis M, von Dohren H, Wagner C, Wortman J, Bovenberg RA (2008) Genome sequencing and analysis of the filamentous fungus *Penicillium chrysogenum*. Nature Biotechnology 26 (10):1161-1168. doi:10.1038/nbt.1498

van der Nest MA, Beirn LA, Crouch JA, Demers JE, de Beer ZW, De Vos L, Gordon TR, Moncalvo JM, Naidoo K, Sanchez-Ramirez S, Roodt D, Santana QC, Slinski SL, Stata M, Taerum SJ, Wilken PM, Wilson AM, Wingfield MJ, Wingfield BD (2014) Draft genomes of *Amanita jacksonii*, *Ceratocystis albifundus*, *Fusarium circinatum*, *Huntiella omanensis*, *Leptographium procerum*, *Rutstroemia sydowiana*, and *Sclerotinia echinophila*. IMA Fungus 5 (2):473-486. doi:10.5598/imafungus.2014.05.02.11

Van der Walk JP, Yarrow D (1984) Methods for isolation, maintenance, classification, and identification of yeasts. In:Kregervan Rij NJW (ed) The Yeasts: a Taxonomic Study. Elsevier, Amsterdam, pp 45-104

van Driel KG, Humbel BM, Verkleij AJ, Stalpers J, Muller WH, Boekhout T (2009) Septal pore complex morphology in the Agaricomycotina (Basidiomycota) with emphasis on the Cantharellales and Hymenochaetales. Mycological Research 113 (5):559-576. doi:10.1016/j.mycres.2008.12.007

Vilgalys R, Hester M (1990) Rapid genetic identification and mapping of enzymatically amplified ribosomal DNA from several *Cryptococcus* species. Journal of Bacteriology 172 (8):4238-4246

Visagie CM, Hirooka Y, Tanney JB, Whitfield E, Mwange K, Meijer M, Amend AS, Seifert KA, Samson RA (2014) *Aspergillus*, *Penicillium* and *Talaromyces* isolated from house dust samples collected around the world. Studies in Mycology 78:63-139. doi:j.simyco.2014.07.002

von Arx JA (1970) The Genera of Fungi Sporulating in Pure Culture. Cramer Verlag, Lehre

Vytrasova J, Pribanova P, Marvanova L (2002) Occurrence of xerophilic fungi in bakery gingerbread production. International Journal of Food Microbiology 72:91-96

Weiss M, Bauer R, Sampaio JP, Oberwinkler F (2014) Tremellomycetes and related groups. In:McLaughlin D, Spatafora J (eds) Systematics and Evolution (Part A). The Mycota. Springer

Wheeler KA, Hocking AD, Pitt JI (1988) Effects of temperature and water activity on germination and growth of *Wallemia sebi*. Transactions of the British Mycological Society 90:365-368. doi:10.1016/S0007-1536(88)80144-X

White TJ, Bruns T, Lee S, Taylor JW (1990) Amplification and direct sequencing of fungal ribosomal RNA genes for phylogenetics. In:Innis MA, Gelfand DH, Sninsky JJ, White TJ (eds) PCR protocols: a guide to methods and applications. Academic Press, New York, pp 315-322

Wood GM, Mann PJ, Lewis DF, Reid WJ, Moss MO (1990) Studies on a toxic metabolite from the mould *Wallemia*. Food Additives and Contaminants 7 (1):69-77. doi:10.1080/02652039009373822

Wyatt TT, Wosten HA, Dijksterhuis J (2013) Fungal spores for dispersion in space and time. Advances in Applied Microbiology 85:43-91. doi:10.1016/B978-0-12-407672-3.00002-2

Xu J, Saunders CW, Hu P, Grant RA, Boekhout T, Kuramae EE, Kronstad JW, Deangelis YM, Reeder NL, Johnstone KR, Leland M, Fieno AM, Begley WM, Sun Y, Lacey MP, Chaudhary T, Keough T, Chu L, Sears R, Yuan B, Dawson TL, Jr. (2007) Dandruff-associated *Malassezia* genomes reveal convergent and divergent virulence traits shared with plant and human fungal pathogens. Proceedings of the National Academy of Sciences of the United States of America 104 (47):18730-18735. doi:10.1073/pnas.0706756104

Yang J, Wang L, Ji X, Feng Y, Li X, Zou C, Xu J, Ren Y, Mi Q, Wu J, Liu S, Liu Y, Huang X, Wang H, Niu X, Li J, Liang L, Luo Y, Ji K, Zhou W, Yu Z, Li G, Liu Y, Li L, Qiao M, Feng L, Zhang KQ (2011) Genomic and proteomic analyses of the fungus *Arthrobotrys oligospora* provide insights into nematode-trap formation. PLoS Pathogens 7 (9):e1002179. doi:10.1371/journal.ppat.1002179

Yang Z (1993) Maximum-likelihood estimation of phylogeny from DNA sequences when substitution rates differ over sites. Molecular Biology and Evolution 10 (6):1396-1401

Yang Z, Rannala B (1997) Bayesian phylogenetic inference using DNA sequences: a Markov Chain Monte Carlo Method. Molecular Biology and Evolution 14 (7):717-724

Yang Z, Rannala B (2010) Bayesian species delimitation using multilocus sequence data. Proceedings of the National Academy of Sciences of the United States of America 107 (20):9264-9269. doi:10.1073/pnas.0913022107

Zajc J, Liu Y, Dai W, Yang Z, Hu J, Gostincar C, Gunde-Cimerman N (2013) Genome and transcriptome sequencing of the halophilic fungus *Wallemia ichthyophaga*: haloadaptations present and absent. BMC Genomics 14:617. doi:10.1186/1471-2164-14-617

Zajc J, Zalar P, Sepcic K, Gunde-Cimerman N (2011) Xerophilic fungal genus *Wallemia*: Bioactive inhabitants of marine solar salterns and salty food. Zbornik Matice Srpske za Prirodne Nauke 120:7-18. doi:10.2298/ZMSPN1120007Z

Zak JC, Wildman HG (2004) Fungi in stressful environments. In:Mueller G, Bills G, Foster M (eds) Biodiversity of Fungi: inventory and monitoring methods. Academic Press, Boston, pp 303-316

Zalar P, Sybren de Hoog G, Schroers HJ, Frank JM, Gunde-Cimerman N (2005) Taxonomy and phylogeny of the xerophilic genus *Wallemia* (Wallemiomycetes and Wallemiales, cl. et ord. nov.). Antonie van Leeuwenhoek 87 (4):311-328. doi:10.1007/s10482-004-6783-x

Appendix

Supplementary Table 2.1. Strain information and GenBank accession numbers. Sequences for *MCM7*, *TSR*1, *RPB*1 and *RPB*2 from strain CBS 633.66 were extracted from the Joint Genome Institute (JGI) MycoCosm website.

Strain Number[a]	Genus	Species	Clade	Country	City	Isolation source	Isolation method	ITS	*MCM7*	*TSR*1	*RPB*1	*RPB*2
CBS 818.96[T]	Wallemia	sebi	1	Sweden	?	Sunflower seed	?	AY328915[b]	KM034937	KM035026	KM035115	KM035204
DAOM 226641	Wallemia	sebi	1	Canada	Ottawa	Indoor of residence	Air sample	—	KM034935	KM035024	KM035113	KM035202
EXF 8748	Wallemia	sebi	1	South Africa	Stellenbosch	Office dust	Dilution to extinction	KJ409896	KM034956	KM035045	KM035134	KM035223
CBS 136841	Wallemia	sebi	1	Germany	Berlin	Indoor environment	Air sample	KJ409907	KM034972	KM035061	KM035150	KM035239
CBS 136843	Wallemia	sebi	1	The Netherlands	Hoornaar	Archive	Swab	KJ409909	KM034974	KM035063	KM035152	KM035240
CBS 136845	Wallemia	sebi	1	The Netherlands	Zutphen	Office building	Swab	KJ409911	KM034976	KM035065	KM035154	KM035242
CBS 136847	Wallemia	sebi	1	The Netherlands	Ospel	Boiled eggs plant	Air sample	KJ409913	KM034978	KM035067	KM035156	KM035244
CBS 196.56[c]	Wallemia	sebi	1	The Netherlands	Groningen	Chronic ulcerative skin lesion	?	KJ409916	KM034983	KM035072	KM035161	KM035249
CBS 110595	Wallemia	sebi	1	United Kingdom	Surrey	Domestic interior	?	AY302511[b]	KM034984	KM035073	KM035162	KM035250
CBS 110620	Wallemia	sebi	1	United Kingdom	Surrey	Domestic interior	?	AY302515[b]	KM034985	KM035074	KM035163	KM035251
CBS 633.66[d]	Wallemia	sebi	2	?	?	Date honey	?	AY328916[b]	JGI	JGI	JGI	JGI
EXF 8738	Wallemia	sebi	2	Uruguay	Montevideo	House dust	Dilution to extinction	KJ409875	KM034931	KM035020	KM035109	KM035198
DAOM 242694	Wallemia	sebi	2	Uruguay	Montevideo	House dust	Dilution to extinction	KJ409876	KM034932	KM035021	KM035110	KM035199
DAOM 242799	Wallemia	sebi	2	Uruguay	Montevideo	House dust	Dilution to extinction	KJ409877	KM034933	KM035022	KM035111	KM035200
EXF 8740	Wallemia	sebi	2	Micronesia	Malem	Dust in house A	Dilution to extinction	KJ409881	KM034939	KM035028	KM035117	KM035206
DAOM 242695	Wallemia	sebi	2	Micronesia	Malem	Dust in house A	Dilution to extinction	KJ409882	KM034940	KM035029	KM035118	KM035207
EXF 8741	Wallemia	sebi	2	Micronesia	Malem	Dust in house A	Dilution to extinction	KJ409883	KM034941	KM035030	KM035119	KM035208
DAOM 242696	Wallemia	sebi	2	Micronesia	Malem	Dust in house A	Dilution to extinction	KJ409884	KM034942	KM035031	KM035120	KM035209
DAOM 242800	Wallemia	sebi	2	Micronesia	Malem	Dust in house B	Dilution to extinction	KJ409885	KM034943	KM035032	KM035121	KM035210
DAOM 242697	Wallemia	sebi	2	Micronesia	Malem	Dust in house A	Dilution to extinction	KJ409886	KM034944	KM035033	KM035122	KM035211
DAOM 242702	Wallemia	sebi	2	Micronesia	Malem	Dust in house B	Dilution to extinction	KJ409887	KM034945	KM035034	KM035123	KM035212
EXF 8745	Wallemia	sebi	2	Micronesia	Tofol	Dust in association office	Dilution to extinction	—	KM034946	KM035035	KM035124	KM035213
DAOM 242703	Wallemia	sebi	2	Micronesia	Tofol	Dust in association office	Dilution to extinction	—	KM034948	KM035037	KM035126	KM035215
DAOM 242698	Wallemia	sebi	2	Uruguay	Montevideo	House dust	Dilution to extinction	KJ409889	KM034949	KM035038	KM035127	KM035216
DAOM 242699	Wallemia	sebi	2	Uruguay	Montevideo	House dust	Dilution to extinction	KJ409890	KM034950	KM035039	KM035128	KM035217
DAOM 242700	Wallemia	sebi	2	Indonesia	Yogyakarta	House dust	Dilution to extinction	KJ409892	KM034952	KM035041	KM035130	KM035219
DAOM 242701	Wallemia	sebi	2	Indonesia	Yogyakarta	House dust	Dilution to extinction	KJ409893	KM034953	KM035042	KM035131	KM035220
DAOM 242704	Wallemia	sebi	2	Indonesia	Yogyakarta	House dust	Dilution to extinction	KJ409894	KM034954	KM035043	KM035132	KM035221
EXF 8747	Wallemia	sebi	2	Indonesia	Yogyakarta	House dust	Dilution to extinction	KJ409895	KM034955	KM035044	KM035133	KM035222
EXF 8749	Wallemia	sebi	2	Thailand	Makham Tia	Dust in apartment	Dilution to extinction	KJ409897	KM034957	KM035046	KM035135	KM035224
DAOM 242705	Wallemia	sebi	2	Thailand	Makham Tia	Dust in apartment	Dilution to extinction	—	KM034958	KM035047	KM035136	KM035225
CBS 136827	Wallemia	sebi	2	Germany	?	Indoor environment	Air sample	KJ409898	KM034959	KM035048	KM035137	KM035226
CBS 136836	Wallemia	sebi	2	The Netherlands	Rijswijk	Archive	Swab	—	KM034967	KM035056	KM035145	KM035234
CBS 136837	Wallemia	sebi	2	The Netherlands	Amsterdam	Bat cage	Air sample	—	KM034968	KM035057	KM035146	KM035235
CBS 136838	Wallemia	sebi	2	Germany	Stuttgart	Indoor environment	Air sample	—	KM034969	KM035058	KM035147	KM035236
CBS 136842	Wallemia	sebi	2	Germany	Stuttgart	Indoor environment	Air sample	KJ409908	KM034973	KM035062	KM035151	—
CBS 136849	Wallemia	sebi	2	Thailand	Songkla	Indoor environment	Air sample	KJ409914	KM034981	KM035070	KM035159	KM035247
EXF 8754[c]	Wallemia	sebi	2	India	Varanasi	Subcutaneous lesion on foot	Scraping	KJ409915	KM034982	KM035071	KM035160	KM035248
CBS 112378	Wallemia	sebi	2	Germany	Stuttgart	Indoor environment	Air sample	KJ409917	KM034987	KM035076	KM035165	KM035253
EXF 8757	Wallemia	sebi	2	Mexico	Sayulita	Dust in rental studio	Dilution to extinction	—	KM034989	KM035078	KM035167	KM035255
EXF 8758	Wallemia	sebi	2	Mexico	Sayulita	Dust in rental studio	Dilution to extinction	—	KM034990	KM035079	KM035168	KM035256
EXF 5918	Wallemia	sebi	2	Slovenia	Kamnik	Ceiling in children's room	Swab	KJ494632	KM034999	KM035088	KM035177	—

Supplementary Table 2.1. Continued

Strain Number[a]	Genus	Species	Clade	Country	City	Isolation source	Isolation method	ITS	*MCM7*	*TSR1*	*RPB1*	*RPB2*
DAOM 226642[e]	Wallemia	sebi	3	Canada	Ottawa	Indoor of residence	Air sample	KJ409879	KM034936	KM035025	KM035114	KM035203
DAOM 242571	Wallemia	sebi	3	Canada	Ottawa	Indoor environment	Air sample	—	KM034988	KM035077	KM035166	KM035254
DAOM 242570	Wallemia	sebi	3	Canada	Ottawa	Indoor environment	Air sample	KJ409918	KM034991	KM035080	KM035169	KM035257
EXF 8739	Wallemia	sebi	4	Uruguay	Montevideo	House dust	Dilution to extinction	KJ409878	KM034934	KM035023	KM035112	KM035201
EXF 8746	Wallemia	sebi	4	Micronesia	Tofol	Dust in association office	Dilution to extinction	KJ409888	KM034947	KM035036	KM035125	KM035214
EXF 8744	Wallemia	sebi	4	Indonesia	Yogyakarta	House dust	Dilution to extinction	KJ409891	KM034951	KM035040	KM035129	KM035218
CBS 116628[f]	Wallemia	muriae	—	Slovenia	?	Hypersaline water of saltern	?	KJ409880	KM034938	KM035027	KM035116	KM035205
CBS 136829	Wallemia	muriae	—	The Netherlands	Amsterdam	Archive in justice department	Air sample	—	KM034960	KM035049	KM035138	KM035227
CBS 136830	Wallemia	muriae	—	The Netherlands	Tilburg	Moist wall of archive	Swab	KJ409899	KM034961	KM035050	KM035139	KM035228
CBS 136831	Wallemia	muriae	—	The Netherlands	Tiel	Directly from wallpaper	Swab	KJ409900	KM034962	KM035051	KM035140	KM035229
CBS 136832	Wallemia	muriae	—	The Netherlands	Gorinchem	Archive	Swab	KJ409901	KM034963	KM035052	KM035141	KM035230
CBS 136833	Wallemia	muriae	—	The Netherlands	Utrecht	Directly from filter flowcabinet	Swab	KJ409902	KM034964	KM035053	KM035142	KM035231
CBS 136834	Wallemia	muriae	—	The Netherlands	Eindhoven	Bedroom	Air sample	KJ409903	KM034965	KM035054	KM035143	KM035232
CBS 136835	Wallemia	muriae	—	The Netherlands	Eindhoven	Bathroom	Air sample	KJ409904	KM034966	KM035055	KM035144	KM035233
CBS 136839	Wallemia	muriae	—	Germany	Cologne	Indoor environment	Air sample	KJ409905	KM034970	KM035059	KM035148	KM035237
CBS 136840	Wallemia	muriae	—	Germany	Berlin	Indoor environment	Air sample	KJ409906	KM034971	KM035060	KM035149	KM035238
CBS 136844	Wallemia	muriae	—	The Netherlands	Zutphen	Office building	Air sample	KJ409910	KM034975	KM035064	KM035153	KM035241
CBS 136846	Wallemia	muriae	—	The Netherlands	Ospel	Boiled eggs plant	Air sample	—	KM034977	KM035066	KM035155	KM035243
CBS 110599	Wallemia	muriae	—	United Kingdom	Surrey	Interior of unoccupied house	?	AY863021[b]	KM034979	KM035068	KM035157	KM035245
CBS 136848	Wallemia	muriae	—	The Netherlands	Born	Cheese factory	Air sample	—	KM034980	KM035069	KM035158	KM035246
CBS 110624	Wallemia	muriae	—	United Kingdom	Surrey	Interior of unoccupied house	?	AY863022[b]	KM034986	KM035075	KM035164	KM035252
EXF 8592	Wallemia	muriae	—	Denmark	Lyngby	Living room	Air sample	KJ409919	KM034992	KM035081	KM035170	KM035258
EXF 8591	Wallemia	muriae	—	Denmark	Lyngby	Living room	Air sample	KJ409920	KM034993	KM035082	KM035171	KM035259
EXF 8590	Wallemia	muriae	—	Denmark	Lyngby	Living room	Air sample	KJ409921	KM034994	KM035083	KM035172	KM035260
EXF 8588	Wallemia	muriae	—	Denmark	Lyngby	Living room	Air sample	KJ409922	KM034995	KM035084	KM035173	KM035261
EXF 8587	Wallemia	muriae	—	Denmark	Lyngby	Living room	Air sample	—	KM034996	KM035085	KM035174	KM035262
EXF 8586	Wallemia	muriae	—	Denmark	Lyngby	Living room	Air sample	—	KM034997	KM035086	KM035175	KM035263
EXF 5919	Wallemia	muriae	—	Slovenia	Kamnik	Ceiling in children's room	Swab	KJ494614	KM034998	KM035087	KM035176	KM035264
EXF 5917	Wallemia	muriae	—	Slovenia	Kamnik	Ceiling in children's room	Swab	KJ494613	KM035000	KM035089	KM035178	—
EXF 5916	Wallemia	muriae	—	Slovenia	Ljubljana	Kitchen wall	Swab	KJ494594	KM035001	KM035090	KM035179	KM035265
EXF 5915	Wallemia	muriae	—	Slovenia	Vrhnika	Living room wall	Swab	KJ494593	KM035002	KM035091	KM035180	KM035266
EXF 5914	Wallemia	muriae	—	Slovenia	Radomlje	Kitchen wall	Swab	KJ494611	KM035003	KM035092	KM035181	KM035267
EXF 8356	Wallemia	muriae	—	Slovenia	Lasko	Furnace room	Air sample	KJ409929	KM035004	KM035093	KM035182	KM035268
EXF 8355	Wallemia	muriae	—	Slovenia	Lasko	Furnace room	Air sample	—	KM035005	KM035094	KM035183	KM035269
EXF 8354	Wallemia	muriae	—	Slovenia	Lasko	Furnace room	Air sample	—	KM035006	KM035095	KM035184	KM035270
EXF 8353	Wallemia	muriae	—	Slovenia	Lasko	Basement	Air sample	KJ409930	KM035007	KM035096	KM035185	—
EXF 8352	Wallemia	muriae	—	Slovenia	Lasko	Basement	Air sample	KJ409931	KM035008	KM035097	KM035186	—
EXF 8351	Wallemia	muriae	—	Slovenia	Lasko	Basement	Air sample	KJ409932	KM035009	KM035098	KM035187	KM035271
EXF 8345	Wallemia	muriae	—	Slovenia	Radovljica	Living room	Air sample	—	KM035010	KM035099	KM035188	KM035272
EXF 8344	Wallemia	muriae	—	Slovenia	Radovljica	Living room	Air sample	KJ409933	KM035011	KM035100	KM035189	KM035273
EXF 8343	Wallemia	muriae	—	Slovenia	Radovljica	Living room	Air sample	KJ409934	KM035012	KM035101	KM035190	KM035274
EXF 8342	Wallemia	muriae	—	Slovenia	Radovljica	Bedroom	Air sample	KJ409935	KM035013	KM035102	KM035191	KM035275
EXF 8341	Wallemia	muriae	—	Slovenia	Radovljica	Bedroom	Air sample	KJ409936	KM035014	KM035103	KM035192	KM035276
EXF 8327	Wallemia	muriae	—	Slovenia	Lasko	Kitchen	Air sample	—	KM035015	KM035104	KM035193	KM035277
EXF 8315	Wallemia	muriae	—	Slovenia	Ljubljana	Kitchen	Air sample	KJ409937	KM035016	KM035105	KM035194	KM035278
EXF 8314	Wallemia	muriae	—	Slovenia	Ljubljana	Kitchen	Air sample	—	KM035017	KM035106	KM035195	KM035279
EXF 8313	Wallemia	muriae	—	Slovenia	Ljubljana	Kitchen	Air sample	KJ409938	KM035018	KM035107	KM035196	KM035280
EXF 8299	Wallemia	muriae	—	Slovenia	Ljubljana	Bathroom	Air sample	KJ409939	KM035019	KM035108	KM035197	KM035281

Supplementary Table 2.1. Continued

a: CBS = CBS-KNAW Fungal Biodiversity Centre, Utrecht, the Netherlands
DAOM = Canadian Collection of Fungal Cultures, Agriculture and Agri-Food Canada, Ottawa, Canada
EXF = Ex Culture Collection of the Department of Biology, Biotechnical Faculty, University of Ljubljana in Ljubljana, Infrastructural Centre Mycosmo, MRIC UL, Ljubljana, Slovenia
b: GenBank accession numbers from the Zalar et al. (2005)
c: Strains reported to cause subcutaneous lesions. EXF 8754 = FMR 8645 from Guarro et al. (2008)
d: This is the strain with its genome sequenced at the Joint Genome Institute (JGI)
e: Strain producing metabolites that react to human antibodies
T: neotype strains

Supplementary Table 2.2. Primer sequences. ITS primers are from White et al. (1990).

Primer	Gene	Direction	Sequence (5'-3')
ITS1[a]	ITS	Forward	TCCGTAGGTGAACCTGCGG
ITS4[a]	ITS	Reverse	TCCTCCGCTTATTGATATGC
MCM7WF	*MCM7*	Forward	AGAGCAATGAGGGCAGGTTT
MCM7WR	*MCM7*	Reverse	CGGCCAAGGAGAGGGTTAG
RPB1WF	*RPB1*	Forward	AAGACGAAGAGGCCAAGCAGT
RPB1WR	*RPB1*	Reverse	ACGCAAATAGACAATCGGAACCT
RPB2WF	*RPB2*	Forward	AAATCATTGAAAGYATYTGTGTTA
RPB2WR	*RPB2*	Reverse	CGAAGWGWTGCRGTGTATTT
TSR1WF	*TSR1*	Forward	AGATTAGATTTGGGTGGTCCTT
TSR1WR	*TSR1*	Reverse	ATTCCATAACACCRTCKGACATC

Supplementary Table 2.3. List of haplotypes.

Haplotype ID	Frequency	Clade No.	Strains number, Geography (Country & City)
1	5	*W. sebi* clade 1	CBS818.96, Sweden, ? CBS136843, The Netherlands, Hoornaar CBS196.56, The Netherlands, Groningen CBS110595, United Kingdom, Surrey CBS110620, United Kingdom, Surrey
2	1	*W. sebi* clade 1	DAOM226641, Canada, Ottawa
3	1	*W. sebi* clade 1	EXF8748, South Africa, Stellenbosch
4	2	*W. sebi* clade 1	CBS136841, Germany, Berlin CBS136847, The Netherlands, Ospel
5	1	*W sebi* clade 1	CBS136845, The Netherlands, Zutphen
6	1	*W. sebi* clade 2	CBS633.66, ?, ?
7	1	*W. sebi* clade 2	EXF8738, Uruguay, Montevideo
8	1	*W. sebi* clade 2	DAOM242694, Uruguay, Montevideo
9	1	*W. sebi* clade 2	DAOM242799, Uruguay, Montevideo
10	1	*W. sebi* clade 2	EXF8740, Micronesia, Malem
11	1	*W. sebi* clade 2	DAOM242695, Micronesia, Malem
12	5	*W. sebi* clade 2	EXF8741, Micronesia, Malem DAOM242696, Micronesia, Malem DAOM242800, Micronesia, Malem DAOM242697, Micronesia, Malem DAOM242702, Micronesia, Malem
13	6	*W. sebi* clade 2	EXF8745, Micronesia, Tofol DAOM242703, Micronesia, Tofol CBS136827, Germany, ? CBS136837, The Netherlands, Amsterdam CBS136838, Germany, Stuttgart CBS112378, Germany, Stuttgart
14	1	*W. sebi* clade 2	DAOM242698, Uruguay, Montevideo
15	1	*W. sebi* clade 2	DAOM242699, Uruguay, Montevideo
16	4	*W. sebi* clade 2	DAOM242700, Indonesia, Yogyakarta DAOM242704, Indonesia, Yogyakarta CBS136836, The Netherlands, Rijswijk EXF8754, India, Varanasi
17	2	*W. sebi* clade 2	DAOM242701, Indonesia, Yogyakarta EXF8749, Thailand, MarkhamTia
18	2	*W. sebi* clade 2	EXF8747, Indonesia, Yogyakarta CBS136849, Thailand, Songkla
19	1	*W. sebi* clade 2	DAOM242705, Thailand, MarkhamTia
20	1	*W. sebi* clade 2	CBS136842, Germany, Stuttgart
21	1	*W. sebi* clade 2	EXF8757, Mexico, Sayulita
22	1	*W. sebi* clade 2	EXF8758, Mexico, Sayulita
23	1	*W. sebi* clade 2	EXF5918, Slovenia, Kamnik
24	3	*W. sebi* clade 3	DAOM226642, Canada, Ottawa DAOM242571, Canada, Ottawa DAOM242570, Canada, Ottawa
25	3	*W. sebi* clade 4	EXF8739, Uruguay, Montevideo EXF8746, Micronesia, Tofol EXF8744, Indonesia, Yogyakarta

Supplementary Table 2.3. Continued.

Haplotype ID	Frequency	Clade No.	Strains number, Geography (Country & City)
26	27	*W. muriae*	CBS116628, Slovenia, ? CBS136832, The Netherlands, Gorinchem CBS136834, The Netherlands, Einhoven CBS136835, The Netherlands, Einhoven CBS136840, Germany, Berlin CBS136844, The Netherlands, Zutphen EXF8591, Denmark, Lyngby EXF8590, Denmark, Lyngby EXF8588, Denmark, Lyngby EXF8586, Denmark, Lyngby EXF5916, Slovenia, Ljubljana EXF5915, Slovenia, Vrhnika EXF5914, Slovenia, Radomlje EXF8356, Slovenia, Lasko EXF8355, Slovenia, Lasko EXF8353, Slovenia, Lasko EXF8352, Slovenia, Lasko EXF8351, Slovenia, Lasko EXF8345, Slovenia, Radovljica EXF8344, Slovenia, Radovljica EXF8343, Slovenia, Radovljica EXF8342, Slovenia, Radovljica EXF8341, Slovenia, Radovljica EXF8327, Slovenia, Lasko EXF8315, Slovenia, Ljubljana EXF8313, Slovenia, Ljubljana EXF8299, Slovenia, Ljubljana
27	10	*W. muriae*	CBS136829, The Netherlands, Amsterdam CBS136830, The Netherlands, Tilburg CBS136831, The Netherlands, Tiel CBS136833, The Netherlands, Utrecht CBS136846, The Netherlands, Ospel CBS110624, United Kingdom, Surrey EXF8587, Denmark, Lyngby EXF5919, Slovenia, Kemnik EXF5917, Slovenia, Kemnik EXF8354, Slovenia, Lasko
28	2	*W. muriae*	CBS136839, Germany, Cologne EXF8314, Slovenia, Ljubljana
29	1	*W. muriae*	CBS110599, United Kingdom, Surrey
30	1	*W. muriae*	CBS136848, The Netherlands, Born
31	1	*W. muriae*	EXF8592, Denmark, Lyngby

Supplementary Table 2.4. Support values for monophyly of each clade in our species hypothesis. Low or unsupported values are bolded and italicized. NJ = neighbor joining. MP = Maximum parsimony strict consensus. ML = Maximum likelihood. BI = Bayesian inference.

		Methods of phylogenetic reconstruction			
Clade	**Gene**	**NJ**	**MP**	**ML**	**BI**
W. sebi clade 1	ITS	96	yes	98	1.00
	MCM7	100	yes	87	1.00
	RPB1	90	yes	96	1.00
	RPB2	91	yes	***51***	1.00
	TSR1	100	yes	100	1.00
W. sebi clade 2	ITS	***0***	***no***	***0***	***0.00***
	MCM7	100	yes	95	1.00
	RPB1	100	yes	99	1.00
	RPB2	100	yes	89	1.00
	TSR1	100	yes	100	1.00
W. sebi clade 3	ITS	93	yes	87	1.00
	MCM7	100	yes	99	1.00
	RPB1	100	yes	100	1.00
	RPB2	100	yes	97	1.00
	TSR1	100	yes	100	1.00
W. sebi clade 4	ITS	80	yes	83	1.00
	MCM7	100	yes	100	1.00
	RPB1	100	yes	100	1.00
	RPB2	100	yes	100	1.00
	TSR1	100	yes	100	1.00
W. muriae	ITS	98	yes	100	1.00
	MCM7	100	yes	100	1.00
	RPB1	100	yes	100	1.00
	RPB2	100	yes	100	1.00
	TSR1	100	yes	100	1.00

Supplementary Table 3.1. Information on strains, source and sequences.

Taxon	Culture DAOM[1]	Culture CBS[2]	GenBank Accession No. ITS	GenBank Accession No. LSU	GenBank Accession No. SSU	Country	State/Province	Region	Substrate and plants
Basidioascus undulatus	241956[ET]	133763	JX242863	JX242883	JX242889	Canada	MB	Between Thompson and Nelson House	Soil from the site of a forest fire; jack pine and trembling aspen with understory of black spruce
	241958	133764	JX242859	—	—	Canada	BC	Quamichan Lake	Soil from a stand of black cottonwood (*Populus trichocarpa*)
	241959	133765	JX242875	—	—	Canada	BC	Shesta Lake, Prince George	Soil from a stand of spruce
	241961	133766	JX242862	JX242884	JX242890	Canada	BC	Helliwell Park, Hornby Island	Soil from a stand of old-growth Douglas fir
	241962	133767	JX242864	—	—	Canada	AB	AAFC Experimental Farm, Fort Vermillion	Soil from a field of barley stubble
	241963	133768	JX242865	—	—	Canada	BC	Rolla Research Farm, Dawson Creek	Soil from a fallow field
	241964	133769	JX242866	—	—	Canada	AB	AAFC Research Farm, Beaverlodge	Soil from a mature pine/spruce stand
	242122	133770	JX242876	—	—	Canada	AB	Stavely	Soil from from rough fescue grasslands
	229809	133771	JX242882	—	—	Canada	ON	Matawatchan Township, Renfrew County, Cooper Hill Road	Soil from mixed woods
Basidioascus magus	241948[HT]	133772	JX242869	JX242885	JX242891	United States	OR	Wizard Island, Crater Lake National Park	Forest soil near *Goodyera oblongifolia*
	241949	133773	JX242868	—	—	United States	OR	Wizard Island, Crater Lake National Park	Forest soil near *Vaccinium*
	241950	133774	JX242870	—	—	United States	OR	Wizard Island, Crater Lake National Park	Forest soil near *Goodyera oblongifolia*
	241951	133775	JX242871	—	—	United States	OR	Wizard Island, Crater Lake National Park	Forest soil near *Ceanothus velatinus*
	241952	133776	JX242872	—	—	United States	OR	Wizard Island, Crater Lake National Park	Forest soil near *Vaccinium*
	241953	133777	JX242873	—	—	United States	OR	Wizard Island, Crater Lake National Park	Forest soil near *Ceanothus velatinus*
	242123	133778	JX242874	—	—	United States	OR	Wizard Island, Crater Lake National Park	Forest soil near *Ceanothus velatinus*
	241954	133779	JX242857	—	—	Canada	ON	Madawaska Highlands, Morrow Cr. Trail, Centennial Lake	Soil from a stand of red and white pine
	241955	133780	JX242861	—	—	Canada	BC	Helliwell Park, Hornby Island	Soil from a stand of *Arbutus menziesii* with some Douglas fir
Basidioascus sp.	241957	133781	JX242858	—	—	Canada	ON	Big Island, Centennial Lake	Soil from a stand of oak interspersed with white pine
	241960	133782	JX242860	—	—	Canada	BC	Rocky Point near Metchosin, west of Victoria, Vancouver Island	Soil from an old-growth Garry oak and Douglas fir forest
	241965	133783	JX242867	—	—	Canada	MB	Between Thompson and Nelson House	Soil from the site of a forest fire in July 2003. Sampled underneath burnt moss and areas where organic material was completely burnt off
Geminibasidium donsium	241966[HT]	133784	JX242877	JX242886	JX242892	Canada	NS	Sable River	Soil from a commercial field of lowbush blueberries
	241967	133785	JX242878	JX242887	JX242893	Canada	NS	5 km from Grafton Lake, Kejimkujik National Park	Soil from a stand of white pine (*Pinus strobus*)
	242124	133786	JX242881			Canada	NS	Colquist Road, Shelburne County, Nova Scotia	Soil from a stand of jack pine (*Pinus banksiana*)
Geminibasidium hirsutum	241969[HT]	133787	JX242880	JX242888	JX242894	Canada	BC	Shingle Bolt Trail, Capilano Gorge, base of Grouse Mountain, North Vancouver	Soil from coniferous forest of mainly Douglas fir with understory of *Vaccinium parvifolium*
	241968	133788	JX242879	—	—	Canada	BC	Shingle Bolt Trail, Capilano Gorge, base of Grouse Mountain, North Vancouver	Soil from coniferous forest of mainly Douglas fir with understory of *Vaccinium parvifolium*

[1] DAOM = Canadian Collection of Fungal Cultures in Ottawa, Canada. All type strains were also deposited as dried cultures.
[2] CBS = Centraalbureau voor Schimmelcultures in Utrecht, The Netherlands.
[HT] Holotype.
[ET] Epitype.

Supplementary Table 3.2. Amount of solutes estimated from previous studies to achieve water activities ranging from 1.00 to 0.77.

Water activity (a_w)	Glycerol (g/100 mL)	NaCl (g/100mL)	Sucrose (g/100mL)
1.00	0.0	0.0	0.0
0.98	16.5	3.5	13.0
0.95	22.9	7.8	26.0
0.91	31.4	13.5	43.4
0.87	39.9	19.2	60.8
0.83	48.4	24.9	78.2
0.77	61.2	33.5	104.3

Supplementary Table 3.3. AFTOL GenBank accession numbers, associated strains, and GenBank classification.

Phylum/Subphylum	Class	Order	Organism	Strain or Voucher No.	AFTOL-ID	SSU	5.8S	LSU
Ustilaginomycotina	Exobasidiomycetes	Tilletiales	*Tilletia controversa*	MP 2525	493	DQ832245	DQ832246	DQ832244
		Exobasidiales	*Exobasidium rhododendri*	CBS 101457	1851	DQ667152	DQ667153	DQ667151
		Georgefischeriales	*Tilletiaria anomala*	CBS 436.72	865	AY803752	DQ234558	AY745715
		Microstromatales	*Sympodiomycopsis paphiopedili*	IAM13459	1772	DQ832239	DQ832240	DQ832238
		Doassansiales	*Rhamphospora nymphaeae*	CBS 72.38	1645	DQ831033	DQ831034	DQ831032
		Malasseziales	*Malassezia pachydermatis*	CBS 1879	856	DQ457640	DQ411532	AY745724
	Ustilaginomycetes	Ustilaginales	*Ustilago tritici*	CBS 669.70	1398	DQ846895	DQ846894	DQ094784
		Ustilaginales	*Schizonella melanogramma*	CBS 174.42	1722	DQ832211	DQ832212	DQ832210
		Ustilaginales	*Cintractia limitata*	HAJB 10488	446	DQ645507	DQ645508	DQ645506
		Urocystales	*Melanotaenium endogenum*	CBS 481.91	1918	DQ789980	DQ789981	DQ789979
		Urocystales	*Thecaphora spilanthis*	JAG 53	1913	DQ832242	DQ832243	DQ832241
Pucciniomycotina	Microbotryomycetes	Microbotryales	*Microbotryum violaceum*	CBS 438.34	1819	DQ789983	DQ789984	DQ789982
		Leucosporidiales	*Leucosporidium scottii*	CBS 614	718	AY707092	DQ221110	AY646098
		Sporidiobolales	*Rhodosporidium toruloides*	PYCC4416	1547	DQ832192	DQ832193	DQ832191
	Agaricostilbomycetes	incertae sedis	*Kondoa malvinella*	CBS 6082	859	DQ667164	DQ667165	AY745720
		incertae sedis	*Sterigmatomyces halophilus*	CBS 4609	863	DQ092916	DQ832237	AY745716
	Cystobasidiomycetes	Erythrobasidiales	*Sakaguchia dacryoidea*	PYCC 4491	1551	DQ832206	DQ832207	DQ832205
		Erythrobasidiales	*Occultifur externus*	CBS 8732	860	DQ457639	AF444567	AY745723
	Pucciniomycetes	Pucciniales	*Chrysomyxa arctostaphyli*	CFB 22246	442	AY657009	DQ200930	AY700192
		Pucciniales	*Puccinia poarum*	PBM 2567, clone 19 (*)	1027, N/A (*)	DQ831029	AF468043 (*)	DQ831028
		Septobasidiales	*Auriculoscypha anacardiicola*	Unknown	1885	DQ419921	DQ419922	DQ419920
		Platygloeales	*Platygloea disciformis*	IFO 32431	710	DQ234563	DQ234556	AY629314
	Tritirachiomycetes	Tritirachiales	*Tritirachium sp*	CBS 265.96	N/A	JF779653	JF779668	JF779652
Agaricomycotina	Agaricomycetes	Agaricales	*Agaricus bisporus*	RWK 1885	448	AY787216	DQ404388	AY635775
		Agaricales	*Bolbitius vitellinus*	MTS 5020	730	AY705955	DQ200920	AY691807
		Agaricales	*Chrysomphalina chrysophylla*	PBM 684	1523	DQ435814	DQ192180	DQ457656
		Agaricales	*Psilocybe montana*	PBM 961	820	DQ465342	DQ494692	DQ470823
		Boletales	*Aureoboletus thibetanus*	HKAS 41151	450	AY654882	DQ200917	AY700189
		Boletales	*Boletellus projectellus*	MB03-118	713	AY662660	AY789082	AY684158
		Boletales	*Calostoma cinnabarinum*	AW136MA	439	AY665773	AY854064	AY645054
		Boletales	*Paxillus vernalis*	MB-062	715	AY662662	DQ647827	AY645059
		Auriculariales	*Auricularia sp*	PBM 2295	676	DQ234542	DQ200918	AY634277
		Auriculariales	*Exidia uvapsassa*	"TA s.n. JAPAN"	461	AY654890	DQ241776	AY645056

Supplementary Table 3.3. Continued.

Phylum/Subphylum	Class	Order	Organism	Strain or Voucher No.	AFTOL-ID	SSU	5.8S	LSU
Agaricomycotina		Polyporales	*Ganoderma tsugae*	ZWsn	771	AY705969	DQ206985	AY684163
		Polyporales	*Polyporus squamosus*	"Andy Wilson s.n. Mass"	704	AY705963	DQ267123	AY629320
		Trechisporales	*Trechispora alnicola*	CBS 577.83	665	AY657012	DQ411529	AY635768
		Trechisporales	*Trechispora sp*	PBM 418	678	AY803753	DQ411534	AY647217
		Russulales	*Hericium americanum*	PBM 2498	469	AY665778	DQ206987	DQ411538
		Russulales	*Lactarius deceptivus*	PBM 2462	682	AY707093	AY854089	AY631899
		Hymenochaetales	*Fomitiporia mediterranea*	3/22-7	688	AY662664	AY854080	AY684157
		Hymenochaetales	*Hydnochaete duportii*	CBS 939.96	666	AY662669	DQ404386	AY635770
		Thelephorales	*Hydnellum geogenium*	PBM 2382	680	AY752971	DQ218304	AY631900
		Thelephorales	*Polyozellus multiplex*	PBM 2412	677	AY771600	DQ411528	AY634275
		Thelephorales	*Tomentella sp*	"MB s.n."	1016	DQ092920	DQ835998	DQ835997
		Sebacinales	*Sebacina incrustans*	PBM 2709, MW 573 (*)	1626, 1876 (*)	DQ521407	DQ520095 (*)	DQ521406
		Sebacinales	*Tremellodendron sp*	PBM 2324	699	AY766081	DQ411526	AY745701
		Phallales	*Phallus hadriani*	KH11092003-1	683	AY771601	DQ404385	AY885165
	Dacrymycetes	Dacrymycetales	*Calocera cornea*	GEL 5359	438	AY771610	AY789083	AY701526
		Dacrymycetales	*Dacryopinax spathularia*	GEL 5052	454	AY771603	AY854070	AY701525
		Dacrymycetales	*Guepiniopsis buccina*	PBM 2264	888	DQ667157	DQ206986	AY745711
	Tremellomycetes	Tremellales	*Cryptococcus humicola*	PYCC3387T	1552	DQ645515	DQ645516	DQ645514
		Tremellales	*Cryptococcus sp*	CBS 681.93	719	DQ645520	DQ205681	AY646103
		Tremellales	*Tremella aurantia*	E6123	1519	DQ836000	DQ182508	DQ156127
		Cystofilobasidiales	*Cystofilobasidium capitatum*	CBS 6358, ATCC 24507 (*)	1886, N/A (*)	D12801 (*)	DQ645522	DQ645521
		Cystofilobasidiales	*Itersonilia perplexans*	CBS 286.50	1896	DQ667162	DQ667163	DQ667161
		Cystofilobasidiales	*Mrakia frigida*	CBS 5266	1818	DQ831017	DQ831018	DQ831016
		Cystofilobasidiales	*Udeniomyces puniceus*	CBS 5689	1822	DQ836006	DQ836007	DQ836005
		Filobasidiales	*Filobasidium globisporum*	CBS 7642, JCM 10633 (*)	N/A	AB075546 (*)	AF444336	AF075495
		Filobasidiales	*Filobasidium uniguttulatum*	JCM 3685, WH84 (*)	N/A	AB032664	AB032692	HM769334 (*)
incertae sedis	Wallemiomycetes	Wallemiales	*Wallemia ichthyophaga*	EXF1059, EXF994 (*)	1901, N/A (*)	AY741382 (*)	AY302521	DQ847516
			Wallemia muriae	MZKI B-952, EXF1054 (*)	N/A, 1909 (*)	AY741381	AY302534	DQ847517 (*)
			Wallemia sebi	EXF483, EXF757 (*)	1910, N/A (*)	AY741380 (*)	AY328917	DQ847518
	Entorrhizomycetes	Entorrhizales	*Entorrhiza aff fineranae*	PDD70949	1873	DQ645526	DQ645527	DQ645525
Glomeromycota	Glomeromycetes	Glomerales	*Glomus mosseae*	UT101	139	AY635833	AY997053	DQ273793

Supplementary Table 3.4. Information on ITS environmental sequences from GenBank related to *Geminibasidium* and *Basidioascus*.

GenBank No.	Region/Country	Source	Author(s)	Reference
FN397319	Cahors, France	*Tuber melanosporum* truffle-ground soil, burnt area	Napoli et al. (2010)	New Phytol. 185 (1):237–247
DQ388859	Peachester State Forest, Queensland, Australia	burnt soil	Bastias et al. (2006)	New Phytol. 172 (1):149–158
HM240157	California, USA	grassland soil	Hawkes et al.	Unpublished
GU366683	USA, Oregon	temperate forest soil	Yarwood et al.	Unpublished
FJ553224	Skulow Lake, British Columbia, Canada	forest soil from the long-term soil productivity (LTSP) site	Hartmann et al. (2009)	Environ Microbiol. 2009 (12):3045–62
AY970141	Duke Forest, Durham, North Carolina, USA	mixed hardwood B-horizon soil	O'Brien et al. (2005)	Appl. Environ. Microbiol. 71 (9):5544–5550
JF927043	Leonessa (Vallunga), Italy	soil Sample	Belfiori et al. (2012)	FEMS Microbiol. Ecol. In press
JN889968	Guyana	ectomycorrhizal monodominant lowland tropical rainforest; soil 0-20cm	McGuire et al.	Unpublished
HQ022165	Barlett, New Hampshire, USA	high nitrogen, soil, Bartlett Experimental Forest	Vineis et al.	Unpublished
AB520603	Ibaraki, Japan	soil at Field Science Center of Ibaraki University College of Agriculture	Nishizawa et al. (2010)	Microbes Environ. 25 (3):204–210
GQ219822	Hainich, Germany	soil	Christ et al. (2011)	Soil Biol. Biochem. 43 (6):1292–1299
HM044636	Italy	ectomycorrhized root tips	Bacher and Peintner	Unpublished
AB251808	Morioka, Japan	*Pinus densiflora* forest	Lian et al. (2006)	Published Only in Database
DQ421228	Cedar Creek, Minnesota, USA	soil	Waldrop et al. (2006)	Ecol. Lett. 9 (10):1127–1135
EF040855	Albareto, Parma, Italy	Soil from forest of *Castanea sativa* (chestnut), *Juniperus* and *Pseudotsuga menziesii* (Douglas-fir)	Peintner et al. (2007)	Environ. Microbiol. 9 (4):880–889
EU480315	Sevilleta National Wildlife Refuge, New Mexico, USA	biological soil crust	Porras-Alfaro et al. (2011)	Mycologia 103 (1):10–21
EU626069	Beijing, China	hill soil	Thanh	Unpublished

Supplementary Table 4.1. Information on the genomes downloaded from JGI MycoCosm. The chosen file type was Filtered models (best).

Organism	File name	Download date	No. of gene models	PubMed ID	Reference
Pyronema confluens CBS100304	Pyrco1_GeneCatalog_proteins_20131110.aa.fasta	11-Dec-14	13,367	24068976	Traeger et al. (2013)
Neurospora crassa OR74A v2.0	Neucr2_GeneCatalog_proteins_20130412.aa.fasta	11-Dec-14	10,785	12712197	Gal.agan et al. (2003)
Cryptococcus neoformans var *neoformans* JEC21	Cryne_JEC21_1_GeneCatalog_proteins_20120305.aa.fasta	10-Oct-14	6,475	15653466	Loftus et al. (2005)
Ustilago maydis	Ustilago_maydis.proteins.fasta	10-Oct-14	6,522	17080091	Kamper et al. (2006)
Malassezia globosa	Malassezia_globosa.proteins.fasta	10-Oct-14	4,286	18000048	Xu et al. (2007)
Penicillium chrysogenum Wisconsin 54-1255	PenchWisc1_1_GeneCatalog_proteins_20140114.aa.fasta	10-Oct-14	13,671	18820685	van den Berg et al. (2008)
Coccidioides immitis RS	Cocim1_GeneCatalog_proteins_20130907.aa.fasta	11-Dec-14	9,910	19717792	Sharpton et al. (2009)
Tuber melanosporum	Tubme1_GeneCatalog_proteins_20111120.aa.fasta	11-Dec-14	7,496	20348908	Martin et al. (2010)
Coprinopsis cinerea	Coprinopsis_cinerea.proteins.fasta	11-Dec-14	13,393	20547848	Stajich et al. (2010)
Trichoderma atroviride v2.0	Tatroviridev2_FrozenGeneCatalog_20100319.proteins.fasta	10-Oct-14	11,863	21501500	Kubicek et al. (2011)
Sclerotinia sclerotiorum v1.0	Sclsc1_GeneCatalog_proteins_20110903.aa.fasta	11-Dec-14	14,503	21876677	Amselem et al. (2011)
Arthrobotrys oligospora ATCC 24927	Artol1_GeneCatalog_proteins_20131209.aa.fasta	11-Dec-14	11,479	21909256	Yang et al. (2011)
Puccinia striiformis f. sp. *tritici* PST-130	Pucst1_GeneCatalog_proteins_20130920.aa.fasta	10-Oct-14	18,021	21909385	Cantu et al. (2011)
Wallemia sebi v1.0	Walse1_GeneCatalog_proteins_20100910.aa.fasta	10-Oct-14	5,284	22326418	Padamsee et al. (2012)
Auricularia subglabra v2.0	Aurde3_1_GeneCatalog_proteins_20130729.aa.fasta	10-Oct-14	25,459	22745431	Floudas et al. (2012)
Dacryopinax sp. DJM 731 SSP1 v1.0	Dacsp1_GeneCatalog_proteins_20110131.aa.fasta	10-Oct-14	10,242	22745431	Floudas et al. (2012)
Fomitopsis pinicola FP-58527 SS1 v3.0	Fompi3_GeneCatalog_proteins_20120705.aa.fasta	10-Oct-14	13,885	22745431	Floudas et al. (2012)
Fomitiporia mediterranea v1.0	Fomme1_GeneCatalog_proteins_20101122.aa.fasta	11-Dec-14	11,333	22745431	Floudas et al. (2012)
Tremella mesenterica Fries v1.0	Treme1_best_proteins.fasta	10-Oct-14	8,313	22745431	Floudas et al. (2012)
Agaricus bisporus var *bisporus* (H97) v2.0	Abisporus_varbisporusH97.v2.FilteredModels3.proteins.fasta	10-Oct-14	10,438	23045686	Morin et al. (2012)
Botrytis cinerea v1.0	Botci1_GeneCatalog_proteins_20110903.aa.fasta	11-Dec-14	16,447	23104368	Staats and van Kan (2012)
Alternaria brassicicola	Alternaria.brassicola.proteins.fasta	11-Dec-14	10,688	23236275	Ohm et al. (2012)
Taphrina deformans	Tapde1_1_GeneCatalog_proteins_20130601.aa.fasta	10-Oct-14	4,609	23631913	Cisee et al. (2013)
Wallemia ichthyophaga EXF-994	Walic1_GeneCatalog_proteins_20131017.aa.fasta	10-Oct-14	4,863	24034603	Zajc et al. (2013)
Monacrosporium haptotylum CBS 200.50	Monha1_GeneCatalog_proteins_20131210.aa.fasta	11-Dec-14	10,959	24244185	Meerupati et al. (2013)
Rhizophagus irregularis DAOM 181602 v1.0	Gloin1_GeneCatalog_proteins_20120510.aa.fasta	11-Dec-14	30,282	24277808	Tisserant et al. (2013)
Mixia osmundae IAM 14324 v1.0	Mixos1_GeneCatalog_proteins_20120207.aa.fasta	10-Oct-14	6,903	24372469	Toome et al. (2014)
Tilletiaria anomala	Tilan2_GeneCatalog_proteins_20140224.aa.fasta	11-Dec-14	6,810	24926052	Toome et al. (2014)
Aureobasidium pullulans var. *pullulans* EXF-150	Aurpu_var_pul1_GeneCatalog_proteins_20130219.aa.fasta	11-Dec-14	11,866	24984952	Gostincar et al. (2014)
Saccharomyces cerevisiae S288C	Sacce1_GeneCatalog_proteins_20101210.aa.fasta	10-Oct-14	6,575	8849441	Goffeau et al. (1996)
Basidioascus undulatus DAOM 241956 v1.0	NA	NA	6,123	NA	NA

Supplementary Table 4.2. Nuclear single copy genes selected for phylogenomic analysis and molecular dating.

FUNYbase Locus ID	*B. undulatus* Locus ID	FUNYbase Annotation
FG465	E727869117	Protein component of the small 40S subunit essential for control of translational accuracy; has similarity to E. coli S5 and rat S2 ribosomal proteins; Rps2p
FG533	02234A5766	Histone acetyltransferase subunit of the Elongator complex which is a component of the RNA polymerase II holoenzyme; activity is directed specifically towards histones H3 and H4; disruption confers resistance to K. lactis zymotoxin; Elp3p
FG542	9D615CA107	Essential protein involved in transcription regulation; component of chromatin remodeling complexes; required for assembly and function of the INO80 complex; member of the RUVB-like protein family; Rvb2p
FG559	EC0665F929	Putative endonuclease subunit of the mRNA cleavage and polyadenylation specificity complex required for 3 processing of mRNAs; Ysh1p
FG570	C324541578	NAD+-dependent glutamate dehydrogenase degrades glutamate to ammonia and alpha-ketoglutarate; expression sensitive to nitrogen catabolite repression and intracellular ammonia levels; Gdh2p
FG598	7454061A47	Subunit of the core complex of translation initiation factor 3eIF3 which is essential for translation; Tif34p
FG610	19753F50F1	Subunit of the cytosolic chaperonin Cct ring complex related to Tcp1p required for the assembly of actin and tubulins in vivo; Cct8p
FG638	4110B48967	Cytosolic leucyl tRNA synthetase ligates leucine to the appropriate tRNA; Cdc60p
FG659	DADD1B1545	Protein required for the transport of amino acid permease Gap1p from the Golgi to the cell surface; component of the TOR signaling pathway; associates with both Tor1p and Tor2p; contains a WD-repeat; Lst8p
FG668	1CA2C89CDA	Bifunctional enzyme exhibiting both indole-3-glycerol-phosphate synthase and anthranilate synthase activities forms multifunctional hetero-oligomeric anthranilate synthase:indole-3-glycerol phosphate synthase enzyme complex with Trp2p; Trp3p
FG692	F62669A9B5	Catalytic subunit of the DNA polymerase alpha-primase complex required for the initiation of DNA replication during mitotic DNA synthesis and premeiotic DNA synthesis; Pol1p
FG730	8FD073A678	Protein that forms a heterotrimeric complex with Erp1 Erp2p and Emp24 member of the p24 family involved in endoplasmic reticulum to Golgi transport; Erv25p
FG735	CFF85B6CD3	Subunit of the 26S proteasome substrate of the N-acetyltransferase Nat1p; Rpn2p
FG821	15F0B3ED4E	ER membrane glycoprotein subunit of the glycosylphosphatidylinositol transamidase complex that adds glycosylphosphatidylinositol GPI anchors to newly synthesized proteins; human PIG-K protein is a functional homolog; Gpi8p
FG832	E25ABAA10B	Translation initiation factor eIF-5; N-terminal domain functions as a GTPase-activating protein to mediate hydrolysis of ribosome-bound GTP; C-terminal domain is the core of ribosomal preinitiation complex formation; Tif5p
FG848	D2C3637D3E	Ubiquitin activating enzyme involved in ubiquitin-mediated protein degradation and essential for viability; Uba1p
FG898	CC15B8EEC8	Chorismate mutase catalyzes the conversion of chorismate to prephenate to initiate the tyrosine/phenylalanine-specific branch of aromatic amino acid biosynthesis; Aro7p
FG948	4439A5EB63	RNA polymerase III subunit C11; mediates pol III RNA cleavage activity and is important for termination of transcription; Rpc11p
FG1010	DEE696ECBF	Subunit of the eukaryotic translation initiation factor 3 eIF3 involved in the assembly of preinitiation complex and start codon selection; Nip1p
FG1024	0883B62FA7	Conserved 90S pre-ribosomal component essential for proper endonucleolytic cleavage of the 35 S rRNA precursor at A0 A1 and A2 sites; contains eight WD-repeats; PWP2 deletion leads to defects in cell cycle and bud morphogenesis; Pwp2p
MS277	D19C551101	Protein required for processing of 20S pre-rRNA in the cytoplasm associates with pre-40S ribosomal particles; Tsr1p
MS320	9BB3DBA68D	Gamma glutamylcysteine synthetase catalyzes the first step in the gamma-glutamyl cycle for glutathione GSH biosynthesis; expression induced by oxidants cadmium and mercury; Gsh1p
MS358	01F18419DC	Cytoplasmic alanyl-tRNA synthetase required for protein synthesis; point mutation cdc64-1 allele causes cell cycle arrest at G1; lethality of null mutation is functionally complemented by human homolog; Ala1p
MS379	7A551CB330	Metalloprotease subunit of the 19S regulatory particle of the 26S proteasome lid; couples the deubiquitination and degradation of proteasome substrates; Rpn11p

Supplementary Table 4.2. Continued.

FUNYbase Locus ID	*B. undulatus* Locus ID	FUNYbase Annotation
MS384	D8AA9812B8	Essential beta-coat protein of the COPI coatomer involved in ER-to-Golgi and Golgi-to-ER transport; contains WD40 domains that mediate cargo selective interactions; 45% sequence identity to mammalian beta-COP; Sec27p
MS398	7110A9996B	Alpha subunit of COPI vesicle coatomer complex which surrounds transport vesicles in the early secretory pathway; Cop1p
MS407	CAB37B876A	Essential protein involved in transcription regulation; component of chromatin remodeling complexes; required for assembly and function of the INO80 complex; member of the RUVB-like protein family; Rvb1p
MS413	E4381E6DDD	Component of the holoenzyme form of RNA polymerase transcription factor TFIIH has DNA-dependent ATPase/helicase activity and is required with Rad3p for unwinding promoter DNA; involved in DNA repair; homolog of human ERCC3; Ssl2p
MS431	7F6ED5B406	Mismatch repair protein forms dimers withMSh2p that mediate repair of insertion or deletion mutations and removal of nonhomologous DNA ends contains a PCNA Pol30p binding motif required for genome stability;MSh3p
MS432	DFE71D6A4B	Protein of unknown function that associates with ribosomes and has a putative RNA binding domain; interacts with Tma20p; has homology to human protein DRP1 which interacts with human Tma20p homolog MCT-1; Tma22p
MS444	506950BFEE	Cytoplasmic isoleucine-tRNA synthetase target of the G1-specific inhibitor reveromycin A; Ils1p
MS456	01B7A5A97D	Component of the hexameric MCM complex which is important for priming origins of DNA replication in G1 and becomes an active ATP-dependent helicase that promotes DNA melting and elongation when activated by Cdc7p-Dbf4p in S-phase; Cdc47p
MS463	CB29C89B7F	Protein involved in DNA replication; component of the Mcm2-7 hexameric complex that binds chromatin as a part of the pre-replicative complex; Mcm2p
MS484	87D911C03D	Phosphatidylinositol 3-kinase responsible for the synthesis of phosphatidylinositol 3-phosphate; forms membrane-associated signal transduction complex with Vps15p to regulate protein sorting; similar to p110 subunit of mammalian PI 3-kinase; Vps34p
MS561	F58D360C78	Subunit of the oligosaccharyltransferase complex of the ER lumen which catalyzes asparagine-linked glycosylation of newly synthesized proteins; forms a subcomplex with Ost3p and Ost4p and is directly involved in catalysis; Stt3p

Supplementary Table 4.3. Molecular clock calibrations in molecular dating analysis.

Calibration	Mya lower bounds	Mya upper bounds (minimum age)	Represented by		Reference
Ascomycota-Basidiomycota split	1489	452	*Taphrina deformans*	*Mixia osmundae*	Berbee and Taylor (2006), Berbee and Taylor (2010)
Ascomycota crown	715	408	*Rhizophagus irregularis*	*Taphrina deformans*	Prieto and Wedin (2013)
Pezizomycotina crown	614	417	*Saccharomyces cerevisiae*	*Pyronema confluens*	Prieto and Wedin (2013)
Orbiliomycetes crown	201	32	*Arthrobotrys oligospora*	*Monacrosporium haptotylum*	Prieto and Wedin (2013)
Pezizomycetes crown	448	192	*Tuber melanosporum*	*Pyronema confluens*	Prieto and Wedin (2013)
Sordariomycetes crown	194	64	*Trichoderma atroviride*	*Neurospora crassa*	Prieto and Wedin (2013)
Leotiomycetes crown	209	61	*Sclerotinia sclerotiorum*	*Botrytis cinerea*	Prieto and Wedin (2013)
Dothideomycetes crown	252	93	*Alternaria brassicicola*	*Aureobasidium pullulans*	Prieto and Wedin (2013)
Eurotiomycetes crown	386	231	*Penicillium chrysogenum*	*Coccidioides immitis*	Prieto and Wedin (2013)
Agaricales	?	90	*Coprinopsis cinerea*	*Agaricus bisporus*	Hibett et al. (1997), Berbee and Taylor (2010)
Polypores	?	130	*Fomitiporia mediterranea*	*Fomitopsis pinicola*	Smith et al. (2004), Berbee and Taylor (2010)

Supplementary Table 4.4. List of known and putative meiosis genes in the genome of *Saccharomyces cerevisiae*, *Cryptococcus neoformans* and *Basidioascus undulatus*. Meiosis specific proteins are highlighted in red.

Process	Gene name	*Saccharomyces cerevisiae*	*Cryptococcus neoformans*	*Basidioascus undulatus vs. Saccharomyces cerevisiae*					*Basidioascus undulatus vs. Cryptococcus neoformans*					*Basidioascus undulatus*	*Basidioascus undulatus* scaffold
		Locus ID		Locus ID	Score	E-value	% identity	% positive	Locus ID	Score	E-value	% identity	% positive	Probable Locus ID	
DSB generation	SPO11	YHL022C	XM_767420.1	102794F55C	72.8	2E-14	25.46	43.54	102794F55C	191	2E-54	32.92	51.49	**102794F55C**	286
DSB generation	REC107/MEI2	YJR021C	Absent	Not detected					NA					Absent or not detected	
DSB generation	MEI4	YER044C	Absent	Not detected					NA					Absent or not detected	
DSB generation	REC102	YLR329W	Absent	Not detected					NA					Absent or not detected	
DSB generation	REC104	YHR157W	Absent	Not detected					NA					Absent or not detected	
DSB generation	REC114	YMR133W	Absent	Not detected					NA					Absent or not detected	
DSB generation	SKI8	YGL213C	XP_567964.1	Not detected					A5C17B7D33	79.3	1E-18	40	54.29	A5C17B7D33	261
DSB generation	MER1	YNL210W	Absent	Not detected					NA					Absent or not detected	
DSB generation	HFM1/MER3	YGL251C	XP_774045.1	268E1B92EF	286	2E-79	30.69	50.14	268E1B92EF	285	3E-78	29.55	48.66	**268E1B92EF**	125
DSB generation	NAM8/MRE2*	YHR086W	XP_568215.1	012CC612A1	88.6	2E-19	27.24	46.24	C3284824DB	211	7E-69	75.57	83.21	Conflict	
Removal of Spo11	MRE11*	YMR224C	XP_571170.1	550A163039	365	6E-116	40.59	58.02	550A163039	629	0	56.55	74.34	**550A163039**	331
Removal of Spo11	RAD50*	YNL250W	XP_771929.1	1CAAD52FF0	543	2E-170	30.88	52.16	1CAAD52FF0	869	0	38.91	61.16	**1CAAD52FF0**	25
Removal of Spo11	XRS2/NBS1	YDR369C	Absent	Not detected					NA					Absent or not detected	
Removal of Spo11	SAE2/COM1	YGL175C	Absent	Not detected					NA					Absent or not detected	
Strand invasion	RAD51*	YER095W	XP_567016.1	D36F2DAE01	481	9E-170	69.28	85.58	D36F2DAE01	533	0	77.71	84.46	**D36F2DAE01**	922
Strand invasion	DMC1	YER179W	XP_772121.1	1B6A6FD704	376	3E-128	58.13	75.94	1B6A6FD704	388	4E-133	67.13	80.28	**1B6A6FD704**	11
Strand invasion	RAD52*	YML032C	XP_569087.1	EA2B481C23	186	3E-55	51.9	74.05	EA2B481C23	237	4E-73	60.57	78.29	**EA2B481C23**	986
Strand invasion	RAD54*	YGL163C	XP_570462.1	4E6C655AE5	525	5E-179	61.26	78.21	4E6C655AE5	599	0	71.22	82.93	**4E6C655AE5**	1630
Strand invasion	RDH54	YBR073W	Absent	ED83E37023	476	1E-152	42.43	60.41	NA					ED83E37023	705
Strand invasion	RFA1	YAR007C	XP_775959.1	1512E55FF2	350	7E-114	41.02	62.08	1512E55FF2	489	6E-168	51.93	70.39	**1512E55FF2**	2007
Strand invasion	RFA2	YNL312W	XP_776149.1	C06D199EC7	95.9	1E-23	37.78	55.56	C06D199EC7	174	3E-53	40.51	61.18	**C06D199EC7**	444
Strand invasion	RFA3	YJL173C	Absent	Not detected					NA					Absent or not detected	
Strand invasion	SAE3	YHR079C-A	Absent	Not detected					NA					Absent or not detected	
Strand invasion	RAD55	YDR076W	Absent	Not detected					NA					Absent or not detected	
DNA damage checkpoint	PCH2	YBR186W	XP_567632.1	1586D154C9	177	3E-49	36.88	53.49	1586D154C9	418	1E-140	47.79	66.81	**1586D154C9**	703
DNA damage checkpoint	MEC1	YBR136W	XP_568889.1	E568B50733	483	2E-138	24.05	43.61	87D911C03D	713	0	61.72	76.24	Conflict	
DNA damage checkpoint	RAD17	YOR368W	XP_569244.1	Not detected					D5120AB0E3	171	4E-46	34.76	48.66	D5120AB0E3	127
DNA damage checkpoint	RAD24	YER173W	Absent	D5120AB0E3	54.3	3E-08	27.48	43.51	NA					D5120AB0E3	127
DNA damage checkpoint	DDC1	YPL194W	Absent	Not detected					NA					Absent or not detected	
Regulation of crossover frequency	MLH1*	YMR167W	XP_571158.1	F0BB260AD1	361	3E-113	53.03	70.03	F0BB260AD1	642	0	51.99	66.51	**F0BB260AD1**	1233
Regulation of crossover frequency	MLH3*	YPL164C	XP_570272.1	BC2D40152B	115	4E-27	23.47	44.13	BC2D40152B	178	7E-48	37.67	57.88	**BC2D40152B**	17
Regulation of crossover frequency	MSH4	YFL003C	XP_773414.1	CAE76A5567	347	1E-105	31.07	50.64	CAE76A5567	546	0	39.76	59.04	**CAE76A5567**	116
Regulation of crossover frequency	MSH5	YDL154W	XP_566842.1	A5F9B81D55	304	3E-90	30.46	52.12	A5F9B81D55	436	6E-139	39.91	58.36	**A5F9B81D55**	274
Regulation of crossover frequency	SGS1	YMR190C	XP_776787.1	FAB5DF8B5F	526	2E-167	45.14	64.24	FAB5DF8B5F	597	0	43.47	60.52	**FAB5DF8B5F**	297
Regulation of crossover frequency	MEI5	YPL121C	Absent	Not detected					NA					Absent or not detected	
Regulation of crossover frequency	MUM2	YBR057C	Absent	Not detected					NA					Absent or not detected	
Regulation of crossover frequency	NDJ1	YOL104C	Absent	Not detected					NA					Absent or not detected	
Regulation of crossover frequency	RAD1	YPL022W	XP_772313.1	29F5BE17B9	258	2E-75	33.14	50.95	29F5BE17B9	374	3E-117	40.1	56.48	**29F5BE17B9**	609
Regulation of crossover frequency	Rad2*	YGR258C	XP_566738.1	41955FBDBD	248	1E-69	44.04	67.51	41955FBDBD	355	9E-106	54.75	70.82	**41955FBDBD**	2155
Synaptonemal complex	HOP1	YIL072W	50255507	D659917BB2	141	4E-37	31.54	56.54	D659917BB2	170	7E-46	34.16	50	**D659917BB2**	170
Synaptonemal complex	HOP2	YGL033W	50255433	Not detected					Not detected					Absent or not detected	
Synaptonemal complex	MND1	YGL183C	XP_772550.1	5756414F12	62	2E-12	20.94	43.59	5756414F12	115	2E-31	37.13	51.05	**5756414F12**	1606
Synaptonemal complex	ZIP1	YDR285W	Absent	2C075CC8D6	204	1E-68	79.7	86.47	NA					2C075CC8D6	1813
Synaptonemal complex	ZIP2	YGL249W	Absent	Not detected					NA					Absent or not detected	
Synaptonemal complex	ZIP3	YLR394W	Absent	Not detected					NA					Absent or not detected	
Synaptonemal complex	Zip4/Spo22	YIL073C	134115038	Not detected					Not detected					Absent or not detected	

Supplementary Table 4.4. Continued.

Process	Gene name	*Saccharomyces cerevisiae*	*Cryptococcus neoformans*	*Basidioascus undulatus* vs. *Saccharomyces cerevisiae*					*Basidioascus undulatus* vs. *Cryptococcus neoformans*					*Basidioascus undulatus*	*Basidioascus undulatus* scaffold
		Locus ID		Locus ID	Score	E-value	% identity	% positive	Locus ID	Score	E-value	% identity	% positive	Probable Locus ID	
DNA Repair	HTA1*	YDR225W	XP_567962.1	2C075CC8D6	204	1E-68	79.7	86.47	2C075CC8D6	130	3E-39	57.98	73.11	**2C075CC8D6**	1813
DNA Repair	HTA2 *	YBL003C	XP_569065.1	2C075CC8D6	206	2E-69	80.45	87.22	F84A4F188E	205	6E-69	79.39	87.79	Conflict	
DNA Repair	RED1	YLR263W	Absent	Not detected					NA					Absent or not detected	
DNA Repair	SMC5	YOL034W	XP_570071.1	8388BCCBA3	362	3E-107	27.24	48.17	8388BCCBA3	529	1E-168	32.52	51.9	**8388BCCBA3**	691
DNA Repair	SMC6*	YLR383W	XP_775824.1	13E0CFCD07	340	1E-99	27.58	47.32	13E0CFCD07	476	4E-149	29.98	50.65	**13E0CFCD07**	542
DNA Repair	EXO1*	YOR033C	XP_777034.1	36DFC1EC56	276	3E-85	43.67	65.33	36DFC1EC56	389	1E-124	54.49	71.07	**36DFC1EC56**	117
DNA Repair	HRR25	YPL204W	XP_570121.1	22D0CDA5D9	464	6E-162	65.33	83.28	22D0CDA5D9	594	0	95.22	98.63	**22D0CDA5D9**	2927
DNA Repair	RAD23*	YEL037C	XP_777611.1	0FBB054DC3	54.7	5E-10	40.54	60.81	0FBB054DC3	91.3	3E-23	60.81	78.38	**0FBB054DC3**	113
Mismatch repair	MSH2	YOL090W	XP_567098.1	E449052477	746	0	43.93	63.77	E449052477	1087	0	58.26	73.21	**E449052477**	333
Mismatch repair	MSH3	YCR092C	XP_569494.1	7F6ED5B406	354	1E-106	29.13	49.57	7F6ED5B406	790	0	45.31	65.61	**7F6ED5B406**	45
Mismatch repair	MSH6*	YDR097C	XP_772722.1	122F99619E	672	0	36.44	56.87	122F99619E	1026	0	51.24	66.83	**122F99619E**	68
Mismatch repair	MLH2	YLR035C	Absent	8C03A290CE	86.7	2E-19	31.93	53.61	NA					8C03A290CE	258
Mismatch repair	PMS1	YNL082W	57225775	8C03A290CE	176	2E-50	48.65	67.03	8C03A290CE	236	4E-72	60.51	75.38	**8C03A290CE**	258
Resolution of recombination intermediates	MMS4	YBR098W	58260752	Not detected					Not detected					Not detected or absent	
Resolution of recombination intermediates	MUS81*	YDR386W	XP_777360.1	E55E7AB0BD	84	2E-17	30.49	49.78	E55E7AB0BD	101	2E-22	32.39	50.7	**E55E7AB0BD**	1192
Resolution of recombination intermediates	SLX1	YBR228W	XP_567159.1	A74C037F01	83.2	7E-20	52.44	68.29	A74C037F01	108	3E-28	61.54	74.36	**A74C037F01**	521
Resolution of recombination intermediates	TOP1*	YOL006C	XP_572925.1	DB366D3081	439	4E-147	49.78	66.89	DB366D3081	518	2E-176	56.71	70.56	**DB366D3081**	520
Resolution of recombination intermediates	TOP2*	YNL088W	XP_566700.1	4AE1080675	1197	0	52.97	71.47	4AE1080675	1491	0	66.48	79.24	**4AE1080675**	12
Resolution of recombination intermediates	TOP3*	YLR234W	XP_773035.1	BCF17A4E2A	266	3E-82	43.67	60.54	BCF17A4E2A	518	1E-174	57.95	70.91	**BCF17A4E2A**	2738
Resolution of recombination intermediates	SLX4	YLR135W	Absent	Not detected										Not detected or absent	
Resolution of recombination intermediates	SLX5	YDL013W	Absent	Not detected										Not detected or absent	
Resolution of recombination intermediates	SLX8	YER116C	Absent	52369A1C42	52.4	3E-08	35.9	48.72						52369A1C42	695
Nonhomologous end joining	YKU70*	YMR284W	XP_573016.1	AD4E738F04	115	2E-27	24.21	42.14	AD4E738F04	228	3E-66	32.28	47.76	**AD4E738F04**	46
Nonhomologous end joining	YKU80*	YMR106C	XP_568810.1	1FC448F440	60.8	3E-10	30.29	48.57	1FC448F440	241	7E-68	28.83	46.23	**1FC448F440**	180
Nonhomologous end joining	DNL4	YOR005C	XP_572602.1	9206958189	223	5E-62	27.5	43.38	E8D29BB570	902	0	71.5	83.49	Conflict	
Nonhomologous end joining	LIF1	YGL090W	Absent	Not detected					NA					Absent or not detected	
Other	MSC1	YML128C	XP_570348.1	6453C9DC91	53.1	2E-08	22.02	45.83	6453C9DC91	168	1E-47	34.33	51.12	**6453C9DC91**	702
Other	MSC7*	YHR039C	XP_773481.1	AE68F812D8	179	1E-49	26.57	46.65	AE68F812D8	185	8E-52	28.6	45.59	**AE68F812D8**	122
Other	MSC3	YLR219W	Absent	Not detected					NA					Absent or not detected	
Other	MSC6	YOR354C	Absent	Not detected					NA					Absent or not detected	
Other	SRS2	YJL092W	Absent	C8820A864B	273	3E-76	28.95	44.65	NA					C8820A864B	94
Other	MPS3	YJL019W	Absent	Not detected					NA					Absent or not detected	
Other	REC8	YPR007C	134090540	Not detected					130D4D9937	65.1	1E-11	38.04	59.78	130D4D9937	2597
Other	Mcd1/Rad21*	6320201	58266400	130D4D9937	68.6	6E-13	35.05	57.73	130D4D9937	142	4E-37	32.61	46.65	**130D4D9937**	2597
Other	SMC1	BAA09230.1	XP_568851.1	82DC381A41	534	3E-170	31.89	54.54	82DC381A41	894	0	44.85	64.74	**82DC381A41**	636
Other	SMC2	P38989.1	XP_572171.1	68E0241B20	516	7E-168	42.44	63.29	68E0241B20	720	0	58.48	70.98	**68E0241B20**	353
Other	SMC3	CAA74655.1	XP_570201.1	10D8B5FBE4	248	4E-73	41.53	60.17	10D8B5FBE4	404	2E-129	57.95	72.56	**10D8B5FBE4**	2002
Other	SMC4*	EDV09389.1	XP_571168.1	C71F05C621	895	0	41.41	60.31	C71F05C621	1367	0	56.6	73.61	**C71F05C621**	619
Other	SCC3	P40541.1	XP_567136.1	Not detected					Not detected					Absent or not detected	
Other	PDS5	Q04264.1	XP_567466.1	062A151CC3	326	3E-93	24.85	45.12	062A151CC3	681	0	35.27	55.63	**062A151CC3**	36

Supplementary Table 4.5. List of mating genes.

Gene	*Saccharomyces cerevisiae* Database Description (SGD)	*Saccharomyces cerevisiae*	*Basidioascus undulatus vs. Saccharomyces cerevisiae*					*Basidioascus undulatus* scaffold
	Mating response	Locus ID	Locus ID	Score	E-value	% identity	% positive	
STE3	Receptor for a factor pheromone, couples to MAP kinase cascade to mediate pheromone response; transcribed in alpha cells and required for mating by alpha cells, ligand bound receptors endocytosed and recycled to the plasma membrane; GPCR	YKL178C	601070A992	84.7	2E-18	25.17	44.37	10
KSS1	Mitogen-activated protein kinase (MAPK) involved in signal transduction pathways that control filamentous growth and pheromone response; the KSS1 gene is nonfunctional in S288C strains and functional in W303 strains	YGR040W	03DD35A234	341	4E-116	58.5	72.45	2837
FUS3	Mitogen-activated serine/threonine protein kinase involved in mating; phosphoactivated by Ste7p; substrates include Ste12p, Far1p, Bni1p, Sst2p; inhibits invasive growth during mating by phosphorylating Tec1p, promoting its degradation	YBL016W	03DD35A234	355	7E-122	57.48	74.83	2837
STE7	Signal transducing MAP kinase kinase involved in pheromone response, where it phosphorylates Fus3p, and in the pseudohyphal/invasive growth pathway, through phosphorylation of Kss1p; phosphorylated by Ste11p, degraded by ubiquitin pathway	YDL159W	C56EA11F93	209	1E-61	49.32	66.06	2123
STE11	Signal transducing MEK kinase involved in pheromone response and pseudohyphal/invasive growth pathways where it phosphorylates Ste7p, and the high osmolarity response pathway, via phosphorylation of Pbs2p; regulated by Ste20p and Ste50p	YLR362W	A726A87E58	319	6E-103	52.6	67.86	2300
GPA1	GTP-binding alpha subunit of the heterotrimeric G protein that couples to pheromone receptors; negatively regulates the mating pathway by sequestering G(beta)gamma and by triggering an adaptive response; activates Vps34p at the endosome	YHR005C	00D128FF38	243	8E-78	55	75.5	2046
STE4	G protein beta subunit, forms a dimer with Ste18p to activate the mating signaling pathway, forms a heterotrimer with Gpa1p and Ste18p to dampen signaling; may recruit Rho1p to the polarized growth site during mating; contains WD40 repeats	YOR212W	51579617AB	195	3E-59	43.67	61.22	1054
STE18	G protein gamma subunit, forms a dimer with Ste4p to activate the mating signaling pathway, forms a heterotrimer with Gpa1p and Ste4p to dampen signaling; C-terminus is palmitoylated and farnesylated, which are required for normal signaling	YJR086W	Not detected					
STE20	Cdc42p-activated signal transducing kinase of the PAK (p21-activated kinase) family; involved in pheromone response, pseudohyphal/invasive growth, vacuole inheritance, down-regulation of sterol uptake; GBB motif binds Ste4p	YHL007C	ABF41DDAEF	375	5E-122	59.26	76.09	2163
STE12	Transcription factor that is activated by a MAP kinase signaling cascade, activates genes involved in mating or pseudohyphal/invasive growth pathways; cooperates with Tec1p transcription factor to regulate genes specific for invasive growth	YHR084W	Not detected					
FAR1	Cyclin-dependent kinase inhibitor that mediates cell cycle arrest in response to pheromone; also forms a complex with Cdc24p, Ste4p, and Ste18p that may specify the direction of polarized growth during mating; potential Cdc28p substrate	YJL157C	Not detected					
STE5	Pheromone-response scaffold protein that controls the mating decision; binds Ste11p, Ste7p, and Fus3p kinases, forming a MAPK cascade complex that interacts with the plasma membrane and Ste4p-Ste18p; allosteric activator of Fus3p	YDR103W	Not detected					

Supplementary Table 4.5. Continued.

Gene	*Saccharomyces cerevisiae* Database Description (SGD)	*Saccharomyces cerevisiae*	*Basidioascus undulatus* vs. *Saccharomyces cerevisiae*					*Basidioascus undulatus* scaffold
	Pheromone processing	**Locus ID**	Locus ID	Score	E-value	% identity	% positive	
KEX1	Protease involved in the processing of killer toxin and alpha factor precursor; cleaves Lys and Arg residues from the C-terminus of peptides and proteins	YGL203C	C1EB8324D8	249	5E-72	34.79	51.2	316
KEX2	Subtilisin-like protease (proprotein convertase), a calcium-dependent serine protease involved in the activation of proproteins of the secretory pathway	YNL238W	1DAB65F8AC	480	8E-160	47.45	63.53	37
STE13	Dipeptidyl aminopeptidase, Golgi integral membrane protein that cleaves on the carboxyl side of repeating -X-Ala- sequences, required for maturation of alpha factor, transcription is induced by a-factor	YOR219C	C51BE5DE56	131	5E-35	42.11	63.16	2060
RAM1	Beta subunit of the CAAX farnesyltransferase (FTase) that prenylates the a-factor mating pheromone and Ras proteins; required for the membrane localization of Ras proteins and a-factor; homolog of the mammalian FTase beta subunit	YDL090C	B544DBFB4B	169	4E-48	37.09	53.31	27
RAM2	Alpha subunit of both the farnesyltransferase and type I geranylgeranyltransferase that catalyze prenylation of proteins containing a CAAX consensus motif; essential protein required for membrane localization of Ras proteins and a-factor	YKL019W	B2B303A077	82.4	2E-19	30.73	45.31	1520
RCE1	Type II CAAX prenyl protease involved in the proteolysis and maturation of Ras and the a-factor mating pheromone	YMR274C	Not detected					
STE24	Highly conserved zinc metalloprotease that functions in two steps of a-factor maturation, C-terminal CAAX proteolysis and the first step of N-terminal proteolytic processing; contains multiple transmembrane spans	YJR117W	Not detected					
STE14	Farnesyl cysteine-carboxyl methyltransferase, mediates the carboxyl methylation step during C-terminal CAAX motif processing of a-factor and RAS proteins in the endoplasmic reticulum, localizes to the ER membrane	YDR410C	CC90F4A946	99.8	9E-26	45.45	58.68	159
AXL1	Haploid specific endoprotease that performs one of two N-terminal cleavages during maturation of a-factor mating pheromone; required for axial budding pattern of haploid cells	YPR122W	98D2221B58	129	5E-31	30.38	51.9	1187
STE6	Plasma membrane ATP-binding cassette (ABC) transporter required for the export of a-factor, catalyzes ATP hydrolysis coupled to a-factor transport; contains 12 transmembrane domains and two ATP binding domains; expressed only in MATa cells	YKL209C	ED8249ED54	359	2E-103	25.6	43.36	102

Gene	Description	*Interproscan domains*	*Basidioascus undulatus* Locus ID	*Basidioascus undulatus* scaffold
HD1 & HD2	Homeodomain encoding proteins 1 and 2. These proteins are transcription factors that contain DNA binding domains whose role is to regulate genes related to mating. They are called the following in these basidiomycete fungi: *Coprinopsis cinera* (a1/b1, a2/b2), *Ustilago maydis* (bE, bW), *Cryptococcus neoformans* (Sxi1alpha, Sxi2a), *Schizophyllum commune* (Z, Y).	Homeodomain, Homeobox KN domain	8946F71C4C, AF24C22F02	20, 667
HMG	Pheromone response factor, High Mobility Group (HMG) DNA binding protein. These proteins are involved in the regulation of DNA-dependent processes such as transcription, replication, and strand repair, all of which require the bending and unwinding of chromatin. Many of these proteins are regulators of gene expression and are involved in the fungal sexual reproduction cycle of fungi. In *Ustilago maydis*, the gene is called Prf.	DNA-binding motif,DNA binding domain with preference for A/T rich regions, High mobility group protein (HMGY) signature, High mobility group (HMG) box domain, HMG boxes A and B DNA-binding domains profile, High mobility group (HMG1/HMG2) protein signature	B013112742, C8B77D01D8, C1AD40EA22, 9CC40B0A26	92, 127, 360, 1388